VISUALIZATION OF ULTRASOUND INDUCED CAVITATION BUBBLES USING SYNCHROTRON ANALYZER BASED IMAGING

A Thesis Submitted to the College of
Graduate Studies and Research
In Partial Fulfillment of the Requirements
For the Degree of Doctor of Philosophy
In the Division of Biomedical Engineering
University of Saskatchewan
Saskatchewan

By

ZAHRA IZADIFAR

PERMISSION TO USE

In presenting this thesis in partial fulfilment of the requirements for a Postgraduate degree from the University of Saskatchewan, I agree that the libraries of this University may make it freely available for inspection. I further agree that permission for copying of this thesis in any manner, in whole or in part, for scholarly purposes may be granted by the professor or professors who supervised my thesis work or, in their absence, by the Head of the Department or the Dean of the College in which my thesis work was done. It is understood that any copying or publication or use of this thesis or parts thereof for financial gain shall not be allowed without my written permission. It is also understood that due recognition shall be given to me and to the University of Saskatchewan in any scholarly use which may be made of any material in my thesis.

Requests for permission to copy or to make other use of material in this thesis in whole or part should be addressed to:

Head of the Division of Biomedical Engineering

57 Campus Drive, University of Saskatchewan

Saskatoon, Saskatchewan S7N 5A9

Canada

ABSTRACT

Ultrasound is recognized as the fastest growing medical modality for imaging and therapy. Being noninvasive, painless, portable, X-ray radiation-free and far less expensive than magnetic resonance imaging, ultrasound is widely used in medicine today. Despite these benefits, undesirable bioeffects of high-frequency sound waves have raised concerns; particularly, because ultrasound imaging has become an integral part of prenatal care today and is increasingly used for therapeutic applications. As such, ultrasound bioeffects must be carefully considered to ensure optimal benefits-to-risk ratio. In this context, few studies have been done to explore the physics (i.e. 'cavitation') behind the risk factors. One reason may be associated with the challenges in visualization of ultrasound-induced cavitation bubbles *in situ*. To address this issue, this research aims to develop a synchrotron-based assessment technique to enable visualization and characterization of ultrasound-induced microbubbles in a physiologically relevant medium under standard ultrasound operating conditions.

The first objective is to identify a suitable synchrotron X-ray imaging technique for visualization of ultrasound-induced microbubbles in water. Two synchrotron X-ray phase-sensitive imaging techniques, in-line phase contrast imaging (PCI) and analyzer-based imaging (ABI), were evaluated. Results revealed the superiority of the ABI method compared to PCI for visualization of ultrasound-induced microbubbles.

The second main objective is to employ the ABI method to assess the effects of ultrasound acoustic frequency and power on visualization and mapping of ultrasound-induced microbubble patterns in water. The time-averaged probability of ultrasound-induced microbubble occurrence along the ultrasound beam propagation in water was determined using the ABI method. Results showed the utility of synchrotron ABI for visualizing cavitation bubbles formed in water by

clinical ultrasound systems working at high frequency and output powers as low as used for therapeutic systems. It was demonstrated that the X-ray ABI method has great potential for mapping ultrasound-induced microbubble patterns in a fluidic environment under different ultrasound operating conditions of clinical therapeutic devices.

Taken together, this research represents an advance in detection techniques for visualization and mapping of ultrasound-induced microbubble patterns using the synchrotron X-ray ABI method without usage of contrast agents. Findings from this research will pave the road toward the development of a synchrotron-based detection technique for characterization of ultrasound-induced cavitation microbubbles in soft tissues in the future.

ACKNOWLEDGMENTS

I would like to express my gratitude and appreciation to my supervisors, Dr. Dean Chapman and Dr. Paul Babyn, for their support and research advice throughout my Ph.D. studies.

I would like to thank my Advisory Committee members, Dr. Ingrid J Pickering, Dr. Angela Baerwald, and Dr. Chris Zhang, for their support and guidance. Also, I appreciate the dedicated technical support from Dr. George Belev on the experiments performed at the CLS Biomedical Imaging and Therapy Beamline. I acknowledge the assistance of Dr. Kaushik Desai at the Western College of Veterinary Medicine in providing access to ultrasound processors used during my research experiments. I additionally thank the Canadian Institute of Health Research (CIHR)-Training in Health Research Using Synchrotron Techniques (THRUST) training program (through the fellowship to me).

Special thank goes to the staff at the Biomedical Imaging and Therapy (BMIT) beamline at the Canadian Light Source (CLS), where I performed all the synchrotron imaging experiments. The CLS is supported by the Canada Foundation for Innovation, Natural Sciences and Engineering Research Council of Canada (NSERC), the National Research Council Canada, CIHR, the Government of Saskatchewan, Western Economic Diversification Canada, and the University of Saskatchewan.

I acknowledge financial support from the University of Saskatchewan (through the Dean's Scholarship), and the Natural Science and Engineering Research Council of Canada (NSERC) Discovery Grant program.

Finally, my deep gratitude and thanks go to my dearest parents for their unconditional love and support throughout my life, and showing me the value of education and constantly

supporting and encouraging me in this regard. I am grateful to my lovely siblings, Mohammad, Maryam, and Zohreh for their help, guidance, and always being there for me.

TABLE OF CONTENTS

PERMISSION TO USE i
ABSTRACT ii
ACKNOWLEDGMENTS iv
TABLE OF CONTENTS vi
LIST OF TABLES xi
LIST OF FIGURES xii
ABBREVIATIONS xvi
Chapter 1 Introduction 1
1.1. Therapeutic applications of ultrasound 2
1.2. Ultrasound-induced cavitation (non-thermal) effects 4
1.3. Safety concerns of ultrasound applications 4
1.4. Safety assessment detection techniques 6
1.5. Synchrotron detection technique 7
1.6. Research objectives 8
1.7. Contributions of the primary investigator 10
1.8. References 11
Chapter 2 Applications and safety of therapeutic ultrasound: current trends and future potential 13
2.1 Abstract 13
2.2 Introduction 14
2.3 Basic principles of ultrasound tissue interaction 15
2.4 Cavitation effect 19
2.5 Cavitation-based applications of ultrasound 20
2.6 Heating effect of ultrasound 22
2.7 Heating-based applications of ultrasound 23
2.7.1 Ultrasound for physical therapy 23
2.7.2 Hyperthermia 25
2.7.3 High-intensity focused ultrasound 26
2.8 Therapeutic applications of ultrasound based on combined mechanisms 29
2.9 New research areas for therapeutic applications of ultrasound 30

2.10 Summery 31
2.11 References 33
Chapter 3 High Intensity Focused Ultrasound: a Review of Principles, Devices, and Clinical Applications 40
3.1 Abstract 40
3.2 Introduction 41
3.3 High intensity focused ultrasound 42
3.4 Principles behind HIFU 46
3.5 HIFU devices for clinical applications 47
3.6 Clinical Application of HIFU 53
3.6.1 Liver 53
3.6.2 Prostate 54
3.6.3 Breast Cancer 58
3.6.4 Uterine fibroids 60
3.6.5 Kidney tumor 63
3.6.6 Esophageal tumor 64
3.6.7 Pancreas tumor 66
3.6.8 Bone cancer 68
3.6.9 Brain Disorders 73
3.6.10 Essential Tremor 75
3.6.11 Chronic and non-malignant pain 76
3.6.12 Trigeminal Neuralgia 77
3.6.13 Brain tumor 78
3.7 Potential future clinical applications of focused ultrasound 80
3.7.1 Vessel occlusion by HIFU 80
3.7.2 Disruption of blood brain barrier 81
3.7.3 Histotripsy 83
3.7.4 Parkinson's disease 84
3.7.5 Psychiatric disease 86
3.7.6 Stroke and Thrombolysis 87
3.7.7 Abscesses 88
3.8 Combined mechanisms for therapeutic application of ultrasound 89
3.9 Prospective new research areas for application of therapeutic ultrasound 90

3.10 Conclusions 91
3.11 References 93
Chapter 4 Mechanical and biological effects of ultrasound: A review of present knowledge 110
4.1 Abstract 110
4.2 Introduction 110
4.3 Ultrasound mechanisms 111
4.4 Mechanical (non-thermal) bioeffects 115
4.4.1 Lung 115
4.4.2 Intestine 116
4.5 Urinary tract system 118
4.6 Cardiac 121
4.7 Blood vessels and microvasculature 123
4.8 Prenatal exposure 126
4.9 Biological Responses to Acoustic Mechanisms 126
4.10 Cellular bioeffects 128
4.11 Studies on Biological Effects of Ultrasound 131
4.12 Fetus and embryo 138
4.13 Summary 141
4.14 References 145
Chapter 5 Medical applications and detection techniques of ultrasound cavitation and microbubble contrast agents 162
5.1 Abstract 162
5.2 Introduction 163
5.3 Understanding cavitation phenomenon 165
5.4 Effect of cavitation/microbubbles on tissue and body fluid 169
5.5 Ultrasound microbubble contrast agents application 171
5.5.1 Diagnosis and monitoring 171
5.5.2 Ultrasound drug delivery 173
5.5.3 Gene therapy with microbubbles 176
5.5.4 Smart microbubbles in diagnostic applications 176
5.6 Detection and imaging of cavitation and microbubbles 178
5.7 Optical methods 179

5.7.1 Detection of physical and chemical responses 179
5.7.2 High speed photography 180
5.7.3 Optical detection technique 183
5.7.4 Acoustic detection of bubbles (active and passive imaging) 185
5.8 Scattering methods 189
5.8.1 Laser scattering technique 189
5.8.2 Synchrotron X-ray imaging technique 189
5.9 Summary and recommendations for future research 193
5.10 References 196
Chapter 6 Visualization of ultrasound induced cavitation bubbles using synchrotron X-ray Analyzer Based Imaging technique 204
6.1 Abstract 204
6.2 Introduction 204
6.2.1 X-ray ABI 208
6.2.2 X-ray PCI 211
6.3 Materials and method 212
6.3.1 Materials 212
6.3.2 Ultrasound treatment 212
6.3.3 Synchrotron imaging 214
6.4 Result and discussion 218
6.4.1 Phase contrast 218
6.4.2 ABI Images 219
6.5 Conclusion 224
6.6 References 226
Chapter 7 Application of Analyzer Based X-ray Imaging technique for detection of ultrasound induced cavitation bubbles from a physical therapy unit 228
7.1 Abstract 228
7.2 Introduction 229
7.2.1 X-ray ABI 233
7.3 Materials and method 235
7.3.1 Materials 235
7.3.2 Ultrasound treatment 235
7.3.3 Synchrotron imaging 237

7.4 Result and discussion 239
7.4.1 Preliminary experiments 239
7.4.2 Main experiments 240
7.5 Conclusion 245
7.6 References 247
Chapter 8 Conclusion and future research 250
8.1 Conclusion 250
8.2 Recommendation for future work 253

LIST OF TABLES

Table 2-1 Ultrasound attenuation coefficients of different body tissues at a frequency of 1 MHz [26] 16

Table 2-2 Different therapeutic applications of ultrasound and a comparison between ultrasound frequency, therapeutic outcome, and related bioeffect mechanism (thermal or non-thermal) (table design based on [3]). 17

Table 2-3 Typical frequencies used in physical therapy ultrasound units and their associated wavelengths, temperatures generated, and target organs. 25

Table 5-1 Advantages and disadvantages of different imaging modalities for visualizing microbubbles. (-) indicates the absence and (+) indicates the presence of each listed assessment capability in detection modalities. 193

LIST OF FIGURES

Figure 2-1 The different shapes of physical therapy ultrasound transducers widely used in clinics. 24

Figure 3-1 Schematic of high-intensity focused ultrasound for tumor therapy 45

Figure 3-2 Schematic of the structure of an extracorporeal HIFU transducer, including both imaging and therapy probes, depicting an ultrasound-guided technique on a patient .. 49

Figure 3-3 Schematic of magnetic resonance-guided extracorporeal focused ultrasound system treatment technique 50

Figure 3-4 Schematic of a typical transrectal transducer for prostate cancer treatment, with both therapy and imaging transducers incorporated into the head of the transducer probe. Longitudinal and lateral rotation movements of the transducer along with the imaging probe enable volume ablation and scanning of prostate cancer. 57

Figure 3-5 Schematic of a transrectal ultrasound transducer (rectal HIFU probe) and the treatment technique used for prostate cancer treatment. The HIFU ultrasound probe is inserted into the rectum and the sound waves target the cancer-affected areas in the prostate gland. 58

Figure 3-6 Schematic of the front and side view of the head of the interstitial transducer used for the treatment of esophageal tumors. The ultrasound imaging probe along with the HIFU transducer are located at the head of the interstitial transducer to image and treat the region of interest. 65

Figure 3-7 Schematic of the application of the interstitial HIFU probe in esophageal cancer treatment. The applicator is inserted into the esophagus through the mouth and the transducer placed inside the cancerous cells that line the inside of the esophagus. Esophageal cancer ablation along with ultrasound scanning of the targeted area are performed simultaneously by this HIFU system. (Courtesy of Mayo Foundation for Medical Education and Research) 66

Figure 3-8 An ExAblate Neuro (InSightec, Haifa, Israel) MRgFUS transducer helmet on an MRI table. Cooled degassed water is carried through the attached hose to the helmet to provide the medium through which the ultrasound travels. This water is also used to fill the space between the patient's head and the transducers to keep the skull bone temperature within a safe range [169]. 74

Figure 3-9 Intra-operative patient setup for MRgFUS procedure on the brain. The patient lies on the MR bed and the head is placed inside the phased-array ultrasound transducer helmet. [222] 86

Figure 5-1 Schematic image of acoustic cavitation process 165

Figure 5-2. Illustration of variety of ways drug delivery can be enhanced by utilizing microbubbles. (a) Microbubbles with drug-laden external membranes are freely circulated in the vessel and bind in the target region, then are ruptured by ultrasound and the drug payload liberated in the target area; (b) Microbubbles carrying drugs inside of them are circulated in the vessel and destroyed by ultrasound and the transported substances thus released into the surrounding targeted tissue; (c) Free circulation of drug particles (yellow circles) along with ultrasound microbubbles (grey circles) in vessels, and the effect of ultrasound on growth and burst of microbubbles results in extravasation of drug; and (d) Schematic of various modes by which microbubbles increase the cell permeability: 1: non inertial cavitation when a bubble behaves as an oscillator and microstreaming around bubble increases the permeability; 2: collapse of a gas bubble and emission of a shock wave; and 3: asymmetric bubble collapse close to a cell wall producing a high speed liquid jet that pierces and ruptures the cell. 175

Figure 5-3 A series of 18 photographs demonstrate the dynamics of the cavitation process very close to a solid surface. Reproduced from Tomita and Shima [104] with permission. 181

Figure 5-4 (a) Sequence of fluorescent images illustrating the interaction of focused ultrasound with the microbubble inside the echogenic drug delivery vehicle and (b) sequence of fluorescent images of the interaction of an echogenic drug delivery vehicle and an artificial cell membrane under ultrasound pulse sequence. Reproduced from Ibsen et al. [106] with permission..... 182

Figure 5-5 (a) Sequence of two-dimensional images of a microbubble oscillation affected by a 2.25-MHz center frequency pulse ultrasound over 10 nanoseconds. (b) Radius-time image of a microbubble oscillation and a distance-time image of a single line through the center of the microbubble oscillation for characterization of the effect of ultrasound on the microbubble. Reproduced from Ferrara et al. [21] with permission. 185

Figure 5-6 (a) ABI of the whole ultrasound beam of a therapeutic ultrasound system at 0.8835 MHz and 14 W and (b) the sequence and location of cavitation bubbles, with approximately the same interval between sequences. From Izadifar et al. [133] 192

Figure 6-1 Schematic of the ABI set up at the Canadian Light Source used for imaging ultrasound induced cavitation bubbles in water. 207

Figure 6-2 Calculated analyzer rocking curve for the reflection and energy used in the ABI experiments; Si (4,4,0) reflection @ 40keV. Note that the rocking angle scale is in microradians (1microradian = 57.3 x 10-6 degree)..... 210

Figure 6-3 Schematic of the PCI set up at the Canadian Light Source used for imaging ultrasound induced cavitation bubbles in water. 211

Figure 6-4 Preparation of the sample for ultrasound treatment and X-ray imaging: (a)mounting the sonicator probe on the scanning stage and inserting sonotrode inside and at the center of sample/water; (b) covering the transducer and sonicator probe with lead shielding and copper and adjusting camera at the sample. 214

Figure 6-5 The comparison of contrast from PCI and ABI. The PCI image shown at the top with the ABI just below with the same contrast scale. The plot below shows the contrast across the field of view for PCI and ABI. PCI shown at the top with the scale on the right and ABI below with the scale at the left. 218

Figure 6-6 Ultrasound beam (a) Vertical scan of the whole ultrasound beam till 24 mm below the tip of the probe at 20 kHz and 90% acoustic output power (117 W) (b). 219

Figure 6-7 The line intensity profile of images taken of the cavitation bubbles at 20 kHz and 90% acoustic output power at different distances from the tip of the probe; 4 mm(a), 8 mm (b), 12 mm (c), 16 mm (d), 20 mm (e), 24 mm (f)..... 220

Figure 6-8 ABI-based images of the cavitation bubbles at location of 4 mm below the tip of the probe at acoustic powers of 26 W(a), 39 W(b), 52 W(c), 78 W(d), 104 W(e), and 130 W(f). 221

Figure 6-9 The line intensity profile of images taken of the cavitation bubbles at a location of 2 mm below the tip of the probe at acoustic powers of 26 W(a), 39 W(b), 52 W(c), 78 W(d), 104 W(e), and 130 W(f)..... 223

Figure 6-10 Representative axial full cross-section ABI of simulated ultrasound beam at different distances from the tip of the probe; (a) 4 mm (b) 8 mm. 224

Figure 7-1 Schematic of the ABI set up performed for imaging therapeutic ultrasound induced cavitation bubbles in water at Canadian Light Source. 235

Figure 7-2 Preparation of the sample for therapeutic ultrasound treatment and X-ray imaging: (a) mounting the ultrasound probe on the scanning stage and inserting probe inside and at 45 degree angle of sample/water; (b) setting the signal generator/amplifier on the table and setting the experimental system..... 237

Figure 7-3 The experimental set up of the preliminary experiments and the observation of the sample container melting (a) the melted sign of container on the wall (b) and at the center bottom of the container (c) 240

Figure 7-4 Vertical scan of the whole ultrasound beam of a therapeutic ultrasound system below the tip of the probe at 0.8835 MHz and 14 W (a) the sequence form of cavitation bubbles' location with approximately same intervals between sequences..... 242

Figure 7-5 The region selected from Figure 7-4(a) for Fourier analysis (a) The power spectrum obtained from Figure 7-4(a). The black line shows the wave vector associated with the

strongest Fourier component whose magnitude is approximately 1.15 line-pairs/mm (b). 244

Figure 7-6 The intensity profile of images taken of the cavitation bubbles at different distances from the tip of the probe; 19.5 mm(a), 23 mm(b), 26.5 mm(c), 30 mm(d). 245

ABBREVIATIONS

ABI: analyser based imaging

ACD: active cavitation detection

BMIT: biomedical imaging and therapy

BPH: benign prostatic hyperplasia

CLS: Canadian Light Source

CT: computed tomography

DNA: DeoxyriboNucleic Acid

DPCD: dual passive cavitation detection

ESR: electron spin resonance

ESWL: Extracorporeal Shock Wave Lithotripsy

ET: Essential tremor

FDA: Food and Drug Administration

HCC: Hepatocellular carcinoma

HIFU: high intensity focused ultrasound

MI: medical index

MPa: mega Pascals

MR: magnetic resonance

MRgFUS: magnetic resonance guided focused ultrasound

MRI: Magnetic Resonance Imaging

MRSA: Methicillin-resistant Staphylococcus aureus

PCa: prostate cancer

PCD: passive cavitation detection

PCI: Phase Contrast Imaging

TACE: Transcatheter arterial chemoembolization technique

TN: Trigeminal neuralgia

USgFUS: ultrasound guided focused ultrasound

VIM: ventral intermediate

Chapter 1 Introduction

Ultrasound, which is high-frequency sound waves inaudible to humans, has been a fast growing tool useful for imaging and therapy in modern medicine. Diagnostic ultrasound, so called 'sonography', is the most widely used non-ionizing medical imaging technique. Sonography offers several distinct advantages including being noninvasive and painless for patients, accurate for most cases without X-ray radiation, portable, and far less expensive than magnetic resonance imaging (MRI). Ultrasound has been useful for therapy over the past 50 years. Since the 1950s, when low power ultrasound (1 MHz) was first used for tendinitis or bursitis, the use of ultrasound has been dramatically extended to different areas such as mechanically resolving kidney stones using high pressure-amplitude shockwaves, so called 'lithotripsy', uterine fibroid ablation, cataract removal, surgical tissue cutting, transdermal drug delivery and bone fracture healing [1].

Despite all benefits of ultrasound, undesirable bioeffects may occur during ultrasound therapy and imaging. Typical benefits and risks of therapeutic ultrasound are well-known to clinicians. Typical safety problems such as burns for ultrasound thermal-based therapy and hemorrhage for lithotripsy are known and relatively tractable [1]. In terms of diagnostic ultrasound, most of epidemiologic investigations are in favour of the safety of ultrasound imaging; however, there have been some reports that indicate a relationship between prenatal ultrasound exposure and adverse effects such as growth restrictions, delayed speech, and dyslexia [2]. These reports indicate that the diagnostic ultrasound safety information can be scattered, confusing or subject to commercial conflicts of interest [1]. In particular, the safety and risk of ultrasound imaging is of great importance because the use of diagnostic ultrasound has become such an integral part of today's prenatal care. For all ultrasound applications, but especially for prenatal care and

diagnosis, minimization of side effects must be taken carefully into consideration to ensure an optimal risk to benefit ratio of the ultrasound [1].

While investigations are mostly concerned about clinically relevant variables such as acoustic output, exposure time, number of exposures per subject, and the timing during the pregnancy for ultrasound risk assessments, little attention has been paid to exploring the physics behind safety issues, such as ‘cavitation’ [2]. One reason may be the difficulties associated with the visualization and characterization of ultrasound-induced cavitation process. Thus, continued research is required to develop technique(s) and protocol(s) for assessing ultrasound-induced cavitation in physiologically relevant media (in-vitro studies), tissue mimicking phantoms (ex-vivo studies) and animal models (in-vivo studies).

To draw a road map toward defining the objectives of this research, this chapter aims to provide an overview of ultrasound medical applications, ultrasound-induced cavitation process and its safety concerns and detection methods, and synchrotron X-ray imaging as a potential detection technique for characterization of cavitation microbubbles.

1.1. Therapeutic applications of ultrasound

Acoustic waves are categorized into three categories of infrasound, sound, and ultrasound based on the three frequency bands in an overall spectrum of acoustic waves. Acoustic waves lower than 20 Hz are called infrasound, between 20 Hz and 20 kHz are called sound (audible sound), and greater than 20 kHz are called ultrasound. At frequency range between 1 and 20 MHz, practical application is made out of ultrasound in clinical medicine for diagnosis and therapeutic purposes. The biological effects associated with high frequency sound wave energy have been used for therapeutic purposes in medicine for many years. While the ultrasound bioeffects must

be minimized in diagnostic applications, they have been employed for therapeutic purposes including physical therapy, lithotripsy, targeted ultrasound drug delivery, trans-dermal ultrasound drug delivery, ultrasound hemostasis, cancer therapy, and ultrasound assisted thrombolysis [3, 4]. In particular, the ability to precisely focus ultrasonic energy onto targets of millimetre dimensions has brought a significant milestone in the development of focused ultrasound therapeutic applications. Focused ultrasound has shown promise for non-invasive thermal ablation of tumors in several organs, and is a promising alternative to standard treatment options including surgery, radiotherapy, gene therapy and chemotherapy. High intensity focused ultrasound (HIFU) has been used for the treatment of different types of solid malignant tumors such as pancreas, liver, kidney, bone, pancreas, prostate, breast, uterine fibroids, and soft-tissue sarcomas [5].

Ultrasonic biological effects can be induced through heating (e.g. tumor ablation), nonthermal (e.g. acoustic cavitation, gas body activation, mechanical stress) and/or undetermined nonthermal mechanisms [6]. While ultrasound-induced cavitation is undesired for the heat-based ultrasound treatments, some therapeutic applications such as extracorporeal shock wave lithotripsy (ESWL), intracorporeal lithotripsy, and surgical ultrasonic instruments are based on the ultrasound-induced cavitation. In contrast, HIFU takes advantage of both ultrasound-induced thermal effects and cavitation to induce required bioeffects for therapy. However, the timing, pattern and location of formation of cavitation bubbles are not well understood and remain unpredictable during therapeutic procedures. As such, continued studies are crucial for a better insight into the cavitation process. More specifically, the formation and collapse of the ultrasound-induced cavitation microbubbles under ultrasonic therapeutic procedures may need to be re-standardized, in terms of safety risks, for a range of therapeutic and diagnosis applications.

1.2. Ultrasound-induced cavitation (non-thermal) effects

Cavitation is defined as the formation of bubbles (cavities) in a liquid due to the strong negative pressure induced by the propagating acoustic waves through the fluidic environment [4]. The term 'cavitation process' refers to the events in which vapour- or gas- filled cavities are formed and then collapsed (implosion) in the ultrasound-exposed host medium. When an ultrasound wave is applied to a liquid (or a fluidic environment), the molecular structure of the medium goes through alternative expansion and compression cycles. As the cyclic expansions (rarefaction) and compressions travel through the medium, the rarefaction pulls molecules apart and the compression pushes them together. If the ultrasound wave is strong enough, the expansion cycle can overcome intermolecular binding forces and leads to a sudden pressure drop and creation of bubbles filled with gaseous substances (vapour) in the medium. These bubbles grow in size with the following expansion cycles of ultrasound until they reach an unstable size and then violently collapse. In succeeding cavitation processes, the cavities can grow and collapse violently with the release of enormous amounts of energy in the form of an acoustic shock wave, elevation in temperature, increased pressure, and release of visible light [5]. Multiple physical effects are associated with the growth and violent collapse of cavitation bubbles including direct physical phenomena such as luminescence, free radical formation, very high-pressure shock wave emissions, shear stress and high speed microjet production.

1.3. Safety concerns of ultrasound applications

Cavitation can cause substantial injury to cells due to the microexplosions associated with the high frequency expansion and collapse of the ultrasound induced microbubbles adjacent to the cells. Extreme temperature and pressure can be generated as a result of the serial ultrasound-induced microbubble explosions. When a microbubble collapses, high-speed liquid jets are

produced and driven into the surface of the surrounding cells at a high speed of about 400 km/h, which causes serious damage in the impact zones and create newly exposed surfaces susceptible to damage [6]. Moreover, the high temperatures and pressures generated within the bubbles can generate highly reactive radical species from any contained vapour that can then chemically attack the surface. In ultrasound therapy (i.e. HIFU), gas generation, caused by cavitation, suddenly changes the pattern of heat transfer induced by ultrasound, which consequently extends the margin of the lesion from the targeted area to surrounding healthy tissue [7].

Furthermore, based on the fact that the ultrasound imaging is widely used in obstetrics and has become an integral part of prenatal care today, the safety risk assessments associated with the ultrasound-induced cavitation is of a great importance. In particular, the increasing trend of the use of ultrasound combined with microbubbles, as contrast agents for diagnostic imaging and drug/gene delivery vehicles, raises additional concerns. The ultrasound safety risks attributed to cavitation become a serious concern when it applies to prenatal care. Samuel and Eugenie (2001) recorded sound via a miniature hydrophone placed in a woman's uterus during a standard sonography and described the sound "as loud as a subway train coming into the station" [8]. This might explain why ultrasound operators have to keep re-positioning the ultrasound transducer over the part of the fetus which they try to visualize; because the fetus moves away from the sound wave stream probably due to the induced heat, vibration or both [9]. In addition, there has been an increasing interest in the use of higher ultrasound frequencies and acoustic power for improved imaging resolution [10]. As the sound wave power increases, the potential cavitation hazard to the local tissue including cell damage and hemorrhage of blood vessels is elevated [11]. When the frequency increases, an inhomogeneous periodic field around the bubble can produce a small steady flow of fluid that is known as microstreaming [12], resulting in extremely

high shear stresses near the bubble surface. Cell membrane destruction and temporary alteration in permeability may be associated with this high shear stress [13] (e.g. at frequency range between 20 kHz and 2 MHz).

1.4. Safety assessment detection techniques

Over the past decades, different techniques have been investigated for detecting and mapping microbubbles. These techniques mainly include optical, acoustic, and scattering methods. Optical methods include high-speed photography, sonoluminescence, sonochemiluminescence, acoustic methods including active cavitation detection (ACD) and passive cavitation detection (PCD), and the Doppler method. Scattering methods include laser and synchrotron based X-ray methods. Each of these techniques has specific strengths and weaknesses for detection and mapping microbubbles. These signatures can be used to detect the microbubbles through physical and chemical techniques. There are a couple of techniques by which either exogenous microbubble or endogenous cavitation bubbles can be measured. Most published studies of visualization and detection of microbubbles come from *in vitro* experiments. There have been few attempts to detect microbubbles in animals [14, 15]. One challenge for in-vivo detection of the cavitation microbubbles is attributed to the high attenuation and inhomogeneous nature of tissues which affect the sound wave propagation and consequently the behavior of the ultrasound-induced microbubbles *in-situ*.

The presence of cavitation can be indirectly assessed through a variety of physical and chemical methods [16]. These methods rely on the detection and measurement of free radicals, sonoluminescence, and acoustic emission created from cavitation bubbles [17]. In order to improve the efficiency of cavitation and microbubble application in clinical use, it has been attempted to optically observe the microbubbles and cavitation process as well as the interaction

between microbubbles and cell membranes. Different imaging systems, such as electron microscopy, flow cytometry [18], atomic force microscopy [19, 20], home-made instruments based on white light illumination [21], and ultra-high speed imaging with the Brandaris camera have been investigated for studying the interaction of pre-made microbubbles with ultrasound and membranes of artificial cells *in-vitro*. In *in-vitro* studies, high-speed cameras have been used for observing cavitation bubble behaviors [22-25]. Fluorescence microscopy imaging combined with high speed photography has been also used for studying the dynamic interaction between microbubbles and cell membranes. Another method of detecting and characterizing cavitation microbubbles is based on laser scattering of individual bubbles, in which the dynamics of the formation of spherically-shaped bubbles can be individually and precisely measured [26]. Acoustic detection of bubbles, either as active cavitation detection (ACD) or passive cavitation detection (PCD), is another technique with potential application for in *in-vivo* studies.

Each imaging technique has its own advantages and disadvantages for studying microbubble behaviour. However, the potential of each technique for *in-vivo* studies and particularly for deep tissue monitoring of the microbubbles in the human body is considered as an important aspect of the detection method for future clinical study.

1.5. Synchrotron detection technique

Synchrotron radiation provides a highly coherent, collimated and brilliant light which offers potential for studying and directly visualizing microbubbles or ultrasound induced cavitation bubbles. Synchrotron X-rays are generated from electron charged particles accelerating in a storage ring. The electrons are ejected from an electron gun by a strong electric field and accelerated in a linear accelerator. The particles then enter a booster ring and are further accelerated to near the speed of light before being directed to the storage ring. In the storage ring,

the trajectory of the electron is changed by applying magnetic fields as the electrons travel through bending magnets. As a result, the electron velocity vector is changed, electrons are accelerated, and synchrotron light is radiated from the bending magnets. The benefits of synchrotron X-ray are high photon flux over a large range of energies, high brilliance, small angular beam divergence and high level of coherence. In addition, synchrotron X-ray enables us to use monochromatic X-rays for implementation of unique synchrotron-based imaging techniques such as K-edge subtraction and phase-based imaging techniques [27, 28]. Synchrotron radiation has led to the development of several biomedical imaging techniques [29-32] with outstanding imaging capabilities, among which X-ray Phase Contrast Imaging (PCI) and analyser based imaging (ABI) have shown potential for the detection of microbubbles.

Analyzer based imaging (ABI) is a phase sensitive imaging technique in which a monochromatic beam is prepared using a double crystal monochromator. The monochromatic X-ray wave field irradiates the object of study and is subsequently diffracted by an analyzer crystal. Depending on the refractive index of different features of the sample, X-ray diffraction takes place as X-rays travel through the sample. Based on properties of the analyzer crystal, the diffracted X-rays at or near the crystal's Bragg angle are filtered and ultimately passed on to the detector, accentuating microstructural features of different components of the object. Due to the significant difference of refractive index between microbubbles and their surrounding medium (fluid), X-ray diffraction at the bubble-medium interface presents high contrast, making the ABI method a potential technique for visualizing ultrasound-induced microbubbles.

1.6. Research objectives

Overall, this thesis work aims to develop a synchrotron based X-ray imaging technique for detection and better understanding of the spatial distribution of ultrasound induced cavitation

bubbles to help optimize clinical ultrasound applications. The hypothesis of this research is that specific synchrotron phase-based X-ray imaging techniques such as Analyzer based imaging and phase contrast imaging techniques could visualize and provide further information regarding the presence and characteristics of ultrasound induced cavitation bubbles. Accordingly, the main objectives of this research are as follows:

- To develop a refraction based synchrotron X-ray imaging technique for visualization of ultrasound-induced microbubbles in water
- To characterize the ultrasound induced cavitation bubbles by observing the distribution of cavitation bubbles in terms of bubble distribution, location and density of cloud cavitation in water at different levels of ultrasound operating conditions.
- To employ the ABI method for assessing the effects of ultrasound acoustic frequency and power on visualization and mapping the ultrasound-induced microbubble patterns in the water.
- To identify the threshold ultrasound parameters causing bubble formation and collapse at different levels of frequencies and intensities. These findings may improve standards of ultrasound safety for a range of diagnostic and therapeutic applications, toward improving the biosafety of ultrasound applications in clinics.

This dissertation has been organized into 8 chapters, including this introductory chapter. A series of comprehensive literature reviews are presented in chapters 2 to 5 as follow: Literature review on current trends and future applications and safety of therapeutic ultrasound in chapter 2 (submitted to the Journal of *Clinical Research*), review on principles, devices, and clinical applications of high intensity focused ultrasound in chapter 3 (submitted to the Journal of

RadioGraphics), review on mechanical and biological effects of ultrasound in chapter 4 (submitted to the Journal of *Ultrasound in Medicine and Biology*), and review on detection techniques of ultrasound cavitation and microbubble contrast agents are presented in chapter 5 (Submitted to the journal of *Measurement Science and Technology*). Chapters 6 presents a novel synchrotron X-ray Analyzer Based Imaging technique for visualization of ultrasound induced cavitation bubbles and identifying the threshold ultrasound parameters causing cavitation bubble formation (published in the journal of *Physics in medicine and Biology*). The Analyzer Based X-ray Imaging (ABI) technique was applied to detect ultrasound induced cavitation bubbles from a physical therapy unit and results were presented in chapter 7 (published in the journal of *Biomedical Engineering Online*). Finally, Chapter 8 concludes this dissertation by presenting the general conclusions drawn from this research.

1.7. Contributions of the primary investigator

The manuscripts included in this thesis are co-authored; however, it is the mutual understanding of all authors that Zahra Izadifar, as the first author, is the primary investigator of the research work. The contributions of other authors are greatly appreciated in this thesis.

1.8. References

1. Miller DL, Smith NB, Bailey MR, Czarnota GJ, Hynynen K, Makin IR: **Overview of therapeutic ultrasound applications and safety considerations.** *J Ultrasound Med* 2012, **31:**623-634.
2. Marinac-Dabic D, Krulewitch CJ, Moore Jr RM: **The safety of prenatal ultrasound exposure in human studies.** *Epidemiology* 2002, **13:**S19-S22.
3. Mo S, Coussios CC, Seymour L, Carlisle R: **Ultrasound-enhanced drug delivery for cancer.** *Expert Opin Drug Deliv* 2012, **9:**1525-1538.
4. Crum L, Bailey M, Kaczkowski P, Makin I, Mourad P, Beach K, Carter S, Schmeidl U, Chandler W, Martin R: **Therapeutic ultrasound: A promising future in clinical medicine.** *Acoustical Society of America University of Washington* 2005, **21**.
5. Zhou Y-F: **High intensity focused ultrasound in clinical tumor ablation.** *World journal of clinical oncology* 2011, **2:**8.
6. Nyborg W, Carson P, Carstensen E, Dunn F, Miller D, Miller M, Thompson H, Ziskin M: **Exposure criteria for medical diagnostic ultrasound: II. Criteria based on all known mechanisms.** *Bethesda, MD: National Council on Radiation Protection and Measurements* 2002.
7. Cleveland RO, Mc Ateer JA: *Extracorporeal shock wave lithotripsy: The physics of shock wave lithotripsy. In: Smith's Textbook on Endourology.* Ontario, Canada: B C Decker; 2012.
8. Suslick K: **The yearbook of science and the future.** *Encyclopedia Britannica, Chicago* 1994, **138**.
9. Luque-García JL, Luque de Castro MD: **Ultrasound: a powerful tool for leaching.** *TrAC Trends in Analytical Chemistry* 2003, **22:**41-47.
10. Lizzi F, Coleman D, Driller J, Silverman R, Lucas B, Rosado A: **A therapeutic ultrasound system incorporating real-time ultrasonic scanning.** In *IEEE 1986 Ultrasonics Symposium*. IEEE; 1986: 981-984.
11. Samuel E: **Fetuses can hear ultrasound examinations.** *New Scientist www newscientist com/article/dn1639-fetuses-can-hear-ultrasound-examinations- html Accessed* 2006, **11**.
12. Food U, Administration D: **FDA cautions against ultrasound 'keepsake'images.** *FDA Consumer Magazine* 2004, **38:**1-5.
13. Holland CK, Deng CX, Apfel RE, Alderman JL, Fernandez LA, Taylor KJ: **Direct evidence of cavitation in vivo from diagnostic ultrasound.** *Ultrasound Med Biol* 1996, **22:**917-925.
14. Nyborg WL: *Acoustic streaming*San Diego,CA: Academic Press; 1998.
15. Kopechek JA, Carson AR, McTiernan CF, Chen X, Hasjim B, Lavery L, Sen M, Grandis JR, Villanueva FS: **Ultrasound targeted microbubble destruction-mediated delivery of a transcription factor decoy inhibits STAT3 signaling and tumor growth.** *Theranostics* 2015, **5:**1378.
16. Holland CK, Deng CX, Apfel RE, Alderman JL, Fernandez LA, Taylor KJ: **Direct evidence of cavitation in vivo from diagnostic ultrasound.** *Ultrasound in medicine & biology* 1996, **22:**917-925.
17. Bailey MR, Pishchalnikov YA, Sapozhnikov OA, Cleveland RO, McAteer JA, Miller NA, Pishchalnikova IV, Connors BA, Crum LA, Evan AP: **Cavitation detection during shock-wave lithotripsy.** *Ultrasound Med Biol* 2005, **31:**1245-1256.

18. Leighton TG: *The Acoustic Bubble.* San Diego, CA: Academic Press; 1994.
19. Hanson MA: **Health effects of exposure to ultrasound and infrasound: report of the independent advisory group on non-ionising radiation.** *Health Protection Agency* 2010.
20. Karshafian R, Bevan PD, Burns PN, Karshafian R, Samac S, Banerjee M, Bevan PD: **Ultrasound-induced uptake of different size markers in mammalian cells.** In *Ultrasonics Symposium, 2005 IEEE*; *18-21 Sept. 2005*. 2005: 13-16.
21. Ross JP, Cai X, Chiu JF, Yang J, Wu J: **Optical and atomic force microscopic studies on sonoporation.** *J Acoust Soc Am* 2002, **111:**1161-1164.
22. Zhao YZ, Luo YK, Lu CT, Xu JF, Tang J, Zhang M, Zhang Y, Liang HD: **Phospholipids-based microbubbles sonoporation pore size and reseal of cell membrane cultured in vitro.** *J Drug Target* 2008, **16:**18-25.
23. Wolfrum B, Mettin R, Kurz T, Lauterborn W: **Observations of pressure-wave-excited contrast agent bubbles in the vicinity of cells.** *Applied Physics Letters* 2002, **81:**5060-5062.
24. Philipp A, Delius M, Scheffczyk C, Vogel A, Lauterborn W: **Interaction of lithotripter-generated shock waves with air bubbles.** *The Journal of the Acoustical Society of America* 1993, **93:**2496-2509.
25. Sass W, Matura E, Dreyer H, Folberth W, J. S: **Lithotripsy-mechanismsof the fragmentation process with focussed shock waves.** *Electromedica* 1993, **61:**2-12.
26. Zhong P, Cioanta I, Cocks FH, Preminger GM: **Inertial cavitation and associated acoustic emission produced during electrohydraulic shock wave lithotripsy.** *J Acoust Soc Am* 1997, **101:**2940-2950.
27. Pishchalnikov YA, Sapozhnikov OA, Bailey MR, Williams JC, Jr., Cleveland RO, Colonius T, Crum LA, Evan AP, McAteer JA: **Cavitation bubble cluster activity in the breakage of kidney stones by lithotripter shockwaves.** *J Endourol* 2003, **17:**435-446.
28. Matula TJ, Hilmo PR, Bailey MR, Crum LA: **In vitro sonoluminescence and sonochemistry studies with an electrohydraulic shock-wave lithotripter.** *Ultrasound Med Biol* 2002, **28:**1199-1207.
29. Dilmanian F: **Computed tomography with monochromatic x rays.** *American journal of physiologic imaging* 1991, **7:**175-193.
30. Bonse U, Hart M: **An X-ray interferometer with Bragg case beam splitting and beam recombination.** *Zeitschrift für Physik* 1966, **194:**1-17.
31. Chapman D, Thomlinson W, Johnston R, Washburn D, Pisano E, Gmür N, Zhong Z, Menk R, Arfelli F, Sayers D: **Diffraction enhanced x-ray imaging.** *Physics in medicine and biology* 1997, **42:**2015.
32. Momose A, Takeda T, Itai Y, Hirano K: **Phase–contrast X–ray computed tomography for observing biological soft tissues.** *Nature medicine* 1996, **2:**473-475.
33. Snigirev A, Snigireva I, Kohn V, Kuznetsov S, Schelokov I: **On the possibilities of x-ray phase contrast microimaging by coherent high-energy synchrotron radiation.** *Review of scientific instruments* 1995, **66:**5486-5492.
34. Pfeiffer F, Weitkamp T, Bunk O, David C: **Phase retrieval and differential phase-contrast imaging with low-brilliance X-ray sources.** *Nature physics* 2006, **2:**258-261.

Chapter 2 Applications and safety of therapeutic ultrasound: current trends and future potential

This chapter has been submitted as “Zahra Izadifar, Paul Babyn, Dean Chapman, 2016, Applications and safety of therapeutic ultrasound: current trends and future potentials, *Clinical Research* (Under Review)” According to the Copyright Agreement, "the authors retain the right to include the journal article, in full or in part, in a thesis or dissertation".

2.1 Abstract

The ability of ultrasound to penetrate deep into tissue and interact with human tissues via thermal and mechanical mechanisms has expanded its various therapeutic applications. In the 1950s, low power (1 MHz) ultrasound began being used for physical therapy of tendinitis or bursitis. In the 1980s, high pressure amplitude shockwaves were used for kidney stone destruction in lithotripsy. Since then, ultrasound therapy has expanded significantly and is rapidly replacing surgery in clinics. Several major benefits of ultrasound derive from its minimally invasive nature compared to conventional open surgeries that disturb the overlying tissues. The minimally invasive therapeutic procedures have resulted in shortened recovery times and hospital stays as well as lowered risk of complications and cost. Ultrasound therapy may require local anesthesia or sedation, which is highly preferred over general anesthesia, especially for elderly patients. Some ultrasonic therapy techniques, such as cataract removal, surgical tissue cutting and hemostasis, transdermal drug delivery, and bone fracture healing, have been approved for widespread use. Other minimally invasive therapy techniques, such as focused ultrasound beam therapy for coagulating tissue, are on the verge of clinical approval. Therapeutic ultrasound methods work based on thermal and/or non-thermal (e.g., mechanical) mechanisms, with well-defined benefits and risks that include complications to the patient. Ensuring the benefits and minimizing

unwanted side effects depends on a clear understanding of the thermal and non-thermal biological effects of ultrasound as well as more accurate guidance of the ultrasound beam. In this chapter the basic principles behind thermal and non-thermal (cavitation) biological effects of ultrasound, as well as general information and safety considerations for a wide range of therapeutic ultrasound methods either under study or in clinical use are reviewed.

2.2 Introduction

Ultrasound can be employed in many therapeutically beneficial applications. In therapeutic ultrasound procedures, energy is deposited in tissue to bring about different biological effects for therapeutic benefit [1, 2]. The very first large-scale use of ultrasound for therapeutic benefit was in the 1930s [3] [4]; during World War II, people realized that the high-intensity ultrasound waves used to navigate submarines were heating and killing fish and the first therapeutic ultrasound mechanism of tissue heating and healing was envisioned [5]. This led to research using a focused ultrasound beam as an alternative to ablative procedures. As early as the 1940s, researchers tried to focus the ultrasound beam, strengthen the mechanism of heating at the focal point, and ablate tissue [6-9]. In the ensuing decades, the application of ultrasound for destruction of tissue in the brain for Parkinson's disease treatment and of the vestibular nerve for Meniere's disease treatment was explored [10, 11]. The use of ultrasound was also established by the 1970s in physiotherapy because of its ability to speed up the healing process (by giving rise to blood flow in the treated area), decrease pain, and gently massage muscles, tendons, and ligaments; research also continued into further applications related to neurosurgery [12] and cancer treatment [13]. In the 1980s, the use of ultrasound in high-pressure amplitude shockwaves for mechanical destruction of calculi such as kidney stones and gallstones into fragments small enough to be passed from the body (lithotripsy) came into use and replaced surgery [3]. In the

last two decades, advances in the fields of imaging, physics, and engineering have expanded ultrasound use to various applications in medicine, including dentistry (for dental cleaning and disinfection) [14], cataract treatment (for ultrasound phacoemulsification cataract surgery) [15], acoustic targeted drug delivery (for delivering drug to different tissues) [16], lipectomy (for internal and external ultrasound-assisted liposuction) [17-19], and high-intensity focused ultrasound (HIFU) and magnetic resonance guided focused ultrasound (MRgFUS) treatment (for non-invasive ablation of soft tissue in the area of cancer therapy and surgery) [20-24]. The purpose of this review is to briefly outline the common and recent developed therapeutic applications of ultrasound, together with general information and safety considerations for a wide range of therapeutic ultrasound methods either under study or in clinical use. The basic principles behind thermal and non-thermal (cavitation) biological effects are discussed. This is followed by the description of a wide range of ultrasound treatment methods using heating, cavitation, or combined mechanisms of action. Prospective new therapeutic ultrasound methods are also presented.

2.3 Basic principles of ultrasound tissue interaction

Ultrasound can interact with biological tissues through heating as well as through non-thermal mechanisms, including acoustic cavitation, gas body activation, mechanical stress, or other unknown non-thermal processes [25]. As the ultrasound beam travels through tissue, the amplitude of the original signal is attenuated due to absorption, reflection, or scattering at interfaces. When ultrasound passes through soft tissue, about 80% of the attenuation (energy loss) of the sound wave occurs through absorption. The amount of attenuation depends on the type of tissue. Table 2-1 shows the attenuation coefficient of different tissues, measured in decibels per centimeter at a frequency of 1 MHz. A higher attenuation coefficient means more

energy loss; the highest attenuation coefficient is for bone, which means bone particularly limits beam transmission [26].

Table 2-1 Ultrasound attenuation coefficients of different body tissues at a frequency of 1 MHz [26]

Type of body tissue	Attenuation coefficient (dB/cm at 1 MHz)
Water	0.002
Blood	0.18
Fat	0.63
Liver	0.5-0.94
Kidney	1.0
Muscle	1.3-3.3
Bone	5.0

The attenuation coefficient is also directly affected by the applied frequency of the ultrasound wave and the distance the ultrasound wave travels in the body. Higher frequency waves are associated with higher attenuation and therefore limited penetration in tissue; in contrast, lower frequency waves have a lower tissue attenuation and therefore higher penetration depth [26]. For example, the attenuation of ultrasound waves by muscle, liver, and blood increases linearly with frequency, considering that muscle has a higher attenuation than liver, and liver has a higher attenuation than blood [26].

The frequency and intensity of ultrasound waves are determined based on the particular therapeutic application being considered and the penetration distance into the body required to reach the target area. For example, in physical therapy applications ultrasound is applied at a relatively low frequency so as only to generate enough heat for pain relief and to speed healing in injured joints or muscle tissue. At frequencies of 1, 3, and 5 MHz, the ultrasound penetrates up to 4, 2, and 0.5 cm into the body and generates tissue temperatures of up to 40, 42, and 44 °C, respectively [27, 28]. Different therapeutic applications of ultrasound and a comparison between

ultrasound frequency, therapeutic outcome, and related bioeffect mechanism are given in Table 2-2.

Table 2-2 Different therapeutic applications of ultrasound and a comparison between ultrasound frequency, therapeutic outcome, and related bioeffect mechanism (thermal or non-thermal) (table design based on [3]).

Ultrasound Therapy Application	Therapeutic Outcome	Bioeffect Mechanism	Frequency	Reference
Physical therapy	Therapy of sports injuries, chronic inflammation, arthritis, and trauma	heating	1 MHz	Newman [28]
Physical therapy	Bone fracture healing	unknown	1.5 MHz	Gebauer et al. [29]
Physical therapy	Treatment of the most superficial of tendon injuries	heating	3 MHz	Draper et al. [27]
Physical therapy	Skin & facial rejuvenation, fat removal, cellulite, scars & scar tissue, sunburn, bruises, superficial cuts & scrapes	heating	5 MHz	Newman [28]
Physical therapy	Bone growth stimulation	heating	1.5 MHz	Szaboo [30]
Hyperthermia	Cancer therapy	heating	1-3.4 MHz	Samulski et al. [31]
HIFU	Uterine fibroid ablation	thermal lesion	0.5-2 MHz	Tempany et al. [32]
HIFU	Glaucoma relief	thermal lesion	4.6 MHz	Burgess et al. [33]
HIFU	Laparoscopic tissue ablation	thermal lesion	4 MHz	Klingler et al.[34]
HIFU	Laparoscopic or open surgery	thermal lesion	3.8-6.4 MHz	Ninet et al. [35]
Focused ultrasound	Skin tissue tightening	thermal lesion	4.4-7.5 MHz	Alam et al. [36]
Extracorporeal lithotripsy	Kidney stone destruction	mechanical stress; cavitation	~150 kHz	Weizer et al.[37]
Intracorporeal lithotripsy	Kidney stone comminution	mechanical stress; cavitation	25 kHz	Lowe and Knudsen [38]
Extracorporeal shock wave therapy	Plantar fasciitis epicondylitis	unknown	~150 kHz	Haak et al. [39]
Phacoemulsification	Lens removal	vibration; cavitation	40 kHz	Packer et al. [40]
Ultrasound-assisted liposuction	Fat tissue removal	fat liquefaction; cavitation	20-30 kHz	Mann et al. [41]
Cutting tissue	Laparoscopic or open surgery	thermal lesion	55.5 kHz	Koch et al. [42]

and scaling vessel		and vibration		
Intravascular ultrasound	Thrombus dissolution	gas body activation; not clear	2.2 MHz	Parikh et al. [43]
Skin permeabilization	Transdermal drug delivery	mechanical effect	55 kHz	Smith [44]
Focused ultrasound	Microbubble-aided gene delivery	cavitation	20 kHz-2 MHz	Porter and Xie [45]

Ultrasound waves can distort and lead to a discontinuity or shock in the waveform as the pressure amplitude, the frequency, or the propagation length rises [3]. Decreasing frequency raises the probability of cavitation and gas body activation. Enhancing power or intensity tends to raise the probability and magnitude of all types of bioeffect mechanisms [3]. When ultrasound waves are transmitted into tissue, the acoustic pressures can become very large compared with the ambient pressure, with rarefactional pressure amplitudes of several megaPascals (MPa). This tensile stress is supported by the medium; for example, a diagnostic ultrasound scanner with a rarefactional pressure of 2 MPa has a negative tension that is 20 times atmospheric pressure (i.e., 0.1 MPa) [3]. Fluid and tissue can withstand acoustic pressures greater than one atmosphere because of their cohesive molecular forces; however, their strength in this regard is limited. For longer times associated with ultrasonic frequencies at the lower end of the spectrum (e.g. approximately 20 kHz) and at high acoustic pressures (e.g. greater than 20 MPa), the fluid may form small gas bubbles [46], a phenomenon termed cavitation (described in the next section).

Other biological effects of ultrasound can be considered the direct action of compressional, tensile, and shear stresses, and second-order phenomena include radiation pressure, forces on particles, and acoustic streaming [3]. Furthermore, secondary physical, biological, and physiological mechanisms such as vasoconstriction, ischemia, extravasation, reperfusion injury, and immune responses [47-49] can cause further effects. Sometimes the impacts of these

secondary effects are greater than the initial direct insult of ultrasound treatment [3]. The beneficial effects of therapeutic ultrasound include thermal and non-thermal effects. Thermal effects are due to the absorption of ultrasound energy, and non-thermal effects are due to cavitation, microstreaming, and acoustic streaming [1]. The ability to focus ultrasound waves enhances both thermal and non-thermal effects to a specific area of the body and has led to additional applications of focused ultrasound or high-intensity focused ultrasound for various therapeutic purposes. Thermal and non-thermal effects along with their related therapeutic applications are reviewed below.

2.4 Cavitation effect

Cavitation is defined as the creation or motion of very small gas bubbles that are produced in tissue due to the alternating expansion and compression of tissue as an ultrasound wave propagates through it. These bubbles are produced in two fashions, either inertial and non-inertial (stable) cavitation [50]. Once the cavitation bubbles are produced, they may undergo nonlinear oscillations during many cycles of the acoustic wave, called “non-inertial cavitation”, or they may grow and collapse more or less violently, called “inertial cavitation”[51]. When low-pressure acoustic ultrasound is applied, non-inertial cavitation bubbles oscillate in size but do not collapse. This oscillating motion causes the rapid movement of fluid near the cavitation bubble that is called “micro-streaming”. This micro-streaming can generate high shear forces that can lead to transient damage to cell membranes. This effect of non-inertial cavitation bubbles plays an important role in ultrasound-enhanced drug or gene delivery [52].

As opposed to non-inertial cavitation, inertial cavitation occurs due to violent oscillation, rapid bubble growth during the rarefaction cycle of the acoustic wave, and then violent collapse and destruction of the bubble. This collapse generates a very high pressure shock wave (20000-30000

bars) and high temperatures (2000-5000 K) in the immediate microenvironment [50]. In addition, bubbles that collapse close to a cell wall or solid surface produce a very high-speed (~111 m/s) liquid jet that drives into the surface and results in pitting of the surface or cell wall [53].

This cavitation activity can be initiated in tissue when suitable cavitation nuclei are present or can be induced directly by pulsating pre-existing gas bodies, such as in the lung or intestine, or those introduced via ultrasound contrast agents. This causes local tissue injury (including cell death and hemorrhage of blood vessels) in the immediate vicinity of the cavitation activity [3].

2.5 Cavitation-based applications of ultrasound

Therapeutic applications of ultrasound based on cavitation include extracorporeal shock wave lithotripsy (ESWL), intracorporeal lithotripsy, and surgical ultrasonic instrumentation. The non-thermal effects of ultrasound in the human body are the basis for ESWL [37, 54] for kidney stone destruction. The mechanism behind ESWL is that ultrasound waves focused over the kidney stone create shear waves that fracture the stone from within. The stone is shaved away from the outside through cavitation, resulting in cracks that are amplified by dynamic fatigue and further break the stone down [55]. To pulverize the stone to pieces less than 2 mm in size, which can pass naturally in urine, about 3000 ultrasound shock waves are triggered at a frequency of 2 Hz repetition rate at the stone location [3]. Shockwaves have also been used for gall stone destruction, but this technique is not yet in widespread use [3]. Some other orthopedic applications for conditions such as plantar fasciitis and epicondylitis have a similar basis as lithotripsy and have been approved and marketed [39]. The biological side effects of lithotripsy affect virtually all patients [56]. The technique breaks blood vessel walls and leads to bleeding into the connective tissue and interstitium. This can cause bruising of the parenchyma or formation of massive subcapsular hematomas [3]. Permanent loss of kidney mass then ensues as

result of inflammation and scar formation [57]. In addition, the lithotripsy-induced injury causes systemic blood pressure increases, kidney function decreases, establishment of hypertension, and an increased rate of stone return, and also exacerbates the problem of stone disease [3, 58]. Krambeck et al. [59] demonstrate a link between lithotripsy and diabetes mellitus. Furthermore, severe skin injury (second-degree skin burns) after ESWL have also been reported [60, 61]. Such challenging clinical side effects can result from the generation of cavitation bubbles in the coupling gel (due to poor gel quality) or a lack of probe surface uniformity.

In intracorporeal lithotripsy, a rigid ultrasonic probe may be percutaneously manipulated and applied via the ureter for treatment of very large stones. In this technique, the stone is imaged by external ultrasound or fluoroscopy, or by ureteroscopy, endoscopy, or laparoscopy [3]. Hemorrhage, ureteral perforation, urinary tract trauma, and infection are considered risks of intracorporeal lithotripsy [3].

Although the benefits of lithotripsy to patients are many, the considerable risks require more investigations toward safer devices as well as optimization of the therapeutic ultrasound safety standards.

In biological research, frequencies as low as 20 to 90 kHz are applied to break up cells and tissues using a sonicator device [3]. Ultrasound-induced cavitation at low frequencies causes the break-up of cell walls and results in cell death. This is the basis behind ultrasound-assisted liposuction, a procedure in which excessive fat tissue is removed [41]; however, this procedure can result in bleeding, scarring, and infection [3].

Ultrasonic cavitation close to the probe tip can be used for very precise cutting in surgery. The ability of ultrasound to break up cells in the kHz frequency regime (e.g., a sonochemistry

device), has found wide applications in biological research for destroying cells for extraction and other reasons. Ultrasound devices working in kHz frequency regimes are routinely used in clinical surgeries. Some advanced surgical procedures operating at frequencies of 20 to 90 kHz for tissue cutting, hemostasis, and tissue removal are routinely applied in clinics [3]. In ophthalmology, the lens of the eye is removed using an ultrasound probe working at kHz frequency during eye surgery for phacoemulsification for cataracts [40]. Another application of kHz-frequency ultrasound probes are as “harmonic scalpels” to rapidly stop bleeding by coagulating blood due to localized frictional heating [42].

2.6 Heating effect of ultrasound

Absorption of ultrasonic energy can lead to heating of tissues [3]. Ultrasonic-induced heating response *in vivo* is modified by the presence of bone, gas, and fluid. Sites in the body with higher absorption experience greater heating than surrounding tissues. For example, a calcified bone surface strongly absorbs ultrasound energy. Fetal bones absorb more energy compared to the surrounding fetal soft tissue, and the difference becomes greater as bone mineralization proceeds [46].

Ultrasound is usually generated from a piezoceramic crystal in very short cycle pulses (i.e., 1- to 5-cycle). Diagnostic ultrasound typically operates in the range of 2 to 12 MHz. Current diagnostic ultrasound equipment is unlikely to cause a temperature rise in tissue outside the normal physiological range [3]. Temperature elevation and potential bioeffects are kept negligible [62] by applying finite temporal average intensities and short exposure time principles [3]. However, hazardous temperature increases in tissue can occur during the use of physiotherapy ultrasound equipment. The heating caused by ultrasound is highly localized and

limited to the region of the ultrasonic beam. It is possible to expose and so heat the whole of the uterus at the very early stages of a human pregnancy [46].

2.7 Heating-based applications of ultrasound

Heating is generated during therapeutic application of ultrasound either in the form of an unfocused beam with longer durations or focused ultrasound with a higher intensity than diagnostic ultrasound [3]. For example, in physical therapy the unfocused beam is utilized to treat tissues such as bone or tendon and enhance healing without injury; in contrast, a focused beam is utilized to concentrate the heat until tissue coagulates for purposes such as tissue ablation. Depending on the heat generated during ultrasound exposure, the effects can result from moderate heat, coagulative necrosis, tissue vaporization, or all three [3]. Therapeutic application of ultrasound based on heating can be subdivided into three categories: physical therapy, hyperthermia, and high intensity focused ultrasound.

2.7.1 Ultrasound for physical therapy

Physical therapists often use “therapeutic ultrasound”, which features an unfocused beam applied with coupling gel to warm tendons, muscles, and other tissues to treat conditions such as bursitis of the shoulder or tendonitis. This method of treatment uses sound waves to treat pain, inflammation, and muscle spasm. The purpose is to stimulate the tissue beneath the skin’s surface [63], improve blood flow, and accelerate healing [3]. Another application of ultrasound is sonophoresis or phonophoresis, in which ultrasound is used to assist transport of a compound into the skin [64]. As reported by Miller et al. [3], these techniques have a modest level of efficacy and patient benefit and a low level of risk. Ultrasound waves are applied to tissue by a round-headed transducer that can come in different shapes (Figure 2-1) to stimulate joints,

ligaments, tendons, muscles, and other tissues. The gel is used on the skin to decrease friction and act as a conductor of the ultrasonic waves [63].

Figure 2-1 The different shapes of physical therapy ultrasound transducers widely used in clinics.

The ultrasonic waves pass through the skin and, through vibration and cavitation, cause deep local heating of tissues, soothe inflammation, and relieve pain. This heating increases blood flow, causes tissues to relax, and helps decrease local swelling and chronic inflammation. The increase in blood flow also delivers more oxygen and a nutrient to the tissue, eliminates cell waste, and aids healing. Ultrasound can decrease the sensitivity and pain related to muscular trigger points. Physical therapy ultrasound can also be used to increase the delivery of applied drugs by enhancing the absorption of analgesics and anti-inflammatory agents to tissue through ultrasound waves.

Physical therapy ultrasound is conducted at low frequency ranges that depend on the deepness of the target area for treatment in the body. The ultrasonic frequency is the inverse of the ultrasound wavelength and its penetration in the body, meaning a lower frequency results in a larger wavelength and deeper penetration, and vice versa. The amount of energy released to the target area depends on the frequency, power, and absorption coefficient of the substance through which the sound waves travel. Table 2-3 shows the typical frequencies used in physical therapy ultrasound units and related wavelengths, temperatures generated, and target organs.

Table 2-3 Typical frequencies used in physical therapy ultrasound units and their associated wavelengths, temperatures generated, and target organs.

Frequency	Ultrasound wavelength	Penetration depth into the skin	Temperature generated	Therapeutic outcome	Reference
1 MHz	1.6 mm	4 cm	40 °C (104 °F)	Treatment of acute or chronic injuries and pain, bone injuries and arthritis treatment, nerve, muscle, tendon injuries and pain, arthritis, bursitis, wound care, exercise recovery; beauty-related applications	Newman [28]; Draper et al. [27]; Enwemeka [65]; Ebenbichler et al. [66, 67]; Langford [68]
3 MHz	0.53 mm	2 cm	42 °C (106 °F)	Treatment of superficial tendon injuries; beauty-related applications for facial treatments such as cheeks, forehead, chin	Draper et al. [27]; Newman [28]; Langford [68]
5 MHz	0.3 mm	0.5 cm	44 °C (108 °F)	Beauty-related applications for facial treatment such as eye area	Draper et al. [27]; Newman [28]; Langford [68]

2.7.2 Hyperthermia

Another heat-based application of ultrasound is hyperthermia (also called thermal therapy or thermotherapy), in which ultrasound is used to heat a relatively large amount of tissue to about 42 °C for reducing tumor growth in cancer therapy [69]. In hyperthermia, multi-element applicators are used at a frequency range of 1 to 3.4 MHz [70, 71]. Hyperthermia is almost always applied in conjunction with other cancer therapies, such as chemotherapy or radiation therapy [72, 73]. Many clinical trials have focused on such combined applications and many have shown a considerable reduction in tumor size [72, 73]. However, increased survival in

patients was not always observed [73, 74]. Research has shown that high temperatures damage and kill cancer cells. High temperatures damage proteins and structures within cells [75], cause less blood flow to the tumor by damaging blood vessels, and ultimately result in the death of cancer cells. However, the moderate heat produced in hyperthermia has not advanced to other clinical applications and has been replaced by high-intensity focused ultrasound [3].

2.7.3 High-intensity focused ultrasound

HIFU is one of the more active and developed research areas among all non-ionizing-energy methods, which include radiography, lasers, and microwaves [3]. The first application of HIFU was for thermal ablation of inoperable tissue related to Parkinson's disease [10, 76]. This non-invasive thermal ablation technique has been used for treatment of tumors in several organs and is on the verge of becoming an alternative to the standard treatment options of surgery, radiotherapy, gene therapy, and chemotherapy in future oncology practice. HIFU has been used for clinical treatment of different types of solid malignant tumors, such as those in the pancreas, liver, kidney, bone, pancreas, prostate, and breast, as well as uterine fibroids and soft-tissue sarcomas. The HIFU technique has FDA approval for clinical use in the USA for the treatment of uterine fibroids [32], cardiac ablation [35], visceral soft tissue ablation [34], and aesthetic treatment to lift the eyebrow [36, 77]. Other HIFU-based therapies are under study for clinical applications such as modulation of nerve conductance [78], benign prostate hyperplasia, and prostate cancer, but do not yet have FDA approval. HIFU has also been utilized in methods for curing glaucoma [33]. Other HIFU-based therapeutic techniques for the treatment of benign prostatic hyperplasia (BPH), prostate cancer [79, 80], hepatic cancer, and pancreatic cancer are still under investigation.

The HIFU technique focuses the ultrasound beam in a small area and generates a tissue lesion typically a few mm in diameter and in length. The absorbed energy raises the tissue to a lethal temperature, with very sharp thermal gradients so that the boundaries of the volume under ablation are clearly confined without damaging the overlying tissues [81]. In a HIFU system, a signal generator connected to a focusing transducer generates very high local intensities (greater than 1 kW/cm^2 at the focal point) at frequencies ranging between 0.5 and 7 MHz [3]. In this method of treatment, the ultrasound beam is focused several millimetres to centimeters away from the transducer plane. In order to determine the location of the treatment zone and also monitor tissue changes in the target area, two image guidance and treatment monitoring methods are applied: magnetic resonance imaging (MRI) and ultrasound imaging. The related treatment techniques are called magnetic resonance guided focused ultrasound (MRgFUS) and ultrasound guided focused ultrasound (USgFUS), respectively. USgFUS systems incorporate both treatment and imaging modalities in one system. The ultrasound-based monitoring in HIFU treatment is based on a combination of sound velocity, attenuation, stiffness, and vapor content variation in the target area [82]. HIFU guided by ultrasound has limited target definition and monitoring capability of the ablation process. MRgFUS provides more accurate targeting and real-time temperature monitoring. MRgFUS surgery is a non-invasive thermal ablation technique in which MRI is used for target definition, treatment planning, and closed-loop control of energy deposition. In fact, MRgFUS as a therapy system allows targeting, localizing, and monitoring in real time without damaging normal structures. This precision has made MRgFUS an attractive method for surgical resection or radiation therapy of benign and incurable tumors. MRgFUS has been approved for treatment of uterine fibroids, and is undergoing clinical trials for the treatment of breast [83, 84], liver [85, 86], prostate [87-89], and brain cancer [90, 91] as well as to relieve

and lessen pain in bone metastasis [92-94]. Because MRI is capable of providing the temperature variation within the treatment zone [95], generating detailed images of soft tissues in the body, discovering a wide spectrum of space-occupying soft-tissue lesions, and creating real-time images and thermographic guidance during the procedure, MRgFUS has become a novel and non-invasive method of treatment. MRgFUS plays an important role in the development of neurotherapeutics and brain-based disorders and has been proposed as an alternative to open neurosurgical procedures for a wide variety of indications. Specialized MRgFUS systems have ultrasound therapy sub-systems integrated into MR-imagers. Such systems are employed in the treatment of uterine fibroids [32], breast cancer [96], and prostate cancer [97].

All of the above HIFU techniques are applied by external devices; however, natural orifices are also employed, such as in transrectal treatment of prostate cancer [98] and endoscopy via an intraductal probe for bile duct tumors [99].

Non-invasive aesthetic applications of HIFU will provide a safer alternative to liposuction for cosmetic applications [100]. The exposure of superficial tissue to HIFU leads to a contraction of the dermis or to demolition of fatty tissue [77, 101]. In this technique, both thermal as well as non-thermal mechanisms of ultrasound are involved.

HIFU has also been utilized to treat atrial fibrillation by tissue ablation to achieve pulmonary vein isolation [3].

During HIFU applications, undesired tissue injury, unwanted burns, and pain can occur as significant ultrasound energy is delivered to a localized area of tissue [3]. In addition, HIFU can cause vasospasm and hemorrhaging when concomitant cavitation is also generated in the tissue [102], impotence and incontinence during prostate cancer treatment [103], or creation of an

atrial-esophageal fistula during atrial fibrillation treatment [104]. Furthermore, fistula formation and rib necrosis with delayed rib fracture [105] are also considered to be serious complications that can occur following hepatic and pancreatic cancer treatment [3].

2.8 Therapeutic applications of ultrasound based on combined mechanisms

Other therapeutic techniques involve multiple mechanisms of ultrasound. In intravascular catheters, a MHz-frequency transducer is placed near the tip for increasing dissolution of thrombi [43]. When the catheter is placed into a deep vein thrombus, the ultrasound is targeted radially into the thrombus or an infusion of a thrombolytic drug, such as tissue plasminogen activator, is delivered into the thrombus [3]. Ultrasound-assisted drug delivery significantly decreases treatment time by increasing the permeability of cell walls and the infusion of drugs into cells.

Another application of ultrasound is skin permeabilization, which may replace multiple use of needles for drug delivery through the skin for medicines such as heparin and insulin [44]. Drug diffusion through the stratum corneum is difficult for molecules with a molecular weight greater than 500 Da [106]. Using low-frequency ultrasound (<100 kHz), the permeability of the stratum corneum (which is considered a protein diffusion barrier) increases [107] and the drug can pass and reach the inner layers and finally the capillary vessels where it is absorbed [108].

The use of low-intensity pulsed ultrasound (about 1.5 MHz) for accelerating the healing of bone fractures for cases such as non-union and non-healing fractures is another therapeutic action of ultrasound [3]. The biophysical mechanism behind this therapeutic action is not yet clear.

2.9 New research areas for therapeutic applications of ultrasound

Several streams of research are investigating other therapeutic applications of ultrasound. These new methods mostly rely on low frequency and power ultrasound aided by microbubbles or very high power ultrasound for the production of vigorous cavitation [3].

The application of low-frequency ultrasound for direct sonothrombolysis for treatment of thrombotic disease such as stroke is a new strategy [109]. However, this method showed increased brain hemorrhage in a clinical trial [110]. Microbubbles play an important role in increasing thrombolysis and improving stroke therapy [111].

Another potential use of ultrasound is to produce cortical and hippocampal stimulation in mice [112]. Non-thermal mechanisms have been hypothesized to be responsible for the neuronal effects in this method, as the temperature gradients were very small (<0.01 °C) [3].

Ultrasound-aided drug delivery is another area of study. This technique is based on microbubbles and is under study for direct and targeted therapies that release drugs at a specific location within the body (such as a cancerous area) without affecting the rest of the body. It can also be used to force drug flow from a vessel out into the surrounding tissue and to increase intracellular delivery [3]. The advantage of ultrasound microbubble techniques over other techniques such as nanoparticle or liposome delivery systems is the capacity for external control [3]. DNA transfer in gene therapy applications has also been under extensive study [113].

Histotripsy, equivalent to lithotripsy but at a higher frequency and with very high amplitude pulses, uses only the cavitation mechanism for tissue ablation [114] to homogenize targeted tissue, such as tumors, with little heating [115].

2.10 Summery

Both thermal and non-thermal (cavitation) effects play very important roles in all therapeutic applications of ultrasound. These effects can be hazardous biologically, and are therefore avoided in diagnostic applications of ultrasound but used in therapeutic applications of ultrasound. The application of ultrasound at high levels of exposure has well-recognized adverse biological effects, which are harnessed for therapeutic purposes in most therapeutic devices. The use of therapy ultrasound devices comes with the risk of affecting healthy organs and causing substantial bioeffects. The benefits and potential risks associated with each therapeutic device should be considered and explained to patients. For example, non-invasive lithotripsy has tremendous benefits compared to conventional surgical treatment even though it has an increased risk of hemorrhage and longer-term kidney injury.

Although measures and guidelines are in place to avoid unwanted bioeffects and deliberate caution on the part of the operator of the device can help decrease the risk of injury, safe and accurate use of ultrasound devices is essential to minimize the risks.

The cavitation mechanism that is exploited to ablate tissue, disrupt cells, destroy kidney and bladder stones, and treat thrombolysis, among many other applications, is secondary to the ultrasound exposure. Microbubble-based therapeutic strategies are still under investigation for direct and targeted therapeutic purposes. The problems of dosimetry and control of cavitation and microbubbles are challenging. Researchers studying cavitation are endeavoring to understand medium and cavitation nuclei, the ultrasound field, and when cavitation occurs [3]. Understanding the connection between the cavitation threshold and the medium and cavitation nuclei is desired and understanding the ultrasound field requires accurate measurement of the ultrasound beam area. Knowing when cavitation occurs requires the direct observation or

indirect monitoring of cavitation events. Different detection techniques can quantify an ultrasound field [116, 117] and measure cavitation through the noise of bubble collapse [118]. However, considering the rapid development of therapeutic ultrasound techniques that mostly work based on cavitation and microbubbles, the emergence of more accurate and new cavitation detection methods is essential to monitor and control cavitation for optimum patient safety. Repeating treatments can serve to accumulate unwanted bioeffects and damage already compromised organs (e.g., the kidney in lithotripsy) and lead to permanent loss of organ function. Therefore, defining the cumulative dose and anticipating the level of bioeffects after each treatment is also required.

Therapeutic applications of ultrasound directly depend on the interaction of the sound field with the tissue to induce the desired beneficial bioeffect. The exposure parameters used for ultrasound therapies are often noticeably different. This requires sufficient knowledge of acoustic mechanisms with respect to the interaction of ultrasound with tissue to improve the safety of ultrasound use and to facilitate the design of new therapeutic applications of biomedical ultrasound. Safety improvements in therapeutic ultrasound devices need to be pursued and more research should be dedicated to this issue. Exposimetry, dosimetry, and accurate and precise evaluation of acoustic fields in water and *in situ* should be done carefully and followed by animal studies to identify possible harmful bioeffects in humans. New accurate and more effective means of detection and monitoring of acoustic cavitation should be in place to continually regulate the acoustic output levels of therapeutic and diagnostic devices for their safe operation.

2.11 References

1. Mo S, Coussios CC, Seymour L, Carlisle R: **Ultrasound-enhanced drug delivery for cancer.** *Expert Opin Drug Deliv* 2012, **9:**1525-1538.
2. Crum L, Bailey M, Kaczkowski P, Makin I, Mourad P, Beach K, Carter S, Schmeidl U, Chandler W, Martin R: **Therapeutic ultrasound: A promising future in clinical medicine.** *Acoustical Society of America University of Washington* 2005, **21**.
3. Miller DL, Smith NB, Bailey MR, Czarnota GJ, Hynynen K, Makin IR: **Overview of therapeutic ultrasound applications and safety considerations.** *J Ultrasound Med* 2012, **31:**623-634.
4. Lehmann JF: **The biophysical basis of biologic ultrasonic reactions with special reference to ultrasonic therapy.** *Archives of physical medicine and rehabilitation* 1953, **34:**139.
5. Woo J: **A short history of the development of ultrasound in obstetrics and gynecology.** *See http://www ob-ultrasound net/history1 html (last checked 14 May 2011)* 2002.
6. Lynn JG, Zwemer RL, Chick AJ: **THE BIOLOGICAL APPLICATION OF FOCUSED ULTRASONIC WAVES.** *Science (New York, NY)* 1942, **96:**119-120.
7. Fry F, Ades H, Fry W: **Production of reversible changes in the central nervous system by ultrasound.** *Science* 1958, **127:**83-84.
8. Fry WJ: **Use of intense ultrasound in neurological research.** *American Journal of Physical Medicine & Rehabilitation* 1958, **37:**143-147.
9. Fry W, Fry F: **Fundamental neurological research and human neurosurgery using intense ultrasound.** *Medical Electronics, IRE Transactions on* 1960**:**166-181.
10. Fry WJ, Mosberg Jr W, Barnard J, Fry F: **Production of focal destructive lesions in the central nervous system with ultrasound.** *Journal of neurosurgery* 1954, **11:**471-478.
11. Newell J: **Ultrasonics in medicine.** *Physics in medicine and biology* 1963, **8:**241.
12. Wells PN: **Ultrasonics in medicine and biology.** *Phys Med Biol* 1977, **22:**629-669.
13. Kremkau FW: **Cancer therapy with ultrasound: a historical review.** *Journal of clinical ultrasound* 1979, **7:**287-300.
14. Chen Y-L, Chang H-H, Chiang Y-C, Lin C-P: **Application and development of ultrasonics in dentistry.** *Journal of the Formosan Medical Association* 2013, **112:**659-665.
15. Day AC, Gore DM, Bunce C, Evans JR: **Laser-assisted cataract surgery versus standard ultrasound phacoemulsification cataract surgery.** *The Cochrane Library* 2016.
16. Schoellhammer CM, Traverso G: **Low-frequency ultrasound for drug delivery in the gastrointestinal tract.** *Expert opinion on drug delivery* 2016**:**1-4.
17. Serdev NP: **Ultrasound Assisted Liposculpture—UAL: A Simplified Safe Body Sculpturing and Aesthetic Beautification Technique.** *Advanced Techniques in Liposuction and Fat Transfer, N Serdev, ed, InTech, Rijeka, Croatia* 2011**:**135-150.
18. Shah YR, Sen DJ, Patel RN, Patel JS, Patel AD, Prajapati PM: **Liposuction: a remedy from obesity.** *International Journal of Drug Development and Research* 2011.
19. Khan MH: **Update on liposuction: clinical pearls.** *Cutis* 2012, **90:**259-265.

20. Cline HE, Hynynen K, Watkins RD, Adams WJ, Schenck JF, Ettinger RH, Freund WR, Vetro JP, Jolesz FA: **Focused US system for MR imaging-guided tumor ablation.** *Radiology* 1995, **194:**731-737.
21. Cline H, Schenck J, Watkins R, Hynynen K, Jolesz F: **Magnetic resonance-guided thermal surgery.** *Magnetic resonance in medicine* 1993, **30:**98-106.
22. Cline HE, Schenck JF, Hynynen K, Watkins RD, Souza SP, Jolesz FA: **MR-guided focused ultrasound surgery.** *Journal of computer assisted tomography* 1992, **16:**956-965.
23. Hynynen K, Damianou C, Darkazanli A, Unger E, Schenck J: **The feasibility of using MRI to monitor and guide noninvasive ultrasound surgery.** *Ultrasound in medicine & biology* 1993, **19:**91-92.
24. Hynynen K, Darkazanli A, Unger E, Schenck J: **MRI-guided noninvasive ultrasound surgery.** *Medical physics* 1993, **20:**107-115.
25. Nyborg W, Carson P, Carstensen E, Dunn F, Miller D, Miller M, Thompson H, Ziskin M: **Exposure criteria for medical diagnostic ultrasound: II. Criteria based on all known mechanisms.** *Bethesda, MD: National Council on Radiation Protection and Measurements* 2002.
26. **Ultrasound Tissue Interaction** [http://usra.ca/tissue.php]
27. Draper DO, Castel JC, Castel D: **Rate of temperature increase in human muscle during 1 MHz and 3 MHz continuous ultrasound.** *Journal of Orthopaedic & Sports Physical Therapy* 1995, **22:**142-150.
28. Newman J: *Physics of the life sciences.* Springer Science & Business Media; 2010.
29. Gebauer D, Mayr E, Orthner E, Ryaby JP: **Low-intensity pulsed ultrasound: effects on nonunions.** *Ultrasound Med Biol* 2005, **31:**1391-1402.
30. Szabo TL: *Diagnostic ultrasound imaging: inside out.* Academic Press; 2004.
31. Samulski TV, Grant WJ, Oleson JR, Leopold KA, Dewhirst MW, Vallario P, Blivin J: **Clinical experience with a multi-element ultrasonic hyperthermia system: analysis of treatment temperatures.** *Int J Hyperthermia* 1990, **6:**909-922.
32. Tempany CM, Stewart EA, McDannold N, Quade BJ, Jolesz FA, Hynynen K: **MR imaging-guided focused ultrasound surgery of uterine leiomyomas: a feasibility study.** *Radiology* 2003, **226:**897-905.
33. Burgess SE, Silverman RH, Coleman DJ, Yablonski ME, Lizzi FL, Driller J, Rosado A, Dennis PH, Jr.: **Treatment of glaucoma with high-intensity focused ultrasound.** *Ophthalmology* 1986, **93:**831-838.
34. Klingler HC, Susani M, Seip R, Mauermann J, Sanghvi N, Marberger MJ: **A novel approach to energy ablative therapy of small renal tumours: laparoscopic high-intensity focused ultrasound.** *European urology* 2008, **53:**810-818.
35. Ninet J, Roques X, Seitelberger R, Deville C, Pomar JL, Robin J, Jegaden O, Wellens F, Wolner E, Vedrinne C: **Surgical ablation of atrial fibrillation with off-pump, epicardial, high-intensity focused ultrasound: results of a multicenter trial.** *The Journal of Thoracic and Cardiovascular Surgery* 2005, **130:**803. e801-803. e808.
36. Alam M, White LE, Martin N, Witherspoon J, Yoo S, West DP: **Ultrasound tightening of facial and neck skin: a rater-blinded prospective cohort study.** *Journal of the American Academy of Dermatology* 2010, **62:**262-269.
37. Weizer AZ, Zhong P, Preminger GM: **New concepts in shock wave lithotripsy.** *Urol Clin North Am* 2007, **34:**375-382.

38. Lowe G, Knudsen BE: **Ultrasonic, pneumatic and combination intracorporeal lithotripsy for percutaneous nephrolithotomy.** *J Endourol* 2009, **23:**1663-1668.
39. Haake M, Buch M, Schoellner C, Goebel F, Vogel M, Mueller I, Hausdorf J, Zamzow K, Schade-Brittinger C, Mueller HH: **Extracorporeal shock wave therapy for plantar fasciitis: randomised controlled multicentre trial.** *BMJ* 2003, **327:**75.
40. Packer M, Fishkind WJ, Fine IH, Seibel BS, Hoffman RS: **The physics of phaco: a review.** *J Cataract Refract Surg* 2005, **31:**424-431.
41. Mann MW, Palm MD, Sengelmann RD: **New advances in liposuction technology.** *Semin Cutan Med Surg* 2008, **27:**72-82.
42. Koch C, Borys M, Fedtke T, Richter U, Pöhl B: **Determination of the acoustic output of a harmonic scalpel.** *Ultrasonics, Ferroelectrics, and Frequency Control, IEEE Transactions on* 2002, **49:**1522-1529.
43. Parikh S, Motarjeme A, McNamara T, Raabe R, Hagspiel K, Benenati JF, Sterling K, Comerota A: **Ultrasound-accelerated thrombolysis for the treatment of deep vein thrombosis: initial clinical experience.** *Journal of Vascular and Interventional Radiology* 2008, **19:**521-528.
44. Smith NB: **Applications of ultrasonic skin permeation in transdermal drug delivery.** 2008.
45. Porter TR, Xie F: **Therapeutic ultrasound for gene delivery.** *Echocardiography-a Journal of Cardiovascular Ultrasound and Allied Techniques* 2001, **18:**349-353.
46. radiation Tiagon-i: **Health effects of exposure to ultrasound and infrasound.** In *documents of the health protection agency, radiation, chemical and environmental hazards*; 2010.
47. Alves EM, Angrisani AT, Santiago MB: **The use of extracorporeal shock waves in the treatment of osteonecrosis of the femoral head: a systematic review.** *Clinical rheumatology* 2009, **28:**1247-1251.
48. Hundt W, Yuh EL, Bednarski MD, Guccione S: **Gene expression profiles, histologic analysis, and imaging of squamous cell carcinoma model treated with focused ultrasound beams.** *American journal of roentgenology* 2007, **189:**726-736.
49. Silberstein J, Lakin CM, Parsons JK: **Shock wave lithotripsy and renal hemorrhage.** *Reviews in urology* 2008, **10:**236.
50. Mason PFsN: **SOUND INVESTMENTS.** 1998.
51. Frohly J, Labouret S, Bruneel C, Looten-Baquet I, Torguet R: **Ultrasonic cavitation monitoring by acoustic noise power measurement.** *The Journal of the Acoustical Society of America* 2000, **108:**2012-2020.
52. Pitt WG, Husseini GA, Staples BJ: **Ultrasonic drug delivery--a general review.** *Expert Opin Drug Deliv* 2004, **1:**37-56.
53. Luque-Garcıa J, De Castro ML: **Ultrasound: a powerful tool for leaching.** *TrAC Trends in Analytical Chemistry* 2003, **22:**41-47.
54. McAteer JA, Bailey MR, Williams Jr JC, Cleveland RO, Evan AP: **Strategies for improved shock wave lithotripsy.** *Minerva Urol Nefrol* 2005, **57:**271-287.
55. Sapozhnikov OA, Maxwell AD, MacConaghy B, Bailey MR: **A mechanistic analysis of stone fracture in lithotripsy.** *J Acoust Soc Am* 2007, **121:**1190-1202.
56. Evan A, McAteer J: **Q-effects of shock wave lithotripsy.** *Kidney stones: Medical and surgical management* 1996**:**549-570.

57. Evan AP, Willis LR, Lingeman JE, McAteer JA: **Renal trauma and the risk of long-term complications in shock wave lithotripsy.** *Nephron* 1998, **78:**1-8.
58. Krambeck AE, Handa SE, Evan AP, Lingeman JE: **Brushite stone disease as a consequence of lithotripsy?** *Urol Res* 2010, **38:**293-299.
59. Krambeck AE, Gettman MT, Rohlinger AL, Lohse CM, Patterson DE, Segura JW: **Diabetes mellitus and hypertension associated with shock wave lithotripsy of renal and proximal ureteral stones at 19 years of followup.** *J Urol* 2006, **175:**1742-1747.
60. Rao SR, Ballesteros N, Short KL, Gathani KK, Ankem MK: **Extra corporeal shockwave lithotripsy resulting in skin burns–a report of two cases.** *International braz j urol* 2014, **40:**853-857.
61. Rangarajan S, Mirheydar H, Sur RL: **CASE REPORTS: Second-degree burn after shock wave lithotripsy: an unusual complication.** In *BJUI international*; 2012.
62. Fowlkes JB: **American Institute of Ultrasound in Medicine consensus report on potential bioeffects of diagnostic ultrasound: executive summary.** *J Ultrasound Med* 2008, **27:**503-515.
63. **How Ultrasound Works, Ultrasound Pain Relief** [http://www.ezultrasound.com/faqs.aspx]
64. Machet L, Boucaud A: **Phonophoresis: efficiency, mechanisms and skin tolerance.** *International journal of pharmaceutics* 2002, **243:**1-15.
65. Enwemeka CS: **The Effects of Therapeutic Ultrasound on Tendon Healing: A Biomechanical Study.** *American journal of physical medicine & rehabilitation* 1989, **68:**283-287.
66. Ebenbichler GR, Erdogmus CB, Resch KL, Funovics MA, Kainberger F, Barisani G, Aringer M, Nicolakis P, Wiesinger GF, Baghestanian M: **Ultrasound therapy for calcific tendinitis of the shoulder.** *New England Journal of Medicine* 1999, **340:**1533-1538.
67. Ebenbichler GR, Resch KL, Nicolakis P, Wiesinger GF, Uhl F, Ghanem A-H, Fialka V: **Ultrasound treatment for treating the carpal tunnel syndrome: randomised "sham" controlled trial.** *Bmj* 1998, **316:**731-735.
68. **Ultrasonic Facial Treatment** [https://www.jellenproducts.com/ultrasonic-facial-treatment/]
69. Sapareto SA, Dewey WC: **Thermal dose determination in cancer therapy.** *International Journal of Radiation Oncology* Biology* Physics* 1984, **10:**787-800.
70. Samulski T, Grant W, Oleson J, Leopold K, Dewhirst MW, Vallario P, Blivin J: **Clinical experience with a multi-element ultrasonic hyperthermia system: analysis of treatment temperatures.** *International Journal of Hyperthermia* 1990, **6:**909-922.
71. Diederich CJ, Hynynen K: **Ultrasound technology for hyperthermia.** *Ultrasound in medicine & biology* 1999, **25:**871-887.
72. van der Zee J: **Heating the patient: a promising approach?** *Ann Oncol* 2002, **13:**1173-1184.
73. Wust P, Hildebrandt B, Sreenivasa G, Rau B, Gellermann J, Riess H, Felix R, Schlag PM: **Hyperthermia in combined treatment of cancer.** *Lancet Oncol* 2002, **3:**487-497.
74. Falk MH, Issels RD: **Hyperthermia in oncology.** *Int J Hyperthermia* 2001, **17:**1-18.
75. Hildebrandt B, Wust P, Ahlers O, Dieing A, Sreenivasa G, Kerner T, Felix R, Riess H: **The cellular and molecular basis of hyperthermia.** *Crit Rev Oncol Hematol* 2002, **43:**33-56.

76. Kennedy J, Ter Haar G, Cranston D: **High intensity focused ultrasound: surgery of the future?** *The British journal of radiology* 2014.
77. Gliklich RE, White WM, Slayton MH, Barthe PG, Makin IRS: **Clinical pilot study of intense ultrasound therapy to deep dermal facial skin and subcutaneous tissues.** *Archives of facial plastic surgery* 2007, **9:**88-95.
78. Foley JL, Little JW, Vaezy S: **Effects of high-intensity focused ultrasound on nerve conduction.** *Muscle Nerve* 2008, **37:**241-250.
79. Gelet A, Chapelon JY, Bouvier R, Rouviere O, Lasne Y, Lyonnet D, Dubernard JM: **Transrectal high-intensity focused ultrasound: minimally invasive therapy of localized prostate cancer.** *J Endourol* 2000, **14:**519-528.
80. Thuroff S, Chaussy C, Vallancien G, Wieland W, Kiel HJ, Le Duc A, Desgrandchamps F, De La Rosette JJ, Gelet A: **High-intensity focused ultrasound and localized prostate cancer: efficacy results from the European multicentric study.** *J Endourol* 2003, **17:**673-677.
81. Hynynen K, Freund WR, Cline HE, Chung AH, Watkins RD, Vetro JP, Jolesz FA: **A clinical, noninvasive, MR imaging-monitored ultrasound surgery method.** *Radiographics* 1996, **16:**185-195.
82. Larrat B, Pernot M, Aubry J-F, Sinkus R, Tanter M, Fink M: **Radiation force localization of HIFU therapeutic beams coupled with magnetic resonance-elastography treatment monitoring in vivo application to the rat brain.** In *Ultrasonics Symposium, 2008 IUS 2008 IEEE*. IEEE; 2008: 451-454.
83. Brenin DR: **Focused ultrasound ablation for the treatment of breast cancer.** *Annals of surgical oncology* 2011, **18:**3088-3094.
84. Pediconi F, Napoli A, Di Mare L, Vasselli F, Catalano C: **MRgFUS: from diagnosis to therapy.** *European journal of radiology* 2012, **81:**S118-S120.
85. Fischer K, Gedroyc W, Jolesz FA: **Focused ultrasound as a local therapy for liver cancer.** *The Cancer Journal* 2010, **16:**118-124.
86. Okada A, Murakami T, Mikami K, Onishi H, Tanigawa N, Marukawa T, Nakamura H: **A case of hepatocellular carcinoma treated by MR-guided focused ultrasound ablation with respiratory gating.** *Magnetic Resonance in Medical Sciences* 2006, **5:**167-171.
87. Napoli A, Anzidei M, De Nunzio C, Cartocci G, Panebianco V, De Dominicis C, Catalano C, Petrucci F, Leonardo C: **Real-time magnetic resonance–guided high-intensity focused ultrasound focal therapy for localised prostate cancer: preliminary experience.** *European urology* 2013, **63:**395-398.
88. Zini C, Hipp E, Thomas S, Napoli A, Catalano C, Oto A: **Ultrasound-and MR-guided focused ultrasound surgery for prostate cancer.** *World journal of radiology* 2012, **4:**247.
89. Lindner U, Ghai S, Spensieri P, Hlasny E, Van der Kwast TH, McCluskey SA, Haider MA, Kucharczyk W, Trachtenberg J: **Focal magnetic resonance guided focused ultrasound for prostate cancer: Initial North American experience.** *Canadian Urological Association Journal* 2012, **6:**E283.
90. Bauer R, Martin E, Haegele-Link S, Kaegi G, von Specht M, Werner B: **Noninvasive functional neurosurgery using transcranial MR imaging-guided focused ultrasound.** *Parkinsonism & related disorders* 2014, **20:**S197-S199.

91. Magara A, Bühler R, Moser D, Kowalski M, Pourtehrani P, Jeanmonod D: **First experience with MR-guided focused ultrasound in the treatment of Parkinson's disease.** *J Therapeut Ultrasound* 2014, **2:**b74.
92. Napoli A, Anzidei M, Marincola BC, Brachetti G, Noce V, Boni F, Bertaccini L, Passariello R, Catalano C: **MR Imaging–guided Focused Ultrasound for Treatment of Bone Metastasis.** *Radiographics* 2013, **33:**1555-1568.
93. Izumi M, Ikeuchi M, Kawasaki M, Ushida T, Morio K, Namba H, Graven-Nielsen T, Ogawa Y, Tani T: **MR-guided focused ultrasound for the novel and innovative management of osteoarthritic knee pain.** *BMC musculoskeletal disorders* 2013, **14:**267.
94. Napoli A, Mastantuono M, Cavallo Marincola B, Anzidei M, Zaccagna F, Moreschini O, Passariello R, Catalano C: **Osteoid osteoma: MR-guided focused ultrasound for entirely noninvasive treatment.** *Radiology* 2013, **267:**514-521.
95. Jolesz FA: **MRI-guided focused ultrasound surgery.** *Annu Rev Med* 2009, **60:**417-430.
96. Gianfelice D, Khiat A, Amara M, Belblidia A, Boulanger Y: **MR imaging–guided focused us ablation of breast cancer: Histopathologic assessment of effectiveness—initial experience 1.** *Radiology* 2003, **227:**849-855.
97. Chopra R, Tang K, Burtnyk M, Boyes A, Sugar L, Appu S, Klotz L, Bronskill M: **Analysis of the spatial and temporal accuracy of heating in the prostate gland using transurethral ultrasound therapy and active MR temperature feedback.** *Phys Med Biol* 2009, **54:**2615-2633.
98. Makin IR, Mast TD, Faidi W, Runk MM, Barthe PG, Slayton MH: **Miniaturized ultrasound arrays for interstitial ablation and imaging.** *Ultrasound Med Biol* 2005, **31:**1539-1550.
99. Prat F, Lafon C, De Lima DM, Theilliere Y, Fritsch J, Pelletier G, Buffet C, Cathignol D: **Endoscopic treatment of cholangiocarcinoma and carcinoma of the duodenal papilla by intraductal high-intensity US: Results of a pilot study.** *Gastrointest Endosc* 2002, **56:**909-915.
100. Moreno-Moraga J, Valero-Altes T, Riquelme AM, Isarria-Marcosy MI, de la Torre JR: **Body contouring by non-invasive transdermal focused ultrasound.** *Lasers Surg Med* 2007, **39:**315-323.
101. White WM, Makin IR, Barthe PG, Slayton MH, Gliklich RE: **Selective creation of thermal injury zones in the superficial musculoaponeurotic system using intense ultrasound therapy: a new target for noninvasive facial rejuvenation.** *Arch Facial Plast Surg* 2007, **9:**22-29.
102. Hynynen K, Chung AH, Colucci V, Jolesz FA: **Potential adverse effects of high-intensity focused ultrasound exposure on blood vessels in vivo.** *Ultrasound Med Biol* 1996, **22:**193-201.
103. Rove KO, Sullivan KF, Crawford ED: **High-intensity focused ultrasound: ready for primetime.** *Urol Clin North Am* 2010, **37:**27-35, Table of Contents.
104. Borchert B, Lawrenz T, Hansky B, Stellbrink C: **Lethal atrioesophageal fistula after pulmonary vein isolation using high-intensity focused ultrasound (HIFU).** *Heart Rhythm* 2008, **5:**145-148.
105. Jung SE, Cho SH, Jang JH, Han J-Y: **High-intensity focused ultrasound ablation in hepatic and pancreatic cancer: complications.** *Abdominal imaging* 2011, **36:**185-195.

106. Boucaud A: **Trends in the use of ultrasound-mediated transdermal drug delivery.** *Drug Discov Today* 2004, **9:**827-828.
107. Pitt WG, Husseini GA, Staples BJ: **Ultrasonic drug delivery-a general review.** *Expert opinion on drug delivery* 2004, **1:**37-56.
108. Mitragotri S, Edwards DA, Blankschtein D, Langer R: **A mechanistic study of ultrasonically-enhanced transdermal drug delivery.** *Journal of pharmaceutical sciences* 1995, **84:**697-706.
109. Siegel RJ, Luo H: **Ultrasound thrombolysis.** *Ultrasonics* 2008, **48:**312-320.
110. Daffertshofer M, Gass A, Ringleb P, Sitzer M, Sliwka U, Els T, Sedlaczek O, Koroshetz WJ, Hennerici MG: **Transcranial low-frequency ultrasound-mediated thrombolysis in brain ischemia: increased risk of hemorrhage with combined ultrasound and tissue plasminogen activator: results of a phase II clinical trial.** *Stroke* 2005, **36:**1441-1446.
111. Hitchcock KE, Holland CK: **Ultrasound-assisted thrombolysis for stroke therapy: better thrombus break-up with bubbles.** *Stroke* 2010, **41:**S50-53.
112. Tufail Y, Matyushov A, Baldwin N, Tauchmann ML, Georges J, Yoshihiro A, Tillery SI, Tyler WJ: **Transcranial pulsed ultrasound stimulates intact brain circuits.** *Neuron* 2010, **66:**681-694.
113. Miller DL: **Ultrasound-mediated gene therapy.** pp. 69-130: World Scientific; 2006:69-130.
114. Kieran K, Hall TL, Parsons JE, Wolf JS, Jr., Fowlkes JB, Cain CA, Roberts WW: **Refining histotripsy: defining the parameter space for the creation of nonthermal lesions with high intensity, pulsed focused ultrasound of the in vitro kidney.** *J Urol* 2007, **178:**672-676.
115. Xu Z, Raghavan M, Hall T, Mycek M-A, Fowlkes JB, Cain C: **Evolution of bubble clouds induced by pulsed cavitational ultrasound therapy-histotripsy.** *Ultrasonics, Ferroelectrics, and Frequency Control, IEEE Transactions on* 2008, **55:**1122-1132.
116. Shaw A, Hodnett M: **Calibration and measurement issues for therapeutic ultrasound.** *Ultrasonics* 2008, **48:**234-252.
117. Harris GR: **Progress in medical ultrasound exposimetry.** *IEEE Trans Ultrason Ferroelectr Freq Control* 2005, **52:**717-736.
118. Hwang JH, Tu J, Brayman AA, Matula TJ, Crum LA: **Correlation between inertial cavitation dose and endothelial cell damage in vivo.** *Ultrasound Med Biol* 2006, **32:**1611-1619.

Chapter 3 High Intensity Focused Ultrasound: a Review of Principles, Devices, and Clinical Applications

This chapter has been submitted as “Zahra Izadifar, Paul Babyn, Dean Chapman, High Intensity Focused Ultrasound: a Review of Principles, Devices, and Clinical Applications, *RadioGraphics* (Under Review)” According to the Copyright Agreement, "the authors retain the right to include the journal article, in full or in part, in a thesis or dissertation".

3.1 Abstract

The ability of ultrasound to penetrate deep into tissue and interact with human tissue via thermal and mechanical mechanisms has expanded its various therapeutic applications. The ability to focus the ultrasound beam and, as a result, ultrasound energy onto millimetre-size targets was a significant milestone in the development of therapeutic applications of focused ultrasound. Focused ultrasound is a non-invasive thermal ablation technique for treatment of tumors in several organs and is on the verge of becoming an alternative to the standard treatment options of surgery, radiotherapy, gene therapy, and chemotherapy in oncology practice. High-intensity focused ultrasound (HIFU) has been used for clinical treatment of different types of solid malignant tumors, including those in the pancreas, liver, kidney, bone, prostate, and breast as well as uterine fibroids and soft-tissue sarcomas. In addition, the capability of magnetic resonance imaging (MRI) to provide detailed images of soft tissues in the body and identify a wide spectrum of space-occupying soft-tissue lesions has accelerated the application of HIFU by providing real-time images and thermographic guidance during the procedure. Magnetic resonance guided focused ultrasound (MRgFUS) is a novel and non-invasive method of treatment that plays an important role in the development of neurotherapeutics and treatment options for brain-based disorders. MRgFUS has been proposed as an alternative to open

neurosurgical procedures for a wide variety of indications. The fundamental principles behind HIFU are the thermal absorption of ultrasound energy during transmission in tissue and the induced cavitation damage. This chapter briefly reviews heating and mechanical therapeutic applications of ultrasound along with an extensive review of the clinical applications of HIFU (MRgFUS). The clinical outcomes of HIFU ablation for tumor therapy, complications after treatment, and current challenges are also described. More recent developments in the application of HIFU for tumor treatment, HIFU-mediated drug delivery, vessel occlusion, histotripsy, movement disorders, and vascular, oncologic, and psychiatric applications are reviewed, along with potential future clinical applications of HIFU.

3.2 Introduction

Ultrasound can be employed in many therapeutically beneficial applications [1, 2] Medical therapeutic applications of ultrasound started in the 1930s [3]. The use of ultrasound for tissue heating represented an early clinical application of ultrasound [4]; this first therapeutic application of ultrasound was envisioned when people realized that the high intensity ultrasound waves used to navigate submarines during World War II were heating and killing fish [5]. As early as the 1940s, researchers tried to focus ultrasound waves on body tissues as an alternative to ablative procedures [6-9]. The application of ultrasound for destruction of tissue in the brain for treatment of Parkinson's disease and of the vestibular nerve for treatment of Meniere's disease was explored in the ensuing decades [10, 11]. The use of ultrasound for physiotherapy was established by the 1970s, and research continued into further applications related to neurosurgery [12] and cancer treatment [13]. In the 1980s, the application of ultrasound in high pressure-amplitude shockwaves for mechanical destruction of kidney stones (lithotripsy) came into use and replaced surgery [3]. In the last two decades, several advances in the fields of

imaging, physics, and engineering led to the possibility of focusing ultrasound onto targets anywhere deep into body. Recently, high-intensity focused ultrasound (HIFU) and magnetic resonance-guided focused ultrasound (MRgFUS) in particular have proven effective as non-invasive ablation modalities for soft tissue and been used to treat thousands of patients globally [14-18]. In fact, HIFU is the only completely non-invasive and extracorporeal method to treat primary solid tumors and metastatic disease. Scientific advances have facilitated the development and acceleration of a wide range of therapeutic methods now in use. Recent technical accomplishments have made MRgFUS a non-invasive and image-guided therapeutic approach that is proposed as an alternative to neurosurgical procedures for a wide variety of indications and brain disorders. This article begins by introducing the heating and mechanical (cavitation) effects of ultrasound in the body and briefly addresses their related therapeutic applications. HIFU therapy techniques are introduced and an overview of actual clinical activities in the field is given, including efficacy and safety measures. Clinical studies and outcomes of HIFU use for tumor therapy on different organs and related complications are presented. Recent investigations on intracranial MRgFUS in a range of clinical applications — from movement disorders, to vascular, oncologic, and psychiatric applications as well as brain-based disorders — are also reviewed. The article concludes with a discussion of some potential future clinical applications for focused ultrasound as well as some prospective new research areas.

3.3 High intensity focused ultrasound

HIFU is one of the research areas that is more active and developed among all non-ionizing energy methods, which include radiography, lasers, and microwaves [3]. The lesion produced in the tissue due to HIFU is a few mm in diameter and in length [3]. The first application of HIFU

was for thermal ablation of inoperable tissue related to Parkinson's disease [10, 19]. HIFU has also been used for treating uterine fibroids [20], cardiac ablation [21], visceral soft tissue ablation [22], and aesthetic treatment to lift the eyebrow [23, 24]. These methods have been approved by the Food and Drug Administration (FDA) for clinical use in the USA [3]. HIFU has also been utilized for curing glaucoma [25]. Other HIFU-based therapeutic techniques are under investigation for the treatment of benign prostatic hyperplasia (BPH) and prostate cancer [26, 27], hepatic, and pancreatic cancer [28]. HIFU treatment is usually assessed, guided, and monitored by one of two image guidance methods: magnetic resonance imaging (MRI) or ultrasound imaging [29]. MRgFUS has proven to be an attractive modality for non-invasive thermal ablation of soft tissue. All of the above HIFU techniques are applied by external devices; however, natural orifices are also employed, such as in transrectal prostate cancer treatment [30] and endoscopy via an intraductal probe for bile duct tumor treatment [31]. Ultrasound monitoring in HIFU treatment is based on a combination of sound velocity, attenuation, stiffness, and vapor content variation in the target area [32].

Energy-based thermal therapies apply various energy sources (e.g., radiofrequency currents, microwaves, laser, thermal conductor sources, and ultrasound) in clinical devices. Ultrasound provides several benefits over other competing technologies, including energy penetration to treat deep target areas, better focusing because of its small wavelengths, and precise control of energy deposition shape and location [33, 34]. HIFU with image guidance demonstrates the advantage of ultrasound energy and is increasingly being applied for tumor ablation [35].

HIFU was developed in the 1940s as a permanent thermal tissue ablation approach [36]. The advantages of HIFU have recently expanded its clinical use to treatment of a variety of solid virulent tumors in a well-defined volume, including those in the pancreas, liver, prostate, and

breast, as well as uterine fibroids and soft tissue sarcomas. The advantage of HIFU with respect to conventional tumor/cancer treatment methods, such as chemotherapy, radiotherapy, and open surgery, is that HIFU is a non-invasive and non-ionizing treatment modality [36]. In fact, among tumor/cancer treatment modalities, HIFU is the only completely non-invasive and extracorporeal technique to treat primary solid tumors and metastatic diseases. Over 100,000 cases have been treated using HIFU, mainly in Asia and Europe, with great success [36]. The key to HIFU treatment is that the energy delivered is sufficient to increase the tissue temperature to a cytotoxic level very fast so that the tissue vasculature does not affect the extent of cell killing. Heat coagulation by HIFU is desired for cell reaction with chronic inflammation, with histological signs of fat necrosis in the surrounding normal fatty tissue [36]. The boundary width between totally disrupted cells and normal tissue is no more than 50 μm [37]. Deadly complications may develop if any vital blood vessels adjacent to the tumors are damaged. Large blood vessels are probably less vulnerable to HIFU damage compared to tumor tissue; however, this speculation is likely due to the fact that the blood flow dissipates the thermal energy from the vessel wall and results in safe ablation of the tumor. Surgical resection of a tumor is often contraindicated and may be dangerous when it is located close to major blood vessels [36]. HIFU has been widely applied in neurosurgery, ophthalmology, urology, gynecology, and oncology [26, 37, 38]. HIFU can pass through overlying skin and tissues without harming them and is focused to a localized tumor area with an upper size limit of approximately 3-4 cm in diameter for tumors; there is a very sharp boundary between dead and live cells when the tumor is ablated [36]. Figure 3-1 is a schematic of a HIFU transducer and the focused ultrasound beam it produces to pass through overlying skin and tissues and necrose a localized tumor region. The

tumor region may lie deep within the tissue. The affected area at the focal point that leads to lesion coagulative necrosis is shown in red in the figure.

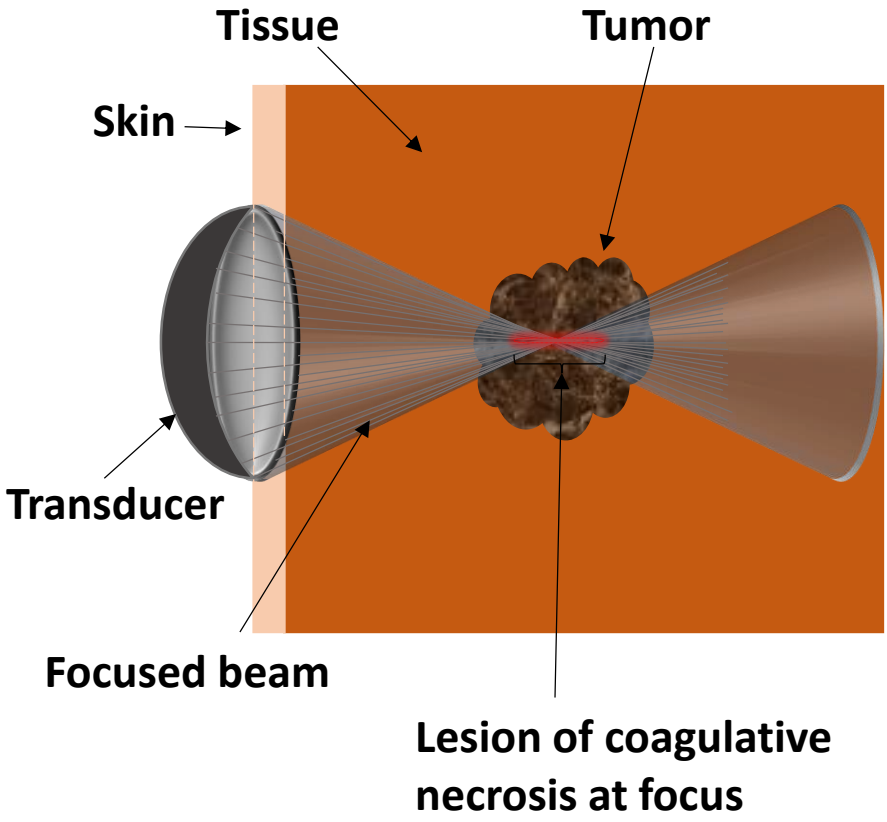

Figure 3-1 Schematic of high-intensity focused ultrasound for tumor therapy

Many benefits justify further exploration of HIFU for additional future clinical applications: HIFU ablation results in reduced toxicity compared with other ablation techniques; it is non-invasive and causes minimal pain; it is a low-cost procedure compared with surgery; it leaves no scars on the patient; recovery is faster compared with traditional surgery techniques; any bleeding that occurs during the procedure can be stopped by ultrasound; it has excellent repeatability as there is no dose limit; as it is guided by MRI or diagnostic ultrasound, as opposed to X-rays, there is no exposure to ionizing radiation; system maintenance costs are low; it causes very limited side effects to normal surrounding tissues [36]; patient comfort and safety are

maximized; undisturbed real-time visualization can occur during the procedure; and the technique is precise and easy to apply. In terms of limitations, HIFU treatment is sensitive to complications including metastasis, patient movement, and near-field heating, and the treatment time can be as long as several hours.

3.4 Principles behind HIFU

The basic principles of HIFU are coagulative thermal necrosis due to the absorption of ultrasound energy during transmission in tissue (thermal effect) and ultrasound-induced cavitation damage [36]. The heat generated by HIFU results in a rapid rise in temperature in the local tissue to more than 60 °C for 1 s, which leads to immediate and irreversible cell death in most tissues[36]. The highly focused ultrasound beam results in a very high intensity at the focal point of the beam within a small volume of about 1 mm in diameter and about 10 mm in length [36], which minimizes the potential damage to tissue outside the focal region. Thermal tissue damage due to high temperature exposure is dependent almost linearly on exposure time and exponentially on the temperature increase [39, 40]. A thermal dose of 43 °C for 120 to 240 minutes coagulates cellular protein and tissue structure components, leading to immediate and irreversible vascular and immediate tissue destruction [33]. However, this threshold may vary with tissue type. The tissue at the border of the target area will die within 2-3 days [36].

Another mechanism involved in HIFU ablation is the mechanical effect. This mechanical effect including cavitation only occurs with high intensity acoustic pulses [36]. Cavitation can generate very high pressures and temperatures, high shear stress, and microstreaming jet liquids that can cause pitting of the cell wall. If the medium is mostly liquid and can freely move, then liquid movement can lead to the production of microscopic streaming, which can cause cell apoptosis [41].

The nuclei of these apoptotic cells are self-destructed with quick degradation of deoxyribonucleic acid (DNA) by endonucleases. One of the delayed bioeffects in tissue exposed to HIFU can be apoptosis, especially in cells such as neurons that regenerate poorly [36].

3.5 HIFU devices for clinical applications

The process of ablation can be monitored by ultrasound imaging (ultrasound guided high intensity focused ultrasound - USgFUS) as shown in Figure 3-2, or by MRgFUS as shown in Figure 3-3.

There are three different ways to apply HIFU to the human body based on the accessibility of the targeted organ. When the organ is readily accessible, such as the kidney, HIFU is applied through an acoustic window on the skin by external or extracorporeal transducers. For cases like prostate cancer, however, a transducer is inserted into the body through the rectum (transrectal transducer) (Figures 3-4 and 3-5). Interstitial probes are being developed for the treatment of biliary duct and esophageal tumors and are inserted into the body through the mouth and placed close to the tumor (Figures 3-6 and 3-7). To focus the high-intensity ultrasound beam, a concave focusing transducer is used (Figure 3-1), or multiple piston transducers are arranged on the truncated surface of a spherical bowl (Figure 3-2), or a flat transducer is used with a fittingly designed acoustic lens (e.g., Model-JC, Chongqing HAIFU™, China) [36] (Figure 3-6). Because an extracorporeal device is used to distribute the incident energy over a large skin area, the device has a wide aperture and long focal length to decrease the acoustic intensity at the entry of the wave site to avoid skin burn. However, severe full skin burns following extracorporeal shock wave lithotripsy (ESWL) for renal calculi [42] or second-degree burns after shock wave lithotripsy [43] are often reported. Also, some patients face post-operative side effects, such as pain, vomiting, and wounds on their skin. For targets lying within the breast, abdomen, brain, or

limbs, an extracorporeal HIFU device is usually employed. The device couples the acoustic energy to the skin surface via a coupling gel or water balloon, with an appropriate entry window site on the skin so that the propagated focused beam is not interrupted by intervening gas.

Transrectal and interstitial transducers usually operate at higher frequencies and lower powers so they can be applied at a closer distance to the target area. The devices developed for transrectal use have both therapy and imaging transducers incorporated into the head of the transducer probe with a fixed but adjustable focal point that can be mechanically moved to treat a larger tissue volume (Figures 3-2, 3-4, and 3-6). Prostate ablation is performed by creating lesions side by side and the ultrasound power is altered to adjust the lesion length (for the Ablatherm probe (Edap Technomed, France)). For thick prostates, deep lesions are achieved either by making separate lesions in two layers or by using a longer focal length [36]. For an interstitial transducer, instead of focusing the probe a plane transducer is usually applied and coagulation of the volume is achieved by rotating the probe [30]. When the probe is set in the body and 360° of rotation is achieved, then under fluoroscopic or MRI guidance the transducer is repositioned and another adjacent ring is produced. This device can be used for biliary and esophageal tumors or bloodless partial nephrectomy [36]. Interstitial devices can be derived from percutaneous, laparoscopic, or catheter-based ultrasound. Catheter-based ultrasound devices can be placed within or adjacent to the target volume directly to treat and coagulate a large volume of the target area, or they can be used as endoluminal and endovascular cardiac devices. The exposure time for catheter-based ultrasound devices is typically 10-30 min and the procedure is more invasive compared to external HIFU; however, this method has better energy localization [44]. Catheter-based ultrasound devices are under development for future clinical use for thermal therapy of cancer and benign tissue in the prostate, uterus (fibroids), liver, and bone. Devices for percutaneous

ablations have been successfully investigated *in vivo* (mostly in pigs) for organs such as the liver [45-47], prostate (*in vivo* studies mostly in pigs) [48, 49], brain (*in vivo* study in dogs) [50], and uterus (*ex vivo* trial on human uterine fibroids) [51]. To the best of our knowledge, no human trials of this device have been reported. Figures 3-2 and 3-3, respectively, show schematics of typical ultrasound- and MRI-guided focused ultrasound systems applied to the target through the skin for ESWL, extracorporeal shock wave therapy (ESWT), or HIFU.

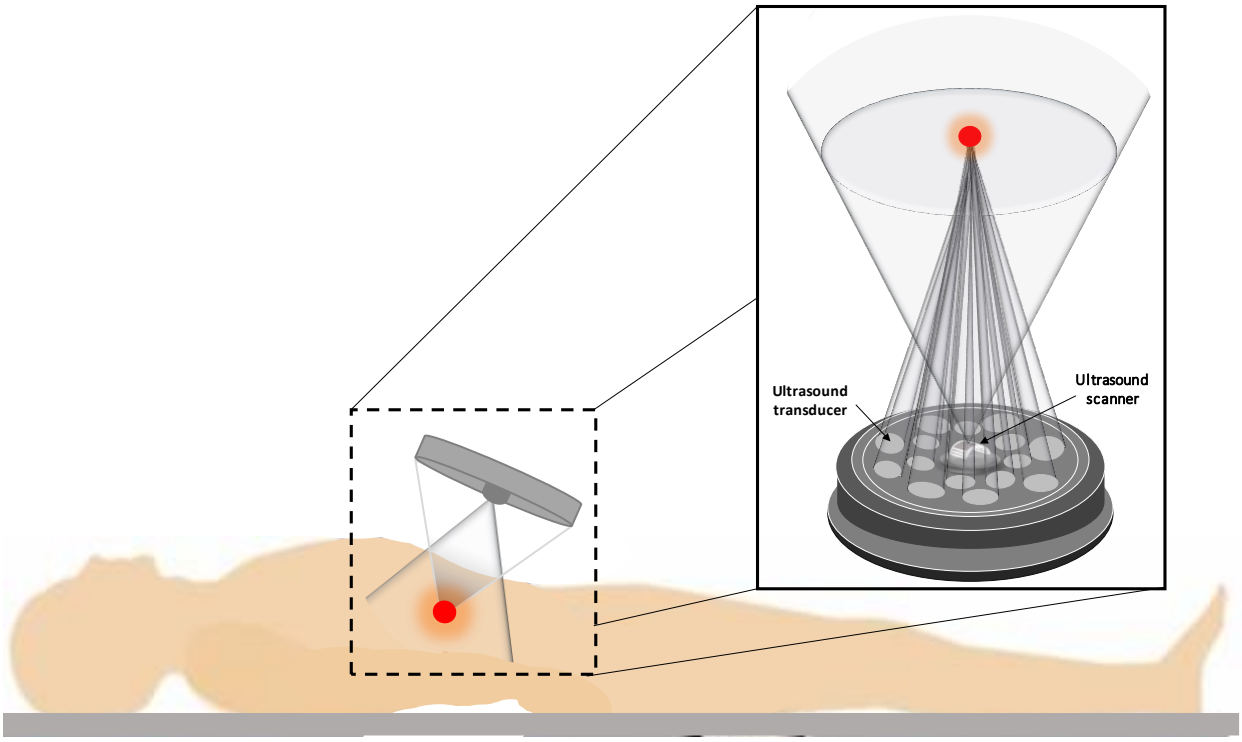

Figure 3-2 Schematic of the structure of an extracorporeal HIFU transducer, including both imaging and therapy probes, depicting an ultrasound-guided technique on a patient

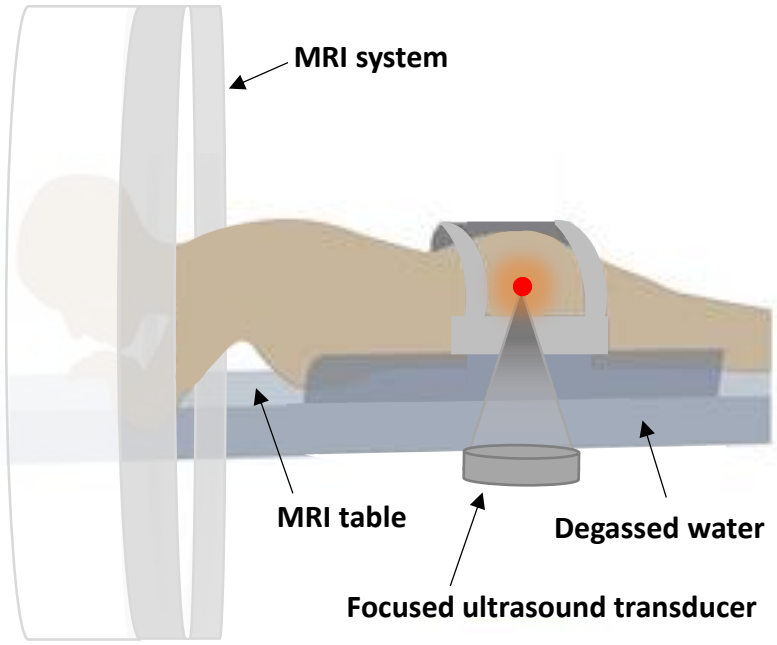

Figure 3-3. Schematic of magnetic resonance-guided extracorporeal focused ultrasound system treatment technique

Depending on the geometrical size and acoustic parameters of the transducers applied in a HIFU system, the beam size of a -6 dB HIFU system at its focal region is typically 1-3 mm in width and approximately 10 mm in length [36]. However, a 1-cm cancerous tumor is detectable and treatable with HIFU. The concern for inhomogeneity of tissue in abdominal-pelvic (such as in uterine fibroids and renal tumors) or transcranial usage that may cause distortion of the focal beam or a drop in focusing ability in deep-seated tissues is solved by application of the phase correction procedure in the HIFU system, as is done with ultrasound imaging systems [36]. When a larger volume is targeted for ablation, the transducers applied in the HIFU system are mechanically or electronically moved in discrete steps and fired at each point until the result is a confluent region of cell killing.

Overall, the therapeutic ultrasound frequency depends on the application-specific treatment depth and the desired rate of heating required for treatment. Higher frequencies lead to lower penetration depths and lower frequencies lead to higher penetration depths. Frequencies as low

as 0.5 MHz have been used for deep treatments (such as transcranial applications) or high absorption situations and as high as 8 MHz for superficial treatments (such as prostate applications) [52]. Frequencies close to 1 MHz have been found to be the most useful for heat deposition and increasing temperature [36].

In order to target and treat the desired region, the HIFU focus point needs to be scanned throughout the entire volume of tissue. Extracorporeal HIFU systems are guided by either ultrasound (USgFUS) or MRI (MRgFUS). MRI with high anatomical resolution and sensitivity for tumor detection offers accurate planning of the tissue to be targeted and treated. In addition, MR thermometry enables calculation of the thermal dose and also superimposes a representation on the anatomical image of the area in which the temperature reaches cytotoxic levels. It provides closed-loop control of energy deposition with a temperature accuracy of 1 °C, spatial resolution of 1 mm, and temporal resolution of 1 s during HIFU treatment [36]. Within seconds of HIFU exposure, MRI can provide temperature data and is superior to sonography for overweight patients [53] as it is not sensitive to fat tissue [54]. However, MRI is expensive, labor-intensive, and its temporal and spatial effects lead to underestimation of temperature. For example, the MRI-measured temperature by water proton resonance frequency of a voxel reached a maximum of only 73 °C after 7 s of continuous HIFU exposure after boiling started; however, the theoretical simulation predicted 100 °C after 7 s of exposure and an average temperature field of 73 °C in the volume of the MRI voxel (0.3 mm^8 × 0.5 mm^8 × 2 mm), which agreed with the MR thermometry measurement [55]. In comparison with MRgFUS, ultrasound imaging is more convenient and mechanically compatible, and provides the same form of energy for imaging as used for therapy. It provides the benefit of verifying the acoustic window with sonography in real time, which means that if the target region is not visualized by ultrasound

imaging before or during HIFU therapy, then it is unlikely that HIFU therapy will be effective in that specific region. The ablated target region is not visualized on standard B-mode images unless the gas bubbles produced in that focal region work as hyperechoic spots and appear in the image [36].

Overall, both USgFUS and MRgFUS have benefits and drawbacks. USgFUS is good for preprocedural positioning of the target tumor, but not for intraprocedural evaluation of therapeutic boundaries [36]. MRgFUS is good for measuring the temperature that is temporally generated in the tissue, but not for measuring the mortal thermal dose [54]. Recently, sensitive microbubbles have been explored for raised ultrasound imaging [56]. MRgFUS as an integrated HIFU therapy system has recently become an attractive method for surgical resection or radiation therapy of benign and incurable tumors. MRgFUS has already been approved for the treatment of uterine fibroids, and is undergoing clinical trials for the treatment of breast [57, 58], liver [59, 60], prostate [61-63], and brain cancer [64, 65] and also to relieve and lessen pain in bone metastasis [66-68].

Non-invasive aesthetic applications of HIFU will provide a safer alternative to liposuction for cosmetic applications [69]. The exposure of superficial tissue to HIFU leads to a contraction of the dermis or to demolition of fatty tissue [23, 70]. In this technique, both thermal as well as non-thermal mechanisms of ultrasound are involved.

HIFU has also been utilized to treat atrial fibrillation by tissue ablation to achieve pulmonary vein isolation [3].

During HIFU applications, undesired tissue injury, unwanted burns, and pain can occur as significant ultrasound energy is delivered to a localized area of tissue [3]. In addition, HIFU can

cause vasospasm and hemorrhaging when concomitant cavitation is also generated in the tissue [71], impotence and incontinence during prostate cancer treatment [72], or creation of an atrial-esophageal fistula during atrial fibrillation treatment [73]. Furthermore, fistula formation and rib necrosis with delayed rib fracture [28] are also considered to be serious complications that can occur following hepatic and pancreatic cancer treatment [3].

3.6 Clinical Application of HIFU

3.6.1 Liver

Hepatocellular carcinoma (HCC) or malignant hepatoma is the most common type of liver cancer in humans and one of the most complicated types of cancer to treat. The common treatment method is liver transplantation. Surgical resection can change the nature of HCC in the early stage of the disease [74, 75], but survival rates for this method of treatment are only 25-30% at 5 years [36]. The transcatheter arterial chemoembolization technique (TACE) that is widely used to achieve the cytoreduction of vital tumor tissue is not capable of complete necrosis of HCC but only embolization of the hepatic artery [76, 77]. HCC is a multifocal tumor and this specific biological behavior leads to poor surgical outcomes and a high risk of postoperative recurrence. Replacing surgery with a therapeutic system capable of selectively destroying multiple tumor nodules distributed throughout the liver would be a better option. In a study performed by Wu et al., the combination of TACE and external focused ultrasound treatment (performed 2-4 weeks after TACE) of advanced-stage HCC in patients showed an absence of or reduction in blood supply in the target area and longer survival time compared with TACE treatment only [78]. In another study in China, 68 patients with advanced primary liver cancer were treated by external HIFU; in 30 cases in which surgical excision followed HIFU, the tumors were completely ablated [79]. A total of 474 patients with primary and metastatic liver cancer

were treated with the same device in China [80]. In another study, 100 patients with liver cancer were treated with external HIFU and the clinical effect evaluated [81]. About 87% of patients showed symptomatic improvement after treatment, and CT and MRI scans after the procedure showed coagulation necrosis and blood supply decrease or complete disappearance of the tumor in the target area [81].

Clinical trials of 68 patients at Royal Marsden Hospital in London showed that HIFU treatment for liver cancer is performed on fully conscious patients who are treated on an outpatient basis and without local anesthesia or sedation [82]. The procedure was well tolerated by all patients. All of the above studies featured ultrasound guided focused ultrasound therapy. However, the safety of focused ultrasound therapy can be greatly improved using MRgFUS [60]. In a case study of MRgFUS treatment of a patient with HCC (15 mm in diameter) [60], MRgFUS was concluded to be superior to USgFUS as it was more feasible and efficient. MRgFUS overcomes the limitations of ultrasonography and allows monitoring of temperature elevation in the treated tissue and detection of lesions deep in the body. Because MR imaging enables the evaluation of the treated volume immediately after treatment, the feasibility and safety of focused ultrasound is significantly improved [60].

3.6.2 Prostate

Transrectal HIFU for treatment of prostate cancer has shown promise in pilot studies. In the past decade, HIFU has been applied to both benign prostate hyperplasia and prostate carcinoma in medical centers in more than 100 sites in Europe, the USA, and Asia. The two commercially available therapy systems are the Ablatherm® (EDAP-Technomed, Lyon, France) and the Sonablate®500 (Focus Surgery, Indianapolis, IN, USA). In these devices, the endorectal probes containing the transducer and a diagnostic ultrasound imager are inserted into the body via the

rectum and placed close to the target (Figure 3-5). The transducer is designed to move both back and forth along the probe axis as well as rotationally 180° around the probe axis (Figure 3-4). This design allows for the production of consecutive lesions in a manner such that the focal lesions overlap laterally and longitudinally and generate the complete targeted prostate volume. Early experiences with HIFU for treatment of benign prostate hyperplasia in patients showed encouraging results [83, 84]. These studies showed the possibility of making irreversible lesions in the prostate tissue without any damage to the rectal wall. Even though these studies concluded that HIFU treatment is a safe treatment technique with minimal side effects and complications to relieve the symptoms of prostatism, the long-term outcome after transrectal HIFU therapy has been disappointing [85]. The effectiveness of treatment in these studies was evaluated by measuring prostate-specific antigen (PSA) nadir level (PSA is a protein produced in prostate) [86-90][88-92][88-92][86-90], biopsy [86, 88, 91], and assessment of quality of life including factors such as urinary incontinence and erectile dysfunction [86, 88, 89, 92] after HIFU treatment. Results showed a significant drop of mean and PSA nadir level after HIFU treatment with a promising survival rate in patients with PSA nadir levels $\leq$ 0.2 ng/mL [90]. Results showed that urinary incontinence was not affected by the treatment [86, 88, 91], except for one study that reported a general decrease in the symptom score for 63% of patients [92]; different erectile dysfunctions were reported depending on the number of patients and follow-up period [88, 91, 93-95]. The 2- to 5-years mid-term follow-up of HIFU treatment has shown that the PSA level stays low and the negative biopsy rate stays about 90% [27, 36, 96, 97]. Repeat biopsy in disease-free patients showed a success rate ranging from 60 [26] to 80% [98]. The evaluation of biochemical disease-free survival rates 5 years after transrectal HIFU treatment of localized prostate cancer showed a decrease of serum PSA values to less than 4 ng/mL [99].

Complications of HIFU treatment, such as urinary retention, urinary infection, and urethral stenosis [94], were reported by many researchers. The rate of complications of HIFU prostate cancer therapy, such as urinary retention, incontinence, urinary infection, impotence, chronic pain, rectal fistulas, and incomplete treatment of disease [100] are higher with repeated HIFU treatment than for a single treatment [101, 102]. Transurethral resection of the prostate before treatment can mitigate urinary retention (ischuria) associated with HIFU treatment [101, 102] and decrease the time an indwelling catheter is required from 40 to 7 days [96].

Interstitial ultrasound applicators such as catheter-based ultrasound applicators were also tried in a clinical pilot study to deliver hyperthermia in connection with high dose rate brachytherapy for treating advanced prostate cancer and cervical cancer [103].

In one study of 98 men for a period of 4 years, 43.8% of patients underwent salvage trans-urethral resection of the prostate after initial HIFU therapy. Therefore, trans-urethral resection is still preferred over the current form of transrectal HIFU, and HIFU is not recommended for treatment of benign prostate hyperplasia [104]. Treatment of benign prostate cancer presents different problems from prostate cancer because prostate cancer is a multi-focal disease and detecting the facies with ultrasound is difficult [36]. HIFU ablation of the whole gland has been the most successful method of treatment [83, 84]. Compared to focal treatment, whole-gland treatment led to a decrease in tumor incidence from 35% to 17% and, in those patients that still had the disease after treatment, a decrease in tumor volume of greater than 90% [98]. In another study, five patients with unifocal, biopsy-proven prostate cancer (PCa) evident on MRI were treated by MRgFUS and then underwent radical prostatectomy [105]. Subsequent histopathology showed wide coagulative necrosis, with no residual tumor in the ablated area. Two patients showed two significant bilateral residual tumors outside the treated area that were not evident in

pre-treatment MRI. They reported an uneventful procedure with no adverse events or surgical difficulties through radical prostatectomy in relation to the previous MRgFUS. Clinical HIFU prostate cancer treatment has increased the control rates for the treated tumor from 50% at 8 months in the early days to 90% in more recent experiments [36, 96, 106]. Overall, HIFU treatment of prostate cancer is more suitable for overweight patients, men over 65 years of age, or those who are not candidates for surgery [107].

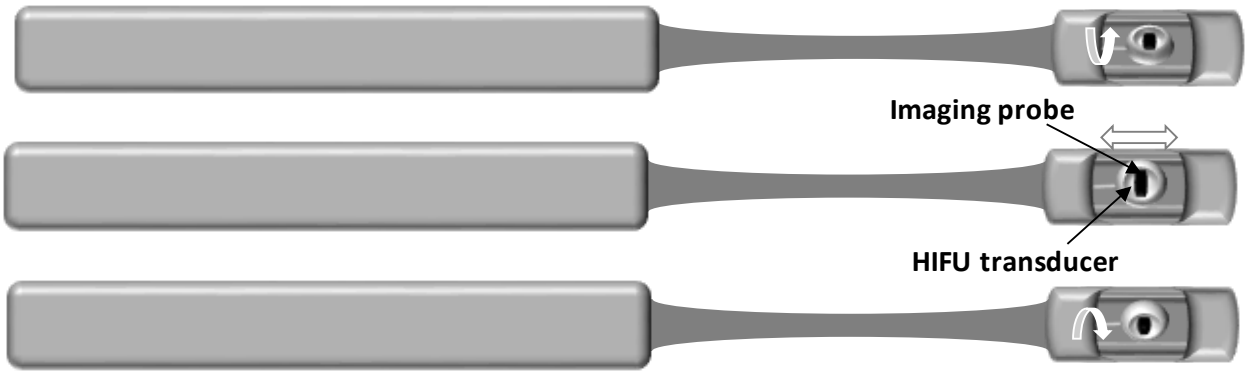

Figure 3-4 Schematic of a typical transrectal transducer for prostate cancer treatment, with both therapy and imaging transducers incorporated into the head of the transducer probe. Longitudinal and lateral rotation movements of the transducer along with the imaging probe enable volume ablation and scanning of prostate cancer.

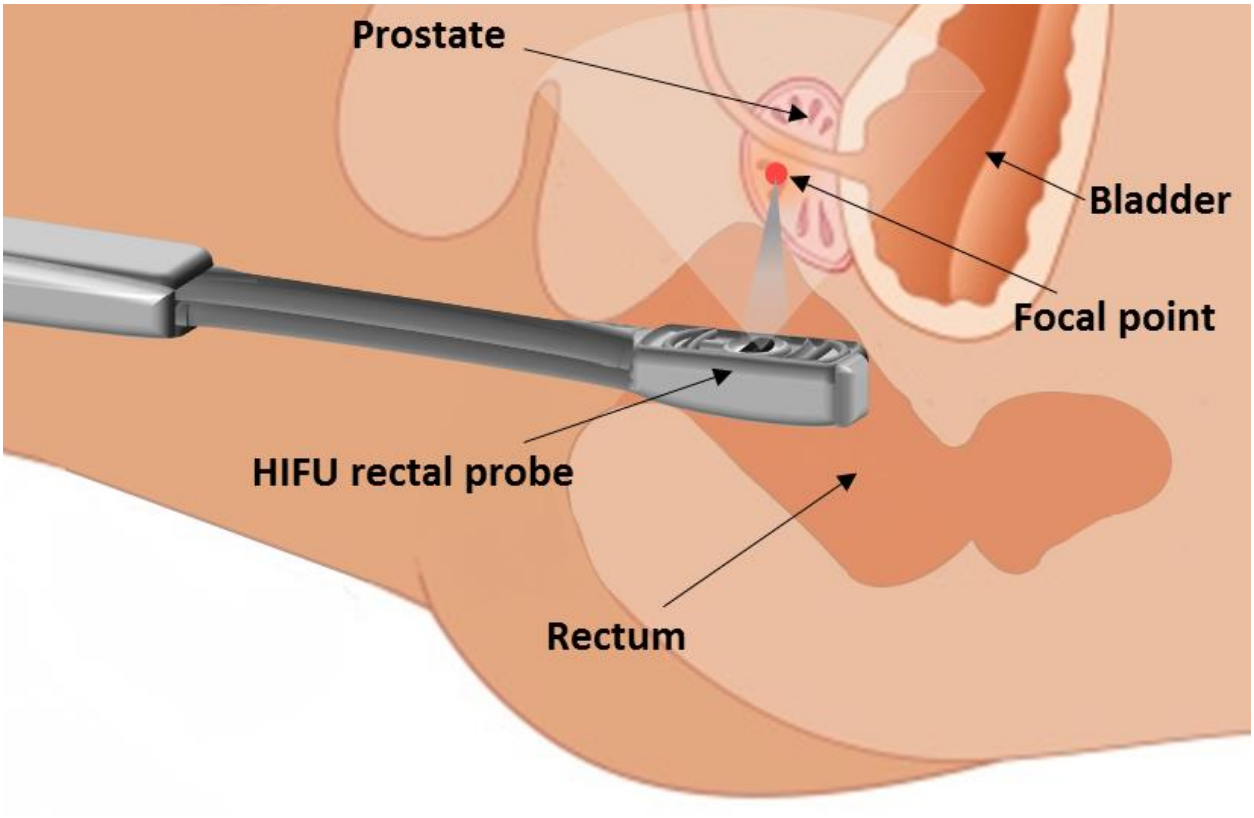

Figure 3-5 Schematic of a transrectal ultrasound transducer (rectal HIFU probe) and the treatment technique used for prostate cancer treatment. The HIFU ultrasound probe is inserted into the rectum and the sound waves target the cancer-affected areas in the prostate gland.

3.6.3 Breast Cancer

Patients with breast cancer who desire breast conservation usually undergo lumpectomy followed by external radiation therapy. Nonsurgical ablation can be a good approach as part of breast-conservation therapy in patients with early-stage breast cancer. This can be cosmetically and psychologically more satisfactory than conventional breast conservation treatment therapy. HIFU is one of the nonsurgical, non-invasive, and effective techniques to affect local tumor necrosis and can be an effective approach for treating patients who are a high surgical risk as it involves less anesthesia, shorter recovery time, lower cost, lower infection risk, and no scar formation [108]. HIFU can precisely deliver energy to a target point in soft tissue without affecting skin integrity. In several clinical studies of breast cancer, tumor ablation treatment with

HIFU was employed [108-116], including applications for invasive lobular carcinoma, invasive ductal carcinoma, and invasive mucinous adenocarcinoma [110, 114]. In most of these studies, the tumors were located a distance of less than 1 cm from the skin, nipple, or rib cage and could be visualized and targeted for treatment [109, 110, 114]. The clinical devices used in these studies included ultrasound guided HIFU using a model JC system [80, 109, 113] that consisted of a 12-cm diameter geometrically focused transducer with a 9-cm focal length operating at a frequency of 1.6 MHz [109-111]; MRI-guided HIFU using an ExAblate 2000 unit (InSightec Ltd., Hifa, Israel) [108, 110, 112, 114] that provided planning and real-time thermal monitoring in a closed-loop procedure [110]; or various kinds of custom-made MRgFUS systems [115, 116] that included focused ultrasound transducers operating at frequencies of 1.7 [115] and 1.5 [116] MHz. Intravenous sedation, general anaesthesia [109, 111], or no anaesthesia [115] were employed in these studies. The size of the ablated breast lesion and margin of breast tissue were about 1.5-2.0 cm around the visible tumor in each case [109, 111, 113]. Local mammary edema in all patients immediately after HIFU treatment, minimal skin burn [44, 45, 46, 47, 49], very few severe (2nd- or 3rd-degree) skin burns [108, 110, 112, 114], and a few minor adverse events were reported. Coagulation necrosis rates of 100% [109, 111, 113], 97% [110], and 88.3% [114] in the treated breast volume were reported. At 5-year follow-up, a disease-free survival rate of 95%, recurrence-free survival rate of 89%, and average 90% reduction in tumor size were reported [111]. HIFU is capable of inducing destructive and sub-lethal damage to tumors with a loss of propagation activity [115]. The main limitation of these HIFU methods for breast cancer treatment is the inability to assess the margin status mainly due to the lack of pathological specimens. Imaging-based assessments such as radiology and post-procedure contrast-enhanced MRI should replace conventional histopathology [36]. In breast fibroadenomata (FAD), which

are benign lesions found in about 10% of women, exceptsurgical removal of the lump or vacuum-assisted mammotomy other techniques such as HIFU, cryo-, or laser ablation have also been applied for treatment. A comprehensive review by Peek et al. compared these ablative techniques for treatment of breast FAD [117]. All of the ablative techniques were minimally invasive and looked promising for the treatment of FAD; however, heterogeneity between studies was observed. Further randomized trials including a larger number of patients are required to determine which ablative technique is most precise [117].

3.6.4 Uterine fibroids

Uterine fibroids (also known as uterine leiomyoma) are benign smooth muscle tumors of the uterus (also of the fallopian tubes, broad ligament, or cervix) and are one of the most common female pelvic tumors, occurring in about 25% of women [118]. Most women have no symptoms while others may have heavy and painful periods, pelvic pain, menorrhagia, dysmenorrhea, dyspareunia, increased urinary frequency, and infertility [36]. As most women are interested in fertility preservation and reduced recovery time after uterine fibroid treatment, a less invasive treatment of uterine fibroids is in high demand. The most recent clinical trials conducted with more than 2000 patients employed four different commercially available systems: an ExAblate 2000 system (Insightec, Haifa, Israel), a Haifu JM therapeutic system (JM2.5C, Chongqing Haifu Technology Co., Ltd., China), a HIFUNIT 9000 tumor therapy system (Shanghai Aishen Technology, Shanghai, China), and a custom made mobile HIFU unit with a 1.07 MHz ultrasound source (Storz Medical AG, Kreuzlingen, Switzerland). The superior soft tissue contrast capability of MRI has led to its use for further characterization of fibroids and also for symptomatic uterine fibroid treatment with MRI-guided focused ultrasound. MRgFUS was approved by the US FDA in 2004 and more than 2000 patients have since been treated in the

United States [119-121], the United Kingdom, Germany, and Israel [36]. A study on the safety and feasibility of MRgFUS in the treatment of fibroids (Phase I/II of study) started in 1999 in the United Kingdom, Germany, and Israel. The results showed that MRgFUS creates hemorrhagic necrosis in the area of non-perfusion on the post-treatment MR images and only 10% of patients experienced pain within 72 h of treatment [36]. A trial on treatment of larger volumes of fibroids in women with symptomatic uterine fibroids (Phase III of study) showed that 79% of treated patients had a 10-point decrease in their symptom severity score with a 13.5% mean decrease in treated fibroid volume at 6-months post-treatment. Most of the improvement was observed at 3 months and 12 months after treatment, as 15% of evaluated patients reported a 10-point decrease in their symptom severity score and only 28% underwent an alternative treatment [122]. Researchers who focused on measuring fibroid volume reduction after HIFU treatment reported a 31.4% volume decrease after three months [123], 31% [119], 15% [124], or 33% [125] after six months, and 9.3% after 12 months [126]. To maximize safety in these FDA approved studies, only 10% of the fibroid volume was treated. Based on FDA guidelines for MRgFUS, the commercial trial time of treatment is limited to 180 min and the allowed distance between serosa and the fibroids must be at least 15 mm [119].

In MRgFUS treatment of uterine fibroids, the patient lies in the prone position and is placed inside the MRI. An MR pelvic coil surrounds the patient to obtain images during treatment (Figure 3-3). HIFU is directed towards the fibroid and during each sonication a small volume of the fibroid is ablated. The treatment is performed under intravenous conscious sedation [119, 123]. Care is taken to avoid sensitive structures adjacent to the fibroid, such as skin, bowel, or sacral nerve [119, 123] and, for cases in which the bowel is in the way, a degassed water balloon is placed on the abdominal wall to compress the bowel away from the acoustic beam [123].

Conventional transabdominal ultrasound imaging guided HIFU systems [127, 128] and interstitial ultrasound applicators have also been used for fibroid treatment [129]. Initial studies on the use of interstitial ultrasound applicators for the treatment of large uterine fibroids were performed on surgically excised human fibroids. The results showed the ablation of a region about 4 cm in diameter and with volumes bigger than 45 cm^3 with a single needle insertion in less than 15 min [129]. In another study conducted in 2014 on the safety and effectiveness of MRgFUS, 32 patients with clinically symptomatic uterine fibroids were treated with MRgFUS and pre- and post-treatment symptom severity scores were assessed at the time of enrolment and at one-, three-, and six-months follow-up [130]. Symptom severity scores decreased notably at the follow-up points with significant positive correlations between non-perfused volume ratios and reduction in fibroid volumes at six-months follow-up.

Gormy et al. assessed the results of MRgFUS on 138 patients with symptomatic uterine fibroids for a long-term follow-up period of 2.8 years [131]. They observed an incidence of additional treatment undertaken at 36- and 48-month follow-up points of 19 and 23%, respectively. Patients with disparate fibroids that show brighter on MRI were more likely to need additional treatment compared with patients with homogeneously dark fibroids. Additionally, younger women (43.0 y ± 5.8) were more likely to need additional treatment compared with older women (46.3 y ± 5.6).

Although clinical results are best estimated using a disease-specific questionnaire, the real reduction of fibroid volume and symptom relief cannot be evaluated until some period of time after treatment. Even though the apparent diffuse coefficient values were notably low within the treated area immediately after treatment (e.g., show cell necrosis and membrane integrity loss), the long-term changes in this value and the reason behind these changes remain to be determined [131]. Overall, HIFU ablation for treatment of symptomatic uterine fibroids appears effective

and safe. Comparison of the long-term rates of additional interventions and related costs after MRgFUS of symptomatic uterine fibroids with other uterine-sparing procedures, such as uterine artery embolization or myomectomy, shows that MRgFUS is a comparable technique [131] with no significant cost difference [132, 133]. Although many women with symptomatic uterine fibroids undergo hysterectomy, MRgFUS is the only non-invasive treatment option. The procedure has been shown to be safe and effective, especially for patients unresponsive to medical treatment [134].

3.6.5 Kidney tumor

Total or partial nephrectomy is still the main method of treatment for kidney tumors [135]; however, because the size of kidney tumors is small in most cases, a non-invasive ablation of the tumor is potentially attractive in addition to available nephron sparing surgical techniques. Few clinical studies have examined ablation of small kidney tumors [22, 136, 137] or metastatic kidney cancer [138] with HIFU. Treatment of kidney tumors using an extracorporeal HIFU device (JC-Model devices C-Model devices [136, 138]), a prototype focused transducer system (Storz Medical, Tägerwilen, Switzerland [137]), and a laparoscopic HIFU system (Sonatherm1 device (Misonix Inc, Farmingdale, NY, USA) [53] have been reported. In one study, an extracorporeal HIFU device was used non-invasively at a frequency of 1 MHz and was guided by an ultrasound imaging transducer [136]; however, another study invasively applied laparoscopic HIFU to bring the laparoscopic probe into direct contact with the tumor at a 4 MHz operating frequency [22]. General or epidural anesthesia was performed for patients during these studies. Histological evidence of irreversible and homogeneous thermal damage within the treated area was shown after excision [22, 139]. MRI assessment of a series of 30 patients with kidney tumors treated with extracorporeal HIFU showed necrosis in two tumors in the lower

kidney pole shortly after HIFU treatment and shrinkage six months after treatment [136, 137]. The ablation of kidney tumors was shown in 67% of treatment cases, assessed radiologically by magnetic resonance imaging 12 days after treatment [136]. Wu et al. [138] reported that 90% of their 13 patients had their pain resolved immediately following HIFU [138]. Kohrman et al. [137] reported unsuccessful HIFU treatment in the upper pole of the kidney due to energy absorption by interposed ribs in the way of the beam [137]. Further investigations continue with respect to the efficiency of HIFU treatment on patients with advanced stage kidney malignancy for both cure and palliation [140].

3.6.6 Esophageal tumor

Esophageal cancer is the eighth most common cancer [141]. Esophageal cancer presents as small localized squamous-cell cancers in the intraluminal part of esophageal tissue. This disease is diagnosed by endoscopic biopsy and is often diagnosed late. The treatment of esophageal cancer depends on the stage of cancer and location, together with the person's general condition [142]. The common current treatment methods include surgery and chemotherapy with or without radiation therapy along with surgery [142]. Results of these treatments are related to the extent of disease and medical conditions, but overall these methods of treatment tend to have poor outcomes [141, 143]. The 5-year survival rates for this disease are about 13 to 18% [144]. Because HIFU is capable of generating rapid, complete, and well-defined coagulation necrosis, it has been considered for esophageal tumor treatment. The first clinical results of treatment of esophageal tumors by HIFU were reported in 2008 [145]. Thermal ablation of esophageal tumors was performed on four patients with a water-cooled interstitial ultrasound transducer operating at a frequency of 10 MHz. A single lesion at 10 mm depth from the surface of the transducer was induced at 14 W/cm^2 for 10 s. The interstitial probe capable of mechanical rotation around its

axis enables treatment of sectorial or cylindrical volumes and is particularly suitable for esophageal tumors. The transducer in this device was such that it could deliver a parallelepiped-shaped high-intensity beam to the target. A schematic of the therapeutic transducer is shown in Figure 3-6. The treatment is monitored using an ultrasound imaging probe located in the head of the applicator. The head of the transducer is round to allow for transesophageal application without risk of injury (Figure 3-6). The applicator is connected to a flexible metallic shaft as long as 80 cm with an outer diameter of 10 mm. The rotation of the applicator is controlled remotely through this shaft. The applicator is inserted into the esophagus through the mouth and is placed inside the esophageal tumor. Ablation of the tumor is performed under ultrasound guidance (Figure 3-7). Complete tumor necrosis was achieved in one patient, while objective tumor response was evident in all patients. Significant dysphagia improvement within 15 days was seen in all patients, with three of them able to eat a solid diet after treatment. This clinical study indicated the efficacy of intraluminal HIFU therapy for local esophageal tumors.

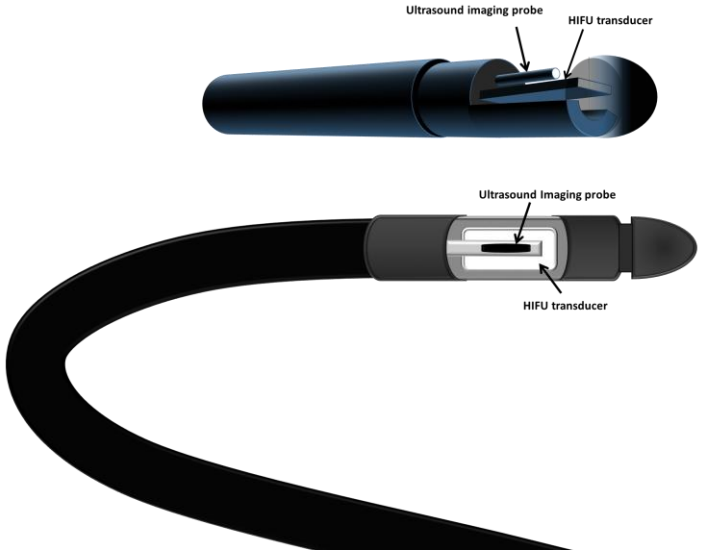

Figure 3-6 Schematic of the front and side view of the head of the interstitial transducer used for the treatment of esophageal tumors. The ultrasound imaging probe along with the HIFU transducer are located at the head of the interstitial transducer to image and treat the region of interest.

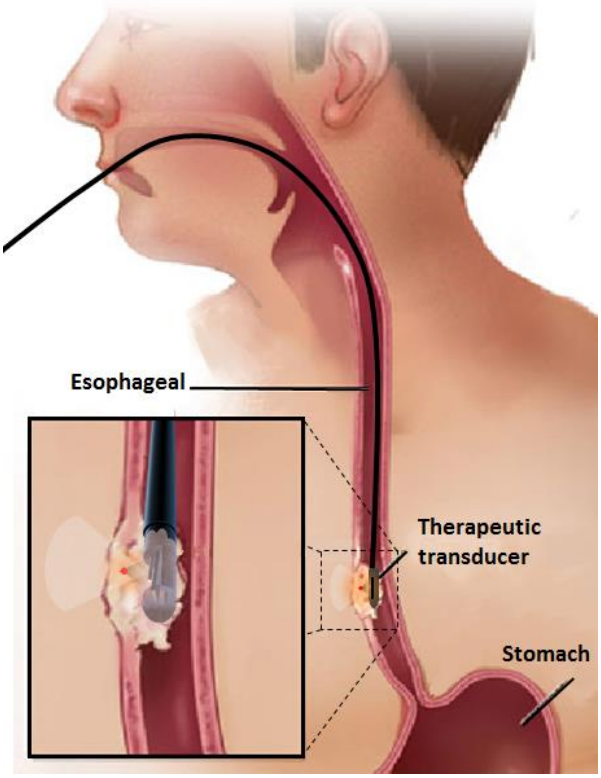

Figure 3-7 Schematic of the application of the interstitial HIFU probe in esophageal cancer treatment. The applicator is inserted into the esophagus through the mouth and the transducer placed inside the cancerous cells that line the inside of the esophagus. Esophageal cancer ablation along with ultrasound scanning of the targeted area are performed simultaneously by this HIFU system. (Courtesy of Mayo Foundation for Medical Education and Research)

3.6.7 Pancreas tumor

In 2008, Pancreatic cancer was the fourth commonest leading cause of cancer-related death across the world [146]. And in 2016, pancreatic cancer moved from fourth to third leading cause of cancer-related death in the U.S. [147]. This disease typically spreads rapidly and is rarely detected in its early stages; signs and symptoms may not appear until the cancer is in its advanced stages. The 5-year survival rate for patients diagnosed with pancreatic cancer is less than 5% [148]. Surgery is possible for only 20% of pancreatic cancers and a non-invasive therapy technique such as HIFU could be a solution. Studies on the treatment of pancreatic tumors in patients not eligible for surgery included approaches that involved only using HIFU

[28, 149, 150], chemotherapy using gemcitabine jointly with HIFU [149, 151], and HIFU therapy after failure of chemotherapy and/or radiotherapy treatment [149]. A study of 251 cases of advanced pancreatic cancer with focused ultrasound surgery in China suggested that HIFU can decrease the size of pancreatic tumors with no signs of pancreatitis [152]. The pain related to unresectable pancreatic cancer was resolved in 80% of patients within 24-48 h after a single session of HIFU treatment and did not return during the follow-up period; the average survival rate was 12.5 (223 patients survived 8 to 36 months and 6 patients survived more than 3 years). No sign of hemorrhage, large blood vessel rupture or gastrointestinal perforation, dilatation of the pancreatic duct in follow-up images, post-interventional pancreatitis, peritonitis, or jaundice was observed in any of the patients [152]. In their study with 35 patients, Jung et al. showed vertebral necrosis in all patients, subcutaneous fat necrosis in 26% of patients, different pain grades in 71% of patients, and transient pancreatitis in 15% of patients [28]. They observed major complications for 8.5% of patients including tumor-duodenal fistulas with severe abdominal pain, duodenal stent, and a third-degree burn of the anterior abdominal wall [28]. Zhao et al. in their study of 30 patients reported no evidence of post-interventional pancreatitis or peritonitis during the follow-up period after HIFU treatment [151]. In another study by Xiong et al. [149], 89 patients were treated with HIFU; subcutaneous sclerosis due to thermal injury to the subcutaneous fat of the anterior abdominal wall was reported in 6.7% of cases, pancreatic pseudocysts were reported in 1.1% of cases, and no treated patient reported severe complications [149].

Other human studies have reported the pain relief associated with pancreatic adenocarcinoma and observed focally ablated malignant tissue [153]. No skin burns were reported by He et al.

[152] or Zhao et al. [151]; however, second-degree skin burns were reported by Jung et al. [28] in all 35 patients and third-degree skin burn in 3% of patients.

Extracorporeal HIFU treatment of pancreatic cancer has been performed using three different devices: an extracorporeal ultrasound-guided Model-JC system (HAIFU, Chongqing, China) [28, 153], HIFUNIT-9000 tumor therapy equipment (Shanghai A&S Sci-Tech Co., Ltd, Shanghai, China) [66], and a FEP-BY system (Yuande Biomedical Engineering Limited Corporation, Beijing, China) [149]. The patients were in either a prone or supine position and, depending on the therapeutic device, the transducer was placed either above or below the patient. Patients can be treated without anesthesia [67] or undergo general anesthesia [69] or regional anesthesia [66].

In these studies, real-time ultrasound images were used to target the tumor during HIFU therapy that ablated it slice by slice until the whole mass was covered [28], [151], [149], [150]. In order to determine and evaluate the tumor response and ablation after HIFU treatment, both contrast enhanced computed tomography (CT) [154] and MRI [28], [150] have been used to determine tumor vascularity before and after HIFU therapy. Color Doppler ultrasound [150] was used in these studies.

Overall, pancreatic cancer treatment with HIFU only achieves an average tumor reduction rate of 50% [150], with concurrent gemcitabine and HIFU treatment showing an overall and partial response rate of 43.6% [151] and 14.6% [149], respectively.

3.6.8 Bone cancer

A bone tumor is an abnormal and uncontrollable growth of tissue in bone that can be either benign (non-cancerous) or malignant (cancerous). The average 5-year survival rate for patients diagnosed with bone and joint cancer in the United States is 67% [155]. Surgery is usually

performed for primary bone tumors and radiation therapy is used for bone metastases. Because of the great difference in acoustic blockage between bone and the surrounding soft tissue, HIFU was not initially considered as a potential treatment technique for bone cancer; however, an experiment performed by Smith et al. [156] on the thermal effect of focused ultrasound on bone tissue showed necrosis of osteocytes in normal rabbits. A pathological study of human malignant bone tumors treated with HIFU showed the destruction of endothelial cells of microvessels and thrombosis, and the potential of HIFU for preventing haematogenous dissemination of the tumor cells [157]. A theoretical study on the optimal external parameters of HIFU for bone tumor treatment [158] showed that the treatable diameter of bone tumors increases with increasing absorption ratio of bone marrow to tumor, acoustic window of surface skin, and bone diameter; the treatable diameter decreases with decreasing muscle thickness and is affected by the specific absorption rate ratio of bone tumor site to the surface skin, bone marrow, and bone. They also indicated that the specific absorption rate at the bone tumor site should be three times higher than that in the surface skin, tumor/marrow, and marrow/bone interfaces to avoid damage to normal tissue [158]. Since 2002, patients with bone tumors have been successfully treated with HIFU in China [159].

HIFU studies have been conducted for solace of pain from bone metastases [160-162] and also to treat primary bone malignancies [163-165]. HIFU devices that are commercially used for these purposes include the MRI-guided therapy system ExAblate 2000 (multielement phased-array transducer with a frequency of 1.0–1.5 MHz) [160], [161], [162] and ultrasound imaging guided therapy unit Model JC (13.5 cm focal length and 0.8 MHz transducers) [163], [164], [165]. Patients undergo either suitable anesthesia [163], [164] [165] or conscious sedation [160],[161] [162].

The application of HIFU alone in 30 patients with malignant solid tumors who refused surgery or were refractory to chemotherapy showed no intensification of all treated regions, with an even, thin intensification rim around the treated region [166]. A survival rate of 87% (26 patients) was reported after a follow-up period of 10 to 38 months (mean 23.1 months). Complete regression of the tumor volume was observed in 10 patients. Shrinkage of the tumor volume of ≥ 50% was observed in 13 patients. Examination of large core needle biopsies on eight of 13 patients showed necrosis and/or fibrosis, although three patients had local recurrence. No local recurrence in most of their treated patients suggested the effectiveness of HIFU alone to manage malignant bone tumors. However, nerves might not be clearly monitored during ultrasound guided HIFU, as two patients in Chen et al. [166] suffered peripheral nerve injuries and one patient developed a skin injury. Bone scan (99mTc-MDP) showed the disappearance of radioactive uptake and production of a radioactive cold region that suggested complete inactivation of the tumor foci.

Further studies were also done using extracorporeal HIFU with or without chemotherapy on 44 patients with primary malignant bone tumors, with a mean follow-up period of 17.6 months [166]. This study had a survival rate of 84.1% and a complication rate of 18.2%. In 34 patients with stage II b disease, 30 survived disease-free, two died due to tumor metastasis to brain and lung, and three developed local recurrence. Among 10 patients with stage III b disease, five survived with tumors, out of which one experienced a local recurrence, and five died due to lung metastasis.

In various other studies, patients were treated using HIFU for ablation therapy of various primary bone malignancies, including osteosarcoma, periosteal osteosarcoma, ewing sarcoma, chondrosarcoma, giant cell bone cancer, periosteal sarcoma and fibrous histiocytoma, and localized painful bone metastases [163], [164], [165].

In a study performed by Li et al. [164] on use of HIFU to treat primary and metastatic bone tumors in 25 patients, MRI or positron emission tomography (PET)-computed tomography (CT) radiological evaluated patients before and after HIFU treatment. Their study on patients with primary bone tumors showed complete tumor ablation in six (46.2%), partial response in five (38.4%), moderate response in one (7.8%), and disease progression in one patient. Comparable results were observed for metastatic bone tumors: five with (41.7%) complete response, four with (33.3%) partial response, one with (8.3%) moderate response, one with (8.3%) stable disease, and one patient with disease progression. They reported 1-, 2-, 3-, and 5-year survival rates for metastatic tumors of 83.3, 16.7, 0, and 0%, respectively. For patients with primary bone tumors, they reported 1-, 2-, 3-, and 5-year survival rates of 100.0, 84.6, 69.2, and 38.5%, respectively, which are considerably better than for patients with metastatic bone tumor.

Another three studies with more focus on palliation of pain of metastasic bone diseases using HIFU showed a pain reduction of 92% [161], 69.5% [160], and 82% [162] after three months of HIFU treatment compared to pain scores before treatment. HIFU for palliation of pain of metastasic bone diseases can be applied with no delay in post-operative chemotherapy as no surgical trauma or repair are involved with HIFU treatment [160].

Mild local pain and edema in all patients, first- and second-degree burns [163-165], and third-degree burns that required further surgical interventions, peripheral nerve damage, bone fracture, ligamentous laxity, epiphysiolyses, and secondary infections [163] were reported as complications of treatment cases in several different studies.

The results of preliminary studies indicated that HIFU was effective and well tolerated, and it was possible to preserve the limb during HIFU treatment of bone tumors as no surgical trauma or

rupture of vessels greater than 2 mm in diameter were reported. In fact, the main vessels could be retained, which is beneficial for revascularization and repair of inactivated tumor bones [36].

Local bone denervation by MRgFUS can be a promising tool for palliation of pain due to bone metastases. Osteoarthritis causes severe knee pain and troubles at elderly ages. In 2013, MRgFUS was used to study the management of osteoarthritic knee pain on eight patients with medial knee pain [67]. MRgFUS was applied to the bone surface just below the rim osteophyte of the medial tibia plateau with follow-up after one month. Immediate pain relief was observed in six patients (75%) after treatment, and a long-lasting effect at 6-months follow-up in four patients with no adverse side effects or complications. A notable rise of the pressure pain threshold in the treated area represents the successful denervation effect on the nociceptive nerve terminals. MRgFUS is an effective, non-invasive, safe, and promising clinical pain management technique for knee osteoarthritis. When the acoustic energy is focused on the intact surface of cortical bone, it causes a sudden temperature rise that mediates critical thermal damage to the adjacent periosteum, the most innervated component of mature bone tissue. This approach is very effective in pain management [167]. In addition, local tumor control, allowing remineralization of trabecular bone or lesion size reduction, is other potential application of this technique [167]. The effectiveness of MRgFUS for treatment of osteoid osteoma, a painful bone tumor, has been demonstrated extensively in a review study by Temple et al. [168]. Creation of a clinical MRgFUS treatment program for the treatment of bone tumors such as osteoid osteoma would not only be a cutting-edge medical treatment but would also help support investigations into the treatment of other bone lesions, such as osteoblastoma, aneurysmal bone cyst, and eosinophilic granuloma [168].

Overall, HIFU alone or combined with chemotherapy can be a safe and very effective way of treating primary malignant bone tumors. The limb-salvaging ability of HIFU (preserving good function in the limbs) can make HIFU a new clinical modality for treatment of bone tumors. Also, MRgFUS can be an alternative non-invasive method for palliation of pain in skeletal metastases. MRgFUS offers several key advantages over other non-invasive treatment modalities. This technology offers three-dimensional treatment planning along with real-time temperature mapping in the target area, and so can be a promising technique for successful palliation of bone metastasis pain and tumor control due to the bony structure remodeling induced by thermo-related coagulative necrosis [167]. Given the positive results of initial pilot studies on MRgFUS, a phase III trial is needed with the results compared to radiofrequency/laser ablation [168].

3.6.9 Brain Disorders

The ability of HIFU to focus acoustic energy through the intact skull onto a target as small as a couple of millimetres would be a considerable milestone in the field of neurosurgery for treating brain-based disorders. Recently, MRgFUS has been used in several studies as an effective and non-invasive thermal ablation technique to disrupt the blood-brain barrier and make intracranial thermal ablation lesions in the brain to overcome certain brain disorders. In MRgFUS, ultrasound can be successfully transmitted through the intact skull and overcome the energy dispersion, reflection, absorption, and distortion due to the bony skull, and allow the user to monitor tissue disruption, ablation, or vascular permeability by real-time MR imaging and MR thermometry. This technique can verify the efficiency of HIFU through patient and imaging feedback [169].

The device usually used for HIFU application to the brain is a spherical, phased array, multielement transducer helmet that allows the ultrasound energy to be focused at a target area

[170]. The helmet is coupled to software that compensates for the wave front distortions induced by passage of ultrasound through the bony skull. An MRgFUS helmet contains more than 1000 individual transducer elements [169]. MRI is performed during treatment for high resolution visualization of the brain target as well as real-time tissue temperature variation mapping [171-173]. Patients undergo local head anesthesia for the procedure. Figure 3-8 shows a model ExAblate Neuro (InSightec, Haifa, Israel) MRgFUS transducer helmet.

Figure 3-8 An ExAblate Neuro (InSightec, Haifa, Israel) MRgFUS transducer helmet on an MRI table. Cooled degassed water is carried through the attached hose to the helmet to provide the medium through which the ultrasound travels. This water is also used to fill the space between the patient's head and the transducers to keep the skull bone temperature within a safe range [169].

Currently, MRgFUS can be used to focally ablate neural tissue or to temporarily disrupt vessel permeability (blood-brain barrier). Current studies on MRgFUS for brain treatments are at

different levels of investigation and status [169]. So far, MRgFUS has been used to treat movement disorders (essential tremor; ET) [174, 175], Parkinson's disease (PD), Alzheimer's disease (AD) [176, 177], brain tumors, depression/anxiety, pain syndromes [178-180], epilepsy, thrombolysis/intracerebral hemorrhage [181-184], and cerebrospinal fluid (CSF) diversion [185].

3.6.10 Essential Tremor

Essential tremor (ET) is a movement disorder that mostly affects the upper extremities and the dominant arm in particular. The tremor is commonly postural, is heightened by movement, and can lead to significant disability and functional impairment over time [169]. ET is often refractory to medical treatment. Up to 25-30% of patients resist common medical treatments, and neurosurgical options may be more appropriate. The target for surgical approaches to treat ET is the ventral intermediate (VIM) nucleus of the thalamus [186]. In common surgical techniques, disruption of the VIM is achieved either by ablating the nucleus through radio frequency (RF) thalamotomy at 75-80 °C or by deep stimulation of the brain. Both of these techniques are invasive and require insertion of probes inside the brain, which incurs surgical risks such as infection and hemorrhage [169]. The first MRgFUS treatment experience was reported in four patients with chronic, medically refractory ET [174]. All patients showed immediate and sustained improvement in tremor. At the 1- and 3-month follow-up points, patients had tremor reductions of 89.4 and 81.3%, respectively. Functional impairment secondary to tremor decreased by an average of 40%. One patient experienced post-operative paraesthesia at three months and another developed deep vein thrombosis; no serious adverse events were reported for the other patients. MRI monitoring of thalamic lesions at time intervals of 1 week and 1 and 3 months showed a gradual evolution of lesions. MRgFUS thalamotomy was attempted by another research group at the University of Virginia on 15 patients with ET [175]. Thermal ablation of

the thalamic target was reported in all patients, and four patients (27%) showed adverse effects of the procedure including transient sensory, cerebellar, motor, and speech abnormalities with persistent paresthesias [175]. At 1-year follow-up, patients had a 75% mean decrease in their dominant arm tremor score and 85% decrease in functional disability. In 2015, Chang et al. studied unilateral MRgFUS thalamotomy on 11 patients with medication-resistant ET and evaluated tremor and neuroimaging at baseline and for a 6-month follow-up period; notably, only 8 patients received the complete MRgFUS treatment and sufficient temperature increase [187]. They assessed tremor severity and functionality at 1 week and 1, 3, and 6 months follow-up points. Immediate and sustained improvement in tremors was observed in all patients through the 6-month follow-up period. One patient experienced mild and delayed post-operative balance issues, but others showed no significant post-surgical complications.

The results of these studies suggest that MRgFUS is a safe, effective, and less invasive surgical modality for the management of disabling, medication-resistant essential tremor; however, long-term follow-up and larger trials are required to validate the safety, efficacy, and durability of this new approach. Issues such as optimal patient selection and management during treatment must also be resolved before clinical application of MRgFUS.

3.6.11 Chronic and non-malignant pain

Chronic and non-malignant pain is considered one of the most challenging conditions to treat. The first treatment approach is usually pharmacological medication; however, for patients who remain symptomatic despite all medications, surgical procedures with ablative or destructive procedures that target either the sensory or affective component of the condition can be used to treat both central- and peripheral-type pain syndromes [188]. Central procedures in which the brain and spinal cord are targeted include thalamotomy, cingulotomy, and dorsal root entry zone-

otomy, and peripheral procedures in which specific nerves or nerve bundles are targeted include ganglionectomy and rhizotomy [188]. The first examination of MRgFUS on chronic, medication-resistant neuropathic pain was a study in 2009 on nine patients [179]. Central lateral thalamotomy was conducted on these patients and the ablation target was the posterior part of the thalamic central lateral nucleus. None of patients showed any side effects or neurological deficits. All patients experienced some level of pain relief during the procedure and in the range of 30 to 100% 48 hours after treatment. The size of the lesion at the target site was determined by MRI to be 3-5 mm in diameter 48 hours after the procedure. This proof-of-concept study of MRgFUS was extended in another study in 2012 on 11 patients with chronic pain [189]. Thermal ablation lesions in the posterior part of the central lateral thalamic nucleus that were 3-4 mm in diameter were produced and peak temperatures of 51 and 64 °C were applied. Patients receiving the MRgFUS treatment were followed for 1 year, with 49% experiencing pain relief at 3 months and 57% at 12 months. Immediate pain relief was reported by six patients following their procedure; however, a small hemorrhage in the area of the motor thalamus was reported in one patient. Also, bleeding complications in the target area with ischemia in the motor thalamus was reported in one case; this was interpreted as a safety issue due to potential cavitation or the maintenance of sonication temperatures below 60°C. MRgFUS avoids mechanical brain tissue shifts and eliminates the risk of infection; in addition, the application of MRI for real-time scanning and thermometry monitoring of the target are major factors for optimizing precision, safety, and efficacy during treatment with this technique [189].

3.6.12 Trigeminal Neuralgia

Trigeminal neuralgia (TN) is a chronic sharp, stabbing electric pain that affects the trigeminal nerve, one of the most distributed nerves in the head, and is a form of neuropathic pain. Surgical

treatments for those patients for whom medication is insufficient or not tolerated focus on the trigeminal nerve and include intentionally damaging the nerve and its divisions in an unrestrictive way or relieving vascular compression of the nerve at its root entry zone [190]. One of the surgical techniques is gamma knife radiosurgery, in which a gamma radiation dose of 80 Gy is administered to the mid-cisternal portion of the nerve [169]. Even though most patients experience pain relief and are pain-free with or without medication, gamma knife radiosurgery includes the variation in susceptibility to radiation between patients, as well as the creation of radiation-related complications, such as secondary malignancy [169]. MRgFUS has been of interest for treatment of TN; however, there are concerns associated with the production of thermal injury next to the trigeminal nerve because of the adjacent petrous bone [169]. This limits applications based on the target location, making the technique only optimal for targets in the center of the brain. The feasibility of MRgFUS for making a trigeminal root entry zone lesion was studied on four unpreserved cadavers in a study in 2013 [178]. The application of MRgFUS along the length of the trigeminal nerve starting at the root entry zone for 10-30 s (at 25-1500 W) increased the temperature by a mean of 10 °C. The petrous bone got as hot as the nerve yet the study concluded that the treatment could be feasible. Some *in vivo* studies are necessary to confirm the safety and efficiency of MRgFUS for TN treatment.

3.6.13 Brain tumor

The most common malignant tumor of the central nervous system is glioblastoma. Treatment of glioblastoma typically involves radiological tissue diagnosis followed by surgical resection and chemo/radiation therapy. In the last 50 years, few advances have been made in the treatment of in malignant brain tumors. Brain tumor management has numerous challenges, including the infiltrative nature of the tumor, which is shown as diffusely spread throughout the brain at the

time of diagnosis, as well as the inability of chemotherapy regiments to effectively cross the blood-brain barrier [169]. MRgFUS as a potential non-invasive method of treatment has been studied in clinical and preclinical trials to address these two typical challenges. Transcranial MRgFUS surgery of brain tumors was studied in three glioblastoma patients in 2010 [191]. The feasibility of MRgFUS through the intact skull and the radiologic effect of thermal ablation in the target tumor with contrast-enhanced MRI were evaluated in this study. One patient underwent the procedure at the highest acoustic power level of 800 W; the other two underwent the procedure at 650 W due to a conservative software setting, and only one reported sonication-related pain. There was difficulty mapping the temperature variation in the tumor in one patient, where signal loss in the MRI was presumably due to blood remaining. The authors of this study, the first study on patients, could not access sufficient power to clearly achieve thermal coagulation and ablation. But, based on extrapolation of their results, they suggest that ablation is possible without overheating the skull. They observed focal heating within the target tumor in all three patients to an overall maximum of 51°C (individual maxima of 42, 51, and 48 °C) for 20 s sonication, which is not clearly above the threshold for thermal damage in the brain [192]. However, based on their measurements, they suggest achieving a peak focal temperature of 55 °C, which is sufficient to produce thermal necrosis, would require a power level of approximately 1200 W for a 20 s period. Cavitation effects are more likely to be generated in tissue and vessels at a lower frequency and higher intensity. Hemorrhage of small capillary blood vessels has been reported in the brain during high-intensity sonication [193-195]. However, Hynynen et al. [71] reported that an ultrasound intensity above 4400 Wcm^{-2} for 1 s generates transient cavitation in tissue and can cause serious effects on blood vessels as small as 1.0-1.3 mm in diameter and cause bleeding. Overall, based on findings of McDannold et al. [191],

ablation of brain tumors appears to be feasible with MRgFUS; however, additional trials investigating MRgFUS ablation for metastatic brain tumors should be conducted to verify these findings. A review by Cohen-Inbar et al. extensively discusses the effect of focused ultrasound on immunomodulatory therapy as a promising treatment approach for patients with glioblastoma multiforme, who exhibit a deficient anti-tumor immune response [196]. Immunotherapy by focused ultrasound mostly relies on mechanical acoustic cavitation and immunomodulation that play key roles in increasing the host anti-tumor immune response. Considering all focused ultrasound-induced pro-inflammatory cytokine secretion and stress responses, changes in the intra-tumoral immune cell population, augmentation of dendritic cell activity, and increased cytotoxic cell potency, it was suggested that focused ultrasound combined with immunotherapy can offer a synergistic treatment to overcome glioblastoma multiforme-induced immune evasion [196].

3.7 Potential future clinical applications of focused ultrasound

3.7.1 Vessel occlusion by HIFU

Blood vessel occlusion aided by HIFU or MRgFUS can be a potential technique in the treatment of arteriovenous malformation (a congenital disorder of blood vessels in different parts of the body, such as the brain, brainstem, or spinal cord) to control abdominal, peritoneal, and pelvic hemorrhage. HIFU or MRgFUS can also be used to block blood supply and interrupt the main blood flow to a tumor and may lead to tumor shrinkage. Recently, studies to interrupt blood flow have been conducted in animals [197]. A complete stoppage of blood flow, and no damage to surrounding soft tissues were observed in color Doppler imaging and MRI, and lack of perfusion in the renal cortex was also observed in color Doppler ultrasound image[197-199]. Histological results show an infarcted tissue volume corresponding to a wedge shape. The animal studies

suggest that HIFU or MRgFUS can be used as a vessel occlusion modality; however, additional studies should be done before clinical application to obtain more data about the relationship between the HIFU intensity required for flow occlusion, blood vessel diameter, and flow velocity, and to investigate possible long-term adverse effects [36].

3.7.2 Disruption of blood brain barrier

The inability of chemotherapy regiments to cross the blood-brain barrier is a challenge that might be addressed by MRgFUS. The blood-brain barrier is a filtering mechanism that blocks the passage of certain substances by tightly bound capillary endothelial cells. The capillaries that carry blood to the brain and spinal cord tissue are lined by a continuous layer of epithelial cells that ban the transport of large and harmful molecules between cells [200]. This rigid biochemical barrier prevents the use of neurotherapeutic treatments for tumors and diseases associated with neurodegeneration of the nervous system (such as Alzheimer's and Parkinson's diseases) that involve the brain. MRgFUS can be a potential technique to disrupt the blood-brain barrier and facilitate the passage of large drugs such as chemotherapy agents and monoclonal antibodies to the brain. Preclinical studies show that the disruption is temporary, occurs without any lesions or irreversible damage [201], and allows drugs to safely pass the blood-brain barrier. The mechanical effect of ultrasound is most often mediated by cavitation bubbles generated in tissue by the pressure wave. The production of cavitation bubbles requires very high exposures that are often accompanied by blood vessel rupture or occlusion[71], and therefore should be controlled for complete tissue disintegration [202] or vaporization [203, 204]. However, these microbubbles are very effective energy concentrators and can mediate ultrasound bioeffects at power levels less than 0.1% of that needed for thermal coagulation. The generation and interaction of

cavitation bubbles in the brain can briefly open the blood-brain barrier with no permanent effect on brain tissue [205].

The introduction of preinjected microbubbles into the capillary along with MRgFUS can also ease the procedure [200]. Premade microbubbles are routinely injected in the bloodstream because the existence of these microbubbles is helpful to increase ultrasound signals from the blood for diagnostic purposes. The oscillation and growth of microbubbles close to endothelial cell membranes leads to opening of the blood-brain barrier within seconds of the start of the sonication procedure [200, 206, 207]. The generated opening is generally healed within 6 hours post-treatment and, in cases with more serious tissue effects, within 24 hours [208]. However, these results were from *in vivo* animal study. Several other animal studies [209-211] have shown the proof of concept that MRgFUS can safely disrupt the blood-brain barrier and achieve significant brain tissue concentrations of complex and large biologic agents.

Another disease with the potential to be treated by MRgFUS is Alzheimer's disease. Alzheimer's disease is one of the most common neurodegenerative disorders, and the very low rate of success in medication therapy is associated with the difficulty of passage of amyloid-beta (Aβ) peptide through the blood-brain barrier. Some animal studies have shown that only 0.1% of intravenously administered anti-Aβ antibodies reach the brain [212, 213]. However, other animal studies have shown that the disruption of the blood-brain barrier by MRgFUS is an effective approach toward introduction of antibodies and decreasing plaque burden [213, 214].

To the best of our knowledge, there are no published reports on human patients. However, a group of neurosurgeons at the University of Toronto are conducting human trials for brain tumor therapy using MRgFUS [169].

3.7.3 Histotripsy

Histotripsy is an experimental extracorporeal ultrasound technology that relies more on the mechanical effect of ultrasound by utilizing cavitational mechanisms of energetic microbubbles to generate non-thermal tissue destruction (fragmentation and subdivision of tissue that results in cellular destruction). In histotripsy, a number of short, high-intensity ultrasound pulses at a 1 kHz pulse repetition rate and 18 MPa rarefactional pressure for 20 μs duration are sent to the target [215]. Delivery of such intense, high pressure, and short bursts to the tissue leads to cavitation bubble formation in the target zone. Subsequent cavitation processes such as oscillation, growth, and collapse of microbubbles will occur close to the cells. The cavitation process leads to mechanical fractionation of targeted tissues to reduce architectural and cellular structures to a fine slurry of acellular debris [216] and a liquefied core with very sharply demarcated boundaries [36]. Histotripsy is very similar to HIFU, with the primary difference being that the transducer in histotripsy has a center frequency around 750 kHz; HIFU applies less intense 3–5 second pulses of acoustic energy to heat tissues and produce thermal coagulation [217]. At a fluid-tissue interface, the cavitation process of histotripsy causes localized tissue removal with sharp boundaries. Histotripsy was used for cardiac tissue removal in the treatment of congenital heart disease (in an *in vitro* animal study with pigs) [218]. Compared to non-invasive thermal therapy, histotripsy has some advantages as a potential clinical tool where precise tissue ablation and removal are needed (e.g., tumor treatment). The cavitation microbubbles produced at the focal point act as a contrast in ultrasound imaging and provide real-time feedback during the procedure. The lesion can be produced in a very controlled and precise manner and is shown as a darker spot in post-operation imaging. Some animal studies are currently underway on applications to the kidney, breast cancer, prostate cancer, several cardiac conditions, and breast fibroadenoma [217, 219, 220].

3.7.4 Parkinson's disease

Parkinson disease is a heterogeneous motor disorder characterized by progressive degeneration of motor neurons. Preclinical studies have shown that disruption of key motor nuclei can lead to significant improvement in motor symptoms [221]. There is a high potential for use of MRgFUS for treatment of Alzheimer's disease and Parkinson's disease because this technique can be used to perform deep stereotactic thermal ablations. The risk of this technique is low due to the absence of penetration of the skin, bone, and brain as well as on-line monitoring of the thermocoagulation process. MRgFUS can be used as an ablative surgery tool in neurosurgery for treatment-resistant Parkinson's disease. The target for ablation in patients with disabling dyskinesias can be the globus pallidus with pallidotomy, and for patients with tremor-dominant disease the target can be ventral intermediate thalamus or VIM thalamotomy [169]. Recently, the interest and possibility of performing subthalamic thermocoagulations by MRgFUS with reduced risk and optimized accuracy has increased. In 2014, the first clinical study on the use of MRgFUS for treatment of Parkinson's disease was reported by Magara et al. [222]. Thirteen patients with chronic (mean average duration of disease for 9.7 years) and therapy-resistant Parkinson's disease were treated with an MRgFUS pallidothalamic tractotomy. The treatment procedure was performed in a 3 Tesla (T) MR imaging system (GE Discovery 750, GE Healthcare, Milwaukee, WI, USA) using the ExAblate Neuro device (InSightec, Haifa, Israel). As shown in Figure 3-9, the patient's head was covered with a flexible silicon membrane that was sealed to outer face of the ultrasound transducer helmet. Degassed and chilled water at a temperature between 15 and 18 °C was circulated in the volume between the head and the transducer to cool down the surface temperature and avoid damage. The target area of treatment, the pallidothalamic tract, was treated by an iterative process guided by MR imaging and MR thermometry. The temperature was increased stepwise by increasing the acoustic power to a

maximum of 1200 W and energy to a maximum of 20400 J for 13 s to reach a final temperature between 52 and 59 °C (average 56.2°C) at the target (considering the temperature of 54°C required for 100% necrosis). The procedure was performed with the patient fully awake. A group of four patients (group 1) received a single application at the peak energy, and a group of nine patients (group 2) received repetitive applications (4-5 times) of the peak energy on the target. Group 1 experienced clear-cut recurrence at 3 months, with thermocoagulation of a volume of 83 mm^3 and no sign of thermal lesion in their MR images. In group 2, the repetitive applications produced larger thermocoagulation volumes of 172 mm^3 that remained visible in MR images for 3 months. Primary relief as a reduction in score on the unified Parkinson disease rating scale was measured as 7.6% in group 1 and 60.9% in group 2. Patients' estimated global symptom relief at 3-months follow-up was 22.5% in group 1 and 56.7% in group 2. The clinical results showed no procedure- or device-related neurological side effects. The targeting accuracy for all patients was measured as 0.5 mm anteroposterior, 0.5 mm mediolateral, and 0.6 mm dorsoventral. This study indicates that that application of MRgFUS pallidothalamic tractotomy is feasible, safe, and accurate.

Figure 3-9 Intra-operative patient setup for MRgFUS procedure on the brain. The patient lies on the MR bed and the head is placed inside the phased-array ultrasound transducer helmet. [222]

3.7.5 Psychiatric disease

Ablation treatment approaches for treatment of refractory psychiatric diseases mainly target and disrupt the limbic pathways connecting the frontal lobe with subcortical structures [169]. In up to a third of patients with mood and anxiety disorders, pharmacologic and psychotherapeutic approaches are not completely satisfactory. These patients are candidates for neuromodulation techniques, including electroconvulsive therapy, transcranial magnetic stimulation, deep brain stimulation, and ablative or lesional procedures [223]. The main targets in cingulotomy (for

treatment of depression and obsessive-compulsive disorder) and capsulotomy (for treatment of refractory depression) are the anterior cingulate gyrus and anterior limb of the internal capsule, respectively [224, 225]. Two different studies on 44 patients with obsessive-compulsive disorder (with 32 months follow-up) and eight patients with refractory depression (with 2-3 years follow-up) showed complete or partial remission in half of the patients [224, 226]. These results suggest that MRgFUS can be a potential alternative to psychiatric treatment because of its non-invasive nature and ability to give real-time MR guidance.

3.7.6 Stroke and Thrombolysis

Deficient blood supply to a part of brain due to obstruction of the inflow of blood and hemorrhagic stroke leads to mortality and morbidity. Thrombolytics and surgery, in the case of intracerebral hemorrhage, are currently available treatment approaches, with surgery showing long-term improved outcomes [227]. For patients with intracerebral hemorrhage, MRgFUS has been proposed with the rationale being that it can liquefy blood to facilitate MR-guided aspiration and also help decrease the clot burden and mass effect and thus avoid a craniotomy [169]. Basically, the mechanical effect of ultrasound and, more specifically, the inertial cavitation effect under high pressure amplitude causes MRgFUS-mediated clot lysis. The power of ultrasound in this procedure is high so that inertial cavitation is sufficient with no need for injection of microbubbles [169]. Preclinical studies have shown liquefaction of intracerebral hemorrhage within seconds in a swine model and of more than 90% of the clot in a human cadaveric head, resulting in almost complete aspiration of blood [178]. In a recent study, Bonow et al. hypothesized that transcranial HIFU may have the ability to induce therapeutic cerebral vasodilation and, as a result, can one day be used for treatment of patients with subarachnoid hemorrhage [228]. Their review suggests the potential of transcranial MRgUS for treatment of

subarachnoid hemorrhage and other cerebral ischemic disorders. In the future, MRgUS systems may find their way to clinical trials and into regular clinical practice for treatment of cerebral vasospasm and other cerebrovascular diseases [228].

3.7.7 Abscesses

Basically, abscesses generated by bacterial infection consist of a localized lesion with an accumulation of pus, surrounded by a capsule built by fibroblasts [229]. Methicillin-resistant *Staphylococcus aureus* (MRSA) is a bacterium responsible for several infections in humans [230]. Abscess related to MRSA infections are difficult to treat as they are resistant to many of the antibiotics used to treat ordinary staph infections. Abscesses in inaccessible areas such as the groin and axillary region or in locations such as the liver, kidney, brain, breast, and bone (osteomyelitis) would benefit from non-invasive therapeutic techniques such as HIFU [231]. The heat generated by HIFU can increase the temperature at the precise location of the abscess and be used for disinfection or reduction of bacterial numbers. The use of heat for treatment and prevention of infection is applied via non-contact radiant heat pads for topical treatment of pressure sores [232] and reduction of intraoperative surgical site infection [233]. MRgFUS can be a very precise and controlled potential tool with the ability to reach deep tissues in body with real-time temperature monitoring. In 2014, an animal study (on mice) was performed to investigate the therapeutic effect of focused ultrasound on abscesses induced by MRSA [231]. The abscess was generated in the left flank of mice and the procedure performed at an ultrasound frequency of 3 MHz. Two different temperatures of 52.3 ± 5.1 and 63.8 ± 7.5 °C were generated by HIFU for two different treatment groups. The effectiveness of the MRgFUS treatment was determined by evaluating the number of bacteria in the treated abscess at 1 and 4 days after treatment. Reduction in the external size of abscess was seen 1 day after treatment, and a

significant reduction in bacterial load was observed 4 days after high temperature (63.8 ± 7.5 °C) treatment. No change in local neutrophil recruitment in the abscess, no systematic inflammatory response, and no open wounds were caused by the treatment. This study suggested MRgFUS is a viable option for the treatment of localized MRSA-related infections, and the results were promising. However, more extensive and realistic studies on human patients are required to draw definitive conclusions. To the best of our knowledge, no human studies have yet to be conducted in this regard.

3.8 Combined mechanisms for therapeutic application of ultrasound

Other therapeutic techniques involve multiple mechanisms of ultrasound. In intravascular catheters, a MHz-frequency transducer is placed near the tip for increasing dissolution of thrombi [234]. When the catheter is placed into a deep vein thrombus, the ultrasound is targeted radially into the thrombus or an infusion of thrombolytic drug such as tissue plasminogen activator is delivered into the thrombus [3]. Ultrasound-assisted drug delivery significantly decreases treatment time by increasing the permeability of cell walls and the infusion of drugs into the cells.

Another application of ultrasound is skin permeabilization, which may replace the multiple use of needles for drug delivery through the skin for medicines such as heparin and insulin [235]. Drug diffusion through the stratum corneum is difficult for molecules with a molecular weight greater than 500 Da [236]. Using low-frequency ultrasound (<100 kHz), the permeability of the stratum corneum (which is considered a protein diffusion barrier) increases [237] and the drug can pass and reach the inner layers and finally the capillary vessels where it is absorbed [238].

The use of low-intensity pulsed ultrasound (about 1.5 MHz) for accelerating the healing of bone fractures for cases such as non-union and non-healing fractures is another therapeutic action of ultrasound [3]. The biophysical mechanism behind this therapeutic action is not yet clear.

3.9 Prospective new research areas for application of therapeutic ultrasound

Several other streams of research are investigating therapeutic applications of ultrasound. These new methods mostly rely on low frequency and power ultrasound aided by microbubbles or very high power ultrasound for the production of vigorous cavitation [3]. The application of low-frequency ultrasound for direct sonothrombolysis for treatment of thrombotic disease such as stroke is a new strategy [239]. However, this method showed increased brain hemorrhage in a clinical trial [240]. Another potential use of ultrasound is to produce cortical and hippocampal stimulation in mice [241]. Non-thermal mechanisms have been hypothesized to be responsible for the neuronal effects in this method [3].

Ultrasound-aided drug delivery is another area of study. This technique is based on microbubbles and is under study for direct and targeted therapies that release drugs at a specific location within the body (such as cancerous area) without affecting the rest of the body. It can also be used to force drug flow from a vessel out into surrounding tissue and to increase intracellular delivery [3]. The advantage of ultrasound-microbubble techniques over other techniques such as nanoparticle or liposome delivery systems is the ability for external control [3]. DNA transfer in gene therapy applications has also been under extensive study [242].

Histotripsy, equivalent to lithotripsy pulses but at higher frequency and very high amplitude pulses, uses only the cavitation mechanism for tissue ablation [243] to homogenize targeted tissue, such as tumors, with little heating [244].

3.10 Conclusions

Both thermal and non-thermal (cavitation) effects play a very important role in all therapeutic applications of ultrasound. The side effects of these two mechanisms of action can be hazardous biologically and are therefore avoided in diagnostic applications of ultrasound but can be beneficial in therapeutic applications of ultrasound. The ability to focus ultrasound in an area a couple of millimeters in size enhances both the thermal and non-thermal effects of ultrasound and results in ablation and necrosis of cells at the applied focal point. This makes ultrasound a non-invasive therapeutic ablation technique for deep-seated targets within the body. HIFU therapy provides a less invasive approach to cancer therapy that minimizes discomfort to the patient and length of hospital stay. Initial studies have demonstrated HIFU to be safe and clinically effective and to have high potential clinical acceptance. However, HIFU is still in its infancy and further studies are necessary (especially in the field of oncology) regarding the long-term medical benefits, technical considerations, and treatment delivery before it transitions to widespread use. The range of HIFU applications may expand in the future with improved imaging; however, MRgFUS is one of the most successful imaging guide approaches in most therapies and seems to be an area of continuing interest. In fact, HIFU is an important milestone in the development of neurotherapeutics. The ability to focus ultrasound energy onto a brain target through the skull with a focal point of only a few millimetres has made HIFU, and especially MRgFUS, a fundamental achievement in the world of neurotherapeutics. Studies show that MRgFUS is a safe and non-invasive modality that has the potential to be an alternative to invasive open neurosurgical approaches. However, there is a need for more studies with long-term follow-up in this area before definitive conclusions are made. Overall, clinical results of therapeutic HIFU applications are encouraging and the method is competing with other

established ablation techniques such as RF-, laser-, or cryo-ablation [245], but more studies are needed to demonstrate the superiority of HIFU over other available surgery/radiotherapy techniques.

3.11 References

1. Mo S, Coussios CC, Seymour L, Carlisle R: **Ultrasound-enhanced drug delivery for cancer.** *Expert Opin Drug Deliv* 2012, **9:**1525-1538.
2. Crum L, Bailey M, Kaczkowski P, Makin I, Mourad P, Beach K, Carter S, Schmeidl U, Chandler W, Martin R: **Therapeutic ultrasound: A promising future in clinical medicine.** *Acoustical Society of America University of Washington* 2005, **21**.
3. Miller DL, Smith NB, Bailey MR, Czarnota GJ, Hynynen K, Makin IR: **Overview of therapeutic ultrasound applications and safety considerations.** *J Ultrasound Med* 2012, **31:**623-634.
4. Lehmann JF: **The biophysical basis of biologic ultrasonic reactions with special reference to ultrasonic therapy.** *Archives of physical medicine and rehabilitation* 1953, **34:**139.
5. Woo J: **A short history of the development of ultrasound in obstetrics and gynecology.** *See http://www ob-ultrasound net/history1 html (last checked 14 May 2011)* 2002.
6. Lynn JG, Zwemer RL, Chick AJ: **THE BIOLOGICAL APPLICATION OF FOCUSED ULTRASONIC WAVES.** *Science (New York, NY)* 1942, **96:**119-120.
7. Fry F, Ades H, Fry W: **Production of reversible changes in the central nervous system by ultrasound.** *Science* 1958, **127:**83-84.
8. Fry WJ: **Use of intense ultrasound in neurological research.** *American Journal of Physical Medicine & Rehabilitation* 1958, **37:**143-147.
9. Fry W, Fry F: **Fundamental neurological research and human neurosurgery using intense ultrasound.** *Medical Electronics, IRE Transactions on* 1960**:**166-181.
10. Fry WJ, Mosberg Jr W, Barnard J, Fry F: **Production of focal destructive lesions in the central nervous system with ultrasound.** *Journal of neurosurgery* 1954, **11:**471-478.
11. Newell J: **Ultrasonics in medicine.** *Physics in medicine and biology* 1963, **8:**241.
12. Wells PN: **Ultrasonics in medicine and biology.** *Phys Med Biol* 1977, **22:**629-669.
13. Kremkau FW: **Cancer therapy with ultrasound: a historical review.** *Journal of clinical ultrasound* 1979, **7:**287-300.
14. Cline HE, Hynynen K, Watkins RD, Adams WJ, Schenck JF, Ettinger RH, Freund WR, Vetro JP, Jolesz FA: **Focused US system for MR imaging-guided tumor ablation.** *Radiology* 1995, **194:**731-737.
15. Cline H, Schenck J, Watkins R, Hynynen K, Jolesz F: **Magnetic resonance-guided thermal surgery.** *Magnetic resonance in medicine* 1993, **30:**98-106.
16. Cline HE, Schenck JF, Hynynen K, Watkins RD, Souza SP, Jolesz FA: **MR-guided focused ultrasound surgery.** *Journal of computer assisted tomography* 1992, **16:**956-965.
17. Hynynen K, Damianou C, Darkazanli A, Unger E, Schenck J: **The feasibility of using MRI to monitor and guide noninvasive ultrasound surgery.** *Ultrasound in medicine & biology* 1993, **19:**91-92.
18. Hynynen K, Darkazanli A, Unger E, Schenck J: **MRI-guided noninvasive ultrasound surgery.** *Medical physics* 1993, **20:**107-115.
19. Kennedy J, Ter Haar G, Cranston D: **High intensity focused ultrasound: surgery of the future?** *The British journal of radiology* 2014.

20. Tempany CM, Stewart EA, McDannold N, Quade BJ, Jolesz FA, Hynynen K: **MR imaging-guided focused ultrasound surgery of uterine leiomyomas: a feasibility study.** *Radiology* 2003, **226:**897-905.
21. Ninet J, Roques X, Seitelberger R, Deville C, Pomar JL, Robin J, Jegaden O, Wellens F, Wolner E, Vedrinne C: **Surgical ablation of atrial fibrillation with off-pump, epicardial, high-intensity focused ultrasound: results of a multicenter trial.** *The Journal of Thoracic and Cardiovascular Surgery* 2005, **130:**803. e801-803. e808.
22. Klingler HC, Susani M, Seip R, Mauermann J, Sanghvi N, Marberger MJ: **A novel approach to energy ablative therapy of small renal tumours: laparoscopic high-intensity focused ultrasound.** *European urology* 2008, **53:**810-818.
23. Gliklich RE, White WM, Slayton MH, Barthe PG, Makin IRS: **Clinical pilot study of intense ultrasound therapy to deep dermal facial skin and subcutaneous tissues.** *Archives of facial plastic surgery* 2007, **9:**88-95.
24. Alam M, White LE, Martin N, Witherspoon J, Yoo S, West DP: **Ultrasound tightening of facial and neck skin: a rater-blinded prospective cohort study.** *Journal of the American Academy of Dermatology* 2010, **62:**262-269.
25. Burgess SE, Silverman RH, Coleman DJ, Yablonski ME, Lizzi FL, Driller J, Rosado A, Dennis PH, Jr.: **Treatment of glaucoma with high-intensity focused ultrasound.** *Ophthalmology* 1986, **93:**831-838.
26. Gelet A, Chapelon JY, Bouvier R, Rouviere O, Lasne Y, Lyonnet D, Dubernard JM: **Transrectal high-intensity focused ultrasound: minimally invasive therapy of localized prostate cancer.** *J Endourol* 2000, **14:**519-528.
27. Thuroff S, Chaussy C, Vallancien G, Wieland W, Kiel HJ, Le Duc A, Desgrandchamps F, De La Rosette JJ, Gelet A: **High-intensity focused ultrasound and localized prostate cancer: efficacy results from the European multicentric study.** *J Endourol* 2003, **17:**673-677.
28. Jung SE, Cho SH, Jang JH, Han J-Y: **High-intensity focused ultrasound ablation in hepatic and pancreatic cancer: complications.** *Abdominal imaging* 2011, **36:**185-195.
29. Jolesz FA: **MRI-guided focused ultrasound surgery.** *Annu Rev Med* 2009, **60:**417-430.
30. Makin IR, Mast TD, Faidi W, Runk MM, Barthe PG, Slayton MH: **Miniaturized ultrasound arrays for interstitial ablation and imaging.** *Ultrasound Med Biol* 2005, **31:**1539-1550.
31. Prat F, Lafon C, De Lima DM, Theilliere Y, Fritsch J, Pelletier G, Buffet C, Cathignol D: **Endoscopic treatment of cholangiocarcinoma and carcinoma of the duodenal papilla by intraductal high-intensity US: Results of a pilot study.** *Gastrointest Endosc* 2002, **56:**909-915.
32. Larrat B, Pernot M, Aubry J-F, Sinkus R, Tanter M, Fink M: **Radiation force localization of HIFU therapeutic beams coupled with magnetic resonance-elastography treatment monitoring in vivo application to the rat brain.** In *Ultrasonics Symposium, 2008 IUS 2008 IEEE*. IEEE; 2008: 451-454.
33. Diederich CJ: **Thermal ablation and high-temperature thermal therapy: overview of technology and clinical implementation.** *International journal of hyperthermia* 2005, **21:**745-753.
34. Lafon C, Melodelima D, Salomir R, Chapelon JY: **Interstitial devices for minimally invasive thermal ablation by high-intensity ultrasound.** *International Journal of Hyperthermia* 2007, **23:**153-163.

35. Schlesinger D, Benedict S, Diederich C, Gedroyc W, Klibanov A, Larner J: **MR-guided focused ultrasound surgery, present and future.** *Medical physics* 2013, **40:**080901.
36. Zhou Y-F: **High intensity focused ultrasound in clinical tumor ablation.** *World journal of clinical oncology* 2011, **2:**8.
37. ter Haar G, Rivens I, Chen L, Riddler S: **High intensity focused ultrasound for the treatment of rat tumours.** *Phys Med Biol* 1991, **36:**1495-1501.
38. Visioli AG, Rivens IH, ter Haar GR, Horwich A, Huddart RA, Moskovic E, Padhani A, Glees J: **Preliminary results of a phase I dose escalation clinical trial using focused ultrasound in the treatment of localised tumours.** *Eur J Ultrasound* 1999, **9:**11-18.
39. Dewey WC: **Arrhenius relationships from the molecule and cell to the clinic.** *Int J Hyperthermia* 1994, **10:**457-483.
40. Dewey WC: **Arrhenius relationships from the molecule and cell to the clinic.** *International journal of hyperthermia* 2009, **25:**3-20.
41. Lagneaux L, de Meulenaer EC, Delforge A, Dejeneffe M, Massy M, Moerman C, Hannecart B, Canivet Y, Lepeltier MF, Bron D: **Ultrasonic low-energy treatment: a novel approach to induce apoptosis in human leukemic cells.** *Exp Hematol* 2002, **30:**1293-1301.
42. Rao SR, Ballesteros N, Short KL, Gathani KK, Ankem MK: **Extra corporeal shockwave lithotripsy resulting in skin burns–a report of two cases.** *International braz j urol* 2014, **40:**853-857.
43. Rangarajan S, Mirheydar H, Sur RL: **Second-degree burn after shock wave lithotripsy: an unusual complication.** 2012.
44. Salgaonkar VA, Diederich CJ: **Catheter-based ultrasound technology for image-guided thermal therapy: current technology and applications.** *Int J Hyperthermia* 2015, **31:**203-215.
45. Deardorff DL, Diederich CJ, Nau WH: **Control of interstitial thermal coagulation: comparative evaluation of microwave and ultrasound applicators.** *Med Phys* 2001, **28:**104-117.
46. Deardorff DL, Diederich CJ: **Ultrasound applicators with internal water-cooling for high-powered interstitial thermal therapy.** *IEEE Trans Biomed Eng* 2000, **47:**1356-1365.
47. Owen NR, Bouchoux G, Seket B, Murillo-Rincon A, Merouche S, Birer A, Paquet C, Delabrousse E, Chapelon JY, Berriet R, et al: **In vivo evaluation of a mechanically oscillating dual-mode applicator for ultrasound imaging and thermal ablation.** *IEEE Trans Biomed Eng* 2010, **57:**80-92.
48. Nau WH, Diederich CJ, Burdette EC: **Evaluation of multielement catheter-cooled interstitial ultrasound applicators for high-temperature thermal therapy.** *Med Phys* 2001, **28:**1525-1534.
49. Kinsey AM, Diederich CJ, Tyreus PD, Nau WH, Rieke V, Pauly KB: **Multisectored interstitial ultrasound applicators for dynamic angular control of thermal therapy.** *Med Phys* 2006, **33:**1352-1363.
50. Kangasniemi M, Diederich CJ, Price RE, Stafford RJ, Schomer DF, Olsson LE, Tyreus PD, Nau WH, Hazle JD: **Multiplanar MR temperature-sensitive imaging of cerebral thermal treatment using interstitial ultrasound applicators in a canine model.** *J Magn Reson Imaging* 2002, **16:**522-531.

51. Nau WH, Diederich CJ, Simko J, Juang T, Jacoby A, Burdette EC: **Ultrasound interstitial thermal therapy (USITT) for the treatment of uterine myomas.** *Proc SPIE Int Soc Opt Eng* 2007, **6440:**64400F.
52. Haar GT, Coussios C: **High intensity focused ultrasound: physical principles and devices.** *Int J Hyperthermia* 2007, **23:**89-104.
53. Yagel S: **High-intensity focused ultrasound: a revolution in non-invasive ultrasound treatment?** *Ultrasound Obstet Gynecol* 2004, **23:**216-217.
54. Jolesz FA, McDannold N: **Current status and future potential of MRI-guided focused ultrasound surgery.** *J Magn Reson Imaging* 2008, **27:**391-399.
55. Khokhlova TD, Canney MS, Lee D, Marro KI, Crum LA, Khokhlova VA, Bailey MR: **Magnetic resonance imaging of boiling induced by high intensity focused ultrasound.** *J Acoust Soc Am* 2009, **125:**2420-2431.
56. Xu RX, Povoski SP, Martin EW, Jr.: **Targeted delivery of microbubbles and nanobubbles for image-guided thermal ablation therapy of tumors.** *Expert Rev Med Devices* 2010, **7:**303-306.
57. Brenin DR: **Focused ultrasound ablation for the treatment of breast cancer.** *Annals of surgical oncology* 2011, **18:**3088-3094.
58. Pediconi F, Napoli A, Di Mare L, Vasselli F, Catalano C: **MRgFUS: from diagnosis to therapy.** *European journal of radiology* 2012, **81:**S118-S120.
59. Fischer K, Gedroyc W, Jolesz FA: **Focused ultrasound as a local therapy for liver cancer.** *The Cancer Journal* 2010, **16:**118-124.
60. Okada A, Murakami T, Mikami K, Onishi H, Tanigawa N, Marukawa T, Nakamura H: **A case of hepatocellular carcinoma treated by MR-guided focused ultrasound ablation with respiratory gating.** *Magnetic Resonance in Medical Sciences* 2006, **5:**167-171.
61. Napoli A, Anzidei M, De Nunzio C, Cartocci G, Panebianco V, De Dominicis C, Catalano C, Petrucci F, Leonardo C: **Real-time magnetic resonance–guided high-intensity focused ultrasound focal therapy for localised prostate cancer: preliminary experience.** *European urology* 2013, **63:**395-398.
62. Zini C, Hipp E, Thomas S, Napoli A, Catalano C, Oto A: **Ultrasound-and MR-guided focused ultrasound surgery for prostate cancer.** *World journal of radiology* 2012, **4:**247.
63. Lindner U, Ghai S, Spensieri P, Hlasny E, Van der Kwast TH, McCluskey SA, Haider MA, Kucharczyk W, Trachtenberg J: **Focal magnetic resonance guided focused ultrasound for prostate cancer: Initial North American experience.** *Canadian Urological Association Journal* 2012, **6:**E283.
64. Bauer R, Martin E, Haegele-Link S, Kaegi G, von Specht M, Werner B: **Noninvasive functional neurosurgery using transcranial MR imaging-guided focused ultrasound.** *Parkinsonism & related disorders* 2014, **20:**S197-S199.
65. Magara A, Bühler R, Moser D, Kowalski M, Pourtehrani P, Jeanmonod D: **First experience with MR-guided focused ultrasound in the treatment of Parkinson's disease.** *J Therapeut Ultrasound* 2014, **2:**b74.
66. Napoli A, Anzidei M, Marincola BC, Brachetti G, Noce V, Boni F, Bertaccini L, Passariello R, Catalano C: **MR Imaging–guided Focused Ultrasound for Treatment of Bone Metastasis.** *Radiographics* 2013, **33:**1555-1568.
67. Izumi M, Ikeuchi M, Kawasaki M, Ushida T, Morio K, Namba H, Graven-Nielsen T, Ogawa Y, Tani T: **MR-guided focused ultrasound for the novel and innovative**

management of osteoarthritic knee pain. *BMC musculoskeletal disorders* 2013, **14:**267.
68. Napoli A, Mastantuono M, Cavallo Marincola B, Anzidei M, Zaccagna F, Moreschini O, Passariello R, Catalano C: **Osteoid osteoma: MR-guided focused ultrasound for entirely noninvasive treatment.** *Radiology* 2013, **267:**514-521.
69. Moreno-Moraga J, Valero-Altes T, Riquelme AM, Isarria-Marcosy MI, de la Torre JR: **Body contouring by non-invasive transdermal focused ultrasound.** *Lasers Surg Med* 2007, **39:**315-323.
70. White WM, Makin IR, Barthe PG, Slayton MH, Gliklich RE: **Selective creation of thermal injury zones in the superficial musculoaponeurotic system using intense ultrasound therapy: a new target for noninvasive facial rejuvenation.** *Arch Facial Plast Surg* 2007, **9:**22-29.
71. Hynynen K, Chung AH, Colucci V, Jolesz FA: **Potential adverse effects of high-intensity focused ultrasound exposure on blood vessels in vivo.** *Ultrasound Med Biol* 1996, **22:**193-201.
72. Rove KO, Sullivan KF, Crawford ED: **High-intensity focused ultrasound: ready for primetime.** *Urol Clin North Am* 2010, **37:**27-35, Table of Contents.
73. Borchert B, Lawrenz T, Hansky B, Stellbrink C: **Lethal atrioesophageal fistula after pulmonary vein isolation using high-intensity focused ultrasound (HIFU).** *Heart Rhythm* 2008, **5:**145-148.
74. Arii S, Yamaoka Y, Futagawa S, Inoue K, Kobayashi K, Kojiro M, Makuuchi M, Nakamura Y, Okita K, Yamada R: **Results of surgical and nonsurgical treatment for small-sized hepatocellular carcinomas: A retrospective and nationwide survey in Japan.** *Hepatology* 2000, **32:**1224-1229.
75. Bruix J, Castells A, Bosch J, Feu F, Fuster J, Garcia-Pagan JC, Visa J, Bru C, Rodes J: **Surgical resection of hepatocellular carcinoma in cirrhotic patients: prognostic value of preoperative portal pressure.** *Gastroenterology* 1996, **111:**1018-1022.
76. Choi BI, Kim HC, Han JK, Park JH, Kim YI, Kim ST, Lee HS, Kim CY, Han MC: **Therapeutic effect of transcatheter oily chemoembolization therapy for encapsulated nodular hepatocellular carcinoma: CT and pathologic findings.** *Radiology* 1992, **182:**709-713.
77. Ikeda K, Kumada H, Saitoh S, Arase Y, Chayama K: **Effect of repeated transcatheter arterial embolization on the survival time in patients with hepatocellular carcinoma. An analysis by the Cox proportional hazard model.** *Cancer* 1991, **68:**2150-2154.
78. Wu F, Wang ZB, Chen WZ, Zou JZ, Bai J, Zhu H, Li KQ, Jin CB, Xie FL, Su HB: **Advanced hepatocellular carcinoma: treatment with high-intensity focused ultrasound ablation combined with transcatheter arterial embolization.** *Radiology* 2005, **235:**659-667.
79. ZHAI H-j, JIANG L-s, LI N: **The Effect of High Intensity Focused Ultrasound on Patients with Advanced Primary Liver Cancer [J].** *West China Medical Journal* 2005, **2:**037.
80. Wu F, Wang ZB, Chen WZ, Wang W, Gui Y, Zhang M, Zheng G, Zhou Y, Xu G, Li M, et al: **Extracorporeal high intensity focused ultrasound ablation in the treatment of 1038 patients with solid carcinomas in China: an overview.** *Ultrason Sonochem* 2004, **11:**149-154.

81. Li CX, Xu GL, Jiang ZY, Li JJ, Luo GY, Shan HB, Zhang R, Li Y: **Analysis of clinical effect of high-intensity focused ultrasound on liver cancer.** *World J Gastroenterol* 2004, **10:**2201-2204.
82. Ter Haar GR: **High intensity focused ultrasound for the treatment of tumors.** *Echocardiography* 2001, **18:**317-322.
83. Gelet A, Chapelon JY, Margonari J, Theillere Y, Gorry F, Souchon R, Bouvier R: **High-intensity focused ultrasound experimentation on human benign prostatic hypertrophy.** *Eur Urol* 1993, **23 Suppl 1:**44-47.
84. Sullivan LD, McLoughlin MG, Goldenberg LG, Gleave ME, Marich KW: **Early experience with high-intensity focused ultrasound for the treatment of benign prostatic hypertrophy.** *Br J Urol* 1997, **79:**172-176.
85. Madersbacher S, Schatzl G, Djavan B, Stulnig T, Marberger M: **Long-term outcome of transrectal high- intensity focused ultrasound therapy for benign prostatic hyperplasia.** *Eur Urol* 2000, **37:**687-694.
86. Muto S, Yoshii T, Saito K, Kamiyama Y, Ide H, Horie S: **Focal therapy with high-intensity-focused ultrasound in the treatment of localized prostate cancer.** *Japanese journal of clinical oncology* 2008, **38:**192-199.
87. Lee H, Hong J, Choi H: **High-intensity focused ultrasound therapy for clinically localized prostate cancer.** *Prostate cancer and prostatic diseases* 2006, **9:**439-443.
88. Ahmed H, Zacharakis E, Dudderidge T, Armitage J, Scott R, Calleary J, Illing R, Kirkham A, Freeman A, Ogden C: **High-intensity-focused ultrasound in the treatment of primary prostate cancer: the first UK series.** *British journal of cancer* 2009, **101:**19-26.
89. Mearini L, D'Urso L, Collura D, Zucchi A, Costantini E, Formiconi A, Bini V, Muto G, Porena M: **Visually directed transrectal high intensity focused ultrasound for the treatment of prostate cancer: a preliminary report on the Italian experience.** *The Journal of urology* 2009, **181:**105-112.
90. Ganzer R, Rogenhofer S, Walter B, Lunz J-C, Schostak M, Wieland WF, Blana A: **PSA nadir is a significant predictor of treatment failure after high-intensity focussed ultrasound (HIFU) treatment of localised prostate cancer.** *european urology* 2008, **53:**547-553.
91. Uchida T, Ohkusa H, Nagata Y, Hyodo T, Satoh T, Irie A: **Treatment of localized prostate cancer using high-intensity focused ultrasound.** *BJU international* 2006, **97:**56-61.
92. Koch MO, Gardner T, Cheng L, Fedewa RJ, Seip R, Sangvhi NT: **Phase I/II trial of high intensity focused ultrasound for the treatment of previously untreated localized prostate cancer.** *The Journal of urology* 2007, **178:**2366-2371.
93. Uchida T, Sanghvi NT, Gardner TA, Koch MO, Ishii D, Minei S, Satoh T, Hyodo T, Irie A, Baba S: **Transrectal high-intensity focused ultrasound for treatment of patients with stage T1b-2n0m0 localized prostate cancer: a preliminary report.** *Urology* 2002, **59:**394-398.
94. Ripert T, Azémar M-D, Ménard J, Bayoud Y, Messaoudi R, Duval F, Staerman F: **Transrectal high-intensity focused ultrasound (HIFU) treatment of localized prostate cancer: review of technical incidents and morbidity after 5 years of use.** *Prostate cancer and prostatic diseases* 2010, **13:**132-137.

95. Uchida T, Baba S, Irie A, Soh S, Masumori N, Tsukamoto T, Nakatsu H, Fujimoto H, Kakizoe T, Ueda T: **Transrectal high-intensity focused ultrasound in the treatment of localized prostate cancer: a multicenter study.** 2005.
96. Chaussy C, Thuroff S: **The status of high-intensity focused ultrasound in the treatment of localized prostate cancer and the impact of a combined resection.** *Curr Urol Rep* 2003, **4:**248-252.
97. Beerlage HP, Thuroff S, Debruyne FM, Chaussy C, de la Rosette JJ: **Transrectal high-intensity focused ultrasound using the Ablatherm device in the treatment of localized prostate carcinoma.** *Urology* 1999, **54:**273-277.
98. Chaussy C, Thuroff S: **High-intensity focused ultrasound in prostate cancer: results after 3 years.** *Mol Urol* 2000, **4:**179-182.
99. Uchida T, Ohkusa H, Yamashita H, Shoji S, Nagata Y, Hyodo T, Satoh T: **Five years experience of transrectal high-intensity focused ultrasound using the Sonablate device in the treatment of localized prostate cancer.** *Int J Urol* 2006, **13:**228-233.
100. Blana A, Rogenhofer S, Ganzer R, Wild PJ, Wieland WF, Walter B: **Morbidity associated with repeated transrectal high-intensity focused ultrasound treatment of localized prostate cancer.** *World J Urol* 2006, **24:**585-590.
101. Blana A, Walter B, Rogenhofer S, Wieland WF: **High-intensity focused ultrasound for the treatment of localized prostate cancer: 5-year experience.** *Urology* 2004, **63:**297-300.
102. Chaussy C, Thuroff S, Rebillard X, Gelet A: **Technology insight: High-intensity focused ultrasound for urologic cancers.** *Nat Clin Pract Urol* 2005, **2:**191-198.
103. Diederich CJ, Wootton J, Prakash P, Salgaonkar V, Juang T, Scott S, Chen X, Cunha A, Pouliot J, Hsu I: **Catheter-based ultrasound hyperthermia with HDR brachytherapy for treatment of locally advanced cancer of the prostate and cervix.** In *SPIE BiOS*. International Society for Optics and Photonics; 2011: 79010O-79010O-79018.
104. Uchida T, Muramoto M, Kyunou H, Iwamura M, Egawa S, Koshiba K: **Clinical outcome of high-intensity focused ultrasound for treating benign prostatic hyperplasia: preliminary report.** *Urology* 1998, **52:**66-71.
105. Napoli A, Anzidei M, De Nunzio C, Cartocci G, Panebianco V, De Dominicis C, Catalano C, Petrucci F, Leonardo C: **Real-time magnetic resonance-guided high-intensity focused ultrasound focal therapy for localised prostate cancer: preliminary experience.** *Eur Urol* 2013, **63:**395-398.
106. Gelet A, Chapelon JY, Bouvier R, Souchon R, Pangaud C, Abdelrahim AF, Cathignol D, Dubernard JM: **Treatment of prostate cancer with transrectal focused ultrasound: early clinical experience.** *Eur Urol* 1996, **29:**174-183.
107. Rebillard X, Gelet A, Davin JL, Soulie M, Prapotnich D, Cathelineau X, Rozet F, Vallancien G: **Transrectal high-intensity focused ultrasound in the treatment of localized prostate cancer.** *J Endourol* 2005, **19:**693-701.
108. Furusawa H, Namba K, Nakahara H, Tanaka C, Yasuda Y, Hirabara E, Imahariyama M, Komaki K: **The evolving non-surgical ablation of breast cancer: MR guided focused ultrasound (MRgFUS).** *Breast Cancer* 2007, **14:**55-58.
109. Wu F, Wang ZB, Cao YD, Zhu XQ, Zhu H, Chen WZ, Zou JZ: **"Wide local ablation" of localized breast cancer using high intensity focused ultrasound.** *Journal of surgical oncology* 2007, **96:**130-136.

110. Furusawa H, Namba K, Thomsen S, Akiyama F, Bendet A, Tanaka C, Yasuda Y, Nakahara H: **Magnetic resonance–guided focused ultrasound surgery of breast cancer: reliability and effectiveness.** *Journal of the American College of Surgeons* 2006, **203:**54-63.
111. Wu F, Wang Z-B, Zhu H, Chen W-Z, Zou J-Z, Bai J, Li K-Q, Jin C-B, Xie F-L, Su H-B: **Extracorporeal high intensity focused ultrasound treatment for patients with breast cancer.** *Breast cancer research and treatment* 2005, **92:**51-60.
112. Zippel DB, Papa MZ: **The use of MR imaging guided focused ultrasound in breast cancer patients; a preliminary phase one study and review.** *Breast cancer* 2005, **12:**32-38.
113. Wu F, Wang Z-B, Cao Y-D, Chen W, Bai J, Zou J, Zhu H: **A randomised clinical trial of high-intensity focused ultrasound ablation for the treatment of patients with localised breast cancer.** *British journal of cancer* 2003, **89:**2227-2233.
114. Gianfelice D, Khiat A, Amara M, Belblidia A, Boulanger Y: **MR imaging–guided focused us ablation of breast cancer: Histopathologic assessment of effectiveness—initial experience 1.** *Radiology* 2003, **227:**849-855.
115. Huber PE, Jenne JW, Rastert R, Simiantonakis I, Sinn H-P, Strittmatter H-J, von Fournier D, Wannenmacher MF, Debus J: **A new noninvasive approach in breast cancer therapy using magnetic resonance imaging-guided focused ultrasound surgery.** *Cancer research* 2001, **61:**8441-8447.
116. Hynynen K, Pomeroy O, Smith DN, Huber PE, McDannold NJ, Kettenbach J, Baum J, Singer S, Jolesz FA: **MR imaging-guided focused ultrasound surgery of fibroadenomas in the breast: A feasibility study 1.** *Radiology* 2001, **219:**176-185.
117. Peek MC, Ahmed M, Pinder SE, Douek M: **A review of ablative techniques in the treatment of breast fibroadenomata.** *Journal of therapeutic ultrasound* 2016, **4:**1.
118. Stewart EA: **Uterine fibroids.** *Lancet* 2001, **357:**293-298.
119. LeBlang SD, Hoctor K, Steinberg FL: **Leiomyoma shrinkage after MRI-guided focused ultrasound treatment: report of 80 patients.** *AJR Am J Roentgenol* 2010, **194:**274-280.
120. Fennessy FM, Tempany CM: **A review of magnetic resonance imaging-guided focused ultrasound surgery of uterine fibroids.** *Top Magn Reson Imaging* 2006, **17:**173-179.
121. Funaki K, Fukunishi H, Sawada K: **Clinical outcomes of magnetic resonance-guided focused ultrasound surgery for uterine myomas: 24-month follow-up.** *Ultrasound Obstet Gynecol* 2009, **34:**584-589.
122. Stewart EA, Rabinovici J, Tempany CM, Inbar Y, Regan L, Gostout B, Hesley G, Kim HS, Hengst S, Gedroyc WM: **Clinical outcomes of focused ultrasound surgery for the treatment of uterine fibroids.** *Fertil Steril* 2006, **85:**22-29.
123. Zhang L, Chen W-Z, Liu Y-J, Hu X, Zhou K, Chen L, Peng S, Zhu H, Zou H-L, Bai J: **Feasibility of magnetic resonance imaging-guided high intensity focused ultrasound therapy for ablating uterine fibroids in patients with bowel lies anterior to uterus.** *European journal of radiology* 2010, **73:**396-403.
124. Rabinovici J, Inbar Y, Revel A, Zalel Y, Gomori J, Itzchak Y, Schiff E, Yagel S: **Clinical improvement and shrinkage of uterine fibroids after thermal ablation by magnetic resonance-guided focused ultrasound surgery.** *Ultrasound in Obstetrics & Gynecology* 2007, **30:**771-777.

125. Morita Y, Ito N, Hikida H, Takeuchi S, Nakamura K, Ohashi H: **Non-invasive magnetic resonance imaging-guided focused ultrasound treatment for uterine fibroids–early experience.** *European Journal of Obstetrics & Gynecology and Reproductive Biology* 2008, **139:**199-203.
126. Lénárd ZM, McDannold NJ, Fennessy FM, Stewart EA, Jolesz FA, Hynynen K, Tempany CM: **Uterine Leiomyomas: MR Imaging–guided Focused Ultrasound Surgery—Imaging Predictors of Success 1.** *Radiology* 2008, **249:**187-194.
127. Meng X, He G, Zhang J, Han Z, Yu M, Zhang M, Tang Y, Fang L, Zhou X: **A comparative study of fibroid ablation rates using radio frequency or high-intensity focused ultrasound.** *Cardiovascular and interventional radiology* 2010, **33:**794-799.
128. Fruehauf JH, Back W, Eiermann A, Lang M-C, Pessel M, Marlinghaus E, Melchert F, Volz-Köster S, Volz J: **High-intensity focused ultrasound for the targeted destruction of uterine tissues: experiences from a pilot study using a mobile HIFU unit.** *Archives of gynecology and obstetrics* 2008, **277:**143-150.
129. Nau Jr WH, Diederich CJ, Simko J, Juang T, Jacoby A, Burdette EC: **Ultrasound interstitial thermal therapy (USITT) for the treatment of uterine myomas.** In *Biomedical Optics (BiOS) 2007*. International Society for Optics and Photonics; 2007: 64400F-64400F-64408.
130. Himabindu Y, Sriharibabu M, Nyapathy V, Mishra A: **Early evaluation of magnetic resonance imaging guided focused ultrasound sonication in the treatment of uterine fibroids.** *Indian J Med Res* 2014, **139:**267-272.
131. Gorny KR, Borah BJ, Brown DL, Woodrum DA, Stewart EA, Hesley GK: **Incidence of Additional Treatments in Women Treated with MR-Guided Focused US for Symptomatic Uterine Fibroids: Review of 138 Patients with an Average Follow-up of 2.8 Years.** *Journal of Vascular and Interventional Radiology*, **25:**1506-1512.
132. !!! INVALID CITATION !!! {}.
133. Borah BJ, Carls GS, Moore BJ, Gibson TB, Moriarty JP, Stewart EA: **Cost comparison between uterine-sparing fibroid treatments one year following treatment.** *Journal of Therapeutic Ultrasound* 2014, **2:**1-12.
134. Rueff LE, Raman SS: **Clinical and Technical Aspects of MR-Guided High Intensity Focused Ultrasound for Treatment of Symptomatic Uterine Fibroids.** *Semin Intervent Radiol* 2013, **30:**347-353.
135. Reddan DN, Raj GV, Polascik TJ: **Management of small renal tumors: an overview.** *Am J Med* 2001, **110:**558-562.
136. Illing R, Kennedy J, Wu F, Ter Haar G, Protheroe A, Friend P, Gleeson F, Cranston D, Phillips R, Middleton M: **The safety and feasibility of extracorporeal high-intensity focused ultrasound (HIFU) for the treatment of liver and kidney tumours in a Western population.** *British journal of cancer* 2005, **93:**890-895.
137. KÖHRMANN KU, Michel MS, Gaa J, Marlinghaus E, Alken P: **High intensity focused ultrasound as noninvasive therapy for multilocal renal cell carcinoma: case study and review of the literature.** *The Journal of urology* 2002, **167:**2397-2403.
138. Wu F, Wang Z-B, Chen W-Z, Bai J, Zhu H, Qiao T-Y: **Preliminary experience using high intensity focused ultrasound for the treatment of patients with advanced stage renal malignancy.** *The Journal of urology* 2003, **170:**2237-2240.

139. Vallancien G, Chartier-Kastler E, Harouni M, Chopin D, Bougaran J: **Focused extracorporeal pyrotherapy: experimental study and feasibility in man.** *Semin Urol* 1993, **11:**7-9.
140. Wu F, Wang ZB, Chen WZ, Bai J, Zhu H, Qiao TY: **Preliminary experience using high intensity focused ultrasound for the treatment of patients with advanced stage renal malignancy.** *J Urol* 2003, **170:**2237-2240.
141. Montgomery E, Basman F, Brennan P, Malekzadeh R: **Oesophageal cancer.** *Stewart, BW; Wild, CP World Cancer Report* 2014**:**528-543.
142. Stahl M, Mariette C, Haustermans K, Cervantes A, Arnold D, Group EGW: **Oesophageal cancer: ESMO Clinical Practice Guidelines for diagnosis, treatment and follow-up.** *Annals of oncology* 2013, **24:**vi51-vi56.
143. Enzinger PC, Mayer RJ: **Esophageal cancer.** *New England Journal of Medicine* 2003, **349:**2241-2252.
144. Napier KJ, Scheerer M, Misra S: **Esophageal cancer: A Review of epidemiology, pathogenesis, staging workup and treatment modalities.** *World J Gastrointest Oncol* 2014, **6:**112-120.
145. Melodelima D, Prat F, Fritsch J, Theillere Y, Cathignol D: **Treatment of esophageal tumors using high intensity intraluminal ultrasound: first clinical results.** *J Transl Med* 2008, **6:**28.
146. Hariharan D, Saied A, Kocher H: **Analysis of mortality rates for pancreatic cancer across the world.** *HPB* 2008, **10:**58-62.
147. network Pca: **PANCREATIC CANCER ACTION NETWORK**

PANCREATIC CANCER FACTS 2016. Washington, DC: Government Affairs & Advocacy Office; 2016.
148. Jemal A, Siegel R, Ward E, Hao Y, Xu J, Thun MJ: **Cancer statistics, 2009.** *CA Cancer J Clin* 2009, **59:**225-249.
149. Xiong LL, Hwang JH, Huang XB, Yao SS, He CJ, Ge XH, Ge HY, Wang XF: **Early clinical experience using high intensity focused ultrasound for palliation of inoperable pancreatic cancer.** *Jop* 2009, **10:**123-129.
150. Wu F, Wang Z-B, Chen W-Z, Zou J-Z, Bai J, Zhu H, Li K-Q, Xie F-L, Jin C-B, Su H-B: **Extracorporeal focused ultrasound surgery for treatment of human solid carcinomas: early Chinese clinical experience.** *Ultrasound in medicine & biology* 2004, **30:**245-260.
151. Zhao H, Yang G, Wang D, Yu X, Zhang Y, Zhu J, Ji Y, Zhong B, Zhao W, Yang Z: **Concurrent gemcitabine and high-intensity focused ultrasound therapy in patients with locally advanced pancreatic cancer.** *Anti-cancer drugs* 2010, **21:**447-452.
152. He S, Wang G, Niu S, Yao B, Wang X: **The noninvasive treatment of 251 cases of advanced pancreatic cancer with focused ultrasound surgery.** In *2nd International Symposium on Therapeutic Ultrasound, Seattle*. 2002: 51-56.
153. Wu F, Wang ZB, Zhu H, Chen WZ, Zou JZ, Bai J, Li KQ, Jin CB, Xie FL, Su HB: **Feasibility of US-guided high-intensity focused ultrasound treatment in patients with advanced pancreatic cancer: initial experience.** *Radiology* 2005, **236:**1034-1040.
154. Li YY, Sha WH, Zhou YJ, Nie YQ: **Short and long term efficacy of high intensity focused ultrasound therapy for advanced hepatocellular carcinoma.** *Journal of gastroenterology and hepatology* 2007, **22:**2148-2154.

155. DeSantis CE, Lin CC, Mariotto AB, Siegel RL, Stein KD, Kramer JL, Alteri R, Robbins AS, Jemal A: **Cancer treatment and survivorship statistics, 2014.** *CA: a cancer journal for clinicians* 2014, **64:**252-271.
156. Smith NB, Temkin JM, Shapiro F, Hynynen K: **Thermal effects of focused ultrasound energy on bone tissue.** *Ultrasound Med Biol* 2001, **27:**1427-1433.
157. Wu F, Chen WZ, Bai J, Zou JZ, Wang ZL, Zhu H, Wang ZB: **Pathological changes in human malignant carcinoma treated with high-intensity focused ultrasound.** *Ultrasound Med Biol* 2001, **27:**1099-1106.
158. Lu BY, Yang RS, Lin WL, Cheng KS, Wang CY, Kuo TS: **Theoretical study of convergent ultrasound hyperthermia for treating bone tumors.** *Med Eng Phys* 2000, **22:**253-263.
159. Chen W, Zhou K: **High-intensity focused ultrasound ablation: a new strategy to manage primary bone tumors.** *Current Opinion in Orthopaedics* 2005, **16:**494-500.
160. Liberman B, Gianfelice D, Inbar Y, Beck A, Rabin T, Shabshin N, Chander G, Hengst S, Pfeffer R, Chechick A, et al: **Pain palliation in patients with bone metastases using MR-guided focused ultrasound surgery: a multicenter study.** *Ann Surg Oncol* 2009, **16:**140-146.
161. Gianfelice D, Gupta C, Kucharczyk W, Bret P, Havill D, Clemons M: **Palliative Treatment of Painful Bone Metastases with MR Imaging–guided Focused Ultrasound 1.** *Radiology* 2008, **249:**355-363.
162. Catane R, Beck A, Inbar Y, Rabin T, Shabshin N, Hengst S, Pfeffer R, Hanannel A, Dogadkin O, Liberman B: **MR-guided focused ultrasound surgery (MRgFUS) for the palliation of pain in patients with bone metastases—preliminary clinical experience.** *Annals of Oncology* 2007, **18:**163-167.
163. Chen W, Zhu H, Zhang L, Li K, Su H, Jin C, Zhou K, Bai J, Wu F, Wang Z: **Primary bone malignancy: Effective treatment with high-intensity focused ultrasound ablation 1.** *Radiology* 2010, **255:**967-978.
164. Li C, Zhang W, Fan W, Huang J, Zhang F, Wu P: **Noninvasive treatment of malignant bone tumors using high-intensity focused ultrasound.** *Cancer* 2010, **116:**3934-3942.
165. Li C, Wu P, Liang Z, Fan W, Huang J, Zhang F: **Osteosarcoma: limb salvaging treatment by ultrasonographically guided high-intensity focused ultrasound.** *Cancer biology & therapy* 2009, **8:**1102-1108.
166. Chen W, Wang Z, Wu F, Bai J, Zhu H, Zou J, Li K, Xie F, Wang Z: **[High intensity focused ultrasound alone for malignant solid tumors].** *Zhonghua Zhong Liu Za Zhi* 2002, **24:**278-281.
167. Napoli A, Anzidei M, Marincola BC, Brachetti G, Noce V, Boni F, Bertaccini L, Passariello R, Catalano C: **MR imaging-guided focused ultrasound for treatment of bone metastasis.** *Radiographics* 2013, **33:**1555-1568.
168. Temple MJ, Waspe AC, Amaral JG, Napoli A, LeBlang S, Ghanouni P, Bucknor MD, Campbell F, Drake JM: **Establishing a clinical service for the treatment of osteoid osteoma using magnetic resonance-guided focused ultrasound: overview and guidelines.** *Journal of therapeutic ultrasound* 2016, **4:**1.
169. Lipsman N, Mainprize TG, Schwartz ML, Hynynen K, Lozano AM: **Intracranial applications of magnetic resonance-guided focused ultrasound.** *Neurotherapeutics* 2014, **11:**593-605.

170. Clement G, Hynynen K: **A non-invasive method for focusing ultrasound through the human skull.** *Physics in medicine and biology* 2002, **47:**1219.
171. McDannold NJ, Jolesz FA: **Magnetic resonance image-guided thermal ablations.** *Topics in Magnetic Resonance Imaging* 2000, **11:**191-202.
172. Kuroda K, Chung AH, Hynynen K, Jolesz FA: **Invited. Calibration of water proton chemical shift with temperature for noninvasive temperature imaging during focused ultrasound surgery.** *Journal of Magnetic Resonance Imaging* 1998, **8:**175-181.
173. Hynynen K, McDannold N, Mulkern RV, Jolesz FA: **Temperature monitoring in fat with MRI.** *Magnetic resonance in medicine* 2000, **43:**901-904.
174. Lipsman N, Schwartz ML, Huang Y, Lee L, Sankar T, Chapman M, Hynynen K, Lozano AM: **MR-guided focused ultrasound thalamotomy for essential tremor: a proof-of-concept study.** *The Lancet Neurology* 2013, **12:**462-468.
175. Elias WJ, Huss D, Voss T, Loomba J, Khaled M, Zadicario E, Frysinger RC, Sperling SA, Wylie S, Monteith SJ: **A pilot study of focused ultrasound thalamotomy for essential tremor.** *New England Journal of Medicine* 2013, **369:**640-648.
176. Jordão JF, Ayala-Grosso CA, Markham K, Huang Y, Chopra R, McLaurin J, Hynynen K, Aubert I: **Antibodies targeted to the brain with image-guided focused ultrasound reduces amyloid-β plaque load in the TgCRND8 mouse model of Alzheimer's disease.** *PloS one* 2010, **5:**e10549.
177. Jordão JF, Thévenot E, Markham-Coultes K, Scarcelli T, Weng Y-Q, Xhima K, O'Reilly M, Huang Y, McLaurin J, Hynynen K: **Amyloid-β plaque reduction, endogenous antibody delivery and glial activation by brain-targeted, transcranial focused ultrasound.** *Experimental neurology* 2013, **248:**16-29.
178. Monteith SJ, Kassell NF, Goren O, Harnof S: **Transcranial MR-guided focused ultrasound sonothrombolysis in the treatment of intracerebral hemorrhage.** *Neurosurg Focus* 2013, **34:**E14.
179. Martin E, Jeanmonod D, Morel A, Zadicario E, Werner B: **High-intensity focused ultrasound for noninvasive functional neurosurgery.** *Annals of neurology* 2009, **66:**858-861.
180. Jeanmonod D, Werner B, Morel A, Michels L, Zadicario E, Schiff G, Martin E: **Transcranial magnetic resonance imaging–guided focused ultrasound: noninvasive central lateral thalamotomy for chronic neuropathic pain.** *Neurosurgical focus* 2012, **32:**E1.
181. Burgess A, Huang Y, Waspe AC, Ganguly M, Goertz DE, Hynynen K: **High-intensity focused ultrasound (HIFU) for dissolution of clots in a rabbit model of embolic stroke.** *PloS one* 2012, **7:**e42311.
182. Monteith SJ, Kassell NF, Goren O, Harnof S: **Transcranial MR-guided focused ultrasound sonothrombolysis in the treatment of intracerebral hemorrhage.** *Neurosurgical focus* 2013, **34:**E14.
183. Hölscher T, Ahadi G, Fisher D, Zadicario E, Voie A: **MR-guided focused ultrasound for acute stroke a rabbit model.** *Stroke* 2013, **44:**S58-S60.
184. Wright C, Hynynen K, Goertz D: **In vitro and in vivo high intensity focused ultrasound thrombolysis.** *Investigative radiology* 2012, **47:**217.
185. Alkins R, Huang Y, Pajek D, Hynynen K: **Cavitation-based third ventriculostomy using MRI-guided focused ultrasound: Laboratory investigation.** *Journal of neurosurgery* 2013, **119:**1520.

186. Hua S, Lenz F, Zirh T, Reich S, Dougherty P: **Thalamic neuronal activity correlated with essential tremor.** *Journal of Neurology, Neurosurgery & Psychiatry* 1998, **64:**273-276.
187. Chang WS, Jung HH, Kweon EJ, Zadicario E, Rachmilevitch I, Chang JW: **Unilateral magnetic resonance guided focused ultrasound thalamotomy for essential tremor: practices and clinicoradiological outcomes.** *J Neurol Neurosurg Psychiatry* 2015, **86:**257-264.
188. Cetas JS, Saedi T, Burchiel KJ: **Destructive procedures for the treatment of nonmalignant pain: a structured literature review.** *J Neurosurg* 2008, **109:**389-404.
189. Jeanmonod D, Werner B, Morel A, Michels L, Zadicario E, Schiff G, Martin E: **Transcranial magnetic resonance imaging-guided focused ultrasound: noninvasive central lateral thalamotomy for chronic neuropathic pain.** *Neurosurg Focus* 2012, **32:**E1.
190. Haines SJ, Jannetta PJ, Zorub DS: **Microvascular relations of the trigeminal nerve. An anatomical study with clinical correlation.** *J Neurosurg* 1980, **52:**381-386.
191. McDannold N, Clement GT, Black P, Jolesz F, Hynynen K: **Transcranial magnetic resonance imaging- guided focused ultrasound surgery of brain tumors: initial findings in 3 patients.** *Neurosurgery* 2010, **66:**323-332; discussion 332.
192. McDannold N, Vykhodtseva N, Jolesz FA, Hynynen K: **MRI investigation of the threshold for thermally induced blood-brain barrier disruption and brain tissue damage in the rabbit brain.** *Magn Reson Med* 2004, **51:**913-923.
193. Fry F, Kossoff G, Eggleton R, Dunn F: **Threshold ultrasonic dosages for structural changes in the mammalian brain.** *the Journal of the Acoustical Society of America* 1970, **48:**1413-1417.
194. Lele PP: **Effects of ultrasound on "solid" mammalian tissues and tumors in vivo.** In *Ultrasound.* Springer; 1987: 275-306
195. Repacholi MH, Gandolfo M, Rindi A: *Ultrasound: Medical Applications, Biological Effects, and Hazard Potential.* Springer Science & Business Media; 2012.
196. Cohen-Inbar O, Xu Z, Sheehan JP: **Focused ultrasound-aided immunomodulation in glioblastoma multiforme: a therapeutic concept.** *Journal of therapeutic ultrasound* 2016, **4:**1.
197. Delon-Martin C, Vogt C, Chignier E, Guers C, Chapelon JY, Cathignol D: **Venous thrombosis generation by means of high-intensity focused ultrasound.** *Ultrasound Med Biol* 1995, **21:**113-119.
198. Zhou Y: *Principles and Applications of Therapeutic Ultrasound in Healthcare.* CRC Press; 2015.
199. Wu F, Chen W-Z, Bai J, Zou J-Z, Wang Z-L, Zhu H, Wang Z-B: **Tumor vessel destruction resulting from high-intensity focused ultrasound in patients with solid malignancies.** *Ultrasound in medicine & biology* 2002, **28:**535-542.
200. Vykhodtseva N, McDannold N, Hynynen K: **Progress and problems in the application of focused ultrasound for blood-brain barrier disruption.** *Ultrasonics* 2008, **48:**279-296.
201. Hynynen K, McDannold N, Vykhodtseva N, Jolesz FA: **Noninvasive MR Imaging–guided Focal Opening of the Blood-Brain Barrier in Rabbits 1.** *Radiology* 2001, **220:**640-646.

202. Xu Z, Ludomirsky A, Eun LY, Hall TL, Tran BC, Fowlkes JB, Cain CA: **Controlled ultrasound tissue erosion.** *Ultrasonics, Ferroelectrics, and Frequency Control, IEEE Transactions on* 2004, **51:**726-736.
203. Simon JC, Sapozhnikov OA, Khokhlova VA, Wang Y-N, Crum LA, Bailey MR: **Ultrasonic atomization of tissue and its role in tissue fractionation by high intensity focused ultrasound.** *Physics in medicine and biology* 2012, **57:**8061.
204. Smith NB, Hynynen K: **The feasibility of using focused ultrasound for transmyocardial revascularization.** *Ultrasound in medicine & biology* 1998, **24:**1045-1054.
205. Hynynen K, McDannold N, Vykhodtseva N, Jolesz FA: **Noninvasive MR imaging-guided focal opening of the blood-brain barrier in rabbits.** *Radiology* 2001, **220:**640-646.
206. Colen RR, Jolesz FA: **MR-guided focused ultrasound of the brain.** In *Interventional Magnetic Resonance Imaging.* Springer; 2012: 367-380
207. Cho EE, Drazic J, Ganguly M, Stefanovic B, Hynynen K: **Two-Photon Fluorescence Microscopy Study of Cerebrovascular Dynamics in Ultrasound-Induced Blood—Brain Barrier Opening.** *Journal of Cerebral Blood Flow & Metabolism* 2011, **31:**1852-1862.
208. Samiotaki G, Konofagou EE: **Dependence of the reversibility of focused- ultrasound-induced blood-brain barrier opening on pressure and pulse length in vivo.** *IEEE Trans Ultrason Ferroelectr Freq Control* 2013, **60:**2257-2265.
209. Kinoshita M, McDannold N, Jolesz FA, Hynynen K: **Targeted delivery of antibodies through the blood–brain barrier by MRI-guided focused ultrasound.** *Biochemical and biophysical research communications* 2006, **340:**1085-1090.
210. Jolesz F, McDannold N, Clement G, Kinoshita M, Fennessy F, Tempany C: **MRI-guided FUS and its clinical applications.** In *Image-Guided Interventions.* Springer; 2008: 275-307
211. Wei K-C, Chu P-C, Wang H-YJ, Huang C-Y, Chen P-Y, Tsai H-C, Lu Y-J, Lee P-Y, Tseng I-C, Feng L-Y: **Focused ultrasound-induced blood–brain barrier opening to enhance temozolomide delivery for glioblastoma treatment: a preclinical study.** *PloS one* 2013, **8:**e58995.
212. Jordao JF, Ayala-Grosso CA, Markham K, Huang Y, Chopra R, McLaurin J, Hynynen K, Aubert I: **Antibodies targeted to the brain with image-guided focused ultrasound reduces amyloid-beta plaque load in the TgCRND8 mouse model of Alzheimer's disease.** *PLoS One* 2010, **5:**e10549.
213. Burgess A, Ayala-Grosso CA, Ganguly M, Jordao JF, Aubert I, Hynynen K: **Targeted delivery of neural stem cells to the brain using MRI-guided focused ultrasound to disrupt the blood-brain barrier.** *PLoS One* 2011, **6:**e27877.
214. Thevenot E, Jordao JF, O'Reilly MA, Markham K, Weng YQ, Foust KD, Kaspar BK, Hynynen K, Aubert I: **Targeted delivery of self-complementary adeno-associated virus serotype 9 to the brain, using magnetic resonance imaging-guided focused ultrasound.** *Hum Gene Ther* 2012, **23:**1144-1155.
215. Parsons JE, Cain CA, Abrams GD, Fowlkes JB: **Pulsed cavitational ultrasound therapy for controlled tissue homogenization.** *Ultrasound Med Biol* 2006, **32:**115-129.

216. Lake AM, Hall TL, Kieran K, Fowlkes JB, Cain CA, Roberts WW: **Histotripsy: minimally invasive technology for prostatic tissue ablation in an in vivo canine model.** *Urology* 2008, **72:**682-686.
217. Hempel CR, Hall TL, Cain CA, Fowlkes JB, Xu Z, Roberts WW: **Histotripsy fractionation of prostate tissue: local effects and systemic response in a canine model.** *J Urol* 2011, **185:**1484-1489.
218. Xu Z, Fowlkes JB, Rothman ED, Levin AM, Cain CA: **Controlled ultrasound tissue erosion: the role of dynamic interaction between insonation and microbubble activity.** *J Acoust Soc Am* 2005, **117:**424-435.
219. Roberts WW, Hall TL, Ives K, Wolf JS, Jr., Fowlkes JB, Cain CA: **Pulsed cavitational ultrasound: a noninvasive technology for controlled tissue ablation (histotripsy) in the rabbit kidney.** *J Urol* 2006, **175:**734-738.
220. Xu Z, Fowlkes JB, Cain CA: **A new strategy to enhance cavitational tissue erosion using a high-intensity, Initiating sequence.** *IEEE Trans Ultrason Ferroelectr Freq Control* 2006, **53:**1412-1424.
221. Lozano AM, Lipsman N: **Probing and regulating dysfunctional circuits using deep brain stimulation.** *Neuron* 2013, **77:**406-424.
222. Magara A, Bühler R, Moser D, Kowalski M, Pourtehrani P, Jeanmonod D: **First experience with MR-guided focused ultrasound in the treatment of Parkinson's disease.** *Journal of Therapeutic Ultrasound* 2014, **2:**1-8.
223. Lipsman N, Sankar T, Downar J, Kennedy SH, Lozano AM, Giacobbe P: **Neuromodulation for treatment-refractory major depressive disorder.** *CMAJ* 2014, **186:**33-39.
224. Dougherty DD, Baer L, Cosgrove GR, Cassem EH, Price BH, Nierenberg AA, Jenike MA, Rauch SL: **Prospective long-term follow-up of 44 patients who received cingulotomy for treatment-refractory obsessive-compulsive disorder.** *Am J Psychiatry* 2002, **159:**269-275.
225. Dougherty DD, Weiss AP, Cosgrove GR, Alpert NM, Cassem EH, Nierenberg AA, Price BH, Mayberg HS, Fischman AJ, Rauch SL: **Cerebral metabolic correlates as potential predictors of response to anterior cingulotomy for treatment of major depression.** *J Neurosurg* 2003, **99:**1010-1017.
226. Hurwitz TA, Honey CR, Allen J, Gosselin C, Hewko R, Martzke J, Bogod N, Taylor P: **Bilateral anterior capsulotomy for intractable depression.** *J Neuropsychiatry Clin Neurosci* 2012, **24:**176-182.
227. Mendelow AD, Gregson BA, Rowan EN, Murray GD, Gholkar A, Mitchell PM: **Early surgery versus initial conservative treatment in patients with spontaneous supratentorial lobar intracerebral haematomas (STICH II): a randomised trial.** *Lancet* 2013, **382:**397-408.
228. Bonow RH, Silber JR, Enzmann DR, Beauchamp NJ, Ellenbogen RG, Mourad PD: **Towards use of MRI-guided ultrasound for treating cerebral vasospasm.** *Journal of therapeutic ultrasound* 2016, **4:**1.
229. Wallenfang T, Bohl J, Kretzschmar K: **Evolution of brain abscess in cats formation of capsule and resolution of brain edema.** *Neurosurgical review* 1980, **3:**101-111.
230. McDougal LK, Steward CD, Killgore GE, Chaitram JM, McAllister SK, Tenover FC: **Pulsed-field gel electrophoresis typing of oxacillin-resistant Staphylococcus aureus**

isolates from the United States: establishing a national database. *Journal of clinical microbiology* 2003, **41:**5113-5120.
231. Rieck B, Bates D, Zhang K, Escott N, Mougenot C, Pichardo S, Curiel L: **Focused ultrasound treatment of abscesses induced by methicillin resistant Staphylococcus aureus: Feasibility study in a mouse model.** *Medical Physics* 2014, **41:**063301.
232. Ellis SL, Finn P, Noone M, Leaper DJ: **Eradication of methicillin-resistant Staphylococcus aureus from pressure sores using warming therapy.** *Surgical infections* 2003, **4:**53-55.
233. Melling AC, Ali B, Scott EM, Leaper DJ: **Effects of preoperative warming on the incidence of wound infection after clean surgery: a randomised controlled trial.** *The Lancet* 2001, **358:**876-880.
234. Parikh S, Motarjeme A, McNamara T, Raabe R, Hagspiel K, Benenati JF, Sterling K, Comerota A: **Ultrasound-accelerated thrombolysis for the treatment of deep vein thrombosis: initial clinical experience.** *Journal of Vascular and Interventional Radiology* 2008, **19:**521-528.
235. Smith NB: **Applications of ultrasonic skin permeation in transdermal drug delivery.** 2008.
236. Boucaud A: **Trends in the use of ultrasound-mediated transdermal drug delivery.** *Drug Discov Today* 2004, **9:**827-828.
237. Pitt WG, Husseini GA, Staples BJ: **Ultrasonic drug delivery-a general review.** *Expert opinion on drug delivery* 2004, **1:**37-56.
238. Mitragotri S, Edwards DA, Blankschtein D, Langer R: **A mechanistic study of ultrasonically-enhanced transdermal drug delivery.** *Journal of pharmaceutical sciences* 1995, **84:**697-706.
239. Siegel RJ, Luo H: **Ultrasound thrombolysis.** *Ultrasonics* 2008, **48:**312-320.
240. Daffertshofer M, Gass A, Ringleb P, Sitzer M, Sliwka U, Els T, Sedlaczek O, Koroshetz WJ, Hennerici MG: **Transcranial low-frequency ultrasound-mediated thrombolysis in brain ischemia: increased risk of hemorrhage with combined ultrasound and tissue plasminogen activator: results of a phase II clinical trial.** *Stroke* 2005, **36:**1441-1446.
241. Tufail Y, Matyushov A, Baldwin N, Tauchmann ML, Georges J, Yoshihiro A, Tillery SI, Tyler WJ: **Transcranial pulsed ultrasound stimulates intact brain circuits.** *Neuron* 2010, **66:**681-694.
242. Miller DL: **Ultrasound-mediated gene therapy.** pp. 69-130: World Scientific; 2006:69-130.
243. Kieran K, Hall TL, Parsons JE, Wolf JS, Jr., Fowlkes JB, Cain CA, Roberts WW: **Refining histotripsy: defining the parameter space for the creation of nonthermal lesions with high intensity, pulsed focused ultrasound of the in vitro kidney.** *J Urol* 2007, **178:**672-676.
244. Xu Z, Raghavan M, Hall T, Mycek M-A, Fowlkes JB, Cain C: **Evolution of bubble clouds induced by pulsed cavitational ultrasound therapy-histotripsy.** *Ultrasonics, Ferroelectrics, and Frequency Control, IEEE Transactions on* 2008, **55:**1122-1132.
245. Guzmán HR, McNamara AJ, Nguyen DX, Prausnitz MR: **Bioeffects caused by changes in acoustic cavitation bubble density and cell concentration: a unified explanation based on cell-to-bubble ratio and blast radius.** *Ultrasound in medicine & biology* 2003, **29:**1211-1222.

Chapter 4 Mechanical and biological effects of ultrasound: A review of present knowledge

This chapter has been submitted as “Zahra Izadifar, Paul Babyn, Dean Chapman, 2016, Mechanical and biological effects of ultrasound: A review of present knowledge, *Ultrasound in Medicine and Biology* (Under Review)” According to the Copyright Agreement, "the authors retain the right to include the journal article, in full or in part, in a thesis or dissertation".

4.1 Abstract

Ultrasound is widely used for medical diagnosis and increasingly for therapeutic purposes. Understanding the bioeffects of sonography is important for clinicians and scientists working in the field, as permanent damage to biological tissues can occur at high levels of exposure. This chapter reviews the underlying principles of thermal mechanisms and the physical interactions of ultrasound with biological tissues. In this chapter adverse health effects derived from cellular studies, animal studies, and clinical reports are reviewed to provide insight into the *in vitro* and *in vivo* bioeffects of ultrasound.

4.2 Introduction

Therapeutic applications of ultrasound in medicine have been accepted and advantageous for many years [1]. Ultrasound is widely used as a therapeutic tool in physiotherapy, in lithotripsy for kidney stone destruction, in the form of high intensity focused ultrasound (HIFU) for tissue ablation in tumor treatment, and as a surgical tool. It has also been applied as a tool for drug delivery [2], gene delivery [3], and thrombolysis [4]. Current research suggests promising new applications and advancement of biomedical ultrasound in medicine. Further progresses in therapeutic applications of ultrasound require more understanding of the mechanisms of interaction with tissues to safely advance this technique.

4.3 Ultrasound mechanisms

Thermal and non-thermal physical and biological effects of ultrasound in tissues are the basis of various therapeutic applications. Thermal effects of ultrasound that arise from the absorption of ultrasonic energy and creation of heat depend on ultrasound exposure parameters, tissue properties, and beam configuration [5]. Acoustic radiation force, radiation torque, acoustic streaming, shock waves, and cavitation are considered non-thermal effects of ultrasound. Radiation force that results from a transfer of momentum from the ultrasound field to the object [6] is the cause of contrast agent displacement to the wall of blood vessels in laboratory animals [7]. Radiation force is itself an underlying mechanism for radiation torque and acoustic streaming effects. Acoustic streaming is when acoustic field propagation in a fluid causes a rise in fluid flow. Acoustic streaming has been used as a diagnostic method to noninvasively identify cysts [8].

Cavitation is perhaps the most widely studied non-thermal mechanism of ultrasound and is often the basis of a wide range of new therapeutic applications [9]. Ultrasound cavitation is described as the formation and oscillation of a gas bubble. Such bubbles can form from a pre-existing stabilized gas body or nuclei. Gas nuclei can be stabilized in crevices of impurities in the liquid and, as the pressure in the liquid drops, the gas in the crevice expands and forms a microbubble [5]. A variety of biological effects, both *in vivo* and *in vitro*, can be attributed to acoustic cavitation. The non-thermal effects of ultrasound, including cavitation, may play a more important role in treatment of soft tissue lesions than thermal effects [10], but this strongly depends on the type of cavitation. Non-inertial cavitation is when a bubble is exposed to an acoustic field and goes through repetitive oscillations around its equilibrium radius over many acoustic cycles. The oscillation of the bubble can result in heat generation, microstreaming of

nearby fluid, and localized shear stresses [5]. Inertial cavitation, known as microbubble formation and collapse, is induced by ultrasound waves travelling through tissue fluids during ultrasound therapy. When the acoustic field is at higher amplitudes, the radius of a bubble may grow to a maximum radius and then collapse. This kind of bubble is called an inertial (transient) cavitation bubble. Inertial cavitation bubbles can expand and collapse violently during a single ultrasound exposure on the order of one microsecond [11]. Extremely high pressure and temperature, high speed microstreaming [12, 13] and high speed jet liquids [14, 15] are induced as a result of cavitation processes. The high pressure and temperature generated are localized at the minimum radius of the inertial bubble collapse and are temporally limited to the duration of collapse [5]. The motion of the bubble wall during inertial collapse produces a spherically diverging shock wave in the liquid surrounding the collapsing bubble. Inertial cavitation close to a solid surface (such as metal, tissue, cell wall, and stone) generates a high speed jet liquid that drives into the solid surface and results in pitting of the surface [16]. This mechanical outcome of cavitation is used for fragmentation of kidney stones during lithotripsy.

One parameter that can directly change the bubble response from non-inertial to inertial cavitation is the acoustic pressure amplitude. The acoustic pressure at which this transition occurs is called the threshold for inertial cavitation [5]. Another parameter used to determine the likelihood of cavitation is the mechanical index (MI). The MI is based on the derated peak rarefactional pressure and defined as the maximum value of the negative peak pressure divided by the root square of the acoustic center frequency[17].

The mechanical effect of cavitation can cause substantial injury to cells when ultrasound-induced microbubbles expand and then collapse (microexplosion) close to them. Non-inertial cavitation (or stable cavitation in which the microbubble does not violently collapse and instead oscillates

for many cycles around its resonance size) is considered more beneficial to injured tissue while inertial cavitation (transient) causes tissue damage [18, 19]. Many therapeutic applications of ultrasound rely on the ability of ultrasound to focus within tissues at the focal point where the beam converges, and use the energy for non-invasive thermal or mechanical effects. A quantitative analysis of the amount of heat deposited by ultrasound showed that inertial cavitation is key to addressing some of the major challenges of high intensity focused ultrasound [20]. In the context of drug delivery, both inertial and non-inertial cavitation bubbles play roles. When ultrasound is applied *in vivo*, cavitation can occur anywhere that appropriate microbubbles are present, such as the lung, intestine, or tissue containing ultrasound contrast agents. Ultrasound contrast agents are gas-filled microbubbles encapsulated by a protein, lipid, or polymer shell, stabilized from dissolution, and injected intravenously [21]. These ultrasound contrast agents are used clinically to enhance diagnostic images and have new applications in the areas of molecular imaging, drug delivery, and gene therapy [22, 23]. The application of ultrasound contrast agents facilitates drug delivery due to the formation of temporary pores in the cell membrane by ultrasound. Deng et al. (2004) report that ultrasound raises the transmembrane current as a direct result of pore formation that leads to a decline in membrane resistance decline [24]. Microbubbles have also been used as a new therapeutic method for direct deposition of stem cells to the site of injury after acute myocardial infarction [25]. In this new stem cell therapy technique, stem cell-microbubble complexes (StemBells) are assembled by binding dual-targeted microbubbles to adipose-derived stem cells. These complexes target the myocardial infarct area of the heart via microbubbles; specifically, the StemBells were injected into the body of a rat acute myocardial infarction-reperfusion model and unloaded via ultrasound. The effect of ultrasound on directing StemBells to the vessel wall was shown in an *in vitro* flow model. The

feasibility of improving cardiac function was successfully demonstrated in a rat model [25]. Another efficient use of microbubbles and ultrasound is therapeutic gas delivery through microbubbles and liposomes. Gaseous molecules of nitric oxide (NO), carbon monoxide (CO), xenon (Xe), oxygen (O_2), and hydrogen sulfide (H_2S) mediate cell signalling pathways, play an important role is physiology and biological responses, and have great therapeutic potential. However, controlled delivery is a significant challenge for therapeutic techniques using these gases. Researchers are using microbubbles and liposomes in novel therapeutic gas delivery [26]. Extensive studies performed on microbubble gaseous delivery, such as employed for microbubble oxygenation therapy of hypoxic tumors [27]in a rabbit model of hypoxemia [28], in rats with acute respiratory distress syndrome [29], and for pancreatic cancer [30]. Tissues that naturally contain gas, such as the lung and intestine, as well as vessels containing ultrasound contrast agents are more susceptible to ultrasound bioeffects. Mechanical damage (related to cavitation) to the microvasculature in the lung and intestine has been observed in several mammalian laboratory studies [31, 32].

Considering that the therapeutic and imaging mechanisms of ultrasound are based on the interaction of sound waves with tissue, cavitation could also have hazardous bioeffects on tissues. The cavitation that occurs is largely unpredictable and the bioeffects of ultrasound could be hazardous to healthy tissues. Further progress in therapeutic applications of ultrasound with sufficient safety for patients requires greater understanding of the mechanism by which ultrasound interacts with tissues. Therefore, this review concentrates on non-thermal laboratory/clinical-based biological effects of ultrasound both *in vitro* and *in vivo*.

4.4 Mechanical (non-thermal) bioeffects

Discussion of cavitation behavior usually assumes the pre-existence of bubbles of suitable size or bubble nuclei with the potential to grow to a suitable size in the medium propagated by the ultrasound beam. Although liquids can be saturated with gas, suitable cavitation nuclei might not always be present. In some cases, an ultrasound contrast agent is used and injected into the body to improve diagnosis via ultrasound. It is very doubtful if either inertial or non-inertial cavitation occurs at diagnostic levels of ultrasound within soft tissues or fluids in the body in the absence of contrast agents [33, 34].

4.4.1 Lung

Tissues naturally containing gas bodies, such as the lung and intestine, are more sensitive to bioeffects from ultrasound exposure because of the presence of gas. Because fetal lungs are gas-free, they do not exhibit any sign of the lung damage evident in air-filled adult lungs [35]. The trauma at the surface of the lung and in the intestine has been interpreted to result from cavitation-like processes in the body [32, 35]. To explore the hypothesis of cavitation-based bioeffects from diagnostic ultrasound on the lungs of mammals, rat lung was exposed to a 4.0-MHz (the threshold of lung damage in rat) pulsed Doppler and color Doppler ultrasound; then, using a 30-MHz active cavitation detection scheme, the first *in vivo* evidence of cavitation from diagnostic ultrasound pulses was reported [36]. Damage to the microvasculature of the lung was characterized by extravasation of red blood cells from capillaries into the alveolar space [37]. Although this extravasation of red blood cells was reversible, and apparently occurred during exposure without rise in severity in the subsequent 5 minutes, exposure of the lung to pulsed ultrasound was deleterious to the lung [37]. The first report of lung damage was *in situ* and at exposure conditions of about 1 MPa peak positive pressure, 2 MHz frequency, 10 μs pulse

duration, for 3 min [31] and has since been reported in mice, monkey, pigs, rabbits, and rats [38-43]. A human study reported a lack of lung damage after intraoperative transesophageal echocardiography with ultrasound exposure [44]. Lung hemorrhage may be a result of thermal, mechanical, or cavitational effects of ultrasound. Ultrasound-related lung hemorrhage is a function of frequency [31, 45], pulse duration [31, 46], pulse repetition frequency [31, 47], and duration of exposure [35, 47]. Cavitation-related bioeffects are more dependent on frequency [31, 45].

Child et al. (1990) observed haemorrhage in mouse lung tissue after ultrasound exposure (at 1.2 MHz, pulse average intensity 1 mW cm^{-2}, 10 μs pulse, peak positive pressure 0.7 MPa, 3 minute exposure) [31]. Since then, ultrasound-induced lung haemorrhage has been reported *in vivo* in mice [31, 39, 45, 47, 48], rat [46, 47, 49, 50], rabbits [42, 43], and pigs [42, 43, 51, 52]

Lung damage shows itself as localised lesions located on the lung surface, but there has been no report of damage to adult or neonatal human lungs so far [34]. The reason for this effect of ultrasound on the lung surface is not fully understood and is still under investigation. It has been interpreted that the presence of gas in the lung and intestine results in mechanical trauma to adjacent soft tissues as a result of the cavitation process.

4.4.2 Intestine

Acoustic cavitation can be generated in a wide range of intestinal environments, as they contain gas bodies located in a fluid-like medium [5]. Cavitation-related damage is more certain in the intestine and in microvascular with the presence of microbubbles than in the lung [5]. Mammalian studies show the occurrence of intestinal hemorrhage when the thermal effects of ultrasound have been minimized [32, 53, 54]. Petechiae hemorrhage in the intestine of laboratory animals exposed to a lithotripter field is reported in several studies [53, 55, 56]. The threshold of

pressure for intestinal hemorrhage in mice ranges from 1-3 MPa [53, 55]. Further evidence showing cavitation as a mechanism for effects of ultrasound on the intestine relies on studies utilizing ultrasound contrast agents. The area of murine intestinal hemorrhage significantly increased when the vasculature was filled with ultrasound contrast agents and exposed to ultrasound [57, 58]. The threshold of intestinal damage in the presence of a contrast agent was about 3 MPa at 2.4 MHz with a pulse duration of 10 μs [58]. The effect of ultrasound on intestinal damage increases with increasing frequency and decreasing pulse duration [57, 58]. The response of microbubbles to negative pressure is greater than to positive pressure. More damage was noted in the intestine as well as other tissues of mice exposed to negative vs. positive pressure of a lithotripter field in the presence of microbubbles [59]. Lehmann and Herrick (1953) observed vascular damage in the wall of the intestine,[60] followed by an investigation by Dalecki et al. [61] that noted areas of haemorrhage when several abdominal sites of mice were exposed to pulsed ultrasound (10 μs, 100 Hz) at 0.7-3.6 MHz [61]. The haemorrhage area occurs at a level of exposure above the threshold of about 1 MPa; lower frequency levels are more effective at producing haemorrhage than higher frequency levels. Using a piezoelectric lithotripter, Dalecki et al. (1995) determined the threshold of ultrasonically-produced haemorrhage to be about 1-3 MPa [55]. In addition, they found the importance of gas-body activation by observing a very extensive haemorrhage in the (gas-containing) intestine of adult mice and almost no effect in the (gas-free) intestine of their fetuses (at a pressure amplitude of 10 MPa) [32]. Petechiae and haemorrhage in the intestine were also observed by Miller and Gies [62]. They found the threshold level for petechiae to be 0.28 MPa (spatial average, temporal average intensity (I_{SATA})=2.6 W cm^{-2}) and for haemorrhage to be 0.65 MPa (I_{SATA}=14.2 W cm^{-2}) for the longest exposure (up to 1000 s) of the sample (hairless mice) to 0.4 MHz continuous

ultrasound at 37 °C. Pulsed exposures or higher bath temperature affect the threshold level of haemorrhage and particularly petechiae. The threshold level of petechiae increased with pulse exposure. In addition, for both continuous and pulsed exposure, using an ultrasound contrast agent increased the number of petechiae and haemorrhages [57, 58]. Stanton et al. (2001) reported the effect of diagnosis ultrasound on the progression of epithelia cells in the crypts of the small intestine through the cell cycle [63]. Histological examination of the distal portion of the intestine of adult CD 1 mice whose anterior abdomen had been exposed to ultrasound (at 8 MHz for 15 minutes; special peak temporal average intensity (I_{SPTA})=1120 mW/cm^2; P_{MAX}=420 mW) showed that the number of cells undergoing mitosis was considerably decreased 4.5 hours after exposure and the number of apoptotic cells was significantly increased [63]. Overall, investigations on ultrasound-related intestinal damage show that cavitation is the responsible mechanism.

4.5 Urinary tract system

The application of lithotripsy as a clinical treatment for urinary calculosis, or kidney stones, has revolutionized the non-invasive treatment of this disease. During a lithotripsy procedure, high amplitude acoustic pulses are generated at the site of the kidney stone using short pulses of high acoustic pressure ultrasound. The lithotripter shock wave is a short pulse of about 5 μs duration with a near instantaneous jump to a peak positive pressure that typically varies between 30 and 110 MPa. This fast transition in the wave form is called “shock”. The pressure then falls to zero about 1 μs thereafter and is followed by a negative pressure between -5 and -15 MPa. Most of the energy in the shock wave is between 100 kHz and 1 MHz [64]. Most lithotripters generate a similar type of shock wave with an intense compressive wave that produces mechanical force with a tensile component of about -8 to -15 MPa. This negative pressure drives cavitation

bubbles that are critical for stone destruction [64]. Cavitation induced by lithotripters behaves as a cluster of bubbles rather than individual bubbles, and the coherent collapse of the cluster may give rise to its destructive power [65-67]. Almost all patients who receive at least an average dose of shock waves (2,000 shock waves at midrange power or higher) experience some form of tissue trauma and some patients can experience severe, even catastrophic adverse effects [68], including capillary damage and bleeding around the outside of the kidney [69]. The clinical implications of such side effects are still under investigation. The mechanisms that may contribute to tissue injury are shear stress and cavitation. In lithotripsy, cavitation is more likely to create injury within blood vessels and also cause mechanical damage to organs such as the kidney. However, severe full skin burns following extracorporeal shock wave lithotripsy for renal calculi [70] or second-degree burn after shock wave lithotripsy [71] are often reported. Some patients also face post-operative side effects such as pain, vomiting, and wounds on their skin.

Experiments with lithotripsy show the damage to *in vitro* cells and *in vivo* tissue is considerably decreased when cavitation is reduced or eliminated [72, 73]. The cavitation cycle time (time for a bubble to grow and collapse) is on the order of 300 μs in a free field and about 600 μs on the surface of the stone [74]. Based on recent studies, the cavitation bubbles produced by one lithotripsy pulse can be manipulated by a second pulse [75, 76]. Lithotripsy is a form of focused application of ultrasound.

High intensity focused ultrasound (HIFU) is another modality of focused ultrasound used to treat a range of disorders. In HIFU, the ultrasound beam is focused precisely on a target for a non-invasive or minimally invasive method of direct acoustic energy delivery into the body. HIFU is used for treatment purposes including those related to cancer therapy, surgery, and enhancing the

delivery or effect of chemotherapy or immunotherapy. The intention of HIFU is heating a target volume of tissue without affecting the tissue in the ultrasound propagation pathway. HIFU can increase the temperature of a selected area above 55 °C, which results in coagulative necrosis and immediate cell death in a specific volume (the “lesion”) through a focused ultrasound beam. Because the ultrasound wavelength at MHz frequencies has a millimetre-scale beam size and the ultrasound probe has a concave shape, the ultrasound beam can be focused into small, clinically relevant volumes of tissue. The energy absorption raises the temperature at the focus point but only to non-cytotoxic temperatures outside the region [77]. HIFU is applied from sources placed either outside the body for treatment of liver, kidney, breast, uterus, pancreas, and bone cancer or inside the body through the rectum for treatment of prostate cancer [77]. HIFU is gaining rapid clinical acceptance for non-invasive tissue heating and ablation for various applications. However, there are complications and side effects during HIFU treatment of tumors. For example, second-degree skin burns were reported in all patients [78] and third-degree skin burn in 3% of patients [79] during HIFU pancreas tumor treatment. Adverse effects such as tumor or vessel rupture during HIFU can lead to metastasis via the bloodstream. Serious adverse effects such as intrahepatic metastasis [80], lung embolism, deterioration of liver function, renal failure, and death can result from HIFU treatment [81]. The rates of adverse events in both malignant and benign lesions during HIFU largely depend on the disease type and the HIFU device used s [81]. HIFU therapy involves both thermal effects and cavitation that may lead to adverse effects and lesions. Skin burn is considered a thermal lesion and arises from the thermal effects of HIFU. Adverse effects such as tumor or vessel rupture and bleeding, ectopic embolism, and metastasis arise from cavitation during HIFU. The mechanical effect of cavitation can rupture vessel walls from the primary tumor site and at the same time detach cancerous cells/emboli and

lead to their release into circulation where they may cause metastasis or embolism [82, 83]. For example, intrahepatic metastasis [80] and rupture of esophageal varices [84, 85] after HIFU treatment have been reported. Cavitation gives rise to sensitivity of tissue to heat and causes extension of lesions beyond the HIFU focal point [86] that can lead to severe events if the lesion is in the vicinity of vital structures [81]. Peripheral nerve injuries following bone cancer treatment (reversible or irreversible) [87], ischiadic or sacral nerve damage, and hematuria during uterine fibroid treatment (potentially reversible) [88] are some other adverse effects of HIFU treatment. Adverse effects of HIFU frequently happen in tissues adjacent to the target focus as well as in the pathway of the HIFU beam. Therefore, selecting a proper delivery pathway for the HIFU beam [81], and, more importantly, improving cavitation monitoring techniques toward upgrading the accuracy of HIFU devices are necessary for improving the safety profile of this technique.

4.6 Cardiac

Premature ventricular contractions are another effect that results from exposure to a lithotripter ultrasound field [89, 90]; cardiac rhythm can be affected by even a single high-amplitude pulse. The threshold required to generate premature cardiac contractions is below the pressure amplitudes applied in clinical lithotripsy (positive pressure between 30 and 110 MPa and negative pressure between -5 and -15 MPa). To avoid affecting the cardiac rhythm during lithotripsy, the clinical delivery of lithotripter pulses is synchronized with an electrocardiogram [5]. To cause premature contractions, long ultrasound pulse durations and high-pressure amplitudes (e.g., a 5-ms pulse and 2-5 MPa, which is the threshold to cause a premature contraction in mice and frog at 1.2 MHz) are required, but these are not exposure characteristics

of diagnostic ultrasound [5]. Therefore, premature ventricular contractions should not occur during diagnostic ultrasound imaging.

Investigations using ultrasound contrast agents suggest that cavitation may be responsible for ultrasound-related premature cardiac contractions. The threshold for this effect of ultrasound is considerably lower in the presence of ultrasound contrast agents and at shorter pulse durations (e.g., the threshold for production of a premature contraction in the presence of contrast agents in mice exposed to a single 10-μs ultrasound pulse at 1.2 MHz was about 1 MPa [91]) [91-94]. Premature ventricular contractions have been reported in humans with ultrasound contrast agents in their blood and exposed to diagnostic ultrasound [94]. The threshold conditions for such an effect in laboratory animals is a 10-μs pulse of 1-MHz ultrasound and peak pressure amplitudes (positive and negative) on the order of 1 MPa [91, 92]. Microvasculature damage in hearts exposed to ultrasound in the presence of ultrasound contrast agents has also been reported, but without any certain relationship to the generation of arrhythmia [92, 93].

The other mechanical bioeffect of ultrasound on the heart is cardiac contractility, which can be generated by a single pulse of high amplitude ultrasound (peak positive pressure of about 1 MPa) [95, 96]. A series of experimental studies suggests that radiation force is responsible for this effect [96]. Animal studies (frog) showed the direct aortic pressure effect of ultrasound is related to the magnitude of the radiation force extended on the heart [96]. The role of radiation force alone on this effect was confirmed by a study in which an acoustic reflector was placed on the surface of the heart to preclude the possibility of heating and cavitation and instead maximize the radiation force delivered [96].

4.7 Blood vessels and microvasculature

The rupture or destruction of blood cells in the presence of ultrasound contrast agents at diagnostic levels of ultrasound has occurred in *in* vivo studies with laboratory animals [97]. Fetal red blood cells are even more susceptible to lysis from exposure to ultrasound in the presence of contrast agents *in vitro* [98]. However, this is not known to occur in mammals at diagnostic levels of ultrasound in the absence of ultrasound contrast agents [5]. In an *in vivo* study, hemolysis occurred when mice were exposed to ultrasound at a frequency of 1.1 MHz (10-μs pulse duration) and ~2 MPa negative pressure with ultrasound contrast agents [99].

To study the effects of ultrasound and contrast agents on microvasculature, isolated rabbit hearts were treated by a cardiac ultrasound system at 1.8 MHz with 1 Hz triggering of imaging frames [100]. Capillary damage and red blood cell (erythrocyte) extravasation was observed at an MI of 1.6 when the treated heart was examined. Chen et al. [101] examined the injurious effects of an ultrasound contrast agent (Optison or Definity) in rat heart *in vivo*, and observed elevation of troponin T in blood plasma as evidence of myocardial damage.

Cavitation is more likely to cause injury within blood vessels than in the surrounding tissue because a bubble surrounded by tissue is constrained and cannot go through the violent growth and collapse cycle compared to a bubble in a fluid environment such as a blood vessel. Bubbles can cause mechanical damage to organs such as the kidney through at least two mechanisms: collapse and expansion. The asymmetrical collapse of cavitation bubbles forms high velocity microjets of fluid that travel at speeds close to 400 km/h [102] as well as the emission of secondary shock waves that are radiated into the bubble and have a comparable amplitude to that of the focused shock wave [103]. The liquid microjets are forceful enough to easily puncture the fragile wall of a capillary or other blood vessel. Vessel walls may also rupture during the

expansion phase of the bubble cavitation cycle [103]. When a bubble undergoes explosive growth in the vessel, it pushes the vessel outward and ruptures it. Experiments using capillary phantoms in an *in vitro* system confirm this hypothesis [104, 105].

The bubble expansion mechanism may also lead to other tissue damage. When blood vessels rupture and blood is collected in pools (for example in a hematoma), then the potential for cavitation increases because the pooling of blood provides a fluid-filled space in which cavitation can occur [103]. Although cavitation is the primary mechanism of tissue injury studied, much more investigation is still required [103].

Damage to the microvasculature in tissues such as the kidney and liver in laboratory animals after exposure to lithotripter high-amplitude ultrasound has been reported in several studies [56, 106-108]. Damage to the microvasculature is considerably increased in the presence of ultrasound contrast agents in the vasculature [109-111]. In the presence of ultrasound contrast agents and an amplitude of only 2 MPa, reversible microvasculature damage has been observed in several soft tissues of mice, including muscle, mesentery, kidney, stomach, bladder, and fat, with persistent sensitivity to lithotripter exposure for several hours [109, 110]. In the absence of ultrasound contrast agents, minimal damage occurs at amplitudes up to 40 MPa. High amplitude pressure lithotripter pulses can cause cavitation *in vivo* and, in the presence of contrast agents, inertial cavitation can cause microvasculature damage. This understanding relies on the fact that hemorrhage in tissue (as a sign of response of microbubbles) at negative pressures is much greater than at positive pressures, as reported in different studies [5, 59].

Evidence indicates that pulsed ultrasound can also produce capillary damage in the presence of ultrasound contrast agents in the blood. Capillary rupture has been observed in muscle [112, 113], kidney [114], and cardiac tissues [92] of laboratory animals exposed to diagnostic levels of

ultrasound. Considering that no damage has been reported in these tissues from exposure to ultrasound in the absence of an ultrasound contrast agent, it can be concluded that normal tissue may contain no cavitation nuclei [5].

The effect of ultrasound on tissues in the presence of ultrasound contrast agents can be decreased by increasing the applied frequency as well as decreasing pressure amplitudes and the amount of contrast agents in the tissue [5]. In general, the mechanical effect of ultrasound increases in the presence of contrast agent microbubbles, which have potential utility in future therapeutic applications of ultrasound. For example, the capillary damage effect of ultrasound in the presence of ultrasound contrast agents facilitates the process of microbubble drug or gene delivery, in which microbubbles are loaded with drug/gene and then unloaded in a specific localized area of body [113, 115-118]; it also facilitates arteriogenesis [119, 120] and tumor therapy [117, 121-123].

In work by Williams et al. [125], therapeutic ultrasound was shown to decrease the recalcification time of anticoagulated whole blood *in vitro*. Therapeutic ultrasound has also been demonstrated to be capable of inducing platelet aggregation and releasing the platelet-specific protein β-thromboglobulin (β-TG), indicating that the platelet is the probable site of interaction and damage [125]. Their study also suggested that ultrasound interacts with blood platelets (the exceptionally fragile cells that play an important role in the early stages of clot formation) possibly via the occurrence of cavitation processes at MHz frequency levels. Furthermore, their *in vivo* study showed the production of platelet thrombi and true clots within the intact vascular system of mice as a result of acoustic microstreaming, similar to that developed around oscillating gas bubbles [125].

4.8 Prenatal exposure

At lower levels of ultrasound, such as for diagnostic purposes, ultrasound does not induce cavitation in the absence of pre-existing gas bubbles and also does not generally cause heating beyond the normal physiological range [34]. Prenatal exposure to a diagnostic level of ultrasound produces changes in neuronal migration in the developing brains of mice [124]. Significant concerns in the study of side effects of ultrasound in human are related to *in utero* exposure to diagnostic ultrasound. Based on available evidence, there are no effects on perinatal mortality and childhood malignancies; however, some observational studies have found an increased prevalence of non-right handedness in males with prenatal ultrasound exposure [34]. This might reflect confounding effects rather than causation; however, randomly comparing individuals who received prenatal ultrasound exposure with those who did not shows weak evidence for an ultrasound effect on non-right-handedness [33, 34]. At high levels of exposure, ultrasound is capable of causing permanent damage to biological tissue as a result of heating, acoustic cavitation, and radiation force [34] that can disturb the development of an embryo or fetus, i.e., teratogenic effects.

4.9 Biological Responses to Acoustic Mechanisms

The interaction of ultrasound with biological systems has been the subject of a considerable body of research. The potential biological changes associated with clinical applications of ultrasound, especially in obstetrics and gynaecology, have been studied in a wide variety of *in vitro* and *in vivo* models and ultrasound exposure conditions. However, sufficient caution must be exercised when extrapolating *in vitro* results to *in vivo* conditions. For example, the mechanism of interaction of sound waves with cells *in vitro* (in the liquid environment), where cell cultures are in suspension in a nutrient liquid medium or attached to a coated surface, may be very different

from the *in vivo* environment that features more solid structures such as tissue and bone [34]. The effect of ultrasound in cell suspensions is also different from monolayers of cells attached to a surface [34]. In the liquid environment, the most dominant physical mechanisms for biological effects of ultrasound are acoustic cavitation and streaming; substantial heating is unlikely because of the low acoustic absorption coefficient [34]. When tissue is exposed to ultrasound *in vivo*, high acoustic absorption energy in tissue causing thermal effects becomes more important compared to *in vitro* systems, while the probability of cavitation occurrence in tissue is less than in liquid. However, the probability of cavitation occurrence in intact tissue depends on temperature, the tissue state, and gas content [33, 34]. Acoustic exposure conditions as well as the mode of energy deposition are also very important for studying the biological effects of ultrasound. Two acoustic exposure conditions with the same exposure time and energy but different modes of energy deposition (one in continuous mode and the other in short pulses at a low repetition rate) may result in very different effects in tissue. Cavitation activity and its associated characteristic cell damage is more probable with short pulses at a low repetition rate, while thermal effects are more likely in continuous mode [34]. Therefore, in diagnostic ultrasound that features short exposures and relatively low temporal average intensities, thermal effects may not be very important in soft tissue; heating is more likely in tone burst and continuous exposure in therapeutic applications. However, high pressure amplitude with even short pulse mode exposure, such as used in lithotripsy, may promote acoustic cavitation in liquid media [34]. Passive cavitation detection has been used in several studies of ultrasound ablation [126-131], lithotripsy-induced cavitation detection [132]. Measurements using passive cavitation detection in both human and pig have shown the presence of bubbles in the perirenal fat, the collecting system, the parenchyma, and in subcapsular hematomas. The onset of detectable

cavitation in the parenchyma of a pig model required approximately 1000 shock waves to be delivered by a Dornier HM3 lithotripter [103]. In addition to acoustic exposure conditions, the maturity of the individuals being exposed is an important consideration, as biological damage to a few cells of the developing embryo is much more significant than to a small volume of adult cells. The acoustic properties of the early embryo are very similar to those of water. Therefore, bulk heating effects may be unimportant in the early embryo while heating at the bone surface may happen in a third trimester fetus in which bone mineralisation has occurred [34].

4.10 Cellular bioeffects

To study the interaction of ultrasound with biological systems, experimental studies with cells and animals have been performed at a variety of exposure conditions. Studies that describe ultrasonically-induced biological changes in cells *in vivo* and *in vitro* have been reviewed by Feril and Kondo [133], Miller [134], ter Haar [135], the National Council on Radiation Protection and Measurements (NCRP) [136], and the American Institute of Ultrasound in Medicine [137]. The most important representative examples of potential adverse effects on cells are cell lysis, changes in cell division capability, ultrastructural changes, chromosomal and cytogenetic effects, and functional changes [34]. The effects of ultrasound on cells fall into two categories: gross effects, such as lysis, effects on cell division capability, and damage to cellular ultrastructure; and subtle effects, such as chromosomal changes, functional changes, and altered growth patterns [34].

There is extensive and unequivocal evidence that ultrasound exposure of cells in suspension leads to cell lysis [34]. Several studies including, for example, Kaufman et al. [138], Morton et al. [139], Hallow et al. [140], and Lai et al [141], have shown that cavitation is a major mechanism resulting in this sort of complete cellular disruption; however, it is not clear if

ultrasound is able to produce lysis in the absence of cavitation effects [34]. Apart from the ultrasound exposure conditions, the amount of cell lysis can depend on the concentration of cells in suspension [142, 143] as well as cell size [144, 145]. Lysis appears to be an immediate consequence of ultrasound exposure effects on cells and this may affect cells in mitosis more than other cell cycle stages [146]. Colonogenic assays enable assessment of cell division capability following a specific insult. Based on studies performed by Bleaney et al. [147] and Morton et al. [139], cells that survive ultrasound exposure and stay intact will continue producing progeny in the same way as their untreated counterparts. However, there are exceptions for ultrasound exposed cells that remain at elevated temperatures [148, 149].

The interaction of ultrasound with the cell membrane has been of interest in ultrasound-mediated drug delivery and sonoporation [150-152] and extraction of medicinal compounds from biological resources [153]. Changes in permeability to ions is one of the usual changes that occurs in cells exposed to ultrasound. Research by Chapman [154] demonstrated that acoustic exposure at 1.8 MHz and I_{SATA}=1 W cm^{-2} *in vitro* resulted in sublethal alteration in the thymocyte plasma membrane, which leads to a decrease in potassium content. A reversible rise in calcium ion uptake in fibroblasts was observed by Mortimer and Dyson [155] at an ultrasound frequency of 1 MHz and intensity of I_{SATA}=0.5-1 W cm^{-2}.

Electron microscopy results of cells and tissues following exposure to ultrasound show damage to a variety of subcellular organelles, primarily mitochondria, and damage to lysosomes with consequent release of lysosomal enzymes in tissue [156-158]. In addition to membrane and mitochondrial damage as a result of cavitation, Harvey et al. (1975) observed dilated rough endoplasmic reticulum and some irregular lesions [159]. Generally, the cell nucleus seems unaffected by ultrasound exposure; the only type of lesion observed is slit-like vacuoles at the

nuclear membrane [160]. Watmough et al. (1977) hypothesized that ultrasound may produce cavitation microbubbles within cells and that nuclear, mitochondrial, and granular endoplasmic reticulum membranes act as nucleation sites; thus, when these organelles are affected, damage might show itself as lesions next to the membrane [161].

Cytogenetic studies on the effect of ultrasound on chromosomes clearly show that high intensity ultrasound can cause degradation of DNA in solution. Damage appears to be due to hydrodynamic shear stresses, free radical formation, or excessive heating as a result of cavitation [162-164]. A large amount of evidence shows that high intensity ultrasound up to a power of I_{SATA}=100 W cm^{-2} does not produce chromosomal damage [165, 166]. However, when an ultrasound exposure at an intensity of 3 W cm^{-2} and frequency of 810 kHz is followed by (not preceded by) X-irradiation to 1 Gy, some synergistic interactions may result in chromosomal aberrations [167]. Diagnostic ultrasound even at intensities up to I_{SATA}=3.0 W cm^{-2} (3.15 MHz) does not produce sister chromatid exchanges (SCEs) *in vitro* [168]. Whether ultrasound may result in chromosomal damage is not certain; however, the most carefully documented studies have returned negative results. It must also be considered that these were *in vitro* studies, and the interaction mechanism *in vitro* may be different from that in intact tissue *in vivo*. Overall, ultrasound may cause epigenetic changes, such as modification of histone protein structure, that can have a long-term influence on gene expression [34]. Ultrasound may also lead to stimulation of cellular functions that mostly involve interactions at the cell membrane level [34]. Taylor and Newman [169] report that ultrasound exposure at treatment conditions of 1 MHz, I_{SATA}=10 W cm^{-2} , pulses of 20 μs-10 ms, for over 2.5 minutes influenced the electrophoretic mobility of cells, which reflects a cell surface charge density change as a result of volume changes [170]. The results of time-lapse photomicrography of cellular movements *in vitro* show ultrasonically

induced changes that may last for several generations of cells [171]; however, such results are far from clear *in vivo* [34]. To obtain a clearer indication of the biological effects of ultrasound, various studies focusing on biological systems such as bone, blood, vasculature, and lung as well as effects on the fetus and embryo have been conducted using small animal models.

4.11 Studies on Biological Effects of Ultrasound

Low intensity pulsed ultrasound (such as 0.5-50 mW/cm^2) has a favorable effect on bone fracture healing [172]. Several studies have shown that low intensity ultrasound increases the rate of tissue repair following injury, especially those associated with bone fracture [173, 174]. The reasons why ultrasound can give rise to tissue repair and also the functional significance of changes in neuronal migration in the developing brains of mice are not known.

In physiotherapy, hyperthermia treatment, and pulsed Doppler exposure at its maximum output power, one of the main concerns and problems has been pain induction due to heating of the highly innervated periosteum. Biologically relevant temperature increases (over 2 °C) at the skull bone of laboratory animals have been recorded during ultrasound exposure [34]. Smith et al. [175] demonstrated that ultrasound exposure at high intensities (over I_{SATA}= 40 W cm^{-2}) in thermal ablation therapies can lead to osteocyte damage and thermal necrosis. Evidence shows that very low intensity ultrasound (I_{SATA}=12-100 mW cm^{-2}) can influence bone regeneration [176] and this fact is used for treatment of fractures. These influences are predominantly due to a non-thermal mechanism that critically depends on the intensity applied [34]. The temperature increase for intensities of I_{SATA}=20-50 mW cm^{-2} was below 1 °C [177]. Duarte et al. [178] also report negligible increases in temperature (0.01±0.005 °C) in rabbit fibula osteotomies following treatment at I_{SATA}=50 mW cm^{-2} for 15 minutes per day. However, even a small rise in

temperature (less than 1 °C) can influence some enzymes, such as matrix metalloproteinase 1 that has been shown to be very sensitive to temperature [179, 180].

The biophysical process behind bone regeneration stimulation is still unknown. However, several studies suggest that low intensity ultrasound can affect cell membrane permeability [155, 181-190] and increase hydrostatic pressure [185] or can induce mechanical stimulation of micromotion [191] and cause acceleration of fracture healing. Relative to an untreated control, high intensity ultrasound (I_{SATA}=0.2-3 W cm^{-2}) gives rise to callus formation and accelerates fracture healing in rabbit radii [192, 193] and tibia [194] and guinea pig ulnae [195]. High intensity ultrasound treatment (I_{SATA}=0.5 W cm^{-2}) of limbs resulted in a 36% increase in new bone formation and an 80% increase in torsional stiffness compared with controls [177].

Studies on the effect of ultrasound on blood have focused on platelets, the most fragile component. *In vitro* experiments show that ultrasound exposure can lead to platelet activation. In the presence of stable bubbles (those that do not collapse violently and instead oscillate for several cycles around their resonance size), a pressure amplitude of 10 MPa and low average ultrasound intensity of I_{SATA}=0.8 W cm^{-2} can cause platelet disruption [196]. Although erythrocytes seem to be more resistant than platelets to ultrasound damage, haemolysis has been reported when inertial cavitation occurs [197-199]. Williams and Miller (1980) suggest that adenosine-5'-triphosphate (ATP) may be released at lower intensities when inertial cavitation occurs [200].

Because of the continual filtration of impurities in whole blood *in vivo*, the probability of cavitation nuclei is reduced and therefore under normal conditions cavitation is unlikely to happen [34]. However, Brayman et al. [143] show cavitation may occur at sufficiently high pressures. Damage to blood components *in vivo* has not been clearly demonstrated [99, 201-203].

In experiments by Dalecki et al. [99], a clinically insignificant level of haemolysis (0.46%) was detected in mice exposed to ultrasound through the chest wall at a frequency of 2.35 MHz and a peak positive pressure amplitude of 10 MPa.

VanBavel (2007) reviewed the effects of ultrasonically-induced shear stresses on endothelial cells and noted that[204], a major stimulus for many endothelia responses is provided by the shear stress associated with normal blood flow. For example, normal shear stress found in large arteries away from branches is on the order of 2-4 Pa [205] and very rarely exceeds 8 Pa. The shear stress that veins experience is around 0.1-0.6 Pa [204]. Microstreaming associated with an ultrasonic field induces shear stresses that may be expected to increase biological effects. These shear stresses are higher than normal physiological levels and can occur on a membrane, rupture it, or alter its permeability [34]. Experiments performed by Dalecki et al. [206] showed that ultrasound at acoustic treatment conditions of 1.2 MHz, peak positive pressure of 4 MPa, peak rarefactional pressure of 2.5 MPa, 10 μs, pulse repetition frequency of 100 Hz for 3 minute exposure may induce haemorrhage near to fetal bone. Haemorrhage has also been observed in the lung and intestine of mice when treated at pressures greater than diagnostic levels. However, haemorrhage and these kinds of effects in other tissues are more associated with ultrasound treatment in the presence of a gas-filled ultrasound contrast agent [34]. Dalecki et al. [206] imputed these effects to the relative motion between partially ossified bones and the surrounding tissues (that may leads to fragile fetal blood vessel damage); however, Bigelow et al. (2007) postulated the involvement of thermal effects[207].

Application of an ultrasound contrast agent (suspensions of stabilised bubbles) seems to give rise to biological effects through gas-body activation [134]. Brayman et al. [208] observed that the contrast agent in suspension adjacent to orientation of the monolayer (i.e., simulatingthe sites of

ultrasound entry or exit from a blood vessel) gave rise to damage and erosion of cells. They modeled the endothelial layer of blood vessels using fibroblast monolayers *in vitro* and ultrasound treatment was performed at 1.0, 2.1, and 3.5 MHz. The lysis or breaking open of erythrocytes leads to the release of hemoglobin into the surrounding fluid. The frequency dependence of haemolysis with a first-generation ultrasound contrast agent (Albunex) in whole blood and a second-generation perfluorocarbon-based ultrasound contrast agent (Optison) was studied by Miller et al. [209] and Miller and Gies [210]. Miller and Gies [211] show that Optison caused more haemolysis than Albunex, especially when ultrasound exposure was in pulsed mode. The ultrasound contrast agent gas bodies can nucleate inertial cavitation [163] as there is good correlation between the amount of haemolysis induced by ultrasound and inertial cavitation activity [212-215]. Ultrasonically-induced haemolysis strongly depends on the frequency [213, 216, 217], with overall biological effects decreasing with frequency [34].

Contrast agent injection may enhance the risk of capillary rupture by diagnostic ultrasound [34]. Miller and Quddus (2000) anaesthetised hairless mice, injected them with Optison (5 mL kg^{-1}), and scanned them using a 2.5 MHz transducer (610 ns pulses with 3.6 kHz repetition frequency and 61 Hz frame rate); this resulted in an increasing number of petechiae (capillary rupture with erythrocyte extravasation) in the intestine and abdominal muscle[112]. The increase in petechiae was considerable above 0.64 MPa for muscle and 1 MPa for intestine [34]. The rat heart was used as a model system to examine microvascular injury of ultrasound by Li et al. [92, 218]. Rats were examined in a water bath using a 1.7 MHz diagnosis ultrasound system and bolus doses of three different ultrasound contrast agents (Optison, Imagent, and Definity). They detected petechiae on the heart surface and also microvascular leakage by injecting Evans blue dye before scanning. The results of their study demonstrated that the contrast agent delivery mode and dose,

as well as the ultrasound parameters, have a considerable effect on cardiomyocytes. Vascular damage might be physiological and not accompanied by irreversible cellular injury [219]. In fact, dynamics of microbubbles both *in vitro* and *in vivo* show that the oscillation of microbubbles increases vascular permeability and even locally injured vasculature [220, 221]. Depending on the amount of temperature rise during ultrasound application, the effects on vasculature can be either reversible/repairable or irreversible. In reversible cases, the effects are temporary and no permanent vascular occlusion is produced. In irreversible cases, the energy deposition is sufficient to produce long-term damage with persistent effects of vascular spasm, obstructed blood flow, and increasing endothelial destruction that lead to a loss of vascular relaxation responses [222]. Therefore, appropriate strategies need to be designed to minimize irreversible damage to capillaries [220].

Kobayashi et al. [223, 224] studied the microvascular injury in rat mesentery by applying a phased array ultrasound system at a frequency of 1.8 MHz. Endothelial cells were damaged in capillaries and venules for all conditions at 0.82 MPa. The influence of contrast-enhanced diagnostic ultrasound (Optison and several experimental agents) in kidney of rat at three different frequencies of 1.8, 4, and 6 MHz was studied by Wible et al. [114]. Glomerular capillary haemorrhage was driven from the glomerular tuft into Bowman's capsule and proximal convoluted tubules. Shigeta et al. [225] demonstrated that platelet aggregation in the liver sinusoids of rat occurred after exposure of the liver to diagnostic ultrasound at 8 and 12 MHz with an ultrasound contrast agent (Levovist). They also observed endothelial cell damage in samples taken five hours after acoustic exposure. Based on experiments by Stroick et al. [226] and Hardig et al. [227] in an animal model, the extent of intracerebral haemorrhage is not enhanced by ultrasound exposure in the presence of an ultrasound contrast agent. The effect of

ultrasound exposure on rat heart was detected using diagnostic imaging with an experimental ultrasound contrast agent by Vancraeynest et al, 2006 [228]. Findings of histologically definable injury in rat hearts were confirmed by [229, 230] and indicate that elevating the parameters for therapeutic efficacy results in severe microscale injury and functional impairment of the heart [228].

New techniques have been developed with respect to the use of ultrasound and specially designed contrast agents to aid drug delivery across the blood-brain barrier (BBB) [34]. It was first thought that opening the BBB was induced by inertial cavitation, although disruption in the absence of indicators of inertial cavitation has been demonstrated [34]. In almost in every study featuring a combination of ultrasound and ultrasound contrast agent, some BBB injury has been observed [34]. Mesiwala et al. [231] showed that HIFU resulted in selective and non-destructive disruption of the BBB in a rat model. It is possible that the BBB is opened at the focal point without sharp neuronal damage if microbubbles are introduced into the bloodstream before focused ultrasound exposure [232]. Therefore, limiting the effect of ultrasound on the vasculature and decreasing the intensity required to produce BBB opening can be achieved by introduction of cavitation nuclei into the bloodstream. This also reduces the risk of damage to tissue [34]. BBB disruption was also detected by Hynynen et al. [232] and Kinoshita et al. [233] after applying contrast-enhanced magnetic resonance imaging (MRI) at the desired location, as well as with post-mortem histology by Mesiwala et al. [231] and Kinoshita et al. [233]. Hynynen et al. [234] studied the localized effects of ultrasound exposure on rabbit brains using contrast-enhanced MRI. Their study showed BBB disruption for pressure amplitudes above 0.4 Mpa, at 10 ms exposure with a frequency level of 690 kHz, a repetition frequency of 1 Hz, and total exposure time of 20 s. The results of a histological study four hours after exposure showed about

70-80% brain tissue necrosis at pressure amplitude levels above 2.3 MPa. Small areas of erythrocyte extravasation were also observed at lower pressure amplitude levels. Another study demonstrated that when rabbit brain is exposed to ultrasound at 1.63 MHz, a pulse length of 100 ms, a pulse repetition frequency of 1 Hz, at 0.7 to 1.0 MPa for 20 s, only a few cells in some of the sonicated areas had ischemia or apoptosis, but no ischemic region that would indicate compromised blood supply was observed. MRI or histology up to 4 weeks after sonication showed no delayed effect [235]. Therefore, it is possible that BBB disruption after ultrasound may occur without any basic vascular damage; however, red blood cell extravasation into tissue indicates BBB injury has occurred and, as such, the method can be harmful especially for therapeutic applications for brain disease [34].

Hynynen et al. [236] studied the effect of burst mode of ultrasound exposure in the presence of an ultrasound contrast agent on brain tissue using contrast-enhanced MRI and histology. Brain tissue damage, including vascular wall damage, haemorrhage, and sometimes necrosis, was induced at a pressure amplitude of 6.3 MPa (exposure conditions of 1.5 MHz, 10 μs bursts repeated at a frequency of 1 kHz for 20 s). At all tested pressure values, occasional smooth vascular damage in almost 50% of the sonicated locations was observed without any signs of ischemia.

Fatar et al. [237] applied ultrasound (at 2 MHz, 1052 peak negative pressure, and temporal intensity of 37.3 W cm^{-2}) and microbubbles (SonoVue) in a middle cerebral artery occlusion model in rats and studied the influence on brain infarct volume, apoptosis, IL-6 and TNF-alpha levels, and disruption of the BBB. They observed a reduction of the infarct volume in treated samples compared with controls. The results showed no additional BBB disruption and also no rise in apoptotical cell death outside the infarction area. Another study showed that rabbit brain

exposure to low intensity ultrasound (at 1.7 MHz for 30 s) and close to the threshold for tissue damage gave rise to apoptotic cells over 48 hours, but the lesions were dominated by necrosis [238]. Adding ultrasound contrast agent (Optison) to the treatment process (at 1.5 MHz, 1.4-8.8 MPa, and for 20 s) resulted in domination of lesions by apoptosis, with the number of apoptotic cells approximately six times that of necrotic cells [239]. Another study on the short-term safety of BBB opening using focused ultrasound and an ultrasound contrast agent (Baseri 2010) reported the feasibility of a safe BBB opening under a specific set of sonication parameters. In this study, a short-term (30-min or 5-h survival) histological assessment was performed on 49 mice with an intravenously injected ultrasound contrast agent. Mice were exposed to ultrasound at a frequency of 1.525 MHz, pulse length of 20 ms, pulse repetition of 10 Hz, peak rare factional acoustic pressure of 0.15-0.98 MPa, and two 30-s sonication intervals with an intermediate 30-s delay. The BBB opening threshold and the safest acoustic pressure were reported to be 0.15-0.3 and 0.3-0.46 MPa, respectively (Baseri 2010). Another study indicated that repeated opening of the BBB through FUS and ultrasound contrast agents at the basal ganglia of non-human primates is safe for up to 20 months with no long-term negative physiological or neurological effects (Downs 2015). This study was conducted using ultrasound parameters of 500 kHz, 200-400 kPa, administration of 4-5 μm microbubbles, and 2 min sonication, resulting in repeated opening of the BBB. These results demonstrate promise for clinical and basic scientific applications[240].

4.12 Fetus and embryo

Concerns regarding the effect of ultrasound on fetal and embryonic development (teratogenic effects) have generated a large number of studies using different animal species and various exposure conditions. The probability of adverse effects of ultrasound on fetal and embryonic

development has been reviewed by Ziskin and Barnett [241], Miller et al. [242], and Church and Miller [243]. Non-thermal interactions of pulsed ultrasound, especially cavitational mechanisms in the presence of an ultrasound contrast agent, may have adverse effects on the integrity of maternal and developing tissue. However, there is a low possibility of occurrence of these interactions in the fetus [244, 245]. In addition, the teratogenic effects of heat as a result of probable localized hyperthermia during pregnancy ultrasound scans have been extensively reviewed by Miller and Ziskin [246], Miller et al. [242], and Edwards et al. [247]. High maternal or fetal temperatures can have adverse effects on many developing tissues, particularly the brain and nervous system [242].

The teratogenic effect of heat on mammals is well accepted and, among all organs and tissues, the developing central nervous systems shows the greatest sensitivity [34]. Miller and Ziskin [246], Miller et al. [242], and Edwards et al. [247] conducted animal studies on the possible pathogenic mechanisms and thermal effects on the embryo and fetus. Embryo death, growth retardation, internal and external abnormalities, developmental deficits, and behavioral changes that persist into adulthood are some of consequences of fetal hyperthermia [247]. The occurrence of these thermal effects depends on three main parameters: the grade of normal core temperature promotion, the duration of the elevation in temperature, and the specific phase of development (pre-implantation, organogenesis, or fetal period) in which the heating happened [34]. Edwards et al. (2003) demonstrated that the sensitivity of the embryo and fetus to heat changes considerably during development and depends on the particular cell cycle, e.g., cell proliferation, differentiation, or migration[247]. They also described the teratogenic or biological effects of heat at different steps of development. Higher temperatures for a shorter time may raise the risk of a certain defect; the best estimate by Miller et al. (2002) is a threshold of 1.5-2.5 °C above

normal body temperature for an hour or so in pregnant animals, acknowledging that each type of defect and species has its own temperature threshold[242]. In addition to the thermal effect of ultrasound, pulsed and continuous-wave ultrasound can affect reproduction and prenatal development of the embryo and fetus [248]; [249]. Notable ultrasound effects such as increased malformation rates or weight changes have been observed in some studies, while others do not report any firm exposure-related effects in either dam or child [250-263]. These studies used different endpoints, pregnancy ages, species, and ultrasonic exposure conditions, making direct comparisons of results problematic. No considerable treatment-related effects were observed on reproductive outcome or maternal weight during gestation, on viability or weight of child, or on the morbidity of skeletal or visceral malformations when rats were exposed to 3 MHz continuous wave [264, 265] or pulsed ultrasound [254, 255] at up to 30 W cm^{-2} (I_{SPTA}). Statistically considerable decreases in body weight of offspring were observed following frequent exposure of cynomolgus macaques to ultrasound (at 7.5 MHz and I_{SATA}=0.28-12 mW cm^{-2}) [250, 266, 267]; this effect occurred during the first three months of life and not for the subsequent nine months. In a study by Arthuis et al. (2013) in which contrast-enhanced ultrasound imaging and Doppler were used to quantitatively monitor uteroplacental perfusion in rat pregnancies, no microbubbles were detected in the umbilical vein or fetal components[268]. The absence of contrast agents in the fetal compartment would suggest the innocuity of contrast-enhanced ultrasound imaging on fetal development [268]. Overall, there may be no real safety concerns with respect to common clinical use of sonography; however, caution must be exercised when high output regimes such as pulsed Doppler are applied in obstetrics (ter Haar 2010). Ultrasound is often used in obstetric including with the Doptone for fetal monitor and hearing the baby's heartbeat. Considering the difficulty in establishing the thresholds for biological effects, it is

suggested that as-low-as-reasonably-possible scanner outputs be used to collect the required diagnostic information. Unnecessary examinations (non-medical sonography) during pregnancy are not advised because of the large number of remaining unknowns (ter Haar 2010).

4.13 Summary

Ultrasound interacts with tissue through both thermal and non-thermal mechanisms (mostly attributed to cavitation and radiation force) and generates a variety of biological effects at the cellular or intact tissue levels (structural or functional changes). Three main factors can result in bioeffects due to ultrasound: heating, radiation pressure, and the presence of gas (ter Haar 2010). The ultrasound beam's energy and frequency as well as the properties of the medium through which the ultrasound beam passes play important roles in the biological effects. Heating is mostly related to absorption of ultrasound energy by tissue. The mechanical effects that arise from cavitation are primarily related to bubbles created during the rarefactional cycle of acoustic pressure, the presence of gas in the solution that turns to microbubbles via the negative pressure of ultrasound, naturally gaseous body tissues, such as lung alveoli or intestine, or introduction of stabilized gas-filled microbubbles (ultrasound contrast agent) into the blood stream by extravasation.

Based on evidence from cellular and animal studies, high-power devices used in therapeutic and surgical applications, in which the purpose is to deliver high intensity ultrasound to a target tissue, can clearly cause potential biological effects in the body. However, these biological effects have brought about unique opportunities for non-invasive ultrasound therapy; concerns apart from safety are mainly with respect to accurate targeting of ultrasound in the desired target volume without damaging other tissues.

At lower levels of exposure, such as diagnostic ultrasound, there is no established evidence of any specific harmful effect; however, too few research data are available to draw firm conclusions, especially with respect to the long-term use of ultrasound. The subtle effects of diagnostic ultrasound, such as neuronal migration or changes in membrane permeability, are not completely understood.

While the application of ultrasound in fetal imaging has evolved beyond medical practice to commercial souvenir scans, detailed 3D facial imaging, or recording of the baby's movement in the womb via 4D sonography, which require prolonged and more intense ultrasound exposure, there are unconfirmed indications from the biological and epidemiological literature of possible neurological influences on *in utero* ultrasound exposure. Therefore, diagnostic ultrasound should be used wisely, especially with respect to newer equipment that can have higher acoustic output levels than earlier models. Furthermore, for continued safety, there is a great need to further study the long-term hazards of exposure, especially *in utero* exposure, to diagnostic ultrasound.

In addition, a better understanding of the direct physical effect of ultrasound (acoustic cavitation) is required to determine the cause of any biological effects in human (e.g., trauma to lung or intestine, capability to improve healing of bone and soft tissue, platelet damage as a result of cavitation) as well as improve the quality of ultrasound applications in many clinical practices (e.g., drug delivery, tumor ablation, etc.). Based on a literature review by ter Haar (2010) [269] presented from a diagnosis safety viewpoint, most bioeffects from clinically relevant practices arise from short, high-amplitude ultrasonic pulses at high repetition rates. However, most studies until recently have focused on continuous-wave (long-tone-burst) exposures. Furthermore, most *in vitro* studies have investigated the effect of ultrasound on either suspended culture cells or monolayers, yet the way ultrasound interacts with cells in an aqueous environment is different

from intact tissues (ter Haar 2010). Because thermal effects can be better observed through energy absorption of tissue, cultured cells may not properly reflect thermal effects and instead may more show more cavitation effects. When an *in vivo* study is performed, the body's physiological response can also be studied. Also, the size of the animal (and consequently the attenuation of the beam in its body) in most *in vivo* studies is much smaller than a human. In small animal studies, it is usual for most of the body to be exposed to the ultrasound beam (ter Haar 2010). Therefore, having the more appropriate model size and measuring the attenuation due to the intervening tissue can ensure the findings are relevant with respect to effects in humans. Although ultrasound bioeffects shown in animal models occur under conditions similar to those used in humans, we cannot confidently relate these results to humans. The absence of human studies on the bioeffects of diagnostic ultrasound does not necessarily mean there are no effects but, rather, a lack of techniques to detect them. Cavitation thresholds are usually determined experimentally through acoustic emission, broad band noise, and subharmonic signals from bubbles. Because of the attenuation of signals in tissue, detection of signals arising from deep in tissue is more difficult than for those from the surface. This makes the detection of cavitation in tissue very difficult. Detection and visualization of cavitation responses in the body at different operating conditions would be very helpful in threshold determination as well as characterization and analysis of cavitation in the human body.

A complete understanding of the interaction of ultrasound with ultrasound contrast agents is required to develop the full potential of ultrasound contrast agents in biomedical ultrasound applications such as drug/gene delivery, tumor therapy, and arteriogenesis. More information regarding the location of microbubbles in the body as well locating the area where microbubbles are in contact with tissue and cells subjected to ultrasound exposure is necessary.

Further advances in the use of ultrasound in medicine require better knowledge of the cellular and molecular events interfering with physical mechanisms of ultrasound combined with their related biological effects. In addition, more effort is required to visualize, detect, and monitor ultrasound-induced cavitation bubbles combined with ultrasound contrast agents deep in body to have more control over the biological effects of ultrasound.

4.14 References

1. Escoffre JM BA: *Therapeutic Ultrasound.* Switzerland: Springier International Publishing; 2016.
2. Escoffre JM, Zeghimi A, Novell A, Bouakaz A: **In-vivo gene delivery by sonoporation: recent progress and prospects.** *Curr Gene Ther* 2013, **13:**2-14.
3. Panje CM, Wang DS, Willmann JK: **Ultrasound and Microbubble–Mediated Gene Delivery in Cancer: Progress and Perspectives.** *Investigative radiology* 2013, **48:**755-769.
4. Kandadai MA, Meunier JM, Hart K, Holland CK, Shaw GJ: **Plasmin-loaded echogenic liposomes for ultrasound-mediated thrombolysis.** *Transl Stroke Res* 2015, **6:**78-87.
5. Dalecki D: **Mechanical bioeffects of ultrasound.** *Annu Rev Biomed Eng* 2004, **6:**229-248.
6. Rooney JA, Nyborg WL: **Acoustic radiation pressure in a traveling plane wave.** *American Journal of Physics* 1972, **40:**1825-1830.
7. Dayton P, Klibanov A, Brandenburger G, Ferrara K: **Acoustic radiation force in vivo: a mechanism to assist targeting of microbubbles.** *Ultrasound in medicine & biology* 1999, **25:**1195-1201.
8. Nightingale KR, Kornguth PJ, Walker WF, McDermott BA, Trahey GE: **A novel ultrasonic technique for differentiating cysts from solid lesions: preliminary results in the breast.** *Ultrasound in medicine & biology* 1995, **21:**745-751.
9. Kooiman K, Vos HJ, Versluis M, de Jong N: **Acoustic behavior of microbubbles and implications for drug delivery.** *Advanced drug delivery reviews* 2014, **72:**28-48.
10. Speed C: **Therapeutic ultrasound in soft tissue lesions.** *Rheumatology* 2001, **40:**1331-1336.
11. Flynn H: **Generation of transient cavities in liquids by microsecond pulses of ultrasound.** *The Journal of the Acoustical Society of America* 1982, **72:**1926-1932.
12. Wu J: **Theoretical study on shear stress generated by microstreaming surrounding contrast agents attached to living cells.** *Ultrasound in medicine & biology* 2002, **28:**125-129.
13. Doinikov AA, Bouakaz A: **Acoustic microstreaming around an encapsulated particle.** *The Journal of the Acoustical Society of America* 2010, **127:**1218-1227.
14. Ohl C-D, Arora M, Ikink R, De Jong N, Versluis M, Delius M, Lohse D: **Sonoporation from jetting cavitation bubbles.** *Biophysical journal* 2006, **91:**4285-4295.
15. Postema M, van Wamel A, ten Cate FJ, de Jong N: **High-speed photography during ultrasound illustrates potential therapeutic applications of microbubbles.** *Med Phys* 2005, **32:**3707-3711.
16. Bekeredjian R, Bohris C, Hansen A, Katus HA, Kuecherer HF, Hardt SE: **Impact of microbubbles on shock wave-mediated DNA uptake in cells in vitro.** *Ultrasound Med Biol* 2007, **33:**743-750.
17. Nelson TR, Fowlkes JB, Abramowicz JS, Church CC: **Ultrasound biosafety considerations for the practicing sonographer and sonologist.** *Journal of Ultrasound in Medicine* 2009, **28:**139-150.
18. Wells PNT: *Biomedical ultrasonics.* Academic Pr; 1977.

19. Sun T, Samiotaki G, Wang S, Acosta C, Chen CC, Konofagou EE: **Acoustic cavitation-based monitoring of the reversibility and permeability of ultrasound-induced blood-brain barrier opening.** *Physics in medicine and biology* 2015, **60:**9079.
20. Coussios CC, Roy RA: **Applications of acoustics and cavitation to noninvasive therapy and drug delivery.** *Annu Rev Fluid Mech* 2008, **40:**395-420.
21. Lammertink BH, Bos C, Deckers R, Storm G, Moonen CT, Escoffre J-M: **Sonochemotherapy: from bench to bedside.** *Frontiers in pharmacology* 2015, **6**.
22. Klibanov AL: **Targeted delivery of gas-filled microspheres, contrast agents for ultrasound imaging.** *Advanced drug delivery reviews* 1999, **37:**139-157.
23. Unger EC, Matsunaga TO, McCreery T, Schumann P, Sweitzer R, Quigley R: **Therapeutic applications of microbubbles.** *European journal of radiology* 2002, **42:**160-168.
24. Deng CX, Sieling F, Pan H, Cui J: **Ultrasound-induced cell membrane porosity.** *Ultrasound Med Biol* 2004, **30:**519-526.
25. Woudstra L, Krijnen P, Bogaards S, Meinster E, Emmens R, Kokhuis T, Bollen I, Baltzer H, Baart S, Parbhudayal R: **Development of a new therapeutic technique to direct stem cells to the infarcted heart using targeted microbubbles: StemBells.** *Stem cell research* 2016, **17:**6-15.
26. Fix SM, Borden MA, Dayton PA: **Therapeutic gas delivery via microbubbles and liposomes.** *Journal of Controlled Release* 2015, **209:**139-149.
27. McEwan C, Owen J, Stride E, Fowley C, Nesbitt H, Cochrane D, Coussios CC, Borden M, Nomikou N, McHale AP: **Oxygen carrying microbubbles for enhanced sonodynamic therapy of hypoxic tumours.** *Journal of Controlled Release* 2015, **203:**51-56.
28. Legband ND, Feshitan JA, Borden MA, Terry BS: **Evaluation of peritoneal microbubble oxygenation therapy in a rabbit model of hypoxemia.** *IEEE Transactions on Biomedical Engineering* 2015, **62:**1376-1382.
29. Legband N, Hatoum L, Thomas A, Kreikemeier-Bower C, Hostetler D, Buesing K, Borden M, Terry B: **Peritoneal Membrane Oxygenation Therapy for Rats With Acute Respiratory Distress Syndrome.** *Journal of Medical Devices* 2016, **10:**020905.
30. McEwan C, Kamila S, Owen J, Nesbitt H, Callan B, Borden M, Nomikou N, Hamoudi RA, Taylor MA, Stride E: **Combined sonodynamic and antimetabolite therapy for the improved treatment of pancreatic cancer using oxygen loaded microbubbles as a delivery vehicle.** *Biomaterials* 2016, **80:**20-32.
31. Child SZ, Hartman CL, Schery LA, Carstensen EL: **Lung damage from exposure to pulsed ultrasound.** *Ultrasound Med Biol* 1990, **16:**817-825.
32. Dalecki D, Raeman CH, Child SZ, Carstensen EL: **A test for cavitation as a mechanism for intestinal hemorrhage in mice exposed to a piezoelectric lithotripter.** *Ultrasound in medicine & biology* 1996, **22:**493-496.
33. radiation Tiagon-i: **Health effects of exposure to ultrasound and infrasound.** In *documents of the health protection agency, radiation, chemical and environmental hazards*; 2010.
34. Hanson MA: **Health effects of exposure to ultrasound and infrasound: report of the independent advisory group on non-ionising radiation.** *Health Protection Agency* 2010.

35. Hartman C, Child S, Mayer R, Schenk E, Carstensen E: **Lung damage from exposure to the fields of an electrohydraulic lithotripter.** *Ultrasound in medicine & biology* 1990, **16:**675-679.
36. Holland CK, Deng CX, Apfel RE, Alderman JL, Fernandez LA, Taylor KJ: **Direct evidence of cavitation in vivo from diagnostic ultrasound.** *Ultrasound Med Biol* 1996, **22:**917-925.
37. Penney D, Schenk E, Maltby K, Hartman-Raeman C, Child S, Carstensen E: **Morphological effects of pulsed ultrasound in the lung.** *Ultrasound in medicine & biology* 1993, **19:**127-135.
38. Baggs R, Penney DP, Cox C, Child SZ, Raeman CH, Dalecki D, Carstensen EL: **Thresholds for ultrasonically induced lung hemorrhage in neonatal swine.** *Ultrasound Med Biol* 1996, **22:**119-128.
39. Dalecki D, Child SZ, Raeman CH, Cox C, Penney DP, Carstensen EL: **Age dependence of ultrasonically induced lung hemorrhage in mice.** *Ultrasound Med Biol* 1997, **23:**767-776.
40. Holland CK, Deng CX, Apfel RE, Alderman JL, Fernandez LA, Taylor KJ: **Direct evidence of cavitation in vivo from diagnostic ultrasound.** *Ultrasound in medicine & biology* 1996, **22:**917-925.
41. Tarantal AF, Canfield DR: **Ultrasound-induced lung hemorrhage in the monkey.** *Ultrasound in medicine & biology* 1994, **20:**65-72.
42. Zachary JF, O'Brien WD, Jr.: **Lung lesions induced by continuous- and pulsed-wave (diagnostic) ultrasound in mice, rabbits, and pigs.** *Vet Pathol* 1995, **32:**43-54.
43. O'Brien WD, Zachary JF: **Lung damage assessment from exposure to pulsed-wave ultrasound in the rabbit, mouse, and pig.** *Ultrasonics, Ferroelectrics, and Frequency Control, IEEE Transactions on* 1997, **44:**473-485.
44. Meltzer RS, Adsumelli R, Risher WH, Hicks GL, Stern DH, Shah PM, Wojtczak JA, Lustik SJ, Gayeski TE, Shapiro JR: **Lack of lung hemorrhage in humans after intraoperative transesophageal echocardiography with ultrasound exposure conditions similar to those causing lung hemorrhage in laboratory animals.** *Journal of the American Society of Echocardiography* 1998, **11:**57-60.
45. Zachary JF, Sempsrott JM, Frizzell LA, Simpson DG, O'Brien WD, Jr.: **Superthreshold behavior and threshold estimation of ultrasound-induced lung hemorrhage in adult mice and rats.** *IEEE Trans Ultrason Ferroelectr Freq Control* 2001, **48:**581-592.
46. O'Brien WD, Simpson DG, Frizzell LA, Zachary JF: **Threshold estimates and superthreshold behavior of ultrasound-induced lung hemorrhage in adult rats: role of pulse duration.** *Ultrasound Med Biol* 2003, **29:**1625-1634.
47. O'Brien WD, Jr., Frizzell LA, Schaeffer DJ, Zachary JF: **Superthreshold behavior of ultrasound-induced lung hemorrhage in adult mice and rats: role of pulse repetition frequency and exposure duration.** *Ultrasound Med Biol* 2001, **27:**267-277.
48. O'Brien WD, Jr., Frizzell LA, Weigel RM, Zachary JF: **Ultrasound-induced lung hemorrhage is not caused by inertial cavitation.** *J Acoust Soc Am* 2000, **108:**1290-1297.
49. Kramer JM, Waldrop TG, Frizzell LA, Zachary JF, O'Brien WD, Jr.: **Cardiopulmonary function in rats with lung hemorrhage induced by pulsed ultrasound exposure.** *J Ultrasound Med* 2001, **20:**1197-1206.

50. O'Brien WD, Jr., Simpson DG, Frizzell LA, Zachary JF: **Superthreshold behavior of ultrasound-induced lung hemorrhage in adult rats: role of pulse repetition frequency and exposure duration revisited.** *J Ultrasound Med* 2005, **24:**339-348.
51. Harrison GH, Eddy HA, Wang JP, Liberman FZ: **Microscopic lung alterations and reduction of respiration rate in insonated anesthetized swine.** *Ultrasound Med Biol* 1995, **21:**981-983.
52. O'Brien Jr WD, Simpson DG, Ho M-H, Miller RJ, Frizzell L, Zachary JF: **Superthreshold behavior and threshold estimation of ultrasound-induced lung hemorrhage in pigs: role of age dependency.** *Ultrasonics, Ferroelectrics, and Frequency Control, IEEE Transactions on* 2003, **50:**153-169.
53. Miller DL, Thomas RM: **Thresholds for hemorrhages in mouse skin and intestine induced by lithotripter shock waves.** *Ultrasound in medicine & biology* 1995, **21:**249-257.
54. Dalecki D, Raeman CH, Child SZ, Carstensen EL: **Intestinal hemorrhage from exposure to pulsed ultrasound.** *Ultrasound in medicine & biology* 1995, **21:**1067-1072.
55. Dalecki D, Raeman C, Child S, Carstensen E: **Thresholds for intestinal hemorrhage in mice exposed to a piezoelectric lithotripter.** *Ultrasound in medicine & biology* 1995, **21:**1239-1246.
56. Raeman CH, Child SZ, Dalecki D, Mayer R, Parker KJ, Carstensen EL: **Damage to murine kidney and intestine from exposure to the fields of a piezoelectric lithotripter.** *Ultrasound in medicine & biology* 1994, **20:**589-594.
57. Miller DL, Gies RA: **Gas-body-based contrast agent enhances vascular bioeffects of 1.09 MHz ultrasound on mouse intestine.** *Ultrasound in medicine & biology* 1998, **24:**1201-1208.
58. Miller DL, Gies RA: **The influence of ultrasound frequency and gas-body composition on the contrast agent-mediated enhancement of vascular bioeffects in mouse intestine.** *Ultrasound in medicine & biology* 2000, **26:**307-313.
59. Dalecki D, Child SZ, Raeman CH, Xing C, Gracewski S, Carstensen EL: **Bioeffects of positive and negative acoustic pressures in mice infused with microbubbles.** *Ultrasound in medicine & biology* 2000, **26:**1327-1332.
60. Lehmann J, Herrick J: **Biologic reactions to cavitation, a consideration for ultrasonic therapy.** *Archives of physical medicine and rehabilitation* 1953, **34:**86-98.
61. Dalecki D, Child SZ, Raeman CH, Carstensen EL: **Tactile perception of ultrasound.** *The Journal of the Acoustical Society of America* 1995, **97:**3165-3170.
62. Miller DL, Gies RA: **The interaction of ultrasonic heating and cavitation in vascular bioeffects on mouse intestine.** *Ultrasound in medicine & biology* 1998, **24:**123-128.
63. Stanton M, Ettarh R, Arango D, Tonra M, Brennan P: **Diagnostic ultrasound induces change within numbers of cryptal mitotic and apoptotic cells in small intestine.** *Life sciences* 2001, **68:**1471-1475.
64. Cleveland RO, McAteer JA: **The physics of shock wave lithotripsy.** *Smith's Textbook on Endourology* 2007, **1:**529-558.
65. Pishchalnikov YA, Sapozhnikov OA, Bailey MR, Williams JC, Jr., Cleveland RO, Colonius T, Crum LA, Evan AP, McAteer JA: **Cavitation bubble cluster activity in the breakage of kidney stones by lithotripter shockwaves.** *J Endourol* 2003, **17:**435-446.

66. Pittomvils G, Lafaut J-P, Vandeursen H, De Ridder D, Baert L, Boving R: **Macroscopic ESWL-induced cavitation: in vitro studies.** *Ultrasound in medicine & biology* 1995, **21:**393-398.
67. Tanguay M, Colonius T: **Numerical investigation of bubble cloud dynamics in shock wave lithotripsy.** In *ASME 2002 Joint US-European Fluids Engineering Division Conference*. American Society of Mechanical Engineers; 2002: 389-394.
68. Tuteja AK, Pulliam JP, Lehman TH, Elzinga LW: **Anuric renal failure from massive bilateral renal hematoma following extracorporeal shock wave lithotripsy.** *Urology* 1997, **50:**606-608.
69. Evan AP, Willis LR, Lingeman JE, McAteer JA: **Renal trauma and the risk of long-term complications in shock wave lithotripsy.** *Nephron* 1998, **78:**1-8.
70. Rao SR, Ballesteros N, Short KL, Gathani KK, Ankem MK: **Extra corporeal shockwave lithotripsy resulting in skin burns–a report of two cases.** *International braz j urol* 2014, **40:**853-857.
71. Rangarajan S, Mirheydar H, Sur RL: **Second-degree burn after shock wave lithotripsy: an unusual complication.** 2012.
72. Williams JC, Woodward JF, Stonehill MA, Evan AP, McAteer JA: **Cell damage by lithotripter shock waves at high pressure to preclude cavitation.** *Ultrasound in medicine & biology* 1999, **25:**1445-1449.
73. Evan AP, Willis LR, McAteer JA, Bailey MR, Connors BA, Shao Y, Lingeman JE, Williams JC, Fineberg NS, Crum LA: **Kidney damage and renal functional changes are minimized by waveform control that suppresses cavitation in shock wave lithotripsy.** *The Journal of urology* 2002, **168:**1556-1562.
74. Bailey MR, Blackstock DT, Cleveland RO, Crum LA: **Comparison of electrohydraulic lithotripters with rigid and pressure-release ellipsoidal reflectors. II. Cavitation fields.** *The Journal of the Acoustical Society of America* 1999, **106:**1149-1160.
75. Sokolov DL, Bailey MR, Crum LA: **Use of a dual-pulse lithotripter to generate a localized and intensified cavitation field.** *The Journal of the Acoustical Society of America* 2001, **110:**1685-1695.
76. Sokolov DL, Bailey MR, Crum LA: **Dual-pulse lithotripter accelerates stone fragmentation and reduces cell lysis in vitro.** *Ultrasound in medicine & biology* 2003, **29:**1045-1052.
77. Haar GT, Coussios C: **High intensity focused ultrasound: physical principles and devices.** *Int J Hyperthermia* 2007, **23:**89-104.
78. Jung SE, Cho SH, Jang JH, Han J-Y: **High-intensity focused ultrasound ablation in hepatic and pancreatic cancer: complications.** *Abdominal imaging* 2011, **36:**185-195.
79. Xiong LL, Hwang JH, Huang XB, Yao SS, He CJ, Ge XH, Ge HY, Wang XF: **Early clinical experience using high intensity focused ultrasound for palliation of inoperable pancreatic cancer.** *Jop* 2009, **10:**123-129.
80. Xin H: **High intensity focused ultrasound in the treatment of abdominal malignant tumors in 60 cases.** *Modern Medicine & Health* 2008, **15:**012.
81. Yu T, Luo J: **Adverse events of extracorporeal ultrasound-guided high intensity focused ultrasound therapy.** *PLoS One* 2011, **6:**e26110.
82. Miller DL, Dou C: **The potential for enhancement of mouse melanoma metastasis by diagnostic and high-amplitude ultrasound.** *Ultrasound in medicine & biology* 2006, **32:**1097-1101.

83. Yi J, Li N, Jiang L, Xiong X: **[The study of clinical application of high intensity focused ultrasound in non-invasive therapy for liver cancer].** *Sichuan da xue xue bao Yi xue ban= Journal of Sichuan University Medical science edition* 2005, **36:**426-428.
84. Wang J, Gao X, Gao F, Zou J, Du G: **Clinical study of treating advanced pancreatic carcinoma by high intensity focused ultrasound.** *Mil Med J South China* 2004, **18:**17-18.
85. Yongjian Z, Yuqiang N, Yuyuan L: **Preliminary study of high intensity focused ultrasound therapy liver cancer.** *Guangzhou Medical Journal* 2002, **4:**002.
86. Yu T, Fan X, Xiong S, Hu K, Wang Z: **Microbubbles assist goat liver ablation by high intensity focused ultrasound.** *European radiology* 2006, **16:**1557-1563.
87. Chen W, Wang Z, Wu F, Bai J, Zhu H, Zou J, Li K, Xie F, Wang Z: **Use of high intensity focused ultrasound for treating malignant tumors.** *Chinese Journal of Clinical Oncology* 2004, **1:**15-20.
88. Ren X-L, Zhou X-D, Yan R-L, Liu D, Zhang J, He G-B, Han Z-H, Zheng M-J, Yu M: **Sonographically guided extracorporeal ablation of uterine fibroids with high-intensity focused ultrasound: midterm results.** *Journal of Ultrasound in Medicine* 2009, **28:**100-103.
89. Dalecki D, Keller BB, Carstensen EL, Neel DS, Palladino JL, Noordergraaf A: **Thresholds for premature ventricular contractions in frog hearts exposed to lithotripter fields.** *Ultrasound in medicine & biology* 1991, **17:**341-346.
90. Delius M, Hoffmann E, Steinbeck G, Conzen P: **Biological effects of shock waves: induction of arrhythmia in piglet hearts.** *Ultrasound in medicine & biology* 1994, **20:**279-285.
91. Dalecki D, Rota C, Raeman CH, Child SZ: **Premature cardiac contractions produced by ultrasound and microbubble contrast agents in mice.** *Acoustics Research Letters Online* 2005, **6:**221-226.
92. Li P, Cao L-q, Dou C-Y, Armstrong WF, Miller D: **Impact of myocardial contrast echocardiography on vascular permeability: an in vivo dose response study of delivery mode, pressure amplitude and contrast dose.** *Ultrasound in medicine & biology* 2003, **29:**1341-1349.
93. Zachary JF, Hartleben SA, Frizzell LA, O'brien WD: **Arrhythmias in rat hearts exposed to pulsed ultrasound after intravenous injection of a contrast agent.** *Journal of ultrasound in medicine* 2002, **21:**1347-1356.
94. van der Wouw PA, Brauns AC, Bailey SE, Powers JE, Wilde AA: **Premature ventricular contractions during triggered imaging with ultrasound contrast.** *Journal of the American Society of Echocardiography* 2000, **13:**288-294.
95. Dalecki D, Keller BB, Raeman CH, Carstensen EL: **Effects of pulsed ultrasound on the frog heart: I. Thresholds for changes in cardiac rhythm and aortic pressure.** *Ultrasound in medicine & biology* 1993, **19:**385-390.
96. Dalecki D, Raeman CH, Child SZ, Carstensen EL: **Effects of pulsed ultrasound on the frog heart: III. The radiation force mechanism.** *Ultrasound in medicine & biology* 1997, **23:**275-285.
97. Miller DL, Averkiou MA, Brayman AA, Everbach EC, Holland CK, Wible JH, Wu J: **Bioeffects considerations for diagnostic ultrasound contrast agents.** *Journal of Ultrasound in Medicine* 2008, **27:**611-632.

98. Miller MW, Brayman AA, Sherman TA, Abramowicz JS, Cox C: **Comparative sensitivity of human fetal and adult erythrocytes to hemolysis by pulsed 1 MHz ultrasound.** *Ultrasound in medicine & biology* 2001, **27:**419-425.
99. Dalecki D, Raeman C, Child S, Cox C, Francis C, Meltzer R, Carstensen E: **Hemolysis in vivo from exposure to pulsed ultrasound.** *Ultrasound in medicine & biology* 1997, **23:**307-313.
100. Ay T, Havaux X, Van Camp G, Campanelli B, Gisellu G, Pasquet A, Denef J-F, Melin JA, Vanoverschelde J-LJ: **Destruction of contrast microbubbles by ultrasound effects on myocardial function, coronary perfusion pressure, and microvascular integrity.** *Circulation* 2001, **104:**461-466.
101. Chen S, Kroll MH, Shohet RV, Frenkel P, Mayer SA, Grayburn PA: **Bioeffects of myocardial contrast microbubble destruction by echocardiography.** *Echocardiography* 2002, **19:**495-500.
102. Chemat S, Lagha A, AitAmar H, Bartels PV, Chemat F: **Comparison of conventional and ultrasound-assisted extraction of carvone and limonene from caraway seeds.** *Flavour and Fragrance Journal* 2004, **19:**188-195.
103. Cleveland RO, James AM: *A brief review of the Physics of Shock Wave Lithotripsy.* BC Decker Inc., Hamilton, ON, Canada; 2007.
104. Zhong P, Cioanta I, Zhu S, Cocks FH, Preminger GM: **Effects of tissue constraint on shock wave-induced bubble expansion in vivo.** *The Journal of the Acoustical Society of America* 1998, **104:**3126-3129.
105. Zhong P, Zhou Y, Zhu S: **Dynamics of bubble oscillation in constrained media and mechanisms of vessel rupture in SWL.** *Ultrasound in medicine & biology* 2001, **27:**119-134.
106. Delius M, Mueller W, Goetz A, Liebich H, Brendel W: **Biological effects of shock waves: kidney hemorrhage in dogs at a fast shock wave administration rate of fifteen Hertz.** *J Lithotripsy Stone Dis* 1990, **2:**103-110.
107. Delius M, Jordan M, Liebich H-G, Brendel W: **Biological effects of shock waves: effect of shock waves on the liver and gallbladder wall of dogs—administration rate dependence.** *Ultrasound in medicine & biology* 1990, **16:**459-466.
108. Mayer R, Schenk E, Child S, Norton S, Cox C, Hartman C, Carstensen E: **Pressure threshold for shock wave induced renal hemorrhage.** *The Journal of urology* 1990, **144:**1505-1509.
109. Dalecki D, Raeman CH, Child SZ, Penney DP, Mayer R, Carstensen EL: **The influence of contrast agents on hemorrhage produced by lithotripter fields.** *Ultrasound in medicine & biology* 1997, **23:**1435-1439.
110. Dalecki D, Raeman CH, Child SZ, Penney DP, Carstensen EL: **Remnants of Albunex® nucleate acoustic cavitation.** *Ultrasound in medicine & biology* 1997, **23:**1405-1412.
111. Miller D, GIES RA: **Consequences of lithotripter shockwave interaction with gas body contrast agent in mouse intestine.** *The Journal of urology* 1999, **162:**606-609.
112. Miller DL, Quddus J: **Diagnostic ultrasound activation of contrast agent gas bodies induces capillary rupture in mice.** *Proceedings of the National Academy of Sciences* 2000, **97:**10179-10184.
113. Price RJ, Skyba DM, Kaul S, Skalak TC: **Delivery of colloidal particles and red blood cells to tissue through microvessel ruptures created by targeted microbubble destruction with ultrasound.** *Circulation* 1998, **98:**1264-1267.

114. Wible JH, Galen KP, Wojdyla JK, Hughes MS, Klibanov AL, Brandenburger GH: **Microbubbles induce renal hemorrhage when exposed to diagnostic ultrasound in anesthetized rats.** *Ultrasound in medicine & biology* 2002, **28:**1535-1546.
115. Song J, Chappell JC, Qi M, VanGieson EJ, Kaul S, Price RJ: **Influence of injection site, microvascular pressureand ultrasound variables on microbubble-mediated delivery of microspheres to muscle.** *Journal of the American College of Cardiology* 2002, **39:**726-731.
116. Chu PC, Chai WY, Tsai CH, Kang ST, Yeh CK, Liu HL: **Focused Ultrasound-Induced Blood-Brain Barrier Opening: Association with Mechanical Index and Cavitation Index Analyzed by Dynamic Contrast-Enhanced Magnetic-Resonance Imaging.** *Sci Rep* 2016, **6:**33264.
117. Aryal M, Park J, Vykhodtseva N, Zhang YZ, McDannold N: **Enhancement in blood-tumor barrier permeability and delivery of liposomal doxorubicin using focused ultrasound and microbubbles: evaluation during tumor progression in a rat glioma model.** *Phys Med Biol* 2015, **60:**2511-2527.
118. Meairs S, Alonso A: **Ultrasound, microbubbles and the blood-brain barrier.** *Prog Biophys Mol Biol* 2007, **93:**354-362.
119. Song J, Qi M, Kaul S, Price RJ: **Stimulation of arteriogenesis in skeletal muscle by microbubble destruction with ultrasound.** *Circulation* 2002, **106:**1550-1555.
120. Chen S, Shimoda M, Chen J, Grayburn PA: **Stimulation of adult resident cardiac progenitor cells by durable myocardial expression of thymosin beta 4 with ultrasound-targeted microbubble delivery.** *Gene Ther* 2013, **20:**225-233.
121. Simon RH, Ho S-Y, Lange SC, Uphoff DF, D'Arrigo JS: **Applications of lipid-coated microbubble ultrasonic contrast to tumor therapy.** *Ultrasound in medicine & biology* 1993, **19:**123-125.
122. Ji Y, Han Z, Shao L, Zhao Y: **Ultrasound-targeted microbubble destruction of calcium channel subunit alpha 1D siRNA inhibits breast cancer via G protein-coupled receptor 30.** *Oncol Rep* 2016.
123. Zhang Y, Chang R, Li M, Zhao K, Zheng H, Zhou X: **Docetaxel-loaded lipid microbubbles combined with ultrasound-triggered microbubble destruction for targeted tumor therapy in MHCC-H cells.** *Onco Targets Ther* 2016, **9:**4763-4771.
124. Ang ES, Gluncic V, Duque A, Schafer ME, Rakic P: **Prenatal exposure to ultrasound waves impacts neuronal migration in mice.** *Proceedings of the National Academy of Sciences* 2006, **103:**12903-12910.
125. Williams AR, Chater BV, Allen KA, Sherwood MR, Sanderson JH: **Release of β-Thromboglobulin from Human Platelets by Therapeutic Intensities of Ultrasound.** *British Journal of Haematology* 1978, **40:**133-142.
126. Li T, Chen H, Khokhlova T, Wang Y-N, Kreider W, He X, Hwang JH: **Passive cavitation detection during pulsed HIFU exposures of ex vivo tissues and in vivo mouse pancreatic tumors.** *Ultrasound in medicine & biology* 2014, **40:**1523-1534.
127. Hoerig CL, Serrone JC, Burgess MT, Zuccarello M, Mast TD: **Prediction and suppression of HIFU-induced vessel rupture using passive cavitation detection in an ex vivo model.** *Journal of therapeutic ultrasound* 2014, **2:**1.
128. McLaughlan J, Rivens I, Leighton T, Ter Haar G: **A study of bubble activity generated in ex vivo tissue by high intensity focused ultrasound.** *Ultrasound Med Biol* 2010, **36:**1327-1344.

129. Farny CH, Holt RG, Roy RA: **Temporal and spatial detection of HIFU-induced inertial and hot-vapor cavitation with a diagnostic ultrasound system.** *Ultrasound in medicine & biology* 2009, **35:**603-615.
130. Mast TD, Salgaonkar VA, Karunakaran C, Besse JA, Datta S, Holland CK: **Acoustic emissions during 3.1 MHz ultrasound bulk ablation in vitro.** *Ultrasound Med Biol* 2008, **34:**1434-1448.
131. Coussios C, Farny C, Ter Haar G, Roy R: **Role of acoustic cavitation in the delivery and monitoring of cancer treatment by high-intensity focused ultrasound (HIFU).** *International Journal of Hyperthermia* 2007, **23:**105-120.
132. Cleveland RO, Sapozhnikov OA, Bailey MR, Crum LA: **A dual passive cavitation detector for localized detection of lithotripsy-induced cavitation in vitro.** *J Acoust Soc Am* 2000, **107:**1745-1758.
133. Feril LB, Jr., Kondo T: **Biological effects of low intensity ultrasound: the mechanism involved, and its implications on therapy and on biosafety of ultrasound.** *J Radiat Res* 2004, **45:**479-489.
134. Miller DL: **Overview of experimental studies of biological effects of medical ultrasound caused by gas body activation and inertial cavitation.** *Progress in biophysics and molecular biology* 2007, **93:**314-330.
135. ter Haar G: **Therapeutic applications of ultrasound.** *Progress in biophysics and molecular biology* 2007, **93:**111-129.
136. Nyborg W, Carson P, Carstensen E, Dunn F, Miller D, Miller M, Thompson H, Ziskin M: **Exposure criteria for medical diagnostic ultrasound: II. Criteria based on all known mechanisms.** *Bethesda, MD: National Council on Radiation Protection and Measurements* 2002.
137. Holland CK: **Mechanical bioeffects from diagnostic ultrasound: AIUM consensus statements.** *Journal of ultrasound in medicine: official journal of the American Institute of Ultrasound in Medicine* 2000, **19:**69.
138. Kaufman GE, Miller MW, Griffiths TD, Ciaravino V, Carstensen EL: **Lysis and viability of cultured mammalian cells exposed to 1 MHz ultrasound.** *Ultrasound in medicine & biology* 1977, **3:**21-25.
139. Morton K, Ter Haar G, Stratford I, Hill C: **The role of cavitation in the interaction of ultrasound with V79 Chinese hamster cells in vitro.** *The British journal of cancer Supplement* 1982, **5:**147.
140. Hallow DM, Mahajan AD, McCutchen TE, Prausnitz MR: **Measurement and correlation of acoustic cavitation with cellular bioeffects.** *Ultrasound in medicine & biology* 2006, **32:**1111-1122.
141. Lai C-Y, Wu C-H, Chen C-C, Li P-C: **Quantitative relations of acoustic inertial cavitation with sonoporation and cell viability.** *Ultrasound in medicine & biology* 2006, **32:**1931-1941.
142. Ellwart JW, Brettel H, Kober LO: **Cell membrane damage by ultrasound at different cell concentrations.** *Ultrasound in medicine & biology* 1988, **14:**43-50.
143. Brayman A, Church C, Miller M: **Re-evaluation of the concept that high cell concentrations "protect" cells in vitro from ultrasonically induced lysis.** *Ultrasound in medicine & biology* 1996, **22:**497-514.
144. Nyborg WL, Miller DL: **Biophysical implications of bubble dynamics.** *Applied Scientific Research* 1982, **38:**17-24.

145. Brayman AA, Miller MW: **Cell density dependence of the ultrasonic degassing of fixed erythrocyte suspensions.** *Ultrasound in medicine & biology* 1993, **19:**243-252.
146. Clarke P, Hill C: **Biological action of ultrasound in relation to the cell cycle.** *Experimental cell research* 1969, **58:**443-444.
147. Bleaney BI, Blackbourn P, Kirkley J: **Resistance of CHLF hamster cells to ultrasonic radiation of 1· 5 MHz frequency.** *The British journal of radiology* 1972, **45:**354-357.
148. ter Haar G, Stratford I, Hill C: **Ultrasonic irradiation of mammalian cells in vitro at hyperthermic temperatures.** *The British journal of radiology* 1980, **53:**784-789.
149. Feril LB, Kondo T: **Biological effects of low intensity therapeutic ultrasound in vitro: The potentials for therapy and the implications on safety of diagnostic ultrasound.** In *International Congress Series*. Elsevier; 2004: 133-140.
150. ter Haar G: **Therapeutic applications of ultrasound.** *Prog Biophys Mol Biol* 2007, **93:**111-129.
151. Escoffre J, Kaddur K, Rols M, Bouakaz A: **In vitro gene transfer by electrosonoporation.** *Ultrasound in medicine & biology* 2010, **36:**1746-1755.
152. de Jong N, Frinking PJ, Bouakaz A, Ten Cate FJ: **Detection procedures of ultrasound contrast agents.** *Ultrasonics* 2000, **38:**87-92.
153. Izadifar Z: **Ultrasound pretreatment of wheat dried distiller's grain (DDG) for extraction of phenolic compounds.** *Ultrasonics sonochemistry* 2013, **20:**1359-1369.
154. Chapman I: **The effect of ultrasound on the potassium content of rat thymocytes in vitro.** *The British journal of radiology* 1974, **47:**411-415.
155. Mortimer A, Dyson M: **The effect of therapeutic ultrasound on calcium uptake in fibroblasts.** *Ultrasound in medicine & biology* 1988, **14:**499-506.
156. Dvorak M, Hrazdira I: **Changes in the ultrastructure of bone marrow cells in rats following exposure to ultrasound.** *Zeitschrift für mikroskopisch-anatomische Forschung* 1966, **75:**451.
157. Hrazdira I: **Changes in cell ultrastructure under direct and indirect action of ultrasound.** In *Ultrasonographia Medica. Volume* 1: Wiener Med. Akad; 1971: 457-463
158. Taylor K, Pond J: **Primary sites of ultrasonic damage on cell systems.** *Interaction of Ultrasound and Biological Tissues* 1972, **3**.
159. Harvey W, Dyson M, Pond J, Grahame R: **The in vitro stimulation of protein synthesis in human fibroblasts by therapeutic levels of ultrasound.** In *Proceedings of the Second European Congress on Ultrasonics in Medicine*. Excerpta Medica Amsterdam; 1975: 10-21.
160. Ter Haar G, Dyson M, Smith SP: **Ultrastructural changes in the mouse uterus brought about by ultrasonic irradiation at therapeutic intensities in standing wave fields.** *Ultrasound in medicine & biology* 1979, **5:**167-179.
161. Watmough D, Dendy P, Eastwood L, Gregory D, Gordon F, Wheatley D: **The biophysical effects of therapeutic ultrasound on HeLa cells.** *Ultrasound in medicine & biology* 1977, **3:**205-219.
162. Thacker J: **The possibility of genetic hazard from ultrasonic radiation.** *Current topics in radiation research quarterly* 1973, **8:**235-258.
163. Miller DL, Thomas RM: **Ultrasound contrast agents nucleate inertial cavitation in vitro.** *Ultrasound in medicine & biology* 1995, **21:**1059-1065.

164. Miller DL, Thomas RM: **Contrast-agent gas bodies enhance hemolysis induced by lithotripter shock waves and high-intensity focused ultrasound in whole blood.** *Ultrasound in medicine & biology* 1996, **22:**1089-1095.
165. Rott H-D: **Zur Frage der Schädigungsmöglichkeit durch diagnostischen Ultraschall.** *Ultraschall in der Medizin* 1981, **2:**56-64.
166. **EFSUMB European Committee for Ultrasound Radiation Safety.** (Ultrasound EJ ed., vol. 1. pp. 91-92; 1994:91-92.
167. Kunze-Mühl E: **Observations on the effect of X-ray alone and in combination with ultrasound on human chromosomes.** *Human genetics* 1981, **57:**257-260.
168. Liebeskind D, Bases R, Mendez F, Elequin F, Koenigsberg M: **Sister chromatid exchanges in human lymphocytes after exposure to diagnostic ultrasound.** *Science* 1979, **205:**1273-1275.
169. Taylor K, Newman D: **Electrophoretic mobility of Ehrlich cell suspensions exposed to ultrasound of varying parameters.** *Physics in medicine and biology* 1972, **17:**270.
170. Mummery CL: **The effect of ultrasound on fibroblasts' In Vitro'.** King's College London (University of London), 1978.
171. Liebeskind D, Padawer J, Wolley R, Bases R: **Diagnostic ultrasound time-lapse and transmission electron microscopic studies of cells insonated in vitro.** *The British journal of cancer Supplement* 1982, **5:**176.
172. Busse JW, Bhandari M, Kulkarni AV, Tunks E: **The effect of low-intensity pulsed ultrasound therapy on time to fracture healing: a meta-analysis.** *Canadian Medical Association Journal* 2002, **166:**437-441.
173. Mundi R, Petis S, Kaloty R, Shetty V, Bhandari M: **Low-intensity pulsed ultrasound: Fracture healing.** *Indian J Orthop* 2009, **43:**132-140.
174. Dijkman BG, Sprague S, Bhandari M: **Low-intensity pulsed ultrasound: Nonunions.** *Indian J Orthop* 2009, **43:**141-148.
175. Smith NB, Temkin JM, Shapiro F, Hynynen K: **Thermal effects of focused ultrasound energy on bone tissue.** *Ultrasound Med Biol* 2001, **27:**1427-1433.
176. Claes L, Willie B: **The enhancement of bone regeneration by ultrasound.** *Progress in biophysics and molecular biology* 2007, **93:**384-398.
177. Chang WHS, Sun JS, Chang SP, Lin JC: **Study of thermal effects of ultrasound stimulation on fracture healing.** *Bioelectromagnetics* 2002, **23:**256-263.
178. Duarte L: **The stimulation of bone growth by ultrasound.** *Archives of orthopaedic and traumatic surgery* 1983, **101:**153-159.
179. Welgus HG, Jeffrey JJ, Eisen AZ, Roswit W, Stricklin G: **Human skin fibroblast collagenase.** *J Biol Chem* 1981, **256:**9516-9521.
180. Welgus HG, Jeffrey JJ, Eisen AZ, Roswit WT, Stricklin GP: **Human skin fibroblast collagenase: interaction with substrate and inhibitor.** *Collagen and related research* 1985, **5:**167-179.
181. Brookes M, Dyson M: **Stimulation of bone repair by ultrasound.** In *Journal of Bone and Joint Surgery-British Volume*. BRITISH EDITORIAL SOC BONE JOINT SURGERY 22 BUCKINGHAM STREET, LONDON, ENGLAND WC2N 6ET; 1983: 659-659.
182. Dinno M, Dyson M, Young S, Mortimer A, Hart J, Crum L: **The significance of membrane changes in the safe and effective use of therapeutic and diagnostic ultrasound.** *Physics in medicine and biology* 1989, **34:**1543.

183. Ryaby J, Bachner E, Bendo J, Dalton P, Tannenbaum S, Pilla A: **Low intensity pulsed ultrasound increases calcium incorporation in both differentiating cartilage and bone cell cultures.** *Trans Orthop Res Soc* 1989, **14:**15.
184. Ryaby J: **Low intensity pulsed ultrasound modulates adenylate cyclase activity and transforming growth factor beta synthesis.** *Electomagnetics in Biology and Medicine* 1991.
185. Rawool NM, Goldberg BB, Forsberg F, Winder AA, Hume E: **Power Doppler assessment of vascular changes during fracture treatment with low-intensity ultrasound.** *Journal of Ultrasound in Medicine* 2003, **22:**145-153.
186. Sun JS, Hong RC, Chang WHS, Chen LT, Lin FH, Liu HC: **In vitro effects of low-intensity ultrasound stimulation on the bone cells.** *Journal of biomedical materials research* 2001, **57:**449-456.
187. Lim K, Kim J, Seonwoo H, Park SH, Choung P-H, Chung JH: **In vitro effects of low-intensity pulsed ultrasound stimulation on the osteogenic differentiation of human alveolar bone-derived mesenchymal stem cells for tooth tissue engineering.** *BioMed research international* 2013, **2013**.
188. Hu B, Zhang Y, Zhou J, Li J, Deng F, Wang Z, Song J: **Low-intensity pulsed ultrasound stimulation facilitates osteogenic differentiation of human periodontal ligament cells.** *PloS one* 2014, **9:**e95168.
189. Chen K, Hao J, Noritake K, Yamashita Y, Kuroda S, Kasugai S: **Effects of low intensity pulsed ultrasound stimulation on bone regeneration in rat parietal bone defect model.** 2013.
190. Montalti CS, Souza NV, Rodrigues NC, Fernandes KR, Toma RL, Renno A: **Effects of low-intensity pulsed ultrasound on injured skeletal muscle.** *Brazilian journal of physical therapy* 2013, **17:**343-350.
191. Wolff J: **Das gesetz der transformation der knochen.** *DMW-Deutsche Medizinische Wochenschrift* 1892, **19:**1222-1224.
192. De Nunno R: **[Effect of ultrasonics on ossification; experimental studies.].** *Annali italiani di chirurgia* 1952, **29:**211-220.
193. Corradi C, Cozzolino A: **Effect of ultrasonics on the development of osseous callus in fractures.** *Archivio di ortopedia* 1953, **66:**77.
194. Klug W, Franke W-G, Knoch H-G: **Scintigraphic control of bone-fracture healing under ultrasonic stimulation: an animal experimental study.** *European journal of nuclear medicine* 1986, **11:**494-497.
195. Murolo C, Claudio F: **Effect of ultrasonics on repair of fractures.** *Giornale italiano di chirurgia* 1952, **8:**897.
196. Miller DL, Nyborg W, Whitcomb C: **Platelet aggregation induced by ultrasound under specialized conditions in vitro.** *Science* 1979, **205:**505-507.
197. Rooney JA: **Hemolysis near an ultrasonically pulsating gas bubble.** *Science* 1970, **169:**869-871.
198. Williams A, Hughes D, Nyborg W: **Hemolysis near a transversely oscillating wire.** *Science* 1970, **169:**871-873.
199. Wong Y, Watmough D: **Haemolysis of red blood cells in vitro and in vivo caused by therapeutic ultrasound at 0.75 MHz.** *Paper C14 in Ultrasound Interaction in Biology and Medicine* 1980.

200. Williams A, Miller D: **Photometric detection of ATP release from human erythrocytes exposed to ultrasonically activated gas-filled pores.** *Ultrasound in medicine & biology* 1980, **6:**251-256.
201. Williams A, Sykes S, O'Brien W: **Ultrasonic exposure modifies platelet morphology and function in vitro.** *Ultrasound in medicine & biology* 1977, **2:**311-317.
202. Deng CX, Xu Q, Apfel RE, Holland CK: **In vitro measurements of inertial cavitation thresholds in human blood.** *Ultrasound in medicine & biology* 1996, **22:**939-948.
203. Poliachik SL, Chandler WL, Mourad PD, Bailey MR, Bloch S, Cleveland RO, Kaczkowski P, Keilman G, Porter T, Crum LA: **Effect of high-intensity focused ultrasound on whole blood with and without microbubble contrast agent.** *Ultrasound in Medicine and Biology* 1999, **25:**991-998.
204. VanBavel E: **Effects of shear stress on endothelial cells: possible relevance for ultrasound applications.** *Progress in biophysics and molecular biology* 2007, **93:**374-383.
205. Davies PF: **Flow-mediated endothelial mechanotransduction.** *Physiological reviews* 1995, **75:**519-560.
206. Dalecki D, Child S, Raeman C, Cox C: **Hemorrhage in murine fetuses exposed to pulsed ultrasound.** *Ultrasound in medicine & biology* 1999, **25:**1139-1144.
207. Bigelow TA, Miller RJ, Blue JP, O'Brien WD: **Hemorrhage near fetal rat bone exposed to pulsed ultrasound.** *Ultrasound in medicine & biology* 2007, **33:**311-317.
208. Brayman AA, Lizotte LM, Miller MW: **Erosion of artificial endothelia in vitro by pulsed ultrasound: acoustic pressure, frequency, membrane orientation and microbubble contrast agent dependence.** *Ultrasound in medicine & biology* 1999, **25:**1305-1320.
209. Miller DL, Gies RA, Chrisler WB: **Ultrasonically induced hemolysis at high cell and gas body concentrations in a thin-disc exposure chamber.** *Ultrasound in medicine & biology* 1997, **23:**625-633.
210. Miller DL, Gies RA: **Enhancement of ultrasonically-induced hemolysis by perfluorocarbon-based compared to air-based echo-contrast agents.** *Ultrasound in medicine & biology* 1998, **24:**285-292.
211. Miller DL, Gies RA: **Enhancement of ultrasonically-induced hemolysis by perfluorocarbon-based compared to air-based echo-contrast agents.** *Ultrasound in Medicine and Biology* 1998, **24:**285-292.
212. Everbach EC, Makin IRS, Azadniv M, Meltzer RS: **Correlation of ultrasound-induced hemolysis with cavitation detector output in vitro.** *Ultrasound in medicine & biology* 1997, **23:**619-624.
213. Miller MW, Everbach EC, Cox C, Knapp RR, Brayman AA, Sherman TA: **A comparison of the hemolytic potential of Optison™ and Albunex® in whole human blood in vitro: Acoustic pressure, ultrasound frequency, donor and passive cavitation detection considerations.** *Ultrasound in medicine & biology* 2001, **27:**709-721.
214. Chen W-S, Brayman AA, Matula TJ, Crum LA: **Inertial cavitation dose and hemolysis produced in vitro with or without Optison®.** *Ultrasound in medicine & biology* 2003, **29:**725-737.

215. Chen W-S, Brayman AA, Matula TJ, Crum LA, Miller MW: **The pulse length-dependence of inertial cavitation dose and hemolysis.** *Ultrasound in medicine & biology* 2003, **29:**739-748.
216. Brayman AA, Strickler PL, Luan H, Barned SL, Raeman CH, Cox C, Miller MW: **Hemolysis of 40% hematocrit, Albunex®-supplemented human erythrocytes by pulsed ultrasound: Frequency, acoustic pressure and pulse length dependence.** *Ultrasound in medicine & biology* 1997, **23:**1237-1250.
217. Miller MW, Everbach EC, Miller WM, Battaglia LF: **Biological and environmental factors affecting ultrasound-induced hemolysis in vitro: 2. Medium dissolved gas (pO 2) content.** *Ultrasound in medicine & biology* 2003, **29:**93-102.
218. Li P, Armstrong WF, Miller DL: **Impact of myocardial contrast echocardiography on vascular permeability: comparison of three different contrast agents.** *Ultrasound in medicine & biology* 2004, **30:**83-91.
219. Zachary JF, Blue JP, Miller RJ, O'Brien WD: **Vascular lesions and s-thrombomodulin concentrations from auricular arteries of rabbits infused with microbubble contrast agent and exposed to pulsed ultrasound.** *Ultrasound in medicine & biology* 2006, **32:**1781-1791.
220. Stieger SM, Caskey CF, Adamson RH, Qin S, Curry FR, Wisner ER, Ferrara KW: **Enhancement of vascular permeability with low-frequency contrast-enhanced ultrasound in the chorioallantoic membrane model.** *Radiology* 2007, **243:**112-121.
221. Hwang JH, Brayman AA, Reidy MA, Matula TJ, Kimmey MB, Crum LA: **Vascular effects induced by combined 1-MHz ultrasound and microbubble contrast agent treatments in vivo.** *Ultrasound Med Biol* 2005, **31:**553-564.
222. Shaw C, ter Haar G, Rivens I, Giussani D, Lees C: **Pathophysiological mechanisms of high-intensity focused ultrasound-mediated vascular occlusion and relevance to non-invasive fetal surgery.** *Journal of The Royal Society Interface* 2014, **11:**20140029.
223. Kobayashi N, Yasu T, Yamada S, Kudo N, Kuroki M, Kawakami M, Miyatake K, Saito M: **Endothelial cell injury in venule and capillary induced by contrast ultrasonography.** *Ultrasound in Medicine and Biology* 2002, **28:**949-956.
224. Kobayashi N, Yasu T, Yamada S, Kudo N, Kuroki M, Miyatake K, Kawakami M, Saito M: **Influence of contrast ultrasonography with perflutren lipid microspheres on microvessel injury.** *Circulation journal* 2003, **67:**630-636.
225. Shigeta K, Itoh K, Ookawara S, Taniguchi N, Omoto K: **Endothelial cell injury and platelet aggregation induced by contrast ultrasonography in the rat hepatic sinusoid.** *Journal of ultrasound in medicine* 2004, **23:**29-36.
226. Stroick M, Alonso A, Fatar M, Griebe M, Kreisel S, Kern R, Gaud E, Arditi M, Hennerici M, Meairs S: **Effects of simultaneous application of ultrasound and microbubbles on intracerebral hemorrhage in an animal model.** *Ultrasound in medicine & biology* 2006, **32:**1377-1382.
227. Härdig BM, Persson HW, Gidö G, Olsson SB: **Does low-energy ultrasound, known to enhance thrombolysis, affect the size of ischemic brain damage?** *Journal of ultrasound in medicine* 2003, **22:**1301-1308.
228. Vancraeynest D, Havaux X, Pouleur A-C, Pasquet A, Gerber B, Beauloye C, Rafter P, Bertrand L, Vanoverschelde J-LJ: **Myocardial delivery of colloid nanoparticles using ultrasound-targeted microbubble destruction.** *European heart journal* 2006, **27:**237-245.

229. Miller DL, Li P, Dou C, Gordon D, Edwards CA, Armstrong WF: **Influence of Contrast Agent Dose and Ultrasound Exposure on Cardiomyocyte Injury Induced by Myocardial Contrast Echocardiography in Rats 1.** *Radiology* 2005, **237:**137-143.
230. Miller DL, Li P, Gordon D, Armstrong WF: **Histological characterization of microlesions induced by myocardial contrast echocardiography.** *Echocardiography* 2005, **22:**25-34.
231. Mesiwala AH, Farrell L, Wenzel HJ, Silbergeld DL, Crum LA, Winn HR, Mourad PD: **High-intensity focused ultrasound selectively disrupts the blood-brain barrier in vivo.** *Ultrasound in medicine & biology* 2002, **28:**389-400.
232. Hynynen K, McDannold N, Vykhodtseva N, Jolesz FA: **Noninvasive MR Imaging–guided Focal Opening of the Blood-Brain Barrier in Rabbits 1.** *Radiology* 2001, **220:**640-646.
233. Kinoshita M, McDannold N, Jolesz FA, Hynynen K: **Targeted delivery of antibodies through the blood–brain barrier by MRI-guided focused ultrasound.** *Biochemical and biophysical research communications* 2006, **340:**1085-1090.
234. Hynynen K, McDannold N, Sheikov NA, Jolesz FA, Vykhodtseva N: **Local and reversible blood–brain barrier disruption by noninvasive focused ultrasound at frequencies suitable for trans-skull sonications.** *Neuroimage* 2005, **24:**12-20.
235. McDannold N, Vykhodtseva N, Raymond S, Jolesz FA, Hynynen K: **MRI-guided targeted blood-brain barrier disruption with focused ultrasound: histological findings in rabbits.** *Ultrasound in medicine & biology* 2005, **31:**1527-1537.
236. Hynynen K, McDannold N, Martin H, Jolesz FA, Vykhodtseva N: **The threshold for brain damage in rabbits induced by bursts of ultrasound in the presence of an ultrasound contrast agent (Optison®).** *Ultrasound in medicine & biology* 2003, **29:**473-481.
237. Fatar M, Griebe M, Stroick M, Kern R, Hennerici M, Meairs S: **Neuroprotective effect of combined ultrasound and microbubbles in a rat model of middle cerebral artery infarction.** In *4TH INTERNATIONAL SYMPOSIUM ON THERAPEUTIC ULTRASOUND*. AIP Publishing; 2005: 62-64.
238. Vykhodtseva N, Mcdannold N, Martin H, Bronson RT, Hynynen K: **Apoptosis in ultrasound-produced threshold lesions in the rabbit brain.** *Ultrasound in medicine & biology* 2001, **27:**111-117.
239. Vykhodtseva N, McDannold N, Hynynen K: **Induction of apoptosis in vivo in the rabbit brain with focused ultrasound and Optison®.** *Ultrasound in medicine & biology* 2006, **32:**1923-1929.
240. Downs ME, Buch A, Sierra C, Karakatsani ME, Teichert T, Chen S, Konofagou EE, Ferrera VP: **Long-Term Safety of Repeated Blood-Brain Barrier Opening via Focused Ultrasound with Microbubbles in Non-Human Primates Performing a Cognitive Task.** *PLoS One* 2015, **10:**e0125911.
241. Ziskin MC, Barnett SB: **Ultrasound and the developing central nervous system.** *Ultrasound in medicine & biology* 2001, **27:**875-876.
242. Miller M, Nyborg W, Dewey W, Edwards M, Abramowicz J, Brayman A: **Hyperthermic teratogenicity, thermal dose and diagnostic ultrasound during pregnancy: implications of new standards on tissue heating.** *International journal of hyperthermia* 2002, **18:**361-384.

243. Church CC, Miller MW: **Quantification of risk from fetal exposure to diagnostic ultrasound.** *Progress in biophysics and molecular biology* 2007, **93:**331-353.
244. Abramowicz JS: **Ultrasonographic Contrast Media Has the Time Come in Obstetrics and Gynecology?** *Journal of ultrasound in medicine* 2005, **24:**517-531.
245. Sienkiewicz Z: **Rapporteur report: Roundup, discussion and recommendations.** *Progress in biophysics and molecular biology* 2007, **93:**414-420.
246. Miller MW, Ziskin MC: **Biological consequences of hyperthermia.** *Ultrasound in medicine & biology* 1989, **15:**707-722.
247. Edwards M, Saunders R, Shiota K: **Effects of heat on embryos and foetuses.** *International journal of hyperthermia* 2003, **19:**295-324.
248. Sikov M: **Effect of ultrasound on development. Part 2: Studies in mammalian species and overview.** *Journal of ultrasound in medicine* 1986, **5:**651-661.
249. Jensh RP, Brent RL: **Intrauterine effects of ultrasound: animal studies.** *Teratology* 1999, **59:**240-251.
250. Tarantal A, O'Brien W, Hendrickx A: **Evaluation of the bioeffects of prenatal ultrasound exposure in the cynomolgus macaque (Macaca fascicularis): III. Developmental and hematologic studies.** *Teratology* 1993, **47:**159-170.
251. Norton S, Kimler B, Cytacki E, Rosenthal S: **Prenatal and postnatal consequences in the brain and behavior of rats exposed to ultrasound in utero.** *Journal of ultrasound in medicine* 1991, **10:**69-75.
252. Carnes K, Hess R, Dunn F: **Effects of in utero ultrasound exposure on the development of the fetal mouse testis.** *Biology of reproduction* 1991, **45:**432-439.
253. Hande MP, Devi PU: **Effect of prenatal exposure to diagnostic ultrasound on the development of mice.** *Radiation research* 1992, **130:**125-128.
254. Fisher JE, Acuff-Smith KD, Schilling MA, Vorhees CV, Meyer RA, Smith NB, O'Brien WD: **Teratologic evaluation of rats prenatally exposed to pulsed-wave ultrasound.** *Teratology* 1994, **49:**150-155.
255. Fisher JE, Acuff-Smith KD, Schilling MA, Meyer RA, Smith NB, Moran MS, O'Brien WD, Vorhees CV: **Behavioral effects of prenatal exposure to pulsed-wave ultrasound in unanesthetized rats.** *Teratology* 1996, **54:**65-72.
256. Devi PU, Suresh R, Hande M: **Effect of fetal exposure to ultrasound on the behavior of the adult mouse.** *Radiation research* 1995, **141:**314-317.
257. Hande MP, Devi PU: **Teratogenic effects of repeated exposures to X-rays and/or ultrasound in mice.** *Neurotoxicology and teratology* 1995, **17:**179-188.
258. Oh H, Lee S, Yang J, Chung C, Ryu S, Huh M, Jo S, Son C, Kim S: **Establishment of a biological indicator for the radiation and safety of diagnostic ultrasound using apoptosis.** *In vivo (Athens, Greece)* 1999, **14:**345-349.
259. Ryo E, Shiotsu H, Takai Y, Tsutsumi O, Okai T, Taketani Y, Takeuchi Y: **Effects of pulsed ultrasound on development and glucose uptake of preimplantation mouse embryos.** *Ultrasound in medicine & biology* 2001, **27:**999-1002.
260. Gu YH, Hasegawa T, Suzuki I: **Combined effects of radiation and ultrasound on ICR mice in the preimplantation stage.** *Ultrasound in medicine & biology* 2002, **28:**831-836.
261. Brown AS, Reid AD, Leamen L, Cucevic V, Foster FS: **Biological effects of high-frequency ultrasound exposure during mouse organogenesis.** *Ultrasound in medicine & biology* 2004, **30:**1223-1232.

262. Jia H, Duan Y, Cao T, Zhao B, Lv F, Yuan L: **Immediate and Long-Term Effects of Color Doppler Ultrasound on Myocardial Cell Apoptosis of Fetal Rats.** *Echocardiography* 2005, **22:**415-420.
263. Karagöz İ, Biri A, Babacan F, Kavutçu M: **Evaluation of biological effects induced by diagnostic ultrasound in the rat foetal tissues.** *Molecular and cellular biochemistry* 2007, **294:**217-224.
264. Vorhees CV, Acuff-Smith KD, Schilling MA, Fisher JE, Meyer RA, Smith NB, Ellis DS, O'Brien WD: **Behavioral teratologic effects of prenatal exposure to continuous-wave ultrasound in unanesthetized rats.** *Teratology* 1994, **50:**238-249.
265. Vorhees CV, Acuff-Smith KD, Weisenburger WP, Meyer RA, Smith NB, O'Brien WD: **A teratologic evaluation of continuous-wave, daily ultrasound exposure in unanesthetized pregnant rats.** *Teratology* 1991, **44:**667-674.
266. Tarantal A, Hendrickx A: **Evaluation of the bioeffects of prenatal ultrasound exposure in the cynomolgus macaque (Macaca fascicularis): I. Neonatal/infant observations.** *Teratology* 1989, **39:**137-147.
267. Tarantal A, Hendrickx A: **Evaluation of the bioeffects of prenatal ultrasound exposure in the cynomolgus macaque (Macaca fascicularis): II. Growth and behavior during the first year.** *Teratology* 1989, **39:**149-162.
268. Arthuis C, Novell A, Escoffre J-M, Patat F, Bouakaz A, Perrotin F: **New insights into uteroplacental perfusion: quantitative analysis using Doppler and contrast-enhanced ultrasound imaging.** *Placenta* 2013, **34:**424-431.
269. Ter Haar G: **Ultrasound bioeffects and safety.** *Proceedings of the Institution of Mechanical Engineers, Part H: Journal of Engineering in Medicine* 2010, **224:**363-373.

Chapter 5 Medical applications and detection techniques of ultrasound cavitation and microbubble contrast agents

This chapter has been submitted as “Zahra Izadifar, Paul Babyn, Dean Chapman, 2016, Medical applications and detection techniques of ultrasound cavitation and microbubble contrast agents, *Measurement Science and Technology* (Under Review)” According to the Copyright Agreement, "the authors retain the right to include the journal article, in full or in part, in a thesis or dissertation".

5.1 Abstract

The presence of microbubbles in the human body can be induced either through cavitation or exogenous introduction of bubbles. One of the effects of ultrasound is cavitation, or microbubble formation and collapse. Cavitation produces high pressures and temperatures, and microbubble expansion and then collapse close to cells can lead to cellular damage or hemorrhage in biological tissues. Cavitation is, in most cases, an undesired event in clinical diagnostic imaging. Considering that cavitation microbubble formation is largely unpredictable, ultrasound imaging may present a rare or yet unknown risk, particularly to fetuses and embryos. Although most therapeutic ultrasound modalities work based on physical and thermal effects of cavitation, the safety of treatment strongly depends on accurate knowledge of the location of the cavitation inception point. Cavitation detection is an important factor with respect to improving the safety of ultrasound imaging and therapy. It is essential to recognize the existence and location of cavitation inception points. In addition, the use of encapsulated microbubbles as contrast agents for diagnostic imaging, as vehicles for local drug or gene delivery, and as tools for microbubble and ultrasound therapy in thrombolysis has increased the demand for an accurate deep tissue microbubble detection technique. Over the past decades, different techniques have been

investigated for detecting microbubbles. In this chapter the state-of-the-art of medical microbubble detection along with therapeutic, monitoring, and diagnostic applications are reviewed. A novel imaging technique for detection of cavitation bubbles deep in tissue is also addressed.

5.2 Introduction

Cavitation is defined as the formation of bubbles (cavities) when the propagation of an acoustic wave through a liquid induces a strong enough negative pressure [1]. The term *cavitation process* is used to describe the process in which vapor- or gas-filled cavities undergo growth and implosion in a liquid host medium on exposure to acoustic radiation. The fundamental physics of the cavitation process in human tissues during clinical ultrasound applications still requires further study. Frenkle [2]and Skripov [3] largely deal with the fundamental physics of nucleation in very pure liquid and clean environments.

Multiple physical effects are associated with the growth and violent collapse of cavitation bubbles, including direct physical phenomena such as luminescence, free radical formation, very high pressure shock wave emissions, shear stress, and high-speed microjet production. In ultrasound diagnostic imaging, cavitation can be an undesired and unwanted phenomenon. Although some therapeutic modalities work based on cavitation, it can also be considered an undesired bioeffect (e.g., giving rise to hemorrhaging) in other therapeutic modalities (e.g., lithotripsy).

There has been interest in the use of higher frequencies and higher acoustic power for improved imaging resolution [4]. In addition, more recent interest in three-dimensional fetal images as souvenirs in obstetric ultrasonography raises concern with respect to potential bioeffects. As a

mechanical bioeffect, cavitation can cause local tissue injury in the immediate vicinity of the cavitation activity, including cell death and hemorrhage of blood vessels [5].

Because cavitation plays a significant role in therapeutic modalities such as extracorporeal shock wave lithotripsy (ESWL), intracorporal lithotripsy, and the ultrasonic cavitation devices used in surgery to dissect or fragment tissues, the safe application of these modalities largely depends on precisely locating the cavitation microbubbles generated by these devices.

Microbubbles can also be introduced into human tissues by injection and are used as microbubble contrast agents for ultrasound diagnostic imaging or as vehicles for drug or gene delivery. Considering that the entrance of medical microbubbles (e.g., ultrasound contrast agents) into the human body is followed by ultrasound radiation, the growth and violent collapse of microbubbles can have the same or similar effect as cavitation on cells, blood vessels, or tissues. Therefore, cavitation bubbles and ultrasound contrast agents should both be further studied in the body to provide safety assurance and minimize the side effects of clinical ultrasound modalities. However, to accurately assess and control cavitation, it is first essential to determine the existence of microbubbles and locate any cavitation inception points.

This review briefly describes the fundamentals and clinical applications of cavitation phenomena and ultrasound microbubble contrast agents. The biological effects of cavitation/microbubbles and concerns regarding their adverse effects on tissue and organs in the human body are discussed. This is followed by a review of the various modalities that have been used for detection of microbubbles/cavitation bubbles, and their relative advantages and disadvantages.

5.3 Understanding cavitation phenomenon

When an ultrasound wave is applied to a liquid, the molecular structure of the medium goes through alternating expansion and compression cycles. As expansion (rarefaction) and compression cycles travel through a medium, rarefaction pulls molecules apart and compression pushes them together. If the ultrasound wave is strong enough, the expansion cycle can overcome intermolecular binding forces and lead to a sudden pressure drop and creation of bubbles of gaseous substances in the liquid. These bubbles grow in size with the ensuing expansion cycles of ultrasound until they reach an unstable size and then violently collapse (Figure 5-1). This physical phenomenon is called acoustic cavitation.

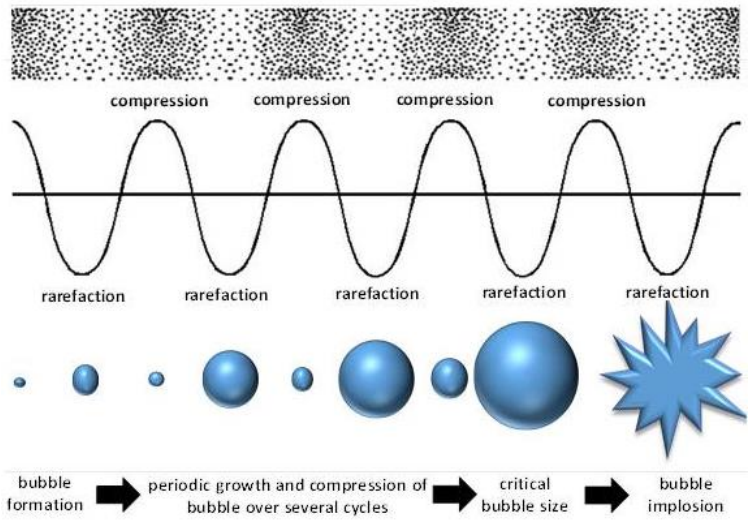

Figure 5-1 Schematic image of acoustic cavitation process

Cavitation bubbles are typically initiated at a micron size in the fluid [6] but, depending on the frequency, power, and environment, their size will vary. For example, in a lithotripter shock wave the bubble can grow from a 1 μm radius to a ~1 mm radius over a period of 150 μs; it then takes a further 150 μs for the bubble to collapse [1]. The size of cavitation bubbles primarily depends on the ultrasonic frequency. At a given ultrasonic power, higher frequencies produce

smaller cavitation bubbles and lower frequencies generate bigger cavitation bubbles [7]. This is partially due to the fact that the increased wavelength at lower frequencies allows more time and space for the bubbles to grow to larger sizes before they implode. The energy released in the zone as the bubbles implode directly relates to the bubble size. Larger bubbles require more energy to grow and, in turn, a larger amount of energy will be released when they implode [7]. Decreasing the frequency enhances the likelihood of cavitation activation [5]. Based on the conservation of energy, at a constant frequency a higher ultrasonic power will lead to a larger number of cavitation bubbles [7].

Two types of cavitation bubbles form based on the behavior of microbubbles within a medium. When a bubble forms in a liquid medium, it grows until it reaches a critical size known as its resonance size, which depends on the frequency of the applied sound field. If the microbubble reaches its resonance size and then becomes unstable and collapses violently within a single cycle or over a small number of acoustic cycles, it is called *inertial cavitation* (or *transient cavitation*). If, however, the microbubble does not violently collapse and instead oscillates for many cycles at, or around, its resonance size, it is called *non-inertial cavitation* (or *stable cavitation*) [8]. In non-inertial cavitation, the ultrasound pressure acts as a driving force that changes the bubble size and shape; the bubble behaves as an oscillator with a stiffness provided by the gas within the bubble and inertia provided by the liquid surrounding the bubble that moves with the bubble wall. Generally, higher acoustic pressures lead to inertial cavitation and lower acoustic pressures result in non-inertial cavitation [9]. Non-inertial cavitation can be as important as inertial cavitation as it includes the initiation of surface oscillations and microstreaming. These bubbles are usually long-lived and their integrated effect can be substantial [10].

The whole inertial cavitation process—in which vapour bubbles form, grow to many times their original size, and undergo rapid implosive collapse—happens within about 400 μs. Normally, cavitation occurs at pre-existing weak points in the fluid, such as gas-filled crevices in suspended material or transient bubbles remaining from previous cavitation events [11]. In successful cavitation processes, the cavities can grow and collapse violently with the release of enormous amounts of energy in the form of an acoustic shock wave, temperature, pressure, and visible light [12]. The estimated rapid adiabatic compression of gases and vapours within the bubbles or cavities produces hot spots with extremely high temperatures and pressures that approach 5000 °C and 1000 atm, respectively, during bubble collapse.

Many theories have been proposed to explain the chemical effects stemming from cavitation bubble collapse. Cook in 1917 theoretically calculated and found the pressure developed when cavitation bubble collapse is arrested by impact against a rigid concentric obstacle is 10300 atm or 68 tons per sq. inch [13]. A hot spot theory was proposed by Noltingk and Neppiras in 1950 [14]. Flint and Suslick in 1991 [15] proposed an electrical discharge theory that states that an electrical charge forms on the surface of the bubble when the cavitation bubble starts to collapse into tiny microbubbles. This was also proposed by Margulis in 1990 [16].

Because the size of the bubbles is very small relative to the total liquid volume, the heat produced by bubble collapse is rapidly dissipated with generally no appreciable change in overall environmental conditions [11]. The cooling following the implosion of a cavitation bubble is estimated to be in the region of 10 billion °C/s [11]. The bubble collapse can cause emission of light and also gas temperatures that can reach over 1000 °C [11]. The inertial cavitation process can potentially create free radicals or give rise to emission of light, which is known as ‘sonoluminescence’.

When the acoustic cavitation bubble collapse is close to or on a solid surface, the dynamics of collapse change dramatically. In the absence of any close physical boundary, the bubble retains it spherical shape during collapse because its surroundings are uniform. However, close to a physical boundary, it can only collapse asymmetrically because the solid surface provides resistance to liquid flow. This asymmetric collapse produces high-speed liquid jets driving into the surface of the solid at speeds close to 400 km/h (111 m/s) [11]. The impact of the jets on the surface is very strong and can result in serious damage to impact zones and cause surface pitting (erosion). After its collapse, the bubble might fragment or may repeat its growth/collapse cycle. The probability of inertial cavitation occurrence for a particular bubble nucleus depends on the acoustic pressure amplitude, the acoustic frequency, and the bubble radius. The influence of the physical characteristics of fluid viscosity and surface tension on the dynamics of cavitation bubbles was studied by Plesset, who derived the Rayleigh-Plesset equation in 1949 [17]. In any cloud of bubbles in the medium within the same ultrasound field, both inertial and non-inertial cavitation may occur simultaneously. However, when the bubbles are small the surface tension prevents initial growth and therefore the bubbles do not grow. When the cavitation nuclei are large, they can grow initially but do not collapse to generate sufficiently high temperatures. Therefore, for a specific frequency and nucleus radius a threshold pressure is required to initiate inertial cavitation. Apfel and Holland studied the theoretical threshold acoustic pressure for inertial cavitation in blood and water [18]. If the bubbles are close to an elastic medium, their motion along the surface (shear motion) can lead to an increase in the heating of the medium (shear loss). In a study by Holt and Roy [19], a considerable temperature rise was generated in agar-based tissue with the application of an ultrasonic pressure above the threshold level for cavitation. Also, when the bubble is pulsing, the inhomogeneous periodic field around the bubble

can produce a small steady flow of fluid known as microstreaming [20]. Extremely high shear stresses near the bubble surface will be produced because of the variation of this flow with distance from the bubble. Cell membrane destruction and temporary alterations in permeability have been associated with this high shear stress.

An excellent review on the subject of acoustic cavitation has been written by Neppiras [10], in which the physics of cavitation are extensively reviewed. The mathematical derivations of the basic theories of cavitation and dynamics of bubbles along with some experimental data for those theories can be found in the books by Young [1], Brennen [10], and Leighton [11]. The fundamental behavior of bubbles in an acoustic field is reviewed by Lauterborn [12].

5.4 Effect of cavitation/microbubbles on tissue and body fluid

The presence of microbubbles in the body can result from either exogenous introduction of microbubbles into the body or endogenous generation of microbubbles in the body as a result of ultrasound propagation. The properties of endogenous microbubbles generated within the area of an ultrasound beam will depend on the ultrasound wave's properties. Cavitation microbubbles or endogenous bubbles can be intentionally produced in the body for clinical applications such as lithotripsy, as explained later in this review.

Ultrasound microbubble contrast agents (medical microbubbles) are exogenous microbubbles generated outside of the body and then injected into the vasculature for different medical applications. Considering that these microbubble contrast agents can easily expand, move, and fragment by ultrasound, additional safety considerations are needed during insonation to avoid thermal and mechanical biological effects [21]. The presence of either endogenous or exogenous microbubbles can have multiple thermal and biological effects.

At high ultrasound pressure (mechanical index (MI)>1.0), microbubbles are forced to expand and then are compressed, which results in their destruction. Destruction of these microbubbles close to a living cell leads to permeability of cell membranes [22]. The destruction of microbubbles with ultrasound has caused rupture of microvessels with extravasation of red blood cells [23]. As a mechanical bioeffect, cavitation activation can cause local tissue injury in the immediate vicinity of the cavitation activity, including cell death and hemorrhage of blood vessels [5]. For example, cavitation-mediated tissue damage in shockwave lithotripsy has been reported [24]. Large surface hemorrhaging over both the targeted and contralateral kidneys along with hemorrhaging of the spleen, intestine, and peritoneum have been observed in small animal or *in vitro* studies [24]. Tissue histology has revealed vascular rupture in the kidney, necrosis of the walls of the intralobular arteries and veins, and diffuse damage to the targeted kidney tissue that may be due to cavitation [24].

The exact mechanism by which microbubbles enhance the permeability of cells is still unresolved [22]. When an ultrasound wave is applied to tissues, it creates cavitation bubbles in the fluid that, along with the cavitation process, result in an incremental increase in cell permeability. In fact, the cavitation process on its own increases cell permeability [25]. However, the presence of additional microbubbles along with the high acoustic pressure due to ultrasound exposure have additional effects on cell permeability [26]. Cavitation in body tissues or blood sets fluid in motion and makes small shock waves that give rise to microstreaming along the endothelial cells [22]. High-energy microstreams or microjets produced by cavitation bubbles during the cavitation process cause shear stress on the membrane of an endothelial cell [27], which increases the cell permeability. This increase is probably due to transient holes in the plasma and nuclear membrane [22]. Other proposed mechanisms for cell permeability increase

include the generation of reactive oxygen species in endothelial cells during the cavitation process [28], an increase in intracellular radical production (which is associated with cell killing *in vitro* and endothelial cell layers), a rise in temperature (which can influence the fluidity of phospholipid bilayer membranes), and endocytosis or phagocytosis (which may activate membrane transport mechanisms) [22]. When a bubble collapses following highly energetic ultrasound, all of these phenomena can result in a local increase in cell permeability. Considering this fact, drugs and genes can be attached to microbubbles that are then used as a vehicle to transport them to specific body areas for delivery to local cells. Unger et al. describe how drugs or genes can be attached to microbubbles [29]. Briefly, drugs can be attached to microbubbles by incorporation within the bubble or within the bubble membrane, attachment to the membrane, attachment to a ligand, or incorporation in a multilayer microbubble [22]. Drug and gene delivery with microbubbles is a promising technique; however, adverse effects such as a rise in blood temperature or hemolysis and possible side effects on tissue and organs in humans have been a cause of concern in several studies [22, 30-32]. Bioeffects are mainly influenced by factors such as the choice of ultrasound frequency and its amplitude, both of which need further investigation.

5.5 Ultrasound microbubble contrast agents application

5.5.1 Diagnosis and monitoring

Many of the ongoing improvements in sonographic diagnosis have been related to the entry of ultrasound microbubble contrast agents (medical microbubbles). Small exogenous gas bubbles are used to increase ultrasound contrast. The first reported use of microbubbles as a contrast agent was in echocardiography by Gramiak and Shah in 1968 [33]. Ultrasound microbubble contrast agents permit reliable, reproducible left ventricular opacification and are currently in

widespread clinical use. Evidence has shown that contrast echocardiography is clinically effective, reduces downstream costs, and precludes patients from further potentially hazardous investigations [34]. These medical microbubbles are used to increase the reflectivity of perfused tissue in cardiology and radiology applications [21].

Microbubbles used in echocardiography as contrast agents are small gas-filled microspheres with specific acoustic properties. First generation microbubbles are room air microspheres [35] that disappear a few seconds after intravenous administration [36, 37]. Second generation microbubble contrast agents are filled with a heavy molecular weight gas such as sulphur hexafluoride and stabilized with a thin shell such as sonicated albumin and (phosphor)lipids to improve survival and stability of microbubbles under high pressure [35]. Second generation microbubbles have a much smaller diameter (about 2.5 μm) than first generation microbubbles to ease their passage through the pulmonary capillary bed [22]. Diagnostic imaging with contrast agents is improved when an acoustic pressure higher that 0.05 is used (mechanical index, MI>0.05). An MI higher than 0.05 causes emission of non-linear harmonic signals at multiples of the transmitted frequency [29]. This improves the signal to noise ratio and creates an acoustic impedance mismatch between body tissues and fluids containing microbubbles, which makes these microbubbles beneficial in diagnostic ultrasound imaging [38].

When ultrasound is applied, small exogenous gas bubbles oscillate and can be deflected to a vessel wall and then fragmented into nanometer-sized particles. Microbubble fragmentation facilitates imaging of multiple targets when single-session molecular imaging is difficult with affinity-based strategies [21]. Clinical ultrasound systems take advantage of the unique nonlinear properties of these small gas nuclei for diagnosis and monitoring.

The application of encapsulated microbubbles as a contrast agent has remarkably improved diagnostic capabilities. The addition of microbubble contrast agents increases the sensitivity of ultrasound to capillary-sized vessels and very low flow rates [21]. Because these microbubble contrast agents are highly compressible and their presence results in strong scattering of ultrasound, their expansion and compression generates nonlinear signals [39, 40] and also appears bright on an ultrasound image [39]. Power Doppler imaging combined with ultrasound contrast agents significantly improves detection of blood flow in small vessels [21]. Tumor diagnosis and monitoring the response of cancers to new anti-angiogenesis treatment can be facilitated by means of combined power Doppler and ultrasound contrast agents. In a study by Yang WT et al. [41], a strong correlation between histologic microvascular density of human breast masses with 2- and 3-D power Doppler sonography was shown. In another study in mice, the ratio of increased pixels to total pixels in the tumor was used to follow antiangiogenic treatment of xenografted tumors [42]. The signal-pixel rate in the treated sample was considerably decreased compared to the controls and correlated with histologic microvascular density [42]. Contrast-enhanced phase inversion imaging can subjectively diagnose neovascularity [43] that can significantly ease detection of tumors. Contrast-enhanced phase inversion harmonic imaging of xenografted tumors correlates with a semi-quantitative scale of immunohistochemical staining as a predictor of tumor angiogenesis [44].

5.5.2 Ultrasound drug delivery

Cell membranes often prohibit large molecules (e.g., drugs and genes) from entering cells. The mechanical force of focused ultrasound through endogenous microbubbles of stable (or non-inertial) cavitation can improve cell membrane permeability and give rise to absorption of drugs or genes. This effect, known as sonoporation, creates pores in cell membranes via stable

cavitation and allows a greater volume of compounds to enter the cell [45]. In addition, the acoustic streaming induced by stable cavitation gives rise to the flow of fluid in the local environment of the cell. This helps open pores in the cell membrane and also directs the molecules of the drug toward the cells [46, 47] .

On the other hand, several properties of exogenous medical microbubbles make them promising tools for delivery of drugs and genes to living cells [36, 29, 48-52, 27, 53]. Ultrasound contrast agents combined with focused ultrasound is uniquely suitable for localized drug delivery. Many diseases such as cancer, inflammatory diseases, or thrombo-embolic processes may require high concentrations of certain drugs. However, high drug concentrations can have toxic side effects on the rest of body. In addition, systematic drug delivery requires plasma concentrations to be within the therapeutic range, but this is limited by the occurrence of potential side effects. In more specific drug delivery, microbubbles can be coated with a drug by attaching it to a ligand on the outside of the drug-laden microbubbles (Figure 5-2a). Focused ultrasound is then applied locally at the targeted area, resulting in selective delivery of the drug in the body [54]. Alternatively, drugs may be incorporated into the microbubbles and released in the region of interest by rupturing the microbubbles with localized focused ultrasound (Figure 5-2b) [55, 56]. Another approach is to systematically and simultaneously inject the drug and an ultrasound contrast agent and then apply focused ultrasound to the target region (Figure 5-2c). The oscillation and destruction of the bubbles in small vessels alters the vessel walls and results in extravasation of the drug [57, 58]. As shown in Figure 5-2d, the permeability of cells during drug delivery can be increased (1) through non-inertial cavitation when the bubble behaves as an oscillator and microstreaming around the bubble increases the permeability (Fig. 5-2d-1), (2) through collapse of the gas bubble and emission of a shock wave (Fig. 5-2d-2), or (3) through

asymmetric bubble collapse close to the cell wall producing a liquid jet that pierces and ruptures the cell (Fig. 5-2d-3).

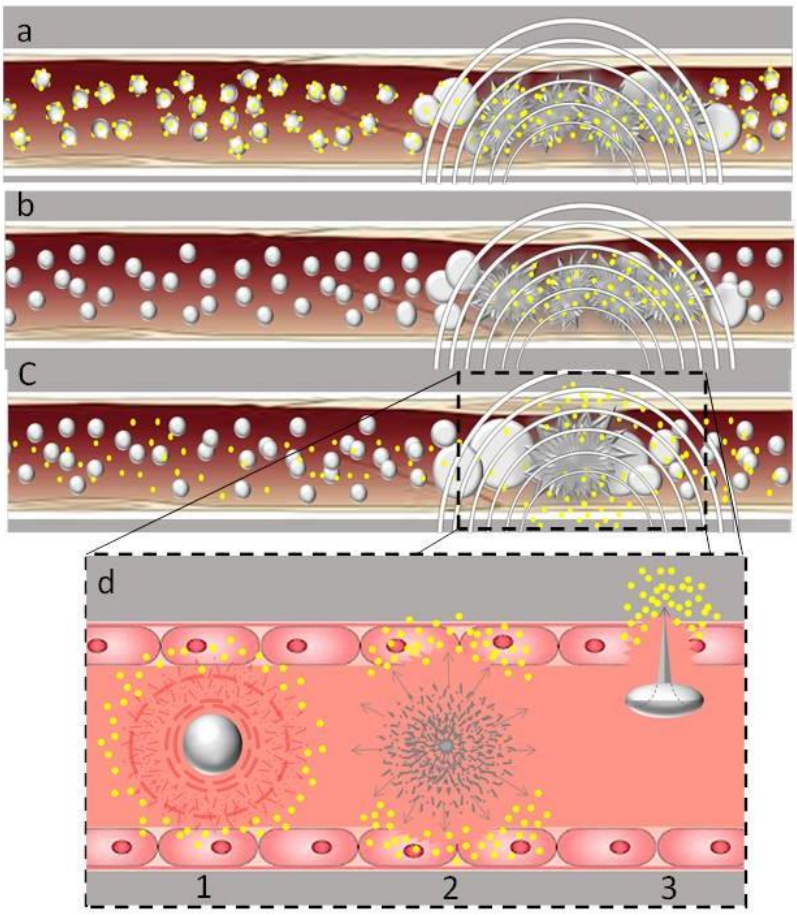

Figure 5-2. Illustration of variety of ways drug delivery can be enhanced by utilizing microbubbles. (a) Microbubbles with drug-laden external membranes are freely circulated in the vessel and bind in the target region, then are ruptured by ultrasound and the drug payload liberated in the target area; (b) Microbubbles carrying drugs inside of them are circulated in the vessel and destroyed by ultrasound and the transported substances thus released into the surrounding targeted tissue; (c) Free circulation of drug particles (yellow circles) along with ultrasound microbubbles (grey circles) in vessels, and the effect of ultrasound on growth and burst of microbubbles results in extravasation of drug; and (d) Schematic of various modes by which microbubbles increase the cell permeability: 1: non inertial cavitation when a bubble behaves as an oscillator and microstreaming around bubble increases the permeability; 2: collapse of a gas bubble and emission of a shock wave; and 3: asymmetric bubble collapse close to a cell wall producing a high speed liquid jet that pierces and ruptures the cell.

Drug delivery via drug-loaded microbubbles that are ruptured with localized ultrasound can result in local drug release in higher concentrations than can be achieved with systemic administration. In addition, the drug will be pushed directly into the cell given the higher cell permeability in this technique [22].

5.5.3 Gene therapy with microbubbles

Gene therapy may play a significant role in the treatment of several (cardiovascular) diseases in the near future. In gene therapy, first the gene needs to be delivered to the tissue and taken up by the cells. Then, it should be incorporated into the genome in the nucleus of the cell without being digested. The direct intravascular injection of genes is not possible as the DNA consists of large molecules and results in the removal of the gene from the blood. In addition, the gene is too long to enter the cell passively [22]. Several studies have shown that ultrasound in combination with microbubbles can be a safe method of gene delivery to cells [25, 59, 60, 48, 61].

5.5.4 Smart microbubbles in diagnostic applications

Considering that microbubbles in current use are comparatively stable and circulate throughout the body, it is possible that the contents of the microbubbles may be deposited in undesired tissues. To avoid this problem, microbubbles can be combined with ligands and receptors that are incorporated in the bubble shell, creating “smart microbubbles” that target specific tissues [22]. These smart microbubbles can also be useful for active attachment of microbubbles to target tissues and provide further potential for diagnosis or localized drug delivery to targeted lesions for therapy.

Smart microbubbles have been described in several studies where they have targeted different types of tissues and processes, including endothelial cells (for diagnosis of preclinical atherosclerosis) [62], non-invasive identification of acute cardiac transplant rejection in mice

[63], inflamed tissue and angiogenesis [64] (for ultrasound imaging of inflamed tissue [65, 66] such as post-ischemic myocardial inflammation [67]), and vascular clots or thrombi (visualization of vascular clots associated with cardiac vascular disease such as stroke and myocardial infarction, which can be used for identification and cure of vascular clots in humans) [68]. Ultrasound is known to improve clot lysis in blood vessels, and ultrasound in combination with targeted microbubbles loaded with thrombolytic agents can further drive this effect by cavitation [22].

Due to the action of microbubbles, ultrasound also became of interest as a potential therapeutic tool in thrombolysis. In several serious cardiovascular diseases such as myocardial infarction and non-hemorrhagic stroke, rapid thrombolysis by fibrinolytic therapy improves morbidity and mortality, but recanalization of the occluded vessel is not easily achieved. Systematic administration of thrombolytic agents can be complicated, especially due to bleeding [69]. The application of ultrasound at low frequencies (from 26 kHz to 10.03 MHz) and high power in the presence of absence of fibrinolytic therapy has been shown to increase clot lysis in both *in vitro* and *in vivo* studies [70-77].

The effect of the cavitation process on the surface of the vascular clot plays an important role in micro fragmentation, which can make the clot more susceptible to fibrinolytic agents [78]. The presence of microbubbles lowers the energy needed for cavitation. Destruction of microbubbles by high power ultrasound creates powerful microjets that accelerate the effect of ultrasound in thrombus dissolution compared to ultrasound alone [22]. Although the influence of different types of microbubbles and different ultrasound operating conditions (170 kHz and 0.5 W/cm [79], 10 MHz and 0.5-1.0 W/cm [80], 20 kHz and 1.5 W/cm [81], 20 kHz and 40 W/cm [82], 10 MHz and 1.02 W/cm [83]) have all shown significant improvement on thrombolysis, there is still

uncertainty about whether the same effects can be reached in humans. These assessments have been reviewed in [22]. Endothelial cell injury of microvessels, which can be a potential clinical danger, has been reported by Kobayashi et al. [84]. Diagnostic ultrasound imaging commonly works at frequencies between 2 and 15 MHz [85]. Most cavitation processes occur at lower frequencies and higher powers, and thrombolysis by ultrasound would require such operating conditions. Considering the bioeffects of ultrasound at low frequency and high power, the safety of all of these techniques requires further study; microbubble detection techniques, especially for future applications in humans, are also needed. At the cellular level, the interaction of fluorescent-labeled microbubbles and myocardial or endothelial cells under high ultrasound pressure can be precisely studied using live-cell imaging techniques (such as multi-dimensional digital imaging microscopy) [22]. But to control the exact area that microbubbles deposit the gene or drug in the body or are interacting with live cells deep in tissue, an imaging technique capable of detecting microbubbles deep in tissue (such as the human body) without disturbing the microbubbles is required.

5.6 Detection and imaging of cavitation and microbubbles

Over the past decades, different techniques have been investigated for detecting and mapping microbubbles. These techniques mainly include optical, acoustic, and scattering methods. Optical methods include high-speed photography, sonoluminescence, and sonochemiluminescence, and acoustic methods include active cavitation detection (ACD) and passive cavitation detection (PCD), and the Doppler method. Scattering methods include laser and synchrotron based X-ray methods. Each of these techniques has specific strengths and weaknesses for detection and mapping microbubbles. These signatures can be used to detect the microbubbles through physical and chemical techniques. Most published studies of visualization and detection of

microbubbles come from in vitro experiments. There have been few attempts to detect microbubbles in animals [86, 87]. One challenge for in-vivo detection of the cavitation microbubbles is attributed to the high attenuation and inhomogeneous nature of tissues which affect the sound wave propagation and consequently the behavior of the ultrasound-induced microbubbles in-situ. A couple of techniques can also measure either exogenous microbubble or endogenous cavitation bubbles. In the following section, the different modalities that have been used to study microbubbles are briefly reviewed.

5.7 Optical methods

5.7.1 Detection of physical and chemical responses

The presence of cavitation can be indirectly assessed through a variety of physical and chemical methods [88]. These methods rely on detection and measurement of free radicals (sonochemiluminescence), and sonoluminescence, created from cavitation bubbles [89]. The results of these measurements must be considered based on a basic interpretation of the cavitation process, which can be complicated. The high temperatures and pressures that result from cavitation can lead to light emission (sonoluminescence) and increased chemical reaction rates (sonochemistry). Some techniques of assessment of the presence of cavitation depend on the creation and detection of free radicals, sonoluminescence, and acoustic emission from cavitation [90]. Sono- and chemiluminescence detection and electron spin resonance (ESR) measurements are two techniques applied to detect the presence of free radicals [91, 92]. Production of light and by-products from chemical reactions as a result of cavitation has been used to quantify cavitation activity [93, 94]. Other techniques to measure cavitation have been developed based on the influence of cavitation on a metal foil; cavitation can lead to pitting on metal foils, so these techniques have used the number and depth of pits to assess the violence of

cavitation [95-97]. The mechanical force exerted on a steel ball by both the incident shock wave and the cavitation phenomenon have been measured using an electromagnetic probe device [98]. However, these methods of quantifying cavitation are secondary measurements of the cavitation field, and interpreting the results can be complicated [1]. Sono- and chemiluminescence and ESR measurement techniques are useful for detecting cavitation bubbles *in vitro* but their use is limited in *in vivo* biological systems. Detecting luminescence is possible either in an optically transparent medium or by introducing an optical probe into the system. ESR is destructive to the sample and real-time measurement is not possible. In addition, cavitation is not directly detected in these techniques, but rather its presence is inferred from the nature of the onset of free radical production [99].

5.7.2 High speed photography

In an *in vitro* setting, cavitation bubble behavior can be observed by means of a high-speed camera [100-103]. High-speed photography has revealed the dynamics of the cavitation process. In principle, the dynamics of a bubble from genesis to extinction may be tracked by this technique; however, this is not feasible in practice. In order to image the bubble during the growth phase, imaging is required at length scales on the order of a millimeter and time scales on the order of tens of microseconds in a transparent media. At the nadir of the collapse, the bubble radius is less than one micrometer and the time scale of the collapse is about a nanosecond. After collapse, the remaining bubble is on the order of 10 micrometers and exists for hundreds of milliseconds before it dissolves. Therefore, it is virtually impossible to capture all bubbles dynamically considering the range of temporal and spatial scales. Another limitation of imaging photography is the limited depth of field, which cannot give an adequate record of bubble dynamics in the substantial volume of the cavitation field [1]. Bubble dynamics in water were

displayed in sequential photographs for the first time by Tomita and Shima [104]. Figure 5-3 shows the series of photographs of the cavitation process very close to a solid surface (top frame). The time interval between each of these numbered images is 2 μs and the frame width is 1.4 mm.

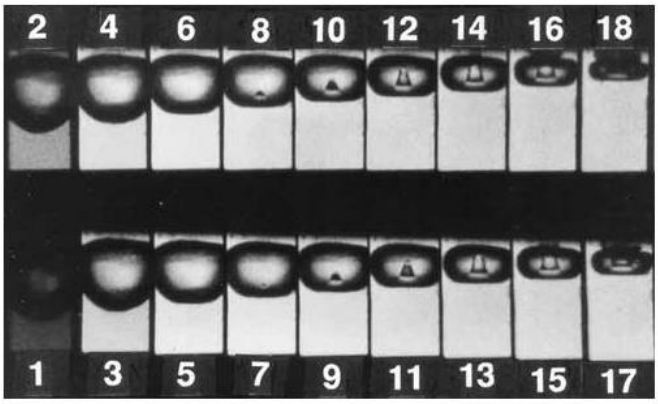

Figure 5-3 A series of 18 photographs demonstrate the dynamics of the cavitation process very close to a solid surface. Reproduced from Tomita and Shima [104] with permission.

One of the techniques that can be used to study the dynamic interaction between microbubbles and cell membranes is high-speed photography along with fluorescence microscopy. Using this technique, Ibsen et al. [105] released optical images of the interaction of a unique drug delivery vehicle (fluorescently labeled microbubbles loaded with drug) with ultrasound. Subsequently, Ibsen et al. designed an analysis system combined with a fluorescent microscope, high-speed camera, and definable pulse sequence of focused ultrasound and observed the real-time interaction between focused ultrasound, echogenic drug delivery vehicles, and live cell membranes [106]. Figure 5-4a shows sequential images of the interaction of focused ultrasound with a microbubble inside the echogenic drug delivery vehicle. The ruptured outer membrane of the microbubble leaves a debris field of fluorescent particles. The membrane fragmentation generates a jet of debris in frame 3 that is followed by the diffusion of a lipid debris cloud in frame 4 [106]. A fluorescent image series of the interaction of the echogenic drug delivery

vehicle with an artificial cell membrane under focused ultrasound pulsation is shown in Figure 5-4b.

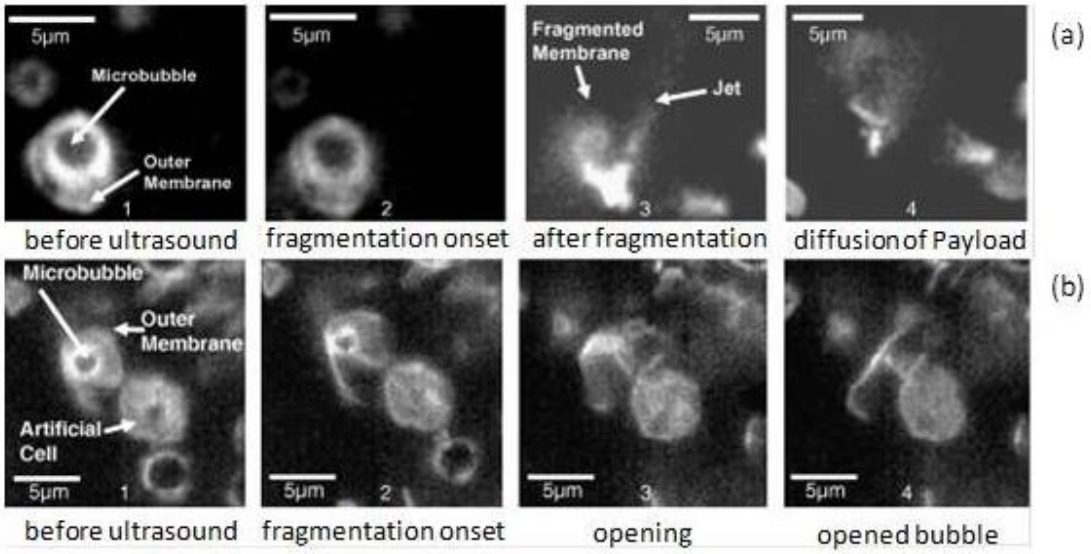

Figure 5-4 (a) Sequence of fluorescent images illustrating the interaction of focused ultrasound with the microbubble inside the echogenic drug delivery vehicle and (b) sequence of fluorescent images of the interaction of an echogenic drug delivery vehicle and an artificial cell membrane under ultrasound pulse sequence. Reproduced from Ibsen et al. [106] with permission.

Another imaging technique is ultra-high-speed imaging using a Brandaris camera. Using this technique, both the interaction of a cavitation bubble with the surface and the sub-microsecond timescale dynamics of the cavitation bubbles are visualized. In a study performed by Zijlstra et al. [107], high-speed imaging of microbubbles driven by a 1-MHz megasonic cleaning device in contact with a rigid wall was achieved. In their experimental setup, one side of a transparent glass microscope slide was coated with a layer of gold nanoparticles, and then removal of the gold nanoparticles with continuous sound illumination under an angle to the slide was observed. Depending on the driving pressure, the time required to visualize a bubble dynamic in their study

was ~1 µs. Using a specialized high-speed imaging system called “Brandaris”, the dynamics of an individual bubble at less than microsecond resolution were also visualized.

In another study by Chen [108], ultra-high-speed optical imaging of ultrasound-activated microbubbles in mesenteric microvessels was performed. The rat mesentery was chosen as it has optical transparency and can be used for imaging of insonated pre-injected microbubbles in microvessels to study the dynamics of microbubbles and their effect on the vessel walls *in vivo*. The mesentery was exteriorized through abdominal midline incision, sandwiched at the edge by two D-shape plates, and placed in a synchronized optical-acoustic system set up for ultra-high-speed imaging. An ultra-high-speed camera (Imacon 200; DRS Hadland, Cupertino, CA, USA) with a minimum exposure time of 5 ns was coupled to one side port of an inverted microscope (TE2000-U; Nikon Inc., Melville, NY, USA) used for imaging of the bubbles. High-intensity focused ultrasound (HIFU) with a center frequency of 1 MHz was used for sonication. The tissue was placed in water and the microbubbles were injected into vessels. When bubbles were in the field of view of the microscope, the ultrasound pulse was sent to the tissue sample and the dynamics of bubble along with its interaction with the vessel walls were studied.

5.7.3 Optical detection technique

In order to improve the efficiency of cavitation and microbubble application in clinical use, optically observing the microbubbles, the cavitation process, and the interaction of microbubbles with membranes has been attempted. Different imaging systems, such as electron microscopy, flow cytometry [109], atomic force microscopy [110, 111], and home-made instruments based on white light illumination [112] have been investigated for studying the interaction of pre-made microbubbles with ultrasound and membranes of artificial cells *in vitro*.

Direct detection of cavitation is possible by imaging bubbles in the medium. However, the very high speed of the cavitation phenomenon as well as the small size of the microbubbles make it difficult to see individual bubbles without a high-speed camera, and bubbles are usually observed as a cavitation cloud. In addition, cavitation detection deep in tissue at different operating conditions can be a difficult task.

If cavitation bubbles are produced at low acoustic frequencies, the bubble size is big enough for human visual perception unaided by a magnifying or light-collecting optical device. However, at higher frequencies the size of the cavitation bubble decreases and is on the order of a couple of microns. The lifetime of each individual bubble (bubble dynamics) is dictated by the period of the driving pressure [107]. The lifetime of cavitation bubbles is very short and visualizing cavitation bubble dynamics at less than microsecond resolution requires a specialized high-speed imaging system.

Another optical imaging technique is based on the microbubble oscillation. During an ultrasound/acoustic pulse, either exogenous or endogenous cavitation-induced microbubbles go through an expansion and contraction cycle as a result of the pressure rarefaction and compression of the applied acoustic beam. Capturing the expansion and breakup of the process requires a shutter speed on the order of tens to hundreds of nanoseconds. This can be done with a high-speed camera capable of nanosecond shutter speeds (Figure 5-5a) [21]. In the absence of a nearby solid boundary, the bubble's symmetric spherical oscillation is observed using a radius-time "streak" imaging technique. In addition, the effect of ultrasound on the microbubble can be characterized by measuring the radial oscillations using a radius-time curve image of a single line through the center of the microbubble (Figure 5-5b) [113, 39].

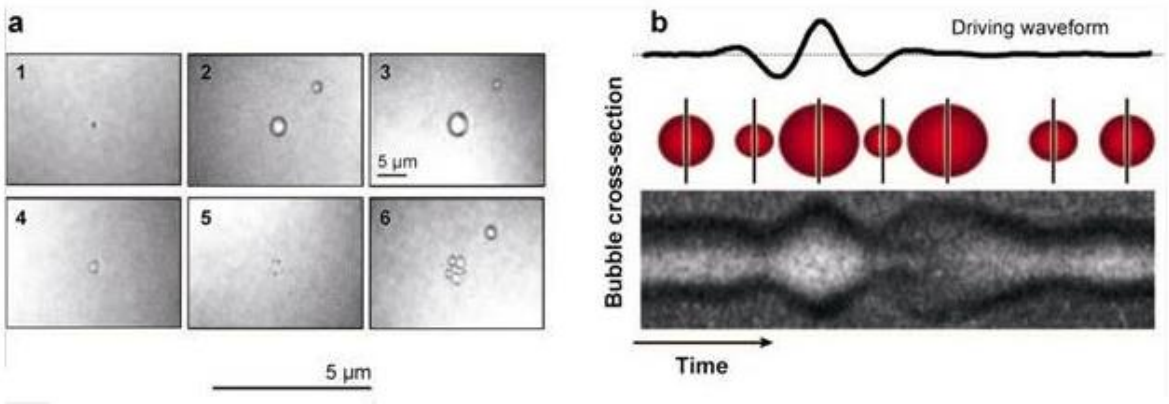

Figure 5-5 (a) Sequence of two-dimensional images of a microbubble oscillation affected by a 2.25-MHz center frequency pulse ultrasound over 10 nanoseconds. (b) Radius-time image of a microbubble oscillation and a distance-time image of a single line through the center of the microbubble oscillation for characterization of the effect of ultrasound on the microbubble. Reproduced from Ferrara et al. [21] with permission.

5.7.4 Acoustic detection of bubbles (active and passive imaging)

An increasing number of ultrasound therapies are trying to harness the potential benefits of cavitation, both with or without intravascular ultrasound contrast agents. In order to precisely guide therapy at the focus and avoid undesirable cavitation events elsewhere within the beam path, cavitation events must be detected and mapped. Magnetic resonance imaging (MRI) can be used for anatomical targeting but is not capable of directly monitoring the effect of cavitation. In addition, cavitation does not necessarily only have a thermal effect and may happen on a very short timescale and therefore magnetic resonance thermometry is not sufficient [114]. Efforts are being made to detect cavitation events by ultrasound. Acoustic detection methods rely on acoustic emission created from cavitation bubbles. When a microbubble is affected by an acoustic field, two acoustic emissions are generated by the bubble: one when the bubble is hit by the acoustic wave and one when the bubble collapses. This unique signature is called “double-bang” and is used for acoustic detection of microbubbles. This method is powerful because it can

be used *in vivo* (living subject). In this method, the sound waves are sent toward the cavitation field and then the sound reflections from the bubbles are picked up. Acoustic detection is usually performed either as active cavitation detection (ACD) or passive cavitation detection (PCD) [115-117]. In ACD, one transducer sends the ultrasound wave toward the cavitation field and another transducer picks up sound reflections from cavitation bubbles, while PCD involves one or more receiving transducers for the double-bang induced acoustic emissions from cavitation bubbles [1]. In dual PCD, it is possible to use two receiving transducers and coincidentally detect a small and discrete cavitation field volume where the transducers intersect [118]. Both ACD and PCD are described in more detail elsewhere [116, 117]. In many thermal therapy applications of ultrasound where cavitation is unwanted, such a system may be used to record the broadband emissions related to inertial cavitation in order to terminate them before inadvertent tissue injury. Such a clinical ultrasound system is now commercially available (ExAblate®, Insightec, Haifa, Israel). Similar systems may be also used to monitor the broadband and harmonic emissions from the desired cavitation or intravascular ultrasound contrast agents. Real-time adjustments to the transmitted acoustic power can be performed with post-processing of signals to obtain a specific treatment effect [114]. In initial work by Hockman et al., cavitation-enhanced thermal lesioning was tested in agar gel and the process controlled using a single passive cavitation detector [119]. Passive cavitation mapping relies upon the scattering of the irradiation field by the bubble clouds, and its use to guide therapy is still in its early stages. More passive cavitation mapping systems with slightly higher coverage have been evaluated *in vitro* using multi elements arrays [120, 121], but for clinical use the detected area of cavitation events should be correlated with histological lesions *in vivo*. Currently, passive cavitation imaging is the only clinically relevant method capable of specifically monitoring cavitation events as well as providing

information about the mode and strength of the oscillations in real time [121, 122]. In this method, which mostly relies on the formation of diverging pressure waves from oscillating bubbles at frequencies different than focused ultrasound device, the final two- or three-dimensional image of the cavitation bubbles (source of emission) can be estimated through back-propagation. The application of this imaging method within a tissue phantom and an *in vitro* flow phantom was described in studies by Gyongy and Coussios [121] and Haworth et al. [122], respectively.

The size of the initial cavitation bubble and the sonic amplitude of the equipment that produced the cavitation bubbles affect the timing and amplitude of cavitation bubble emissions. Therefore, although acoustic detection is not able to provide information on the number and size of bubbles (this method does not image the bubbles), this method provides valuable data that can be helpful in characterizing the acoustic intensity of ultrasound therapeutic equipment (such as a lithotripter or HIFU device) in the body as well as analyzing the environment and dynamics of the cavitation field [102, 118, 94].

In 1996, Christy et al. reported the first direct evidence of *in vivo* cavitation from diagnostic ultrasound pulses [86]. They employed an ACD to detect short-lived cavitation in rat lung exposed to the output of a clinical diagnostic scanner (5 MHz) to identify the cause of damage. They reported observing the 30-MHz interrogating signal scattered by the short-lived bubble as a direct indication of cavitation. They reported that the bubble complex existed for a period of 1 μs, the same as the 5-MHz Doppler pulse duration.

There is a high demand for detection of cavitation occurrence in kidney tissue, as it is a critical step toward determining the mechanisms of tissue injury in shock wave lithotripsy. Both B-mode ultrasound [123, 124] and focused, single-element, passive receivers [125, 102] have been

studied to establish direct evidence of cavitation within the kidney. However, it not possible when using one transducer to differentiate between the occurrence of cavitation within kidney parenchyma and that in the fluid spaces of the collecting system [118]. Bailey et al. developed a cavitation detection system in which dual passive receivers and B-mode ultrasound were coaligned with the focal point of a Dornier HM3 lithotripter to interrogate cavitation occurrence within the renal parenchyma as well as in the collecting system during lithotripsy [87]. Their study provided direct evidence of cavitation occurrence in the renal parenchyma. Monitoring of thermal lesioning with B-mode ultrasound requires interleaving with the treatment beam. It typically displays a hyperechoic area secondary to bubble formation, but these bubbles may be induced through boiling of the tissues and are often undesirable because scattering from the larger bubbles can extend the area of coagulation into the prefocal zone [126].

Ultrasound-guided localized detection of cavitation during lithotripsy has been also studied *in vivo* by a dual passive cavitation detection (DPCD) system in pig kidney [127]. The cavitation appeared as a hyperecho on the B-mode image of the kidney. Following imaging, dissection of the kidney revealed a V-shaped lesion created by the transducer.

Measurement techniques currently used to measure key acoustic output and exposure parameters such as cavitation that might be relevant to biological acoustic effects are performed in water. The acoustic properties of the water medium are very different from those of tissue [128]. Therefore, estimation of *in situ* ultrasound exposure at a site of interest within the patient is very difficult [90].

5.8 Scattering methods

5.8.1 Laser scattering technique

Another method of measuring cavitation is laser scattering of single bubbles, in which the dynamics of a single bubble of spherical shape can be very precisely measured [93]. In this technique, a laser beam illuminates the bubble, and a photodetector collects the scattered light from the bubble. For a single spherical-shaped bubble, the amplitude of the scattered light changes predictably with the radius of the bubble. In this method, most of the temporal and spatial scales related to the dynamics of a cavitation bubble can be captured. However, there are several restrictions related to this method: the volume of the sample is very small; the method requires unrestricted visual access at high magnification; and the theory behind this method that is applied to determine the actual bubble size is based on assumption of a single spherical-shaped bubble [1]. Therefore, this method is not able to give qualitative information about either bubble clouds or non-spherical bubbles produced in clinical applications of ultrasound, such as lithotripsy and HIFU [1].

5.8.2 Synchrotron X-ray imaging technique

Another recent attempt to study and directly visualize microbubbles or ultrasound-induced cavitation bubbles uses synchrotron X-ray imaging. Among the different synchrotron X-ray imaging techniques, X-ray phase contrast imaging (PCI) and analyzer based imaging (ABI) have shown potential for detection of microbubbles. In ABI, which is a phase-sensitive imaging technique, a very bright and highly collimated X-ray beam is sent toward the cavitation field where small structures such as microbubbles will refract and scatter the X-rays through small angles. Using ABI, these small angles can create contrast based on the very narrow reflectivity curve of the analyzer crystal. The refracted and scattered X-ray beams are collected at the

detector behind the sample. This technique is also capable of *in vivo* detection of microbubbles deep in tissue. The advantage of using an X-ray technique such as ABI is that the microbubble properties can be visualized *in vivo* without any effect of the X-rays on the bubbles or vice versa. In 2010, Arfelli et al. studied the feasibility of visualizing the microbubbles as contrast agents using ABI [129]. Microbubble contrast agents commonly used to improve ultrasound imaging are gas-filled microbubbles with shells composed of albumin, galactose, lipids, or polymers [130]. They contain either air or perfluorocarbon gas, and are stable for several minutes. These microbubbles are administered intravascularly and are sized to pass intact through the smallest vascular components. The ideal diameter of microbubble contrast agents is between 2 and 8 μm, which is smaller than red blood cells. These microbubbles are invisible in conventional X-ray absorption techniques. [129]. Arfelli and colleagues evaluated the possibility of visualizing two different microbubble contrast agents commonly used in clinical ultrasound examination (Levovist® and OptisonTM) in sizes ranges between 1 and 8 μm using ABI [129]. In their experiments, different custom-made phantoms based on microbubble contrast agents were prepared to study the potential of scattering-based contrast agents using ABI. They reported that ABI demonstrated high visibility of the details with stronger contrast than normal X-ray absorption techniques. On the other hand, because microbubbles contrast agents can act as an X-ray lens, with individual microbubbles refracting and a population of them scattering the X-rays, PCI was considered a potential synchrotron based X-ray imaging technique for detection of microbubbles by Millard et al. [131]. They developed and validated a model that enables quantification of microbubble concentration for both phase-retrieved images achieved by processing multiple frames and also by “single-shot” images. Their validation was based on ABI with straightforward extension to other phase-based modalities. Millard et al. also studied the

potential of X-ray phase contrast imaging as a functional modality through the use of microbubble contrast agents [131]. In their experiment, imaging the targeted microbubbles injected into the circulatory system was performed by collecting a sequence of X-ray dark field images for varying concentrations of microbubbles flowing through a tube. They reduced the microbubble concentration and acquired images continuously to study the possibility of using PCI as a modality for dynamic functional imaging of microbubbles, enabling quantification of microbubble concentration in a given volume. Their work demonstrated the ability of PCI to quantitatively monitor the concentration of a microbubble suspension and provided the basis for a dynamic imaging technique. All of these studies focused on visualization and monitoring exogenous microbubbles contrast agents that usually contain either air or perfluorocarbon gas with premade shells and have prolonged longevity because of their low solubility (they are stable up to several minutes). Recently, another study attempted to use an ABI modality to visualize microbubbles/ultrasound-induced cavitation bubbles (endogenous microbubbles) at the biomedical imaging and therapy (BMIT) beamline at the Canadian Light Source (CLS). Direct visualization of ultrasound-induced cavitation bubbles was achieved at 20 kHz and 130 W [132] and at a therapeutic clinical system level of 0.88 MHz and 14 W [133]. Figure 5-6a shows the spatial structural pattern of ultrasound-induced cavitation bubbles from a therapeutic clinical system using the ABI technique. The cavitation bubbles appear in a periodic pattern and the distance between two consecutive parallel lines of the pattern (Figure 5-6b) was measured as 0.99 mm. This work demonstrated that ABI has significant utility with respect to detecting and visualizing microbubbles/cavitation bubbles.

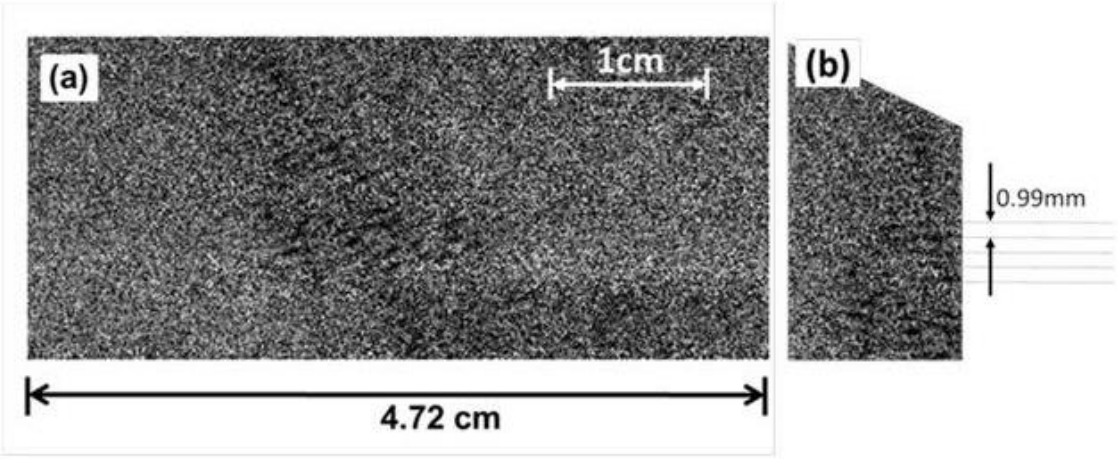

Figure 5-6 (a) ABI of the whole ultrasound beam of a therapeutic ultrasound system at 0.8835 MHz and 14 W and (b) the sequence and location of cavitation bubbles, with approximately the same interval between sequences. From Izadifar et al. [133]

Although this technique is not capable of giving information about the dynamics, size, or behavior of a single bubble, it provides valuable data about the qualitative dynamics of the microbubbles in the cavitation field (the location of microbubble formation or their existence). In the next phase of study by the authors, ABI will be investigated in tissue toward achieving the goal of applying this imaging modality for characterizing and analyzing the environment and dynamics of the cavitation field *in vivo*. A comparison of different imaging methods for visualizing microbubbles in terms of practical advantages and disadvantages is given in Table 5-1.

Table 5-1 Advantages and disadvantages of different imaging modalities for visualizing microbubbles. (-) indicates the inability or limitation of the technique and (+) indicates the capability of each listed assessment capability in detection modalities.

Imaging modalities	In vivo	In vitro	Dynamic detection	Passive detection *	Sample volume independent	Sample area independent	Qualitative assessment
High-speed photography	–	+	+	+	–	–	–
Laser scattering	–	+	+	+	–	–	–
Chemical and physical methods	–	+	–	+	+	+	–
Acoustic detection	+	+	–	–	+	+	+
Synchrotron X-ray detection technique	+	+	–	+	+	+	+

- Passive detection refers to an imaging technique that can detect microbubbles without disturbing the cavitation process and/ or microbubbles

5.9 Summary and recommendations for future research

Advances in diagnostic ultrasound imaging have expanded its use to obstetrics and fetal, embryo, or follicle development imaging. In recent decades, large numbers of fetuses have been scanned on a routine basis. Furthermore, the ability of ultrasound to penetrate deep into soft tissue at low frequencies (0.7-3.3 MHz) has prompted its use for non-invasive therapies such as hyperthermia and extracorporeal shock wave lithotripsy. Although the therapeutic and imaging mechanisms of ultrasound are based on the interaction of sound waves with tissue, cavitation can also occur during ultrasound imaging and therapy and result in hazardous bioeffects on tissues. It is essential to conduct fundamental cavitation studies to identify the threshold parameters of bubble formation and collapse that give rise to bioeffects. These findings may improve standards of ultrasound safety for a range of therapeutic and diagnostic applications, such as fetal and embryo imaging. High levels of ultrasound exposure have well-recognized acute harmful effects

(measures and guidelines exist for medical uses to avoid these). At lower levels of exposure, especially diagnostic ultrasound levels, there is no established evidence of specific hazards; however, few data are available to confirm this, especially over the long term. This concern has been also stated in the report of the advisory group on non-ionizing radiation [90]. In addition, microbubbles and cavitation are playing increasingly important roles in clinical applications of both diagnostic and therapeutic ultrasound. Microbubbles have been used as contrast agents in clinics for decades. They have also been developed as vehicles loaded with therapeutic agents for drug delivery and gene therapy. These vehicles are traced to the target site using diagnostic ultrasound [134]. The use of microbubbles in the future for drug/gene delivery is promising. Also, controlled cavitation is being studied as a means to enhance the speed and efficacy of treatment in HIFU surgery and lithotripsy.

Monitoring the cavitation/microbubbles in different tissues *in vivo* for different treatment conditions will give more insight into the conditions under which ultrasound can be used safely. Furthermore, for high power devices used in therapeutic and surgical applications in which the purpose is to deliver high-intensity ultrasound to a target tissue, the concerns apart from safety are mainly with respect to accurate targeting of the desired target volume to avoid damaging other tissues. Detecting the existence and location of microbubbles/cavitation bubbles in tissue will provide more insight for more precise application of therapeutic ultrasounds such as HIFU, lithotripsy, and drug/gene delivery. Various imaging techniques have been evaluated for detection of microbubbles/cavitation bubbles. Each imaging technique has advantages and disadvantages for studying microbubble behavior. However, their application *in vivo* and particularly deep in tissue for locating microbubbles in the human body is an aspect of interest for future clinical study. Among the different microbubble detection techniques, acoustic and X-

ray detection techniques have advantages for use *in vivo* and particularly in the human body. Also, X-ray imaging techniques can detect microbubbles without disturbing them, which is not the case with acoustic detection methods such as ACD and PCD.

The ABI technique has shown promise for direct visualization of cavitation bubbles deep in tissue through the use of a very bright and collimated X-ray beam from a synchrotron. This imaging technique is under study by the authors at the BMIT beamline at the CLS [132]. ABI has a significant and demonstrated ability to image structures that feature interfaces between materials of different density, such as that between air and water in a bubble. The advantage of using an X-ray technique is the ability to visualize the cavitation bubbles/microbubbles in an optically opaque material, such as tissue, without any physical interaction with the bubbles.

There is no doubt that continuous discoveries and developments in microbubble detection modalities will lead to safer and more efficient therapeutic and diagnostic equipment and also more precise microbubble applications in medicine.

5.10 References

1. Cleveland RO, Mc Ateer JA: *Extracorporeal shock wave lithotripsy: The physics of shock wave lithotripsy. In: Smith's Textbook on Endourology.* Ontario, Canada: B C Decker; 2012.
2. Frenkel J: *Kinetic theory of liquids.* New York: Dover; 1955.
3. Skripov VP, Kondor R, Slutzkin D: *Metastable liquids.* Wiley; 1974.
4. Holland CK, Deng CX, Apfel RE, Alderman JL, Fernandez LA, Taylor KJ: **Direct evidence of cavitation in vivo from diagnostic ultrasound.** *Ultrasound Med Biol* 1996, **22:**917-925.
5. Miller DL, Smith NB, Bailey MR, Czarnota GJ, Hynynen K, Makin IR: **Overview of therapeutic ultrasound applications and safety considerations.** *J Ultrasound Med* 2012, **31:**623-634.
6. Atchley AA, Prosperetti A: **The crevice model of bubble nucleation.** *The Journal of the Acoustical Society of America* 1989, **86:**1065-1084.
7. **Ultrasonics – Number and Size of Cavitation Bubbles** [http://www.ctgclean.com/tech-blog/2011/12/ultrsonics-number-and-size-of-cavitation-bubbles/.]
8. Leong T, Ashokkumar M, Kentish S: **The fundamentals of power ultrasound—a review.** *Acoust Aust* 2011, **39:**54-63.
9. Church CC, Carstensen EL: **"Stable" inertial cavitation.** *Ultrasound in medicine & biology* 2001, **27:**1435-1437.
10. Neppiras EA: **Acoustic cavitation.** *Physics reports* 1980, **61:**159-251.
11. Luque-García JL, Luque de Castro MD: **Ultrasound: a powerful tool for leaching.** *TrAC Trends in Analytical Chemistry* 2003, **22:**41-47.
12. Suslick K: **The yearbook of science and the future.** *Encyclopedia Britannica, Chicago* 1994, **138**.
13. Rayleigh L: **VIII. On the pressure developed in a liquid during the collapse of a spherical cavity.** *The London, Edinburgh, and Dublin Philosophical Magazine and Journal of Science* 1917, **34:**94-98.
14. Noltingk BE, Neppiras EA: **Cavitation produced by ultrasonics.** *Proceedings of the Physical Society Section B* 1950, **63:**674.
15. Flint EB, Suslick KS: **The temperature of cavitation.** *Science* 1991, **253:**1397-1399.
16. Margulis M, Maximenko N: **Advances in Sonochemistry.** *Greenwich Connection, Elsevier, JA, London* 1990**:**49.
17. Plesset M: **The dynamics of cavitation bubbles.** *Journal of applied mechanics* 1949, **16:**277-282.
18. Apfel RE, Holland CK: **Gauging the likelihood of cavitation from short-pulse, low-duty cycle diagnostic ultrasound.** *Ultrasound Med Biol* 1991, **17:**179-185.
19. Holt RG, Roy RA: **Measurements of bubble-enhanced heating from focused, MHz-frequency ultrasound in a tissue-mimicking material.** *Ultrasound Med Biol* 2001, **27:**1399-1412.
20. Nyborg WL: *Acoustic streaming*

San Diego,CA: Academic Press; 1998.

21. Ferrara K, Pollard R, Borden M: **Ultrasound microbubble contrast agents: fundamentals and application to gene and drug delivery.** *Annu Rev Biomed Eng* 2007, **9:**415-447.

22. Dijkmans PA, Juffermans LJ, Musters RJ, van Wamel A, ten Cate FJ, van Gilst W, Visser CA, de Jong N, Kamp O: **Microbubbles and ultrasound: from diagnosis to therapy.** *Eur J Echocardiogr* 2004, **5:**245-256.
23. Skyba DM, Price RJ, Linka AZ, Skalak TC, Kaul S: **Direct in vivo visualization of intravascular destruction of microbubbles by ultrasound and its local effects on tissue.** *Circulation* 1998, **98:**290-293.
24. Matlaga BR, McAteer JA, Connors BA, Handa RK, Evan AP, Williams JC, Lingeman JE, Willis LR: **Potential for cavitation-mediated tissue damage in shockwave lithotripsy.** *Journal of Endourology* 2008, **22:**121-126.
25. Lawrie A, Brisken AF, Francis SE, Tayler DI, Chamberlain J, Crossman DC, Cumberland DC, Newman CM: **Ultrasound enhances reporter gene expression after transfection of vascular cells in vitro.** *Circulation* 1999, **99:**2617-2620.
26. Stride E, Saffari N: **On the destruction of microbubble ultrasound contrast agents.** *Ultrasound in Medicine and Biology* 2003, **29:**563-573.
27. Tachibana K, Tachibana S: **The use of ultrasound for drug delivery.** *Echocardiography-a Journal of Cardiovascular Ultrasound and Allied Techniques* 2001, **18:**323-328.
28. Basta G, Venneri L, Lazzerini G, Pasanisi E, Pianelli M, Vesentini N, Del Turco S, Kusmic C, Picano E: **In vitro modulation of intracellular oxidative stress of endothelial cells by diagnostic cardiac ultrasound.** *Cardiovasc Res* 2003, **58:**156-161.
29. Unger EC, Hersh E, Vannan M, Matsunaga TO, McCreery M: **Local drug and gene delivery through microbubbles.** *Progress in Cardiovascular Diseases* 2001, **44:**45-54.
30. Wu JR: **Temperature rise generated by ultrasound in the presence of contrast agent.** *Ultrasound in Medicine and Biology* 1998, **24:**267-274.
31. Miller DL, Gies RA: **Enhancement of ultrasonically-induced hemolysis by perfluorocarbon-based compared to air-based echo-contrast agents.** *Ultrasound in Medicine and Biology* 1998, **24:**285-292.
32. Poliachik SL, Chandler WL, Mourad PD, Bailey MR, Bloch S, Cleveland RO, Kaczkowski P, Keilman G, Porter T, Crum LA: **Effect of high-intensity focused ultrasound on whole blood with and without microbubble contrast agent.** *Ultrasound in Medicine and Biology* 1999, **25:**991-998.
33. Gramiak R, Shah PM: **Echocardiography of the aortic root.** *Invest Radiol* 1968, **3:**356-366.
34. Chahal NS, Senior R: **Clinical applications of left ventricular opacification.** *JACC Cardiovasc Imaging* 2010, **3:**188-196.
35. Nanda N, Schlief R, Goldberg BB: *Advances in echo imagingusing contrast enhancement.* 2nd edn. Dordrecht: The Netherlands: Kluwer Academic 1997.
36. Mayer S, Grayburn PA: **Myocardial contrast agents: recent advances and future directions.** *Prog Cardiovasc Dis* 2001, **44:**33-44.
37. Bouakaz A, de Jong N, Cachard C, Jouini K: **On the effect of lung filtering and cardiac pressure on the standard properties of ultrasound contrast agent.** *Ultrasonics* 1998, **36:**703-708.
38. Mulvagh SL, DeMaria AN, Feinstein SB, Burns PN, Kaul S, Miller JG, Monaghan M, Porter TR, Shaw LJ, Villanueva FS, Am Soc Echocardiography Task F: **Contrast echocardiography: Current and future applications.** *Journal of the American Society of Echocardiography* 2000, **13:**331-342.

39. Chomas JE, Dayton P, May D, Ferrara K: **Threshold of fragmentation for ultrasonic contrast agents.** *J Biomed Opt* 2001, **6:**141-150.
40. Burns PN, Simpson DH, Averkiou MA: **Nonlinear imaging.** *Ultrasound in medicine & biology* 2000, **26:**S19-S22.
41. Yang WT, Tse GM, Lam PK, Metreweli C, Chang J: **Correlation between color power Doppler sonographic measurement of breast tumor vasculature and immunohistochemical analysis of microvessel density for the quantitation of angiogenesis.** *J Ultrasound Med* 2002, **21:**1227-1235.
42. Tang J, Li S, Li J, Zhang Y, Li X, Dong B, Shi H, Zhang G: **Evaluation of the effect of protamine on human prostate carcinoma PC-3m using contrast enhanced Doppler ultrasound.** *The Journal of urology* 2003, **170:**611-614.
43. Lucidarme O, Nguyen T, Kono Y, Corbeil J, Choi S-H, Varner J, Mattrey RF: **Angiogenesis model for ultrasound contrast research: exploratory study1.** *Academic radiology* 2004, **11:**4-12.
44. Forsberg F, Dicker AP, Thakur ML, Rawool NM, Liu J-b, Shi WT, Nazarian LN: **Comparing contrast-enhanced ultrasound to immunohistochemical markers of angiogenesis in a human melanoma xenograft model: preliminary results.** *Ultrasound in medicine & biology* 2002, **28:**445-451.
45. Liang H, Tang J, Halliwell M: **Sonoporation, drug delivery, and gene therapy.** *Proceedings of the Institution of Mechanical Engineers, Part H: Journal of Engineering in Medicine* 2010, **224:**343-361.
46. Collis J, Manasseh R, Liovic P, Tho P, Ooi A, Petkovic-Duran K, Zhu Y: **Cavitation microstreaming and stress fields created by microbubbles.** *Ultrasonics* 2010, **50:**273-279.
47. Wu J, Ross JP, Chiu J-F: **Reparable sonoporation generated by microstreaming.** *The Journal of the Acoustical Society of America* 2002, **111:**1460-1464.
48. Porter TR, Hiser WL, Kricsfeld D, Deligonul U, Xie F, Iversen P, Radio S: **Inhibition of carotid artery neointimal formation with intravenous microbubbles.** *Ultrasound Med Biol* 2001, **27:**259-265.
49. Price RJ, Kaul S: **Contrast ultrasound targeted drug and gene delivery: an update on a new therapeutic modality.** *J Cardiovasc Pharmacol Ther* 2002, **7:**171-180.
50. Ng KY, Liu Y: **Therapeutic ultrasound: Its application in drug delivery.** *Medicinal Research Reviews* 2002, **22:**204-223.
51. Lindner JR: **Evolving applications for contrast ultrasound.** *American Journal of Cardiology* 2002, **90:**72J-80J.
52. Unger EC, Matsunaga TO, McCreery T, Schumann P, Sweitzer R, Quigley R: **Therapeutic applications of microbubbles.** *European Journal of Radiology* 2002, **42:**160-168.
53. Lindner JR, Kaul S: **Delivery of drugs with ultrasound.** *Echocardiography-a Journal of Cardiovascular Ultrasound and Allied Techniques* 2001, **18:**329-337.
54. Tartis MS, McCallan J, Lum AF, LaBell R, Stieger SM, Matsunaga TO, Ferrara KW: **Therapeutic effects of paclitaxel-containing ultrasound contrast agents.** *Ultrasound Med Biol* 2006, **32:**1771-1780.
55. Chen S, Ding J-h, Bekeredjian R, Yang B-z, Shohet RV, Johnston SA, Hohmeier HE, Newgard CB, Grayburn PA: **Efficient gene delivery to pancreatic islets with**

ultrasonic microbubble destruction technology. *Proceedings of the National Academy of Sciences* 2006, **103:**8469-8474.
56. Hauff P, Seemann S, Reszka R, Schultze-Mosgau M, Reinhardt M, Buzasi T, Plath T, Rosewicz S, Schirner M: **Evaluation of Gas-filled Microparticles and Sonoporation as Gene Delivery System: Feasibility Study in Rodent Tumor Models 1.** *Radiology* 2005, **236:**572-578.
57. Price RJ, Skyba DM, Kaul S, Skalak TC: **Delivery of colloidal particles and red blood cells to tissue through microvessel ruptures created by targeted microbubble destruction with ultrasound.** *Circulation* 1998, **98:**1264-1267.
58. Miller DL, Quddus J: **Diagnostic ultrasound activation of contrast agent gas bodies induces capillary rupture in mice.** *Proceedings of the National Academy of Sciences* 2000, **97:**10179-10184.
59. Bekeredjian R, Chen S, Frenkel PA, Grayburn PA, Shohet RV: **Ultrasound-targeted microbubble destruction can repeatedly direct highly specific plasmid expression to the heart.** *Circulation* 2003, **108:**1022-1026.
60. Frenkel PA, Chen S, Thai T, Shohet RV, Grayburn PA: **DNA-loaded albumin microbubbles enhance ultrasound-mediated transfection in vitro.** *Ultrasound Med Biol* 2002, **28:**817-822.
61. Shohet RV, Chen S, Zhou YT, Wang Z, Meidell RS, Unger RH, Grayburn PA: **Echocardiographic destruction of albumin microbubbles directs gene delivery to the myocardium.** *Circulation* 2000, **101:**2554-2556.
62. Villanueva FS, Jankowski RJ, Klibanov S, Pina ML, Alber SM, Watkins SC, Brandenburger GH, Wagner WR: **Microbubbles targeted to intercellular adhesion molecule-1 bind to activated coronary artery endothelial cells.** *Circulation* 1998, **98:**1-5.
63. Weller GE, Lu E, Csikari MM, Klibanov AL, Fischer D, Wagner WR, Villanueva FS: **Ultrasound imaging of acute cardiac transplant rejection with microbubbles targeted to intercellular adhesion molecule-1.** *Circulation* 2003, **108:**218-224.
64. Ellegala DB, Leong-Poi H, Carpenter JE, Klibanov AL, Kaul S, Shaffrey ME, Sklenar J, Lindner JR: **Imaging tumor angiogenesis with contrast ultrasound and microbubbles targeted to alpha(v)beta3.** *Circulation* 2003, **108:**336-341.
65. Lindner JR, Coggins MP, Kaul S, Klibanov AL, Brandenburger GH, Ley K: **Microbubble persistence in the microcirculation during ischemia/reperfusion and inflammation is caused by integrin- and complement-mediated adherence to activated leukocytes.** *Circulation* 2000, **101:**668-675.
66. Lindner JR, Dayton PA, Coggins MP, Ley K, Song J, Ferrara K, Kaul S: **Noninvasive imaging of inflammation by ultrasound detection of phagocytosed microbubbles.** *Circulation* 2000, **102:**531-538.
67. Christiansen JP, Leong-Poi H, Klibanov AL, Kaul S, Lindner JR: **Noninvasive imaging of myocardial reperfusion injury using leukocyte-targeted contrast echocardiography.** *Circulation* 2002, **105:**1764-1767.
68. Schumann PA, Christiansen JP, Quigley RM, McCreery TP, Sweitzer RH, Unger EC, Lindner JR, Matsunaga TO: **Targeted-microbubble binding selectively to GPIIb IIIa receptors of platelet thrombi.** *Investigative Radiology* 2002, **37:**587-593.

69. **Effectiveness of intravenous thrombolytic treatment in acute myocardial infarction. Gruppo Italiano per lo Studio della Streptochinasi nell'Infarto Miocardico (GISSI).** *Lancet* 1986, **1:**397-402.
70. Akiyama M, Ishibashi T, Yamada T, Furuhata H: **Low-frequency ultrasound penetrates the cranium and enhances thrombolysis in vitro.** *Neurosurgery* 1998, **43:**828-832.
71. Harpaz D, Chen XC, Francis CW, Marder VJ, Meltzer RS: **ULTRASOUND ENHANCEMENT OF THROMBOLYSIS AND REPERFUSION INVITRO.** *Journal of the American College of Cardiology* 1993, **21:**1507-1511.
72. Kornowski R, Meltzer RS, Chernine A, Vered Z, Battler A: **Does external ultrasound accelerate thrombolysis? Results from a rabbit model.** *Circulation* 1994, **89:**339-344.
73. Larsson J, Carlson J, Olsson SB: **Ultrasound enhanced thrombolysis in experimental retinal vein occlusion in the rabbit.** *British Journal of Ophthalmology* 1998, **82:**1438-1440.
74. Lauer CG, Burge R, Tang DB, Bass BG, Gomez ER, Alving BM: **Effect of ultrasound on tissue-type plasminogen activator-induced thrombolysis.** *Circulation* 1992, **86:**1257-1264.
75. Luo H, Nishioka T, Fishbein MC, Cercek B, Forrester JS, Kim CJ, Berglund H, Siegel RJ: **Transcutaneous ultrasound augments lysis of arterial thrombi in vivo.** *Circulation* 1996, **94:**775-778.
76. Riggs PN, Francis CW, Bartos SR, Penney DP: **Ultrasound enhancement of rabbit femoral artery thrombolysis.** *Cardiovasc Surg* 1997, **5:**201-207.
77. Rassin T, Desmet W, Piessens J, Rosenschein U: **Ultrasound thrombolysis in stent thrombosis.** *Catheter Cardiovasc Interv* 2000, **51:**332-334.
78. Porter TR, Xie F: **Ultrasound, microbubbles, and thrombolysis.** *Progress in Cardiovascular Diseases* 2001, **44:**101-110.
79. Tachibana K, Tachibana S: **Albumin microbubble echo-contrast material as an enhancer for ultrasound accelerated thrombolysis.** *Circulation* 1995, **92:**1148-1150.
80. Kondo I, Mizushige K, Ueda T, Masugata H, Ohmori K, Matsuo H: **Histological observations and the process of ultrasound contrast agent enhancement of tissue plasminogen activator thrombolysis with ultrasound exposure.** *Jpn Circ J* 1999, **63:**478-484.
81. Nishioka T, Luo H, Fishbein MC, Cercek B, Forrester JS, Kim CJ, Berglund H, Siegel RJ: **Dissolution of thrombotic arterial occlusion by high intensity, low frequency ultrasound and dodecafluoropentane emulsion: An in vitro and in vivo study.** *Journal of the American College of Cardiology* 1997, **30:**561-568.
82. Porter TR, LeVeen RF, Fox R, Kricsfeld A, Xie F: **Thrombolytic enhancement with perfluorocarbon-exposed sonicated dextrose albumin microbubbles.** *American Heart Journal* 1996, **132:**964-968.
83. Mizushige K, Kondo I, Ohmori K, Hirao K, Matsuo H: **Enhancement of ultrasound-accelerated thrombolysis by echo contrast agents: Dependence on microbubble structure.** *Ultrasound in Medicine and Biology* 1999, **25:**1431-1437.
84. Kobayashi N, Yasu T, Yamada S, Kudo N, Kuroki M, Kawakami M, Miyatake K, Saito M: **Endothelial cell injury in venule and capillary induced by contrast ultrasonography.** *Ultrasound in Medicine and Biology* 2002, **28:**949-956.

85. Cootney RW: **Ultrasound imaging: principles and applications in rodent research.** *Ilar Journal* 2001, **42:**233-247.
86. Holland CK, Deng CX, Apfel RE, Alderman JL, Fernandez LA, Taylor KJ: **Direct evidence of cavitation in vivo from diagnostic ultrasound.** *Ultrasound in medicine & biology* 1996, **22:**917-925.
87. Bailey MR, Pishchalnikov YA, Sapozhnikov OA, Cleveland RO, McAteer JA, Miller NA, Pishchalnikova IV, Connors BA, Crum LA, Evan AP: **Cavitation detection during shock-wave lithotripsy.** *Ultrasound Med Biol* 2005, **31:**1245-1256.
88. Leighton TG: *The Acoustic Bubble.* San Diego, CA: Academic Press; 1994.
89. **Health effects of exposure to ultrasound and infrasound.** In *Report of the independent Advisory Group on Non-ionising Radiation*: Health Protection Agency; 2010.
90. radiation Tiagon-i: **Health effects of exposure to ultrasound and infrasound.** In *documents of the health protection agency, radiation, chemical and environmental hazards*; 2010.
91. Carmichael AJ, Mossoba MM, Riesz P, Christman CL: **Free radical production in aqueous solutions exposed to simulated ultrasonic diagnostic conditions.** *Ultrasonics, Ferroelectrics, and Frequency Control, IEEE Transactions on* 1986, **33:**148-155.
92. Crum L, Fowlkes J: **Acoustic cavitation generated by microsecond pulses of ultrasound.** *Nature* 1986, **319:**52-54.
93. Matula TJ, Hilmo PR, Bailey MR, Crum LA: **In vitro sonoluminescence and sonochemistry studies with an electrohydraulic shock-wave lithotripter.** *Ultrasound Med Biol* 2002, **28:**1199-1207.
94. Coleman AJ, Whitlock M, Leighton T, Saunders JE: **The spatial distribution of cavitation induced acoustic emission, sonoluminescence and cell lysis in the field of a shock wave lithotripter.** *Phys Med Biol* 1993, **38:**1545-1560.
95. Coleman AJ, Saunders JE, Crum LA, Dyson M: **Acoustic cavitation generated by an extracorporeal shockwave lithotripter.** *Ultrasound Med Biol* 1987, **13:**69-76.
96. Bailey MR, Blackstock DT, Cleveland RO, Crum LA: **Comparison of electrohydraulic lithotripters with rigid and pressure-release ellipsoidal reflectors. I. Acoustic fields.** *J Acoust Soc Am* 1998, **104:**2517-2524.
97. Lifshitz DA, Williams Jr JC, Sturtevant B, Connors BA, Evan AP, McAteer JA: **Quantitation of shock wave cavitation damage in vitro.** *Ultrasound in Medicine & Biology* 1997, **23:**461-471.
98. Pye SD, Dineley JA: **Characterization of cavitational activity in lithotripsy fields using a robust electromagnetic probe.** *Ultrasound Med Biol* 1999, **25:**451-471.
99. Atchley A, Frizzell L, Apfel R, Holland C, Madanshetty S, Roy R: **Thresholds for cavitation produced in water by pulsed ultrasound.** *Ultrasonics* 1988, **26:**280-285.
100. Philipp A, Delius M, Scheffczyk C, Vogel A, Lauterborn W: **Interaction of lithotripter-generated shock waves with air bubbles.** *The Journal of the Acoustical Society of America* 1993, **93:**2496-2509.
101. Sass W, Matura E, Dreyer H, Folberth W, J. S: **Lithotripsy-mechanismsof the fragmentation process with focussed shock waves.** *Electromedica* 1993, **61:**2-12.
102. Zhong P, Cioanta I, Cocks FH, Preminger GM: **Inertial cavitation and associated acoustic emission produced during electrohydraulic shock wave lithotripsy.** *J Acoust Soc Am* 1997, **101:**2940-2950.

103. Pishchalnikov YA, Sapozhnikov OA, Bailey MR, Williams JC, Jr., Cleveland RO, Colonius T, Crum LA, Evan AP, McAteer JA: **Cavitation bubble cluster activity in the breakage of kidney stones by lithotripter shockwaves.** *J Endourol* 2003, **17:**435-446.
104. Tomita Y, Shima A: **High-Speed Photographic Observations of Laser-Induced Cavitation Bubbles in Water.** *Acta Acustica united with Acustica* 1990, **71:**161-171.
105. Ibsen S, Benchimol M, Simberg D, Schutt C, Steiner J, Esener S: **A novel nested liposome drug delivery vehicle capable of ultrasound triggered release of its payload.** *J Control Release* 2011, **155:**358-366.
106. Ibsen S, Benchimol M, Esener S: **Fluorescent microscope system to monitor real-time interactions between focused ultrasound, echogenic drug delivery vehicles, and live cell membranes.** *Ultrasonics* 2013, **53:**178-184.
107. Zijlstra A, Janssens T, Wostyn K, Versluis M, Mertens PW, Lohse D: **High speed imaging of 1 MHz driven microbubbles in contact with a rigid wall.** In *Solid State Phenomena*. Trans Tech Publ; 2009: 7-10.
108. Chen H: **Ultra-high Speed Optical Imaging of Ultrasound-activated Microbubbles in Mesenteric Microvessels.** University of Washington, 2011.
109. Karshafian R, Bevan PD, Burns PN, Karshafian R, Samac S, Banerjee M, Bevan PD: **Ultrasound-induced uptake of different size markers in mammalian cells.** In *Ultrasonics Symposium, 2005 IEEE*; *18-21 Sept. 2005*. 2005: 13-16.
110. Ross JP, Cai X, Chiu JF, Yang J, Wu J: **Optical and atomic force microscopic studies on sonoporation.** *J Acoust Soc Am* 2002, **111:**1161-1164.
111. Zhao YZ, Luo YK, Lu CT, Xu JF, Tang J, Zhang M, Zhang Y, Liang HD: **Phospholipids-based microbubbles sonoporation pore size and reseal of cell membrane cultured in vitro.** *J Drug Target* 2008, **16:**18-25.
112. Wolfrum B, Mettin R, Kurz T, Lauterborn W: **Observations of pressure-wave-excited contrast agent bubbles in the vicinity of cells.** *Applied Physics Letters* 2002, **81:**5060-5062.
113. Morgan KE, Allen JS, Dayton PA, Chomas JE, Klibaov AL, Ferrara KW: **Experimental and theoretical evaluation of microbubble behavior: effect of transmitted phase and bubble size.** *Ultrasonics, Ferroelectrics, and Frequency Control, IEEE Transactions on* 2000, **47:**1494-1509.
114. Brahme A: *Comprehensive Biomedical Physics.* Elsevier Science; 2014.
115. Coakley W: **Acoustical detection of single cavitation events in a focused field in water at 1 MHz.** *The Journal of the Acoustical Society of America* 1971, **49:**792-801.
116. Roy RA, Madanshetty SI, Apfel RE: **An acoustic backscattering technique for the detection of transient cavitation produced by microsecond pulses of ultrasound.** *The Journal of the Acoustical Society of America* 1990, **87:**2451-2458.
117. Madanshetty SI, Roy RA, Apfel RE: **Acoustic microcavitation: its active and passive acoustic detection.** *J Acoust Soc Am* 1991, **90:**1515-1526.
118. Cleveland RO, Sapozhnikov OA, Bailey MR, Crum LA: **A dual passive cavitation detector for localized detection of lithotripsy-induced cavitation in vitro.** *J Acoust Soc Am* 2000, **107:**1745-1758.
119. Hockham N, Coussios CC, Arora M: **A real-time controller for sustaining thermally relevant acoustic cavitation during ultrasound therapy.** *Ultrasonics, Ferroelectrics, and Frequency Control, IEEE Transactions on* 2010, **57:**2685-2694.

120. Salgaonkar VA: **Passive Imaging and Measurements of Acoustic Cavitation during Ultrasound Ablation.** University of Cincinnati, 2009.
121. Gyöngy M, Coussios C-C: **Passive cavitation mapping for localization and tracking of bubble dynamics.** *The Journal of the Acoustical Society of America* 2010, **128:**EL175-EL180.
122. Haworth KJ, Mast TD, Radhakrishnan K, Burgess MT, Kopechek JA, Huang SL, McPherson DD, Holland CK: **Passive imaging with pulsed ultrasound insonations.** *J Acoust Soc Am* 2012, **132:**544-553.
123. Delius M, Gambihler S: **Sonographic imaging of extracorporeal shock wave effects in the liver and gallbladder of dogs.** *Digestion* 1992, **52:**55-60.
124. Kuwahara M, Loritani N, Kambe Kea: **Hyper-echoic region induced by focused shock waves in vitro and in vivo: Possibility of acoustic cavitation bubbles.** *Lithotripsy Stone Dis* 1989, **1:**282-288.
125. Coleman AJ, Choi MJ, Saunders JE: **Detection of acoustic emission from cavitation in tissue during clinical extracorporeal lithotripsy.** *Ultrasound Med Biol* 1996, **22:**1079-1087.
126. Coussios C, Farny C, Ter Haar G, Roy R: **Role of acoustic cavitation in the delivery and monitoring of cancer treatment by high-intensity focused ultrasound (HIFU).** *International Journal of Hyperthermia* 2007, **23:**105-120.
127. Sapozhnikov OA, Bailey MR, Crum LA, Miller NA, Cleveland RO, Pishchalnikov YA, Pishchalnikova IV, McAteer JA, Connors BA, Blomgren PM, Evan AP: **Ultrasound-guided localized detection of cavitation during lithotripsy in pig kidney in vivo.** In *Ultrasonics symposium*. 2001
128. Duck FA: **Acoustic saturation and output regulation.** *Ultrasound Med Biol* 1999, **25:**1009-1018.
129. Arfelli F, Rigon L, Menk R: **Microbubbles as x-ray scattering contrast agents using analyzer-based imaging.** *Physics in medicine and biology* 2010, **55:**1643.
130. Lindner JR: **Microbubbles in medical imaging: current applications and future directions.** *Nature Reviews Drug Discovery* 2004, **3:**527-533.
131. Millard T, Endrizzi M, Rigon L, Arfelli F, Menk R, Owen J, Stride E, Olivo A: **Quantification of microbubble concentration through x-ray phase contrast imaging.** *Applied Physics Letters* 2013, **103:**114105.
132. Izadifar Z, Belev G, Izadifar M, Izadifar Z, Chapman D: **Visualization of ultrasound induced cavitation bubbles using the synchrotron x-ray Analyzer Based Imaging technique.** *Physics in medicine and biology* 2014, **59:**7541.
133. Izadifar Z, Belev G, Babyn P, Chapman D: **Application of analyzer based X-ray imaging technique for detection of ultrasound induced cavitation bubbles from a physical therapy unit.** *Biomedical engineering online* 2015, **14:**91.
134. Stride EP, Coussios CC: **Cavitation and contrast: the use of bubbles in ultrasound imaging and therapy.** *Proc Inst Mech Eng H* 2010, **224:**171-191.

Chapter 6 Visualization of ultrasound induced cavitation bubbles using synchrotron X-ray Analyzer Based Imaging technique

"This chapter has been published as "Zahra Izadifar, George Belev, Mohammad Izadifar, Zohreh Izadifar, Dean Chapman, 2014, Visualization of ultrasound induced cavitation bubbles using the synchrotron X-ray Analyzer Based Imaging technique, *Phys Med Biol*., 59(23):7541-55. doi: 10.1088/0031-9155/59/23/7541" According to the Copyright Agreement, "the authors retain the right to include the journal article, in full or in part, in a thesis or dissertation".

6.1 Abstract

The observation of cavitation bubbles deep within tissue is very difficult. The development of a method able to probe cavitation with little concern for the location in tissues would improve the efficiency and application of ultrasound in the clinic. A synchrotron X-ray imaging technique capable of detecting cavitation bubbles induced in water by a sonochemistry system has been reported, with possible extension to study therapeutic ultrasound in tissues. In this study, two different X-ray imaging techniques (Analyzer Based Imaging (ABI) and phase contrast imaging (PCI)) were examined to detect ultrasound induced cavitation bubbles. Cavitation was not observed by PCI, however was detectable with ABI. Acoustic cavitation was imaged at six different acoustic power levels and six different locations through the acoustic beam in water at a fixed power level. The results are promising indicating its utility for cavitation studies in tissues, but time consuming which may be improved by optimization of the imaging method.

6.2 Introduction

Cavitation, known as microbubble formation and collapse, is an effect induced by ultrasound waves travelling through fluids. There are a wide variety of physical phenomena associated with

the onset of cavitation in a liquid such as luminescence, shock wave emissions, free-radicals formation, and high liquid jet speed production as a result of cavitation. Substantial injury to cells and a solid surface can occur when ultrasound induced microbubbles expand and then collapse close to cells or a solid surface. Cavitation can have hazardous bioeffects on the tissue under ultrasound therapy or imaging. Briefly, when the sound waves pass through a liquid medium at high ultrasound power, the traveling compression and rarefaction cycles create and collapse bubbles. Extreme temperature and pressure can be generated within the bubbles at the point of bubble collapse. When the collapse takes place near a solid boundary, high-speed jets of liquid are produced and driven into the surface at speeds close to 400 km/h [1], which can seriously damage the impact zone and create a newly exposed surfaces. Moreover, the high temperatures and pressures generated within the bubbles can generate highly reactive radical species that can chemically attack the surface.

The influence of cavitation on tissues has made ultrasound a potential non-invasive therapy tool for tissue fractionation and treating of benign disease and cancer [2]. Energetic microbubbles fragment tissue resulting in cellular destruction. An experimental study performed by Daniels et al. (1995) revealed damage to red blood cells during irradiation with 0.75 MHz continuous-wave ultrasound. It was found that pulsed ultrasound within the diagnostic imaging range had the ability to induce lung damage in mice [3]. Additional experiments on animals showed that ultrasound is capable of creating lesions on the lungs of pigs, mice, rabbits, rats, monkeys and dogs [4-12]. These bioeffects are mainly concerned in ultrasonography. In ultrasound therapy (i.e. high intensity focused ultrasound), gas generation caused by cavitation abruptly changes the pattern of heat transfer induced by ultrasound which results in the extension of the lesion from

the targeted area to surrounding healthy tissues [13]. These bioeffects are some examples of concern in ultrasonography and therapeutic applications of ultrasound.

The risk of ultrasound, theoretically, would depend on different factors such as: levels of acoustic intensity and frequency, duration of ultrasound exposure, and frequency of ultrasound sessions. Consequently, it is essential to conduct fundamental cavitation studies to identify the threshold ultrasound parameters causing bubble formation and collapse at different levels of frequencies and intensities. These findings may improve standards of ultrasound safety for a range of therapeutic and diagnostic applications, such as imaging susceptible fetuses and embryos. One step toward improving outcomes and safety with this equipment is to have a better understanding of cavitation bubbles, and eventually to determine the safe levels of ultrasound operation below which they are unlikely to form. Thus the goal of this study is to move toward visualization of cavitation bubbles.

So far there have been a number of techniques to measure cavitation. One of these techniques is high speed photography [14-17]. This technique is applicable for in vitro systems and it is virtually impossible to capture all the bubbles considering the range of temporal and spatial scales. Another limitation of this technique is the limited depth of field of the camera [18]. Another method of measuring cavitation is laser scattering of single bubbles. With this method, most of the temporal and spatial scales related to the dynamics of a cavitation bubble can be captured. However, this method is not able to give qualitative information about bubbles or non-spherical bubbles considering that all forms of bubbles, spherical and non-spherical, are produced in clinical application of ultrasound (such as lithotripsy and high intensity focused ultrasound). In this technique the volume of the sample is very small and also this method needs unrestricted visual access at high magnification. In addition, the theory behind this method is

only applied to spherical shape bubbles [18]. Another method of characterizing bubble dynamics is acoustic detection. A positive aspect of this method is that it can be used in vivo, however the size of the initial cavitation bubble and the amplitude of the ultrasound that produced the cavitation bubbles affect the timing and amplitude of the cavitation bubbles' emissions.

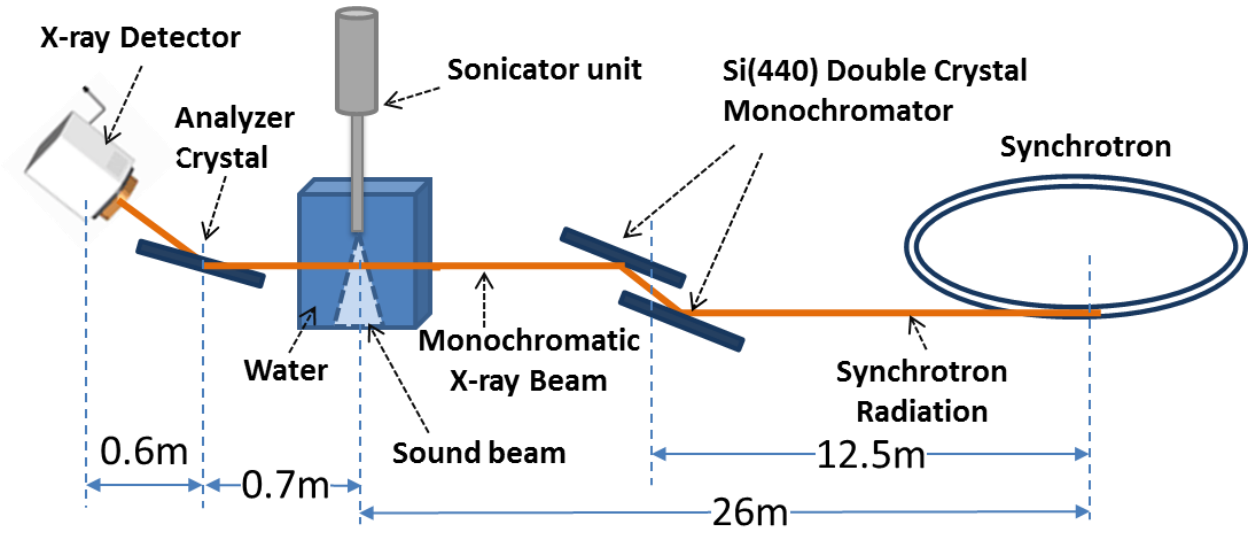

Figure 6-1 Schematic of the ABI set up at the Canadian Light Source used for imaging ultrasound induced cavitation bubbles in water.

Detecting ultrasound cavitation bubbles in vivo and in tissue can be facilitated by Analyzer Based X-ray Imaging (ABI) using a synchrotron [19]. The advantage of using an X-ray technique is that cavitation bubble properties can be visualized even in an optically opaque material, such as tissue. Therefore this method can provide information about cavitation bubbles in vivo without having any effect of X-rays on the bubbles or vice versa.

The operating frequency and acoustic intensity of ultrasound differs based on the clinical application of ultrasound. Both acoustic frequency and power of ultrasound are always considered as important factors in different applications of ultrasound. To improve the safety

level and more efficient usage of ultrasound equipment, a better understanding of the effect of ultrasound frequency and power on occurrence of cavitation is required. In order to study the effect of acoustic frequency on cavitation, a wide variety of frequencies should be investigated. In this pilot study cavitation bubbles were created by a sonochemistry device working at 20 kHz at different operating powers. This frequency was chosen as a starting point for validating the synchrotron visualization methods described below because at this frequency the cavitation bubbles are known to form. Also this type of sonochemistry device was more portable. The information obtained will be used for planning the second phase of the study for visualization and characterization of cavitation bubbles created by clinical acoustic equipment in tissues.

Synchrotron facilities produce X-ray radiation with high photon flux, large range of selectable energies, high brilliance, and monochromatic beams which makes the synchrotron a good source for studying cavitation bubbles. The goal of this study is to use two different synchrotron X-ray imaging techniques for the visualization of ultrasound induced cavitation bubbles.

6.2.1 X-ray ABI

X-ray ABI is a phase sensitive imaging technique with the ability to detect subtle projected density variations in materials such as tissue. As the X-ray travels through the object being imaged, it may be refracted, scattered or absorbed. Small structures such as a bubble will refract the X-rays through small angles and with ABI, these small angles can create contrast based on the very narrow reflectivity curve of the analyzer crystal. Thus the ABI technique is particularly well suited to visualize interfaces of micro scale features in soft tissues. ABI is particularly capable of visualizing bubbles in soft tissues. In animal models, for example lung tissue which has very high ABI contrast, particularly when the analyzer is placed at the peak position. The

alveoli appear as a “bubbly” structure which very effectively refracts the X-rays and thus create contrast.

Detecting ultrasound cavitation bubbles in tissues can be facilitated by ABI. The bubbles will be of a transient nature and should provide sufficient contrast to be imaged in a time averaged exposure. For example, a single bubble the same size as a detector pixel typically generates ~20% contrast compared to a region not containing a bubble. Using ABI the density of stationary and moving bubbles in the tissue and intravascular can be indirectly inferred by measuring the ultra-small angle X-ray scattering distribution in the region of images where bubbles are formed. However, at the top or peak location of the analyzer, there is a distinct loss of intensity due to scattering from the bubbles. In addition, the ABI technique can provide real time imaging of stationary and moving bubble formation during the focused ultrasound treatment on animals.

With ABI, the X-ray imaging beam is prepared by Bragg diffraction from a perfect crystal monochromator which is typically made with silicon crystals (see Figure 6-1). A double crystal arrangement is used so that the imaging energy can be changed while the exit beam is in the same direction as the incident synchrotron beam. The imaging energy is usually selected according to the sample’s composition, thickness and features of interest. The object is placed in this beam with an analyzer crystal downstream of the object before the detector. The analyzer is parallel to the double crystal monochromator crystals and is of the same orientation, reflection and crystal type. In this arrangement, as the analyzer is rocked in angle near the Bragg angle for the energy and lattice plans chosen, the intensity profile is called a rocking curve. An example of the rocking curve is shown in Figure 6-2 for the imaging conditions used in this experiment. Note that the full-width at half maximum is less than two microradians. Thus the analyzer appears to be a very narrow angular slit when located at the peak position and acts like an

extreme scatter rejection element. When the X-ray beam travels through the sample being imaged, the X-rays are refracted at the interfaces of features or structures in the sample through angles of a few nanoradians to microradians. The analyzer can be adjusted over these angular ranges and the character of the image is greatly affected by the angular setting. The analyzer at the peak setting is sensitive to scatter and removes it from the image. The ABI experimental procedure has been described in more detail in other publications [19-21]. ABI has demonstrated a remarkable ability to image structures that have interfaces between materials of different density such as that between air and water in a bubble. The cavitation bubble will be of a transient nature; however, they are continuously created and may provide sufficient contrast to be imaged in a time averaged exposure.

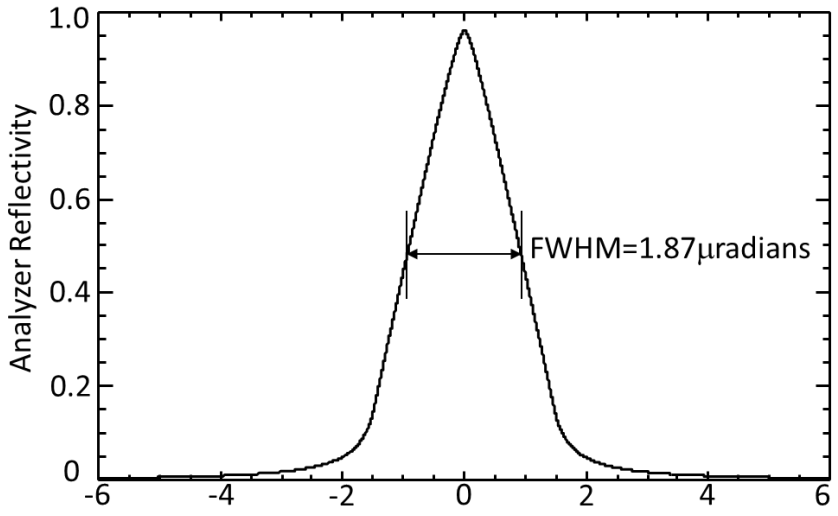

Figure 6-2 Calculated analyzer rocking curve for the reflection and energy used in the ABI experiments; Si (4,4,0) reflection @ 40keV. Note that the rocking angle scale is in microradians (1microradian = 57.3 x 10^{-6} degree)

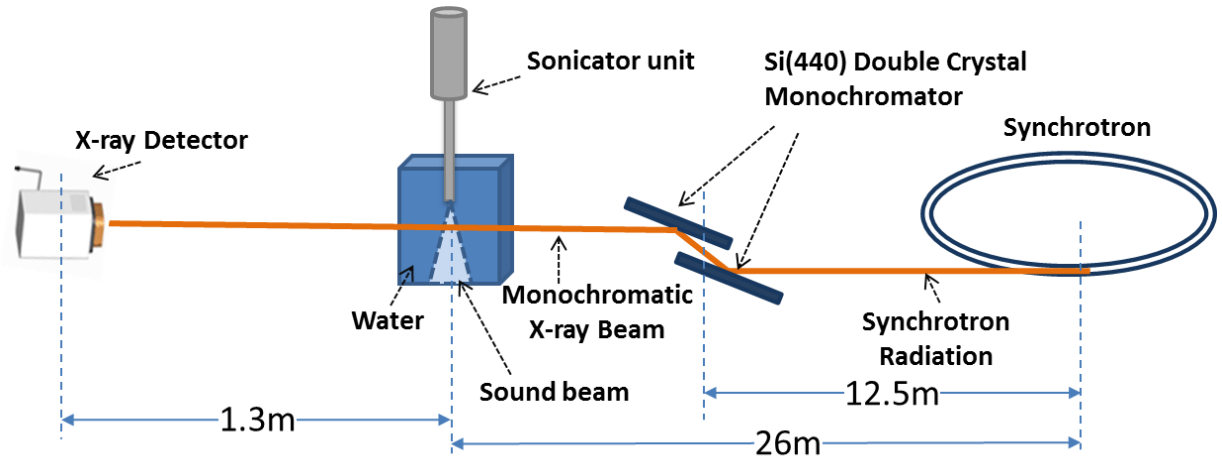

Figure 6-3 Schematic of the PCI set up at the Canadian Light Source used for imaging ultrasound induced cavitation bubbles in water.

6.2.2 X-ray PCI

X-ray in-line or propagation-based PCI is another phase based imaging technique which requires an X-ray source with some degree of transverse coherence. This coherence can be achieved by either having a small source size and/or the source can be placed far from the object and detector (see Figure 6-3). As with ABI, PCI relies on the same sources of contrast within the object, however, the method used is somewhat different and simpler. When the X-ray beam passes through the sample, changes occur in the phase of the X-ray beam. In PCI, information about the beam's phase shift caused by the sample is transformed into intensity variations and is recorded by the detector [22]. Since the X-ray phase shift can be quite high, PCI is very sensitive to density changes in the sample compared to conventional transmission-based X-ray imaging. Even tiny structures can produce phase contrast clearer than absorption contrast. In-Line PCI [23] is particularly easy to apply, especially at a synchrotron. The distance between the object and detector is used to 'tune' the amount of phase contrast from features in the object. Larger separation distances give better phase contrast, however, at the expense of lower resolution. Due

to its simplicity and ability to visualize microstructural details in various biological tissues, in this study PCI was examined for detection of cavitation bubbles.

6.3 Materials and method

6.3.1 Materials

Tap water was used as the sample in which the ultrasound induced cavitation bubbles were produced. The tap water was boiled and left to stand for 48 hours in advance of the experiment to decrease dissolved gases to avoid stationary bubble formation.

6.3.2 Ultrasound treatment

Sonication of tap water was performed by means of an ultrasonic processor (sonochemistry device), with timer and pulser (VCX-130-115V, Cole-Parmer, Montreal, QC, Canada) with the specification of 115 VAC, 20 kHz, 130 W, connecting a sonotrode with a flat tip diameter of 3 mm (1⁄8") titanium probe and tip, and 116 mm length (YO-04712-12, Cole-Parmer, Montreal, QC, Canada). The sonicator output frequency was 20 kHz. The ultrasound processor was brought to CLS and the probe was mounted on the specimen stage at the experimental endstation of BMIT 05B1-1 beamline. The pulse mode was adjusted for continuous acoustic irradiation and the power output of the processor was adjusted at 100% of the maximum output. We developed an electronic switch that was connected to the ultrasonic processor foot switch interface and controlled through National Instrument data acquisition and control system. This arrangement allowed us to control the ultrasonic processor through LabVIEW software (National Instruments Corp., Austin, TX, USA), and collect long image sequences automatically with the sonicator turned on and off as needed in the different parts of the experimental sequence. A 250 ml cell culture container was used as sample holder for this experiment. The top part of the container was cut off using a foam cutter hot knife. Then, the rectangular sample holder, 8 cm wide, 11 cm

high, and 1.3 cm deep was placed on the imaging stage in such a way that the largest surface of the sample holder faces the imaging beam.

The sample holder was filled with the pre-boiled tap water to a height of 8 cm. The tip of the sonicator probe was placed in the sample top at 3.5 cm below the surface of the water (Figure 6-4a), which meant that the tip was about 5.5 cm above the bottom of the container. The sample holder was placed on the scanning stage. The sonicator probe was mounted on the scanning stage using a support stand, and was connected to the ultrasound generator which was placed on the table away from the X-ray beam. Care was taken to prevent any possible damage to the probe by X-ray beam during sonication; the entire probe was protected from the X-ray imaging beam with lead foil, while the tip of the probe was shielded with an additional piece of copper (Figure 6-4b). A visual monitor camera was adjusted at the sample below the probe in order to monitor the sample and the sound jet produced in the sample during the experiment from outside of the hutch (Figure 6-4b). The best mounting position and spatial orientation of the ultrasound processor and sample holder with respect to the incident beam was identified for obtaining as much information as possible. The X-ray beam horizontally covered the entire width of the sample holder for imaging. Images were taken at different positions relative to the probe (different selected distances below the tip of the probe) for different field of views. Changing the experimental system position for different fields of views at each experimental condition was achieved from outside the hutch by adjusting the scanning stage.

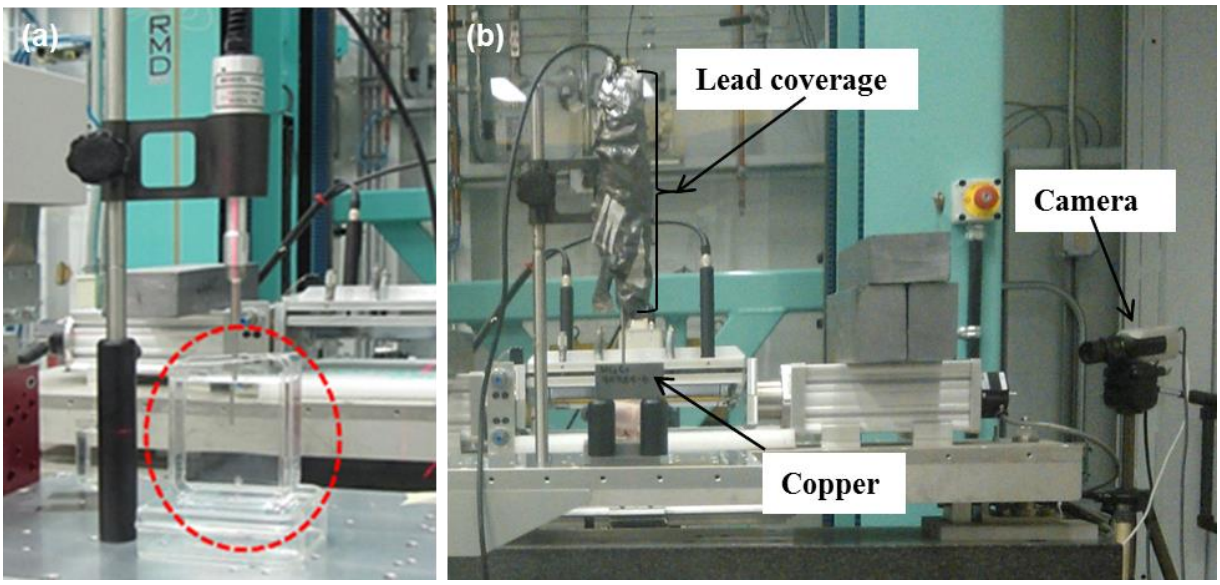

Figure 6-4 Preparation of the sample for ultrasound treatment and X-ray imaging: (a)mounting the sonicator probe on the scanning stage and inserting sonotrode inside and at the center of sample/water; (b) covering the transducer and sonicator probe with lead shielding and copper and adjusting camera at the sample.

6.3.3 Synchrotron imaging

Imaging of ultrasound induced cavitation bubbles was performed at the Biomedical Imaging and Therapy bend magnet (BMIT-BM 05B1-1) beamline of the Canadian Light Source (CLS), Saskatoon, SK, Canada. A highly collimated, monochromatic, X-ray beam with maximum horizontal beam size of 250 mm and maximum vertical beam size of 8.0 mm produced by a bend magnet (1.354T). Preliminary experiments tested the utility of X-ray beams with photon energies of 20 and 40 keV using crystal reflections of (2,2,0) and (4,4,0), respectively. The (4,4,0) crystal reflection at 40 keV provided the highest contrast images and was chosen for this study. Since the usable vertical size of the beam depends on the photon energy, at 40 keV, the X-ray beam with vertical beam size of 4.0 mm and horizontal beam size of 250 mm at the sample location was used for imaging experiments. The size of the beam (scanned region) was 4 mm (vertical) × 240 mm (horizontal) at the detector. Images were taken using a X-ray camera (VHR-90, Photonic Science, Mountfield, East Sussex, UK) with gadolinium oxysulphide scintillator layer having a density of 7.5 mg/cm^2 and area of 74.9 mm × 49.9 mm (4008 × 2672 pixels) with an

effective pixel size of 18.5 μm. Pixel binning of 4 × 4 was used (optical pixel size of 74 μm × 74 μm) and the region of interest of 100 × 77 pixels (7.4 × 5.7 mm) was selected. For the second set of experiments in ABI imaging, the exposure time was about 2500 ms. The images were taken with an average ring current of 170 mA and ring energy of 2.9 GeV.

6.3.3.1 ABI setup

A schematic of the ABI system used for these experiments is shown in Figure 6-1. The distance between the sample and the X-ray source is approximately 26m and the distance between the double crystal monochromator and sample was approximately 13 m. The monochromator - analyzer used in ABI was a silicon (2,2,0) /(4,4,0) configuration. The analyzer was adjusted at the top of the rocking curve. The distance between the analyzer crystal and detector was 0.6 m and the sample was 0.7 m away from the analyzer as shown in the figure. *Single image contrast:* For the first set of experiments, images at different distances from the tip of the probe were taken and the contrast of each image was evaluated. With the tip of the sonicator probe placed 3.5 cm below the surface of the water, the selected distances (field of views) were: 1, 2, 3, 4 cm from the tip of the probe. One image was taken while the sonicator was off and then the sample was sonicated at 100% amplitude (continuous mode) and during the sonication process another image was taken (from the sample at each of the distances from the probe). An earlier, dark image was taken with the X-ray beam off to eliminate non-beam detector response. The dark-corrected sonicator-on images were divided by the dark-corrected sonicator-off images in ImageJ [24], and then the gray value across each image area was evaluated.

Multiple image contrast: For the second part of the experiment a large number of images in sequence mode were collected with the goal to improve the signal to noise ratio and to minimize the effects of the small drift of the analyzer crystal. For this part of study, the X-ray beam was

prepared by the Si (4,4,0) double crystal monochromator at 40 keV, the images were taken at the peak of the rocking curve and the output power of sonicator was set for 90% output power (117 Watt). The imaging sequence contained 700 on-off cycles. In each cycle 2 images were acquired. First the ultrasound was turned on and an image was collected, immediately after that the ultrasound was turned off and after a 500 ms delay another image was collected. The time necessary to complete one cycle is small and both images were collected practically at same point of the analyzer rocking curve. Planar ABI was performed to scan the sample over the 24 mm range below the tip of the probe of sonicator in the sample by taking 6 frames and incrementing the position of the scanning stage by 4 mm between each frame (at six different locations of 4, 8, 12, 16, 20, and 24 mm below the tip of the probe). The exposure time for each frame was 3.5 sec, chosen based on the intensity of the X-ray beam. On completion, all 700 images with ultrasound on were summed and all the 700 images with ultrasound off were summed. Then the two resulting summed images were divided by each other using ImageJ software program. The intensity ratio (on divided by off) was evaluated for each image set. At 40 KeV the total radiation exposure was approximately 1.7 Gy for the 1400 images.

Using the same imaging procedure, ABI-based imaging studies of ultrasound induced cavitation bubbles at 20 kHz level of frequency were performed for seven different acoustic power levels of 26, 39, 52, 78, 104, 117, and 130 Watts (20%, 40%, 60%, 80%, and 100% of output power) at a scanning position of 2 mm below the tip of the probe. The images were analyzed using the ImageJ computer software program.

In addition, in order to have a view of the cross section of the beam (Figure 6-10), software of FileBoss (version 3) and NRecon SkyScan to produce a cross section of the cavitation bubbles

through the acoustic beam. This was possible due to the near rotational symmetry of the probe and beam profile. The sinogram for reconstruction used an image line replicated 2500 times.

6.3.3.2 Phase contrast set up

A schematic of the PCI system used for these experiments is shown in Figure 6-3. The procedure for mounting and setting the sonicator and sample on the scanning stage was the same as described in the ABI section (2.2.1). For the first set of images the distance between the sample and the X-ray source was 26 m and the distance between the sample and detector was 1.3 m. For the second set of experiments, the distance between the detector and sample was increased to 6 m which reduced the source to sample distance to 21.3 m. The PCI images were taken at both 20.05 keV and 40 keV. For taking images, both single image and multiple image contrast procedures described above for ABI were tested.

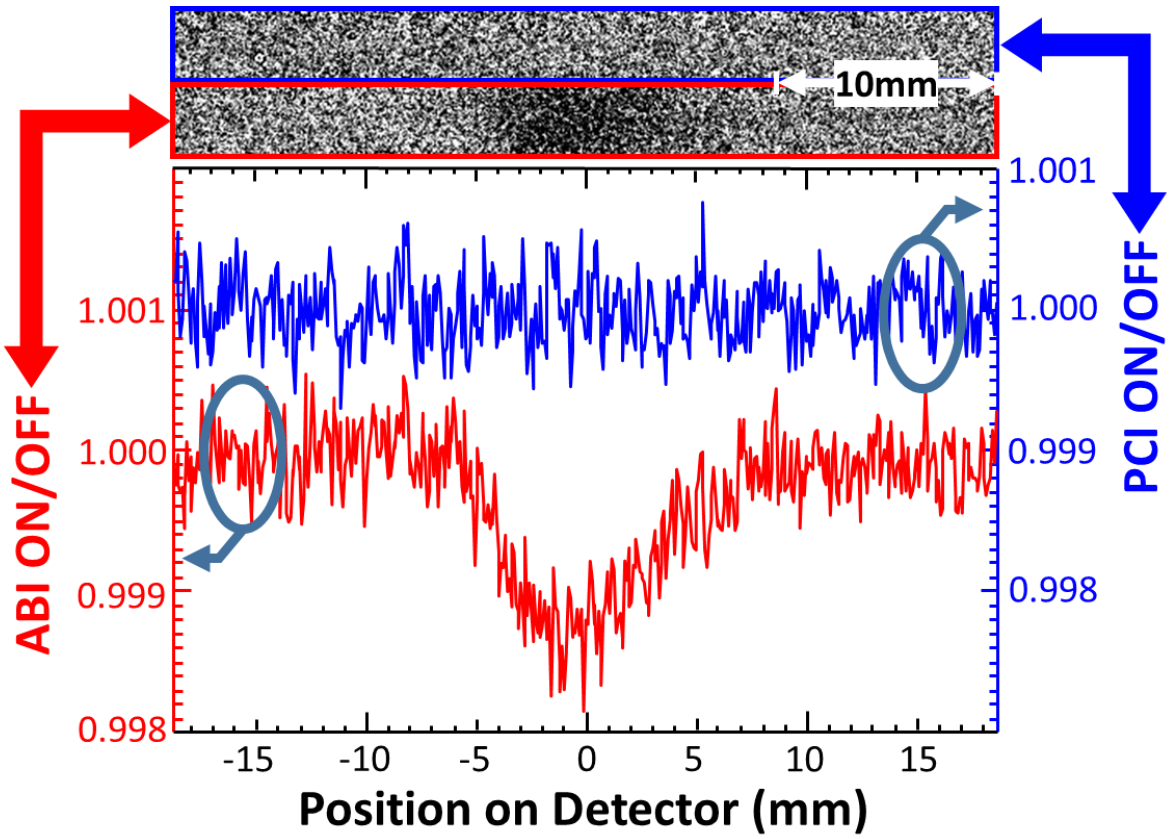

Figure 6-5 The comparison of contrast from PCI and ABI. The PCI image shown at the top with the ABI just below with the same contrast scale. The plot below shows the contrast across the field of view for PCI and ABI. PCI shown at the top with the scale on the right and ABI below with the scale at the left.

6.4 Result and discussion

6.4.1 Phase contrast

Ultrasound induced cavitation bubbles were not detectable beyond the image noise level either with a single image set or with the 700 summed image set. A representative multiple image is shown at the top of Figure 6-5. As can be seen there is no visible contrast from the acoustic beam. That same figure shows a direct comparison with the ABI multiple image obtained under the same conditions which clearly shows contrast. The lower section of Figure 6-5 shows a line plot across the image field of view showing the change in contrast observed by both methods.

6.4.2 ABI Images

Cavitation bubbles were observed in the water sample during multiple image experiments. The processed results obtained from 700 on-off images revealed the region of cavitation bubbles at the center of the image in the area below the ultrasound probe. Since the signal from an ultrasound-induced bubble in the water was very weak (or in the other words, the signal to noise ratio was very low) the features of bubbles in the water were not visible in one single image. By taking more images and summing them, the signal to noise ratio was improved. Also by increasing the number of images, the number of photons in the final, averaged image is increased and more features of bubbles were revealed. Figure 6-6 (a) is a photograph of the ultrasound beam and Figure 6-6 (b) shows the scan of the whole ultrasound beam till 24 mm below the tip of the probe. The presence of cavitation bubbles was detected as decrease in intensity which appears as the dark shadow at the center of the image (Figure 6-6(b)).

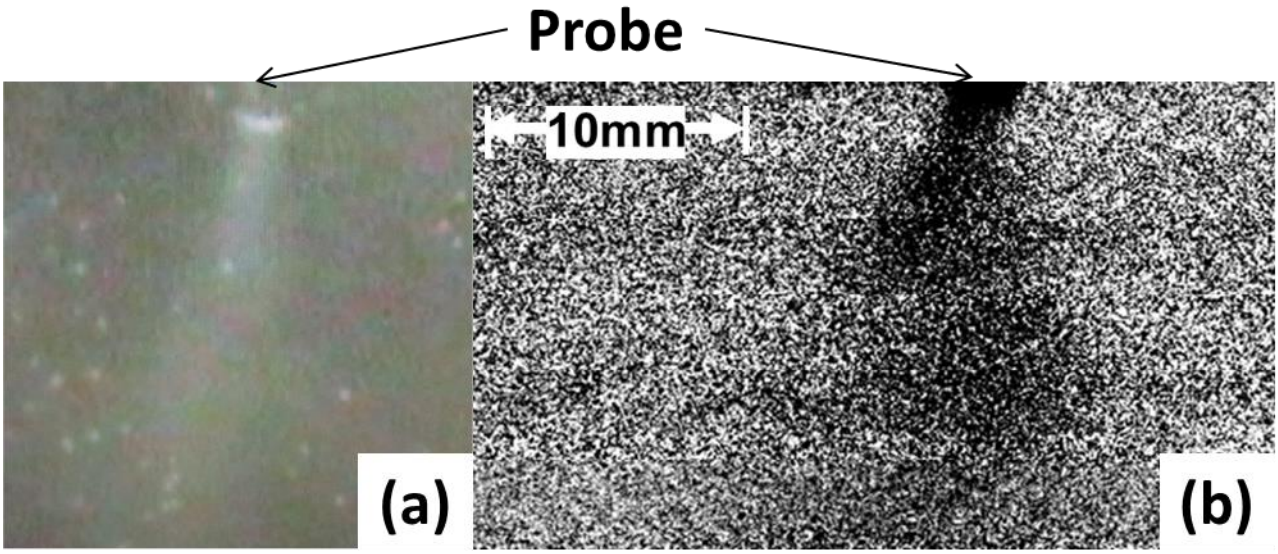

Figure 6-6 Ultrasound beam (a) Vertical scan of the whole ultrasound beam till 24 mm below the tip of the probe at 20 kHz and 90% acoustic output power (117 W) (b).

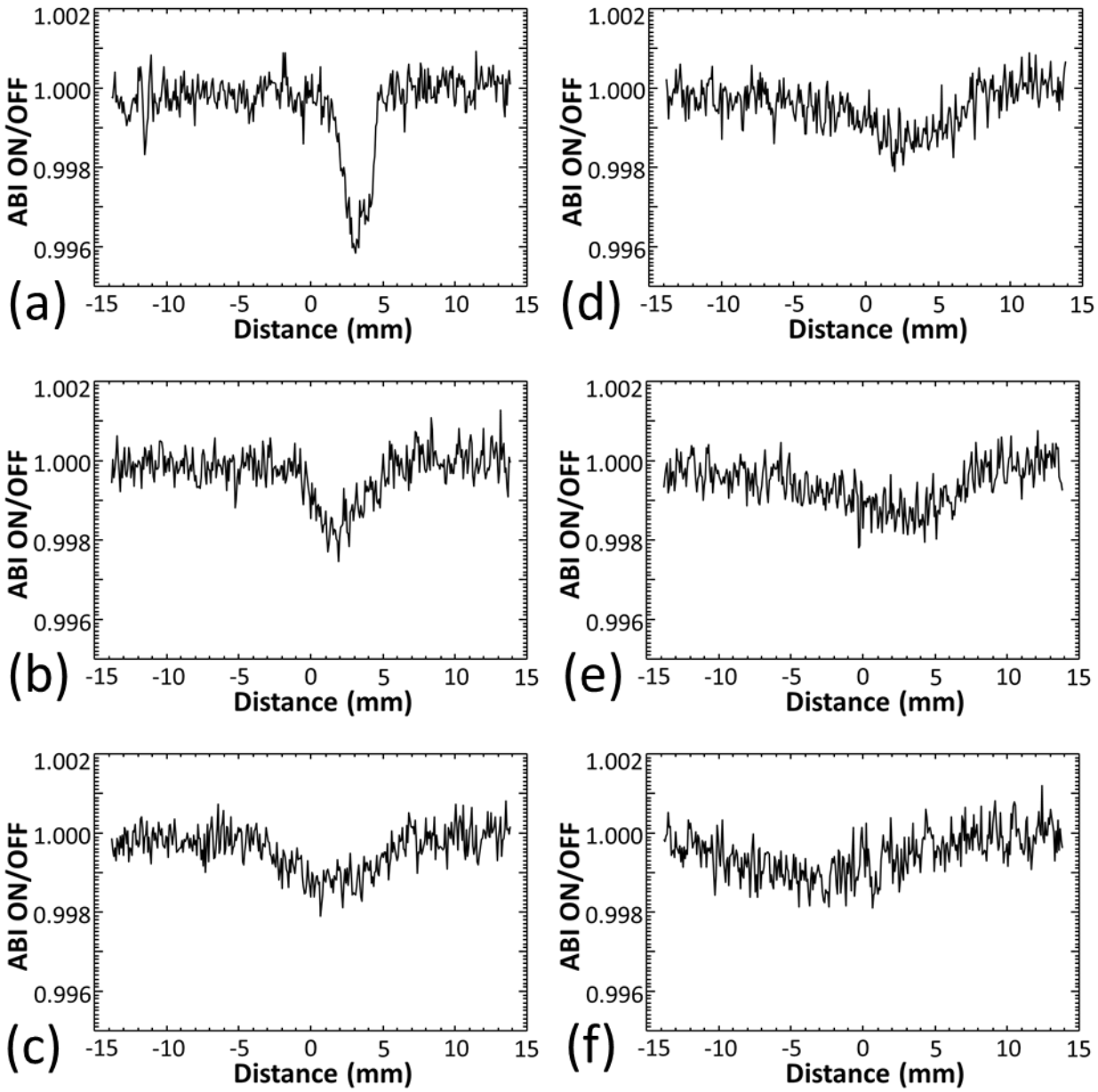

Figure 6-7 The line intensity profile of images taken of the cavitation bubbles at 20 kHz and 90% acoustic output power at different distances from the tip of the probe; 4 mm(a), 8 mm (b), 12 mm (c), 16 mm (d), 20 mm (e), 24 mm (f).

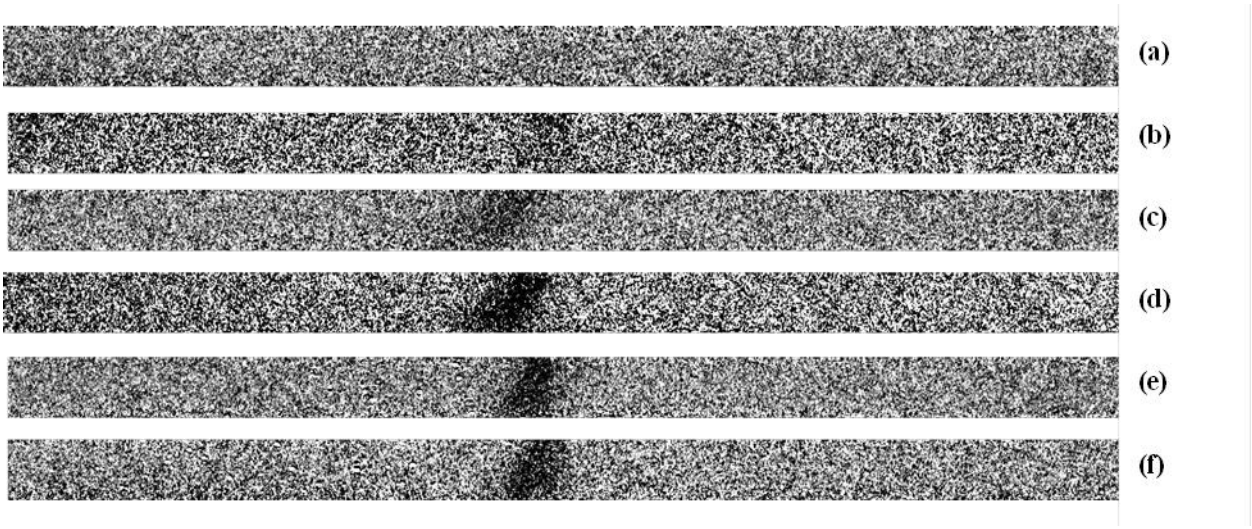

Figure 6-8 ABI-based images of the cavitation bubbles at location of 4 mm below the tip of the probe at acoustic powers of 26 W(a), 39 W(b), 52 W(c), 78 W(d), 104 W(e), and 130 W(f).

As observed in Figure 6-6, the direction of the acoustic beam is not completely straight downward; it tended a little to the left side of the probe direction which may be a result of some non-uniformity on the surface of the probe. This was also visually observed (see Figure 6-6 (a)). The spatial structure of the ultrasonic field will strongly determine the most probable locations of the cavitation bubbles. The shape of the source, its dimension with respect to the wavelength of the ultrasound propagated in the sample and whether it is pulsed or continuous are important factors in controlling the beam structure in the sample. The source of ultrasound in this study was a circularly symmetric source of continuous sound at a single frequency and amplitude. The analysis of such an ultrasound beam has been well developed in the literature [25][26]. As the speed of sound in water is around 1480 ms^{-1}, at 20 kHz, the wavelength in water and soft tissue is about 7.5 cm. The line intensity profile of each image at different distances from the tip of the probe is shown in Figure 6-7.

The line intensity profile of images at different distances from the tip of the probe shows that the intensity decreases as a result of the presence of bubbles. This decrease has the largest magnitude immediately below the probe (4 mm) and weakens with distance from the probe tip. This shows that the density of cavitation bubbles is highest close to the probe and decreases with distance away from the probe. In addition, the width of the dip in the graph increases with distance from the tip of the probe, illustrating the horizontal area in which cavitation bubbles are present. As seen in Figure 6-7, the width of the beam is much smaller in Figure 6-7 (a) than Figure 6-7(f) where the image was taken 24 mm away from the probe. From previous image (Figure 6-6) it is observed that the acoustic beam can be cone shaped meaning that by increasing the distance from the probe the width of distribution of cavitation bubbles is also increased. This is confirmed by the intensity dips in the line plots across the image.

The images of the bubbles at different levels of acoustic powers (26, 39, 52, 78, 104, 117, 130 watt) recorded at the same location of sample (4 mm below the tip of the probe) are shown in Figure 6-8. It is seen that the density of bubbles decreased by decreasing the acoustic output power and the cavitation bubbles were not detectable beyond the noise level at and below 20% amplitude (26 W) of acoustic power (see Figure 6-8(a)).

Figure 6-9 demonstrates the line intensity profile of images taken at 4 mm below the tip of the probe at acoustic powers of 26 W, 39 W, 52 W, 78 W, 104 W, and 130 W, showing that the drop in intensity due to the presence of bubbles decreases as the acoustic power is decreased. At 26 watt level of acoustic power (20% amplitude) no intensity change is observed (Figure 6-9 (a)). Therefore, 26 Watt could be considered as the threshold output power level of ultrasound induced cavitation bubble or the threshold level of capability of ABI for detection of ultrasound induced cavitation bubbles at 20 kHz of frequency.

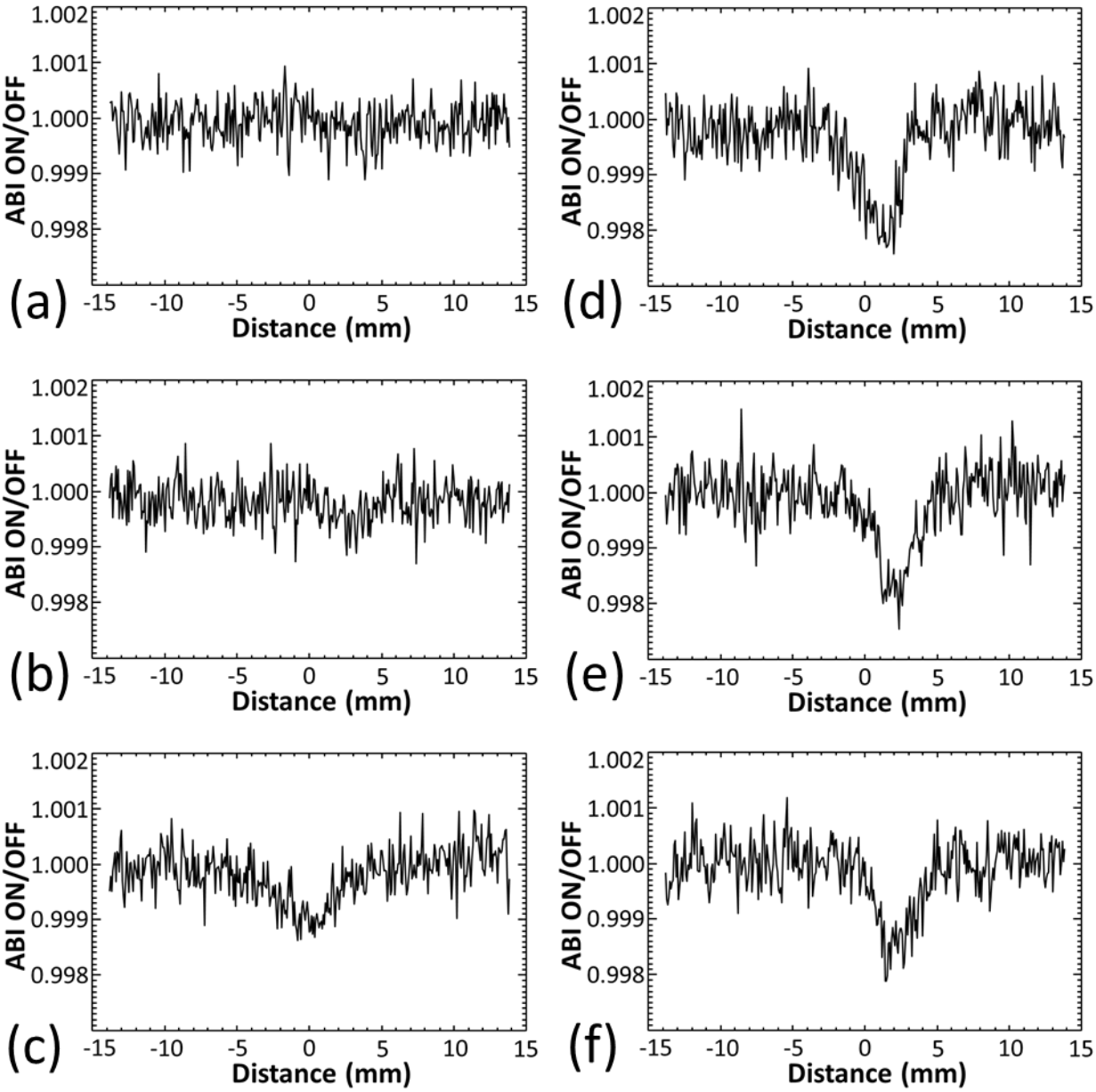

Figure 6-9 The line intensity profile of images taken of the cavitation bubbles at a location of 2 mm below the tip of the probe at acoustic powers of 26 W(a), 39 W(b), 52 W(c), 78 W(d), 104 W(e), and 130 W(f).

As mentioned in section 2.3, the sonotrode was connected to a circle shape probe with a flat tip diameter of 3 mm. Thus the acoustic beam should be rotationally symmetric beam. In order to simulate a view of the cross section of the beam the software tools FileBoss and NRecon (Bruker MicroCT, formerly SkyScan, Kontich, Belgium) were used and all projections of the beam were replicated, constructed and presented in slice sections. As an example, slices for projections of the beam at locations of 4 mm (just below the beam), 8 mm, 16 mm, and 24 mm are shown in Figure 6-10. As observed from Figure 6-10, the diameter of the beam increases at greater distances from the tip of the probe.

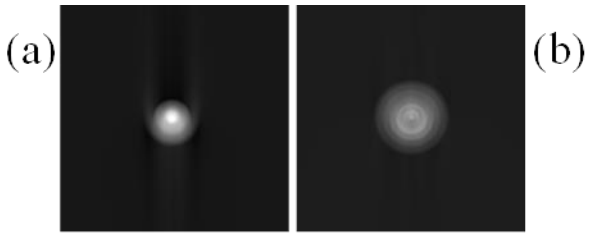

Figure 6-10 Representative axial full cross-section ABI of simulated ultrasound beam at different distances from the tip of the probe; (a) 4 mm (b) 8 mm.

6.5 Conclusion

Cavitation bubbles were successfully detected by ABI giving cloud-like contrast. However, the PCI imaging technique was not able to detect the bubble as implemented on the BMIT beamline. ABI demonstrated the ability to detect cavitation bubbles in water, although the acquisition time was somewhat long. Since the flux at 40 keV on the BMIT beamline is quite low, the imaging time was long. However if the flux was much higher, the imaging time could be shorter and probably bubbles could be detectable at acoustic powers less than 26 W. Considering a very small size and life time of each cavitation bubble, detection of one single bubble was not possible (as it would need a very high speed camera), and the presence of cavitation bubbles were detected as a time-averaged bubble region. Using ABI the density and location of bubbles

in water was indirectly inferred by measuring the ultra-small angle X-ray scattering distribution in the region of images where bubbles (cavitation) were formed. At 26 Watt output power the cavitation bubbles were not detectable anymore as the threshold level of output power or ABI capability in bubble detection. This set of experiments demonstrates the utility of synchrotron ABI for visualizing cavitation bubbles formed in water by ultrasound, providing the first step in more detailed characterization of cavitation bubble formation. Future experiments will investigate both the visualization of cavitation at higher X-ray beam flux, additional frequencies and powers, and the additional challenges of visualizing bubble formation in biological tissues.

6.6 References

1. Chemat S, Lagha A, AitAmar H, Bartels PV, Chemat F: **Comparison of conventional and ultrasound-assisted extraction of carvone and limonene from caraway seeds.** *Flavour and Fragrance Journal* 2004, **19:**188-195.
2. Zhou Y-F: **High intensity focused ultrasound in clinical tumor ablation.** *World journal of clinical oncology* 2011, **2:**8.
3. Child SZ, Hartman CL, Schery LA, Carstensen EL: **Lung damage from exposure to pulsed ultrasound.** *Ultrasound Med Biol* 1990, **16:**817-825.
4. Delius M, Enders G, Heine G, Stark J, Remberger K, Brendel W: **Biological effects of shock waves: lung hemorrhage by shock waves in dogs—pressure dependence.** *Ultrasound in medicine & biology* 1987, **13:**61-67.
5. Holland CK, Deng CX, Apfel RE, Alderman JL, Fernandez LA, Taylor KJ: **Direct evidence of cavitation in vivo from diagnostic ultrasound.** *Ultrasound in medicine & biology* 1996, **22:**917-925.
6. O'Brien WD, Zachary JF: **Comparison of mouse and rabbit lung damage exposure to 30 kHz ultrasound.** *Ultrasound in medicine & biology* 1994, **20:**299-307.
7. O'Brien WD, Zachary JF: **Rabbit and pig lung damage comparison from exposure to continuous wave 30-kHz ultrasound.** *Ultrasound in medicine & biology* 1996, **22:**345-353.
8. O'Brien WD, Zachary JF: **Lung damage assessment from exposure to pulsed-wave ultrasound in the rabbit, mouse, and pig.** *Ultrasonics, Ferroelectrics, and Frequency Control, IEEE Transactions on* 1997, **44:**473-485.
9. O'Brien WD, Jr., Frizzell LA, Schaeffer DJ, Zachary JF: **Superthreshold behavior of ultrasound-induced lung hemorrhage in adult mice and rats: role of pulse repetition frequency and exposure duration.** *Ultrasound Med Biol* 2001, **27:**267-277.
10. O'Brien Jr WD, Kramer JM, Waldrop TG, Frizzell LA, Miller RJ, Blue JP, Zachary JF: **Ultrasound-induced lung hemorrhage: Role of acoustic boundary conditions at the pleural surface.** *The Journal of the Acoustical Society of America* 2002, **111:**1102-1109.
11. O'Brien Jr WD, Simpson DG, Ho M-H, Miller RJ, Frizzell L, Zachary JF: **Superthreshold behavior and threshold estimation of ultrasound-induced lung hemorrhage in pigs: role of age dependency.** *Ultrasonics, Ferroelectrics, and Frequency Control, IEEE Transactions on* 2003, **50:**153-169.
12. Tarantal AF, Canfield DR: **Ultrasound-induced lung hemorrhage in the monkey.** *Ultrasound in medicine & biology* 1994, **20:**65-72.
13. Lizzi F, Coleman D, Driller J, Silverman R, Lucas B, Rosado A: **A therapeutic ultrasound system incorporating real-time ultrasonic scanning.** In *IEEE 1986 Ultrasonics Symposium*. IEEE; 1986: 981-984.
14. Philipp A, Delius M, Scheffczyk C, Vogel A, Lauterborn W: **Interaction of lithotripter-generated shock waves with air bubbles.** *The Journal of the Acoustical Society of America* 1993, **93:**2496-2509.
15. Sass W, Matura E, Dreyer H, Folberth W, J. S: **Lithotripsy-mechanismsof the fragmentation process with focussed shock waves.** *Electromedica* 1993, **61:**2-12.
16. Zhong P, Cioanta I, Cocks FH, Preminger GM: **Inertial cavitation and associated acoustic emission produced during electrohydraulic shock wave lithotripsy.** *J Acoust Soc Am* 1997, **101:**2940-2950.

17. Pishchalnikov YA, Sapozhnikov OA, Bailey MR, Williams JC, Jr., Cleveland RO, Colonius T, Crum LA, Evan AP, McAteer JA: **Cavitation bubble cluster activity in the breakage of kidney stones by lithotripter shockwaves.** *J Endourol* 2003, **17:**435-446.
18. Cleveland RO, James AM: *A brief review of the Physics of Shock Wave Lithotripsy.* BC Decker Inc., Hamilton, ON, Canada; 2007.
19. Chapman D, Thomlinson W, Johnston R, Washburn D, Pisano E, Gmür N, Zhong Z, Menk R, Arfelli F, Sayers D: **Diffraction enhanced X-ray imaging.** *Physics in medicine and biology* 1997, **42:**2015.
20. Kelly ME, Beavis RC, Fourney DR, Schültke E: **Diffraction-enhanced imaging of the rat spine.** *Canadian Association of Radiologists Journal* 2006, **57:**204.
21. Zhong Z, Thomlinson W, Chapman D, Sayers D: **Implementation of diffraction-enhanced imaging experiments: at the NSLS and APS.** *Nuclear Instruments and Methods in Physics Research Section A: Accelerators, Spectrometers, Detectors and Associated Equipment* 2000, **450:**556-567.
22. Keyriläinen J, Bravin A, Fernández M, Tenhunen M, Virkkunen P, Suortti P: **Phase-contrast X-ray imaging of breast.** *Acta radiologica* 2010, **51:**866-884.
23. Davis T, Gureyev T, Gao D, Stevenson A, Wilkins S: **X-ray image contrast from a simple phase object.** *Physical review letters* 1995, **74:**3173.
24. Schneider CA, Rasband WS, Eliceiri KW: **NIH Image to ImageJ: 25 years of image analysis.** *Nat methods* 2012, **9:**671-675.
25. Humphrey V, Duck F: **Ultrasonic fields: Structure and prediction.** *Ultrasound in Medicine* 1998**:**3-22.
26. Kinsler LE, Frey AR, Coppens AB, Sanders JV: **Fundamentals of acoustics.** *Fundamentals of Acoustics, 4th Edition, by Lawrence E Kinsler, Austin R Frey, Alan B Coppens, James V Sanders, pp 560 ISBN 0-471-84789-5 Wiley-VCH, December 1999* 1999, **1**.

Chapter 7 Application of Analyzer Based X-ray Imaging technique for detection of ultrasound induced cavitation bubbles from a physical therapy unit

"This chapter has been published as "Zahra Izadifar, George Belev, Paul Babyn, Dean Chapman, 2015, Application of analyzer based X-ray imaging technique for detection of ultrasound induced cavitation bubbles from a physical therapy unit, *Biomed Eng Online*, 19;14:91. doi: 10.1186/s12938-015-0085-6" According to the Copyright Agreement, "the authors retain the right to include the journal article, in full or in part, in a thesis or dissertation".

7.1 Abstract

The observation of ultrasound generated cavitation bubbles deep in tissue is very difficult. The development of an imaging method capable of investigating cavitation bubbles in tissue would improve the efficiency and application of ultrasound in the clinic. Among the previous imaging modalities capable of detecting cavitation bubbles in vivo, the acoustic detection technique has the positive aspect of in vivo application. However the size of the initial cavitation bubble and the amplitude of the ultrasound that produced the cavitation bubbles, affect the timing and amplitude of the cavitation bubbles' emissions. The spatial distribution of cavitation bubbles, driven by 0.8835 MHz therapeutic ultrasound system at output power of 14 Watt, was studied in water using a synchrotron x-ray imaging technique, Analyzer Based Imaging (ABI). The cavitation bubble distribution was investigated by repeated application of the ultrasound and imaging the water tank. The spatial frequency of the cavitation bubble pattern was evaluated by Fourier analysis. Acoustic cavitation was imaged at four different locations through the acoustic beam in water at a fixed power level. The pattern of cavitation bubbles in water was detected by synchrotron x-ray ABI. The spatial distribution of cavitation bubbles driven by the therapeutic ultrasound system was observed using ABI x-ray imaging technique. It was observed that the

cavitation bubbles appeared in a periodic pattern. The calculated distance between intervals revealed that the distance of frequent cavitation lines (intervals) is one-half of the acoustic wave length consistent with standing waves. This set of experiments demonstrates the utility of synchrotron ABI for visualizing cavitation bubbles formed in water by **clinical** ultrasound systems working at high frequency and output powers as low as a therapeutic system.

7.2 Introduction

One of the main interaction mechanisms that occur during the propagation of an ultrasonic wave through tissues is the possibility of acoustic cavitation. Cavitation is a complex phenomenon that involves creation, oscillation, growth and collapse of bubbles within a liquid medium to local pressure variation. A consequence of the cavitation process is the release of an enormous amount of energy in the form of an acoustic shock wave, temperature, pressure, and as visible light. When the acoustic cavitation bubble collapses close to or on a solid surface, it can collapse asymmetrically and produce high-speed jets of liquid being driving into the surface of the solid have been observed at speeds close to 400km/h [1]. This can seriously damage the impact zone and create a newly exposed surface. This fact makes cavitation one of the important mechanisms in shock wave lithotripsy for kidney stone destruction. Cavitation can also injure tissue during lithotripsy [2]. Studies [3-5] have provided indirect evidence that tissue injury response during shock-wave lithotripsy corresponds to cavitation. A number of studies have been attempted to control cavitation to obtain accelerated fragmentation while minimizing cell lysis and tissue

injury [2]. Furthermore, cloud cavitation (bubble cloud) which is produced during lithotripsy is potentially the most destructive form of cavitation[2]. It has been shown that cloud cavitation is more destructive to high-speed turbo-pumps and ship propellers than the individual bubbles collapse [2]. The effect of cavitation on tissue has made a potential non-invasive therapy application of ultrasound for tissue fractionation and treatment of benign disease and cancer[6, 7]. It has been estimated that rapid adiabatic compression of gases and vapours within the bubbles or cavities produces hot spots with extremely high temperature and pressure approaching 5000°C and 1000atm during this collapse. As ultrasound propagates through tissue, part of its energy is absorbed by tissue which is converted to heat and energetic microbubbles that can result in cellular destruction. Damage to red blood cells [8], lung damage in mice by pulsed ultrasound in the diagnosis imaging range [9], lung lesions of pig, mice, rabbits, rats, monkey and dogs during ultrasound [3, 10-12] [13, 14] [15, 16] [17]bring concern in ultrasonography. Furthermore, high intensity focused ultrasound treatment (HIFU) in which the ultrasound is focused into a small focal zone can damage tissue. Tissue damage occurs as a result of the very high temperature inside the bubbles produced, the collapse that creates a shock wave and jets, and also time duration of tissue exposure. The high temperature produced at the focal point HIFU leads to instantaneous cell death and coagulative necrosis at the focal point and with the margin of six to ten cells between live and dead cells at the edge [18]. Since the onset of cavitation and the resulting tissue damage is not predictable, high acoustic intensity is generally avoided in clinic, however cavitation is under investigation to be used as a means to enhance HIFU ablation. Another application of cavitation is in a relatively new field of medical therapy [19, 20] in which cavitation in HIFU is used for drug delivery in selectively permeable regions of tissue [21, 22]. Direct evidence of cavitation bubbles within the tissue is crucial for further

development and refinement of such applications. In HIFU, gas generation, caused by cavitation, abruptly changes the pattern of heat transfer induced by ultrasound, which results in the extension of lesion from targeted area to surrounding healthy tissues [23]. The lack of cavitation bubble field probes is one of the reasons that limit the clinical development of cavitation. Consequently, it is essential to conduct a fundamental study for cavitation detection and cloud cavitation control to improve the safety and application of ultrasound therapy (such as lithotripsy and HIFU) and possibly for ultrasonography which is pervasively used for neonatal imaging.

The variation in bubble characteristics inside the cavitation field is one of the causes that make the study of cavitation characteristics so complex [24]. Once the cavitation bubbles are generated, they may undergo nonlinear oscillations during many cycles of the acoustic wave, called “stable cavitation”, or they may grow and collapse more or less violently, called “inertial cavitation”[24]. The cavitation state induced in liquid is seldom studied in most experiments. It is important to develop monitoring methods to correlate the cavitation state induced in a liquid to the biological effects observed. Since visualization of cavitation bubble field has been quite complex, workers have used some other indirect observations of macroscopic criteria to describe the induced cavitation state in a liquid[24]. However, the easiest way to study cavitation is the direct observation of the bubble field. In addition, to study the cavitation field in the body, a technique that enables detection of cavitation bubbles in tissue is required.

So far there have been a number of techniques for direct observation of the bubble field such as high speed photography [25-27] [28], laser scattering of single bubbles, and acoustic detection of bubbles [29]. The high speed photography techniques are only applicable in in-vitro systems and it is virtually impossible to capture all the bubbles considering the range of temporal and spatial scales. This technique has a very limited depth of field due to the camera [30], and in addition,

the sound wave that produces the cavitation induces an acoustic-optic effect [24]. Also, the presence of collapsing bubbles can be inferred from second harmonic generation [29]. With laser scattering method, most of the temporal and spatial scales related to the dynamics of a cavitation bubble can be captured; however this method is not able to give qualitative information about bubbles or non-spherical bubbles. In addition, the theory behind this method is only applied to spherical shape bubbles considering that all forms of bubbles, spherical and non-spherical, are produced in clinical application of ultrasound [30]. In this technique the volume of the sample is very small and unrestricted visual access at high magnification is required[30]. The acoustic detection technique has the positive aspect of in vivo application, however the size of the initial cavitation bubble and the amplitude of the ultrasound that produced the cavitation bubbles, affect the timing and amplitude of the cavitation bubbles' emissions.

Analyzer-based X-ray imaging (ABI) [31]has the potential to detect and visualize ultrasound cavitation bubbles in thick, optically opaque materials such as in vivo tissue relying on the high penetration of X-rays and a sensitivity to small angle refraction. As such, ABI can visualize and characterize properties of the cavitation bubbles in vivo without having any influence on the bubbles or vice versa.

The present authors have used ABI for visualizing cavitation bubbles from a high intensity sonochemistry system [32]. In that work, the operating conditions are well beyond that used for any physical therapy or imaging application (130 W and 20 kHz). The system relies on generating cavitation bubbles for cell disruption. The present chapter addresses cavitation bubble formation in a type of ultrasound system commonly used for physical therapy applications (14 W and 0.88 MHz) where one might not expect to observe cavitation bubbles.

Again, the use of an X-ray method can allow observation of cavitation in opaque systems without interacting with the cavitation process.

7.2.1 X-ray ABI

X-ray ABI is a phase sensitive imaging technique that can detect subtle projected density and thickness variations in materials such as tissue. As a collimated X-ray beam travels through the object being imaged, it may be refracted, scattered or absorbed. Small structures such as a bubble in tissue or water will refract the X-rays through very small angles. With ABI, these small angles can create contrast based on the very narrow reflectivity curve of the analyzer crystal placed after the object. Thus the ABI technique is particularly well suited to visualize interfaces between features within soft tissues such as bubbles. This leads to very high contrast for some tissues such as lung particularly when the analyzer is placed at the peak position. The alveoli appear as a "bubbly" structure which very effectively refracts the X-rays and thus create contrast. The effect of multiple refraction events by several alveolar interfaces creates a scatter distribution (ultra-small angle X-ray scattering) of the X-rays which effectively removes X-rays from their original collimated trajectory. This scatter distribution can be very effectively interrogated by the analyzer crystal.

Detecting ultrasound cavitation bubbles in tissues can be simplified by ABI. The bubbles will be of a transient nature and should provide enough contrast to be imaged in a time averaged exposure. For example, a single air bubble the same size as a detector pixel can generate ~20% contrast compared to a region not containing a bubble. Applying ABI the density of stationary and moving bubbles in the tissue and intravascular can be indirectly inferred by measuring the ultra-small angle X-ray scattering distribution in the zone of images where bubbles are formed. However, at the top or peak spot of the analyzer, there is a recognizable loss of intensity due to

scattering from the bubbles. With ABI, the X-ray imaging beam is prepared, or collimated, by Bragg diffraction from a perfect crystal monochromator which is typically made with silicon crystals (seeFigure 7-1). A double crystal arrangement is applied so that the imaging energy can be varied while the exit beam is in the same direction as the incident synchrotron beam. The imaging energy is usually selected based on the sample's composition, thickness and features of interest. The object is located in the beam with an analyzer crystal downstream of the object before the detector. The analyzer is parallel to the double monochromator crystals and is of the same direction, reflection and crystal type. In this arrangement, as the analyzer is locked in angle near the Bragg angle for the energy and lattice plans selected, the intensity profile is called a rocking curve. When the X-ray beam passes through the sample being imaged, the X-rays are refracted at the interfaces of features or structures in the sample through angles of a few nanoradians to microradians. The analyzer can be adjusted over these angular ranges and the character of the image is greatly affected by the angular setting. The analyzer at the peak setting is sensitive to X-rays redirected in angle such as scatter and removes it from the image. The ABI experimental procedure is explained in more detail in other publications [31] [33, 34]. ABI has demonstrated a noticeable ability to image structures that have interfaces between materials of various density such as that between air and water in a bubble. The cavitation bubble will be of a transient nature; however, they are continuously created and may provide enough contrast to be imaged in a time averaged exposure.

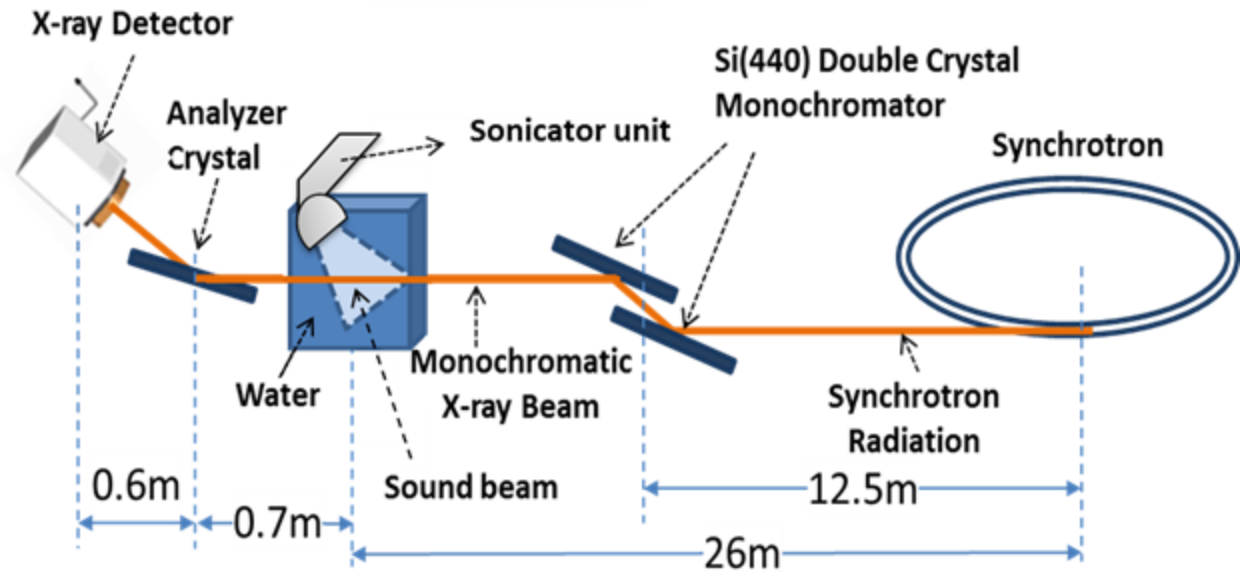

Figure 7-1 Schematic of the ABI set up performed for imaging therapeutic ultrasound induced cavitation bubbles in water at Canadian Light Source.

7.3 Materials and method

7.3.1 Materials

Tap water was used as the sample to produce ultrasound induced cavitation bubbles in it. The tap water was pre-boiled and let stand for 48 hours in advance the experiment.

7.3.2 Ultrasound treatment

Sonication of water was performed by means of a therapeutic ultrasound device (Burdick ultrasound therapy unit model UT-420A), with specifications of 0.8835 MHz, 3.5 W/cm^2, 14 W, connecting a probe with size of 13 cm^2. The ultrasound therapy unit was brought to the Biomedical Imaging and Therapy (BMIT) bend magnet beamline (BM 05B1-1) of the Canadian Light Source (CLS), Saskatoon, SK, Canada. A tissue culture flask (300 cm^2, 1900 ml) was used as sample holder for this experiment. The top part of the flask was cut off by a foam cutter hot knife. Then the sample holder was placed on the imaging stage in such a way that the largest

surface of the flask faces the imaging beam. The probe was mounted on the specimen stage at the experimental endstation of BMIT beamline using a support stand. The sample holder was filled with pre-boiled tap water (to a height of 100 mm) and the probe was placed in the water top at 2.7 cm below the surface of the water with a 60 degree angle (Figure 7-2(a)). The probe was connected to the signal generator/amplifier that was placed on the table away from the X-ray beam (Figure 7-2(b)). The pulse mode was adjusted for continuous acoustic irradiation and the power output of the processor was adjusted at the maximum output. An electronic switch that was connected to the ultrasonic processor foot switch interface was developed and controlled through National Instrument data acquisition and control system. This arrangement allowed the control of the ultrasonic processor through LabVIEW software (National Instruments Corp., Austin, TX, USA), and collect long image sequences automatically with the sonicator turned on and off as needed in the different parts of the experimental sequence. Two visual monitor cameras were adjusted at the sample and at the generator in order to ensure the synchronize operation of the probe and generator along with the Lab VIEW software during image sequence collection. The best mounting position and spatial orientation of the ultrasound and sample holder with respect to the incident beam was identified so that the X-ray beam horizontally covered the entire width of the sample holder for imaging. Images were taken at four different positions. The experimental system position for various fields of views at each experimental condition was changed by adjusting the scanning stage.

Figure 7-2 Preparation of the sample for therapeutic ultrasound treatment and X-ray imaging: (a) mounting the ultrasound probe on the scanning stage and inserting probe inside and at 45 degree angle of sample/water; (b) setting the signal generator/amplifier on the table and setting the experimental system.

7.3.3 Synchrotron imaging

Imaging of therapeutic ultrasound induced cavitation bubbles was performed at the CLS synchrotron source (BMIT-BM 05B1-1). A highly collimated, monochromatic, X-ray beam with maximum horizontal beam size of 250 mm and maximum vertical beam size of 8.0 mm produced by a bend magnet (1.354T) was used for imaging. The X-ray beam with photon energy of 40 keV was prepared by the double crystal monochromator reflection of Si (4,4,0) to provide high contrast images. Depending on the chosen photon energy, the X-ray beam with vertical beam size of 4.0 mm and horizontal beam size of 250 mm at the sample location and the detector was applied for imaging experiments. Images were collected by an X-ray camera (VHR-90, Photonic Science, Mountfield, East Sussex, UK) with gadolinium oxysulphide scintillator layer having a projected density of 7.5 mg/cm^2 and area of 74.9 mm × 49.9 mm (4008 × 2672 pixels) with an effective pixel size of 18.5 μm. Pixel binning of 4 × 4 was applied (optical pixel size of

74 μm × 74 μm) and the region of interest of 100 × 77 pixels (7.4 × 5.7 mm) was selected. Planar ABI was performed for imaging of therapeutic ultrasound induced cavitation bubbles in this study. A schematic of the ABI system applied is shown in Figure 7-2. The distance between the sample and the X-ray source was about 26m and the distance between the double crystal monochromator and sample was approximately 13.5 m. The monochromator - analyzer used in ABI was a silicon (4,4,0) configuration. The analyzer was adjusted very close to the top of the rocking curve. The distance between the analyzer crystal and detector was 0.6 m, and the distance between the sample and the analyzer was 0.7 m as demonstrated in the Figure 7-1. *Multiple image contrast* technique was used for collection of images at each distance from the tip of the probe. In this technique a large number of images in sequence mode were collected to improve the signal to noise ratio and to minimize the effects of the small drift of the analyzer crystal. The imaging sequence contained 7000 on-off cycles. In each cycle 2 images were captured. First an image was collected when the ultrasound was turned on, immediately after that the ultrasound was turned off and after a 500 ms delay another image was collected. The time necessary to complete one cycle is small and both images were collected practically at same point of the analyzer rocking curve. More details on this method of imaging can be found of the previous work of authors [32]. When the ultrasound was on, the output power of sonicator was set for 14 Watt. The sample area of 17.75 to 31.75 mm below the lowest point of the tip of the probe in the sample was imaged. The sample over 14 mm range was scanned by taking 4 frames and incrementing the position of the scanning stage by 3.5 mm between each frame (at four different locations of 19.5, 23, 26.5, and 30 mm below the tip of the probe). The exposure time for each frame was 2.5 sec, selected based on the intensity of the X-ray beam. In total 7000 images with ultrasound on and 7000 images with ultrasound off were acquired. Then the two

resulting summed image sets were divided by each other. The initial results were calculated and analyzed by ImageJ software program. Then, a dedicated program was written in Interactive data language (IDL) software program (Exelis Visual Information Solution, Inc., Boulder, Colorado, USA) and the final results were analyzed. The intensity ratio (on divided by off) was evaluated for each image set. At 40 keV the total radiation exposure was about 17 Gy for the 14000 images.

7.4 Result and discussion

7.4.1 Preliminary experiments

Preliminary experiments were performed by means of a therapeutic ultrasound system (Intelect advanced, Chattanooga group, a division of encore medical, L.P. 2005) with the specification of 0.8835 MHz, Duty cycle 100%, 1 W/cm^2, 4 Watt, Duty frequency 100 Hz, treatment time of 60 min, and probe size of 5 cm^2. During preliminary experiments it was observed that at two specific points of the sample holder, at the wall close to the probe (Figure 7-3(b)), and also at the bottom center of sample holder (Figure 7-3(c)), the sample holder was melting. This means that the transducer field was consistently energetically non-uniform with some spatial 'hot-spots' occurring during the application which lead to burning points (Figure 7-3(a)). These non-uniformities in the acoustic field, simultaneously with the high time-averaged intensities produced, can cause patient burns (Advisory group on non-ionising radiation 2010). This issue has become the issuing of a recent safety in Scotland [35].

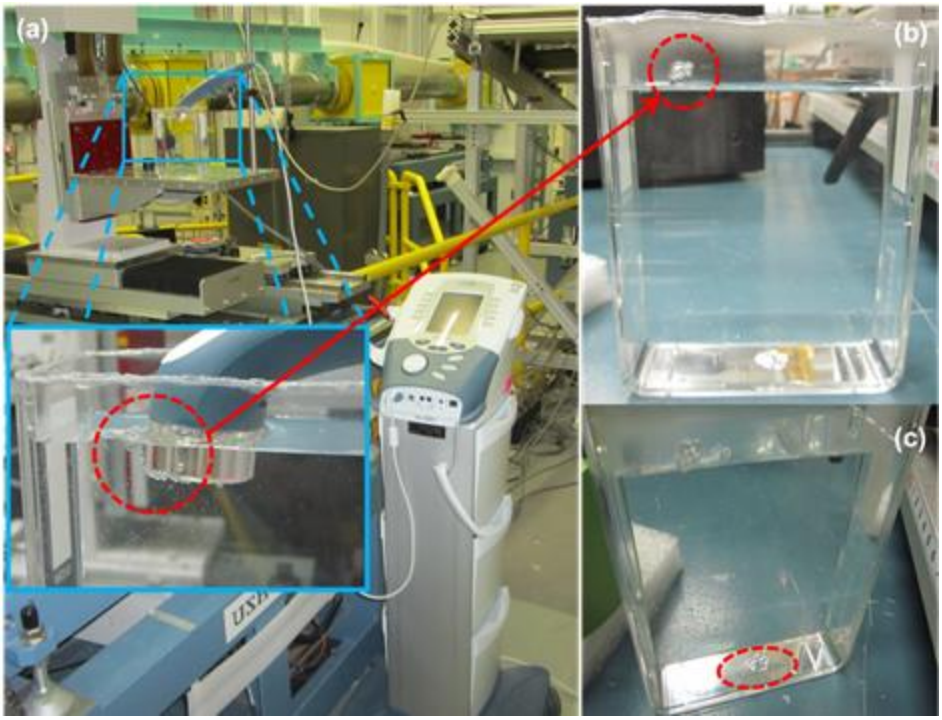

Figure 7-3 The experimental set up of the preliminary experiments and the observation of the sample container melting (a) the melted sign of container on the wall (b) and at the center bottom of the container (c)

7.4.2 Main experiments

Ultrasound induced cavitation bubbles produced by the therapeutic system (physical therapy device with unfocused beam) were detected during multiple image ABI experiments. The processed results from the 7000 on-off images, showed the region of cavitation bubbles in the area below the probe, with 60 degree angle from the water surface along the direction of ultrasound probe. The scan of the ultrasound beam in the area between 17.75 to 31.75 mm below the surface of the probe is shown in Figure 7-4 (a). The presence of cavitation bubbles was detected as loss of intensity that appears as the dark shadow in the area below the ultrasound probe, with a 60 degree angle at the center of the image (Figure 7-4(a)). The spatial structure of the ultrasonic field can determine the most probable location of the cavitation bubbles. The spatial structure of the beam can be controlled by factors such as the shape and dimension of the

source with respect to the wavelength of the ultrasound propagated in the sample, and also the pulsed or continuous mode of sound propagation in sample. In this study the shape of the probe was a circularly symmetric source and the ultrasound was propagated in the sample in a continuous mode at a single frequency and amplitude. The analysis of such ultrasound beams has been well studied in the literature [36, 37]. As the speed of sound in water is around 1480 ms^{-1}, at frequency of 0.8835 MHz, the wavelength in water and soft tissue is approximately 1.675 mm in which the wavelength was calculated as follow:

$$\lambda=c/f \quad (1)$$

where λ is the wavelength in mm, c is the velocity of sound in mm/s, and f is the frequency in Hz. Based on a previous study performed by the authors, the current multiple imaging technique was established for visualization of ultrasound induced cavitation bubbles [32]. The signal to noise ratio from a single ultrasound –induced cavitation bubble is very weak. The features of cavitation bubbles in water are not revealed by a single ABI image and the signal to noise ratio is improved by taking more images and summing them. The number of photons in the final, averaged image is raised by increasing the number of images and as a result more features of bubbles are revealed due to the increased signal-to-noise.

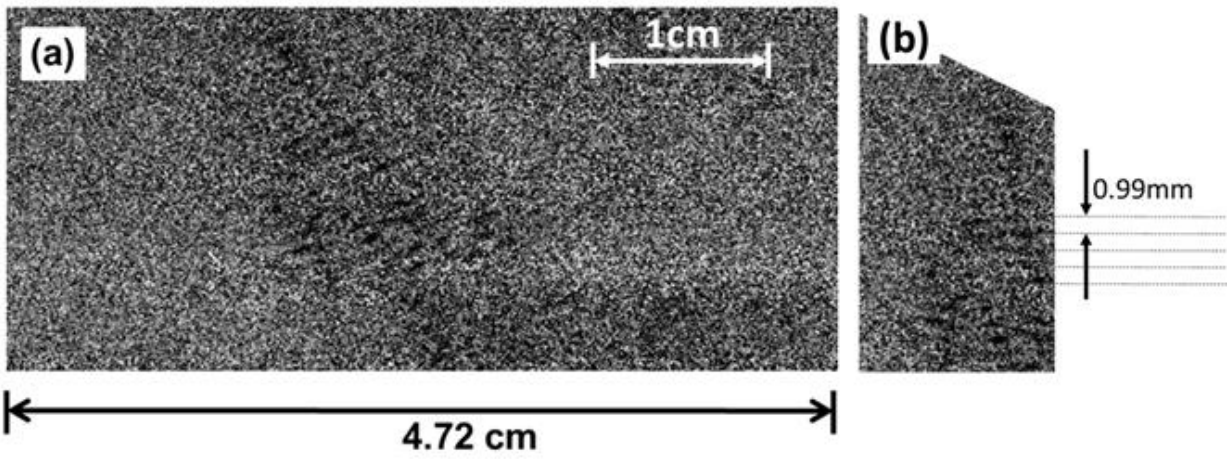

Figure 7-4 Vertical scan of the whole ultrasound beam of a therapeutic ultrasound system below the tip of the probe at 0.8835 MHz and 14 W (a) the sequence form of cavitation bubbles' location with approximately same intervals between sequences

As shown in Figure 7-4(b), it was observed that the cavitation bubbles appeared in a periodic pattern. The most likely reason for this spatial structure can be the production of a standing wave in the sample. In case the pattern in Figure 7-4 is the formation of an acoustic standing wave field due to trapped cavitation induced bubbles, then the standing wave patterns should be one-half of the wave length. To investigate this, the distance between the two consecutive parallel lines of the pattern in Figure 7-4(b) was measured as 0.99 mm. The periodicity can also be obtained from Fourier analysis (Figure 7-5(b)) and was found to be 1.15 line-pairs (lp) per mm. Figure 7-5(b) is a spatial power spectrum of the acoustic field region shown in Figure 7-5a and the bright regions indicate spatial periodicities of higher amplitude. Note the somewhat dual circular appearance of the power spectrum which indicates there are multiple directions which describe the acoustic pattern. We have selected the component that corresponds to the pattern most prominent in Figure 7-5a and 4b. This is the reciprocal of the periodicity distance and leads to a spatial periodicity of 0.870 mm. Therefore, the distance between the two consecutive

parallel lines of the pattern is 0.99 mm from Figure 7-4b and the Fourier analysis giving 0.870 mm is close to the theoretically calculated value of 0.838 mm meaning that the assumption of having acoustic standing wave and also the first harmonic can be correct. However, it should be noted that the geometry of the container did not support the formation of the standing wave completely; there was no surface perpendicular to the acoustic wave (or surface parallel to the probe surface). The pattern of Figure 7-4 indicates that an acoustic standing wave was formed in the container at applied therapeutic ultrasound frequency, and the generated cavitation bubbles were trapped at the nodes or anti-nodes of the acoustic standing wave field, and form the temporary stationary bubbles. The fact that the container surfaces were not parallel to the probe surface may give rise to a complex standing wave pattern as indicated by the Fourier power spectrum (Figure 7-5(b)) where there appear to be several standing waves which in that Figure which form a somewhat circular pattern. The stationary bubbles dance/vibrate at their zone and act as sound scatterers [38]. These bubbles finally collapse as the ultrasound goes through off cycle. Although the vibration of bubbles causes the scattered acoustic energy to modulate the exciting carrier signal, the constant generation of these bubbles at same locations and their collapse afterward can release energy and possibly cause damage.

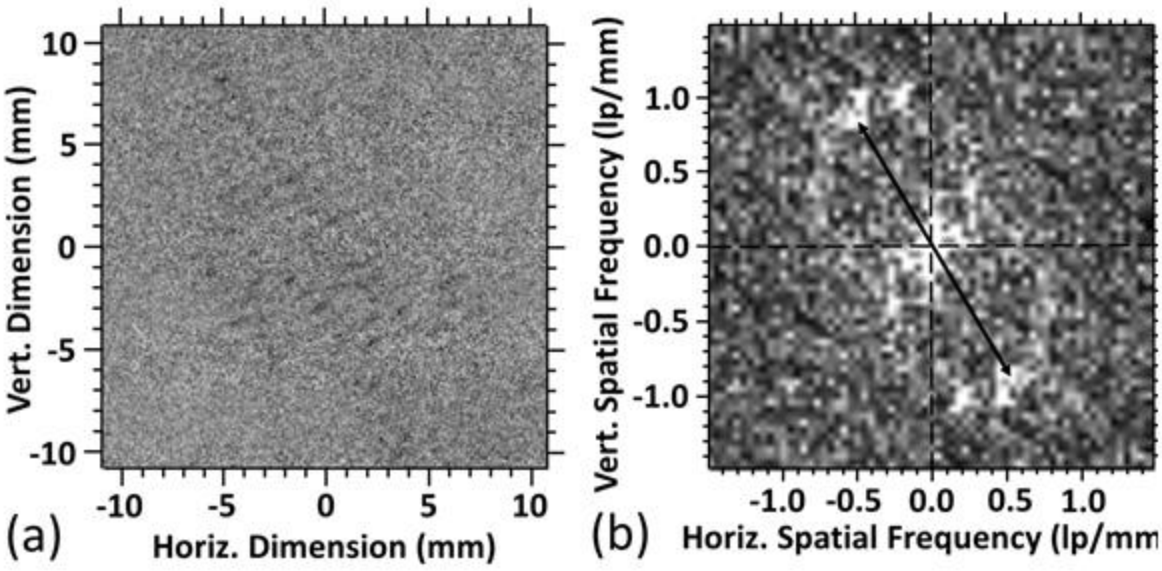

Figure 7-5 The region selected from Figure 7-4(a) for Fourier analysis (a) The power spectrum obtained from Figure 7-4(a). The black line shows the wave vector associated with the strongest Fourier component whose magnitude is approximately 1.15 line-pairs/mm (b).

The line intensity profile of images at different imaging distances from the tip of the probe is shown in Figure 7-6. The line intensity profile of each image obtained from the average of 31 image lines about the center of each image. The intensity profiles demonstrate that the intensity loss as a result of the presence of bubbles. This loss has the highest magnitude at the closest distance to the probe (19.5 mm below tip) and weakens with distance from the probe tip. This demonstrates that the density of cavitation bubbles is higher close to the probe and declines with distance away from the probe. In addition the width of the dip in the graph rises with distance from the tip of the probe, showing the horizontal area in which cavitation bubbles are present. As shown in Figure 7-6, the width of the beam is much smaller at 19.5 mm (Figure 7-6(a)) than 30 mm (Figure 7-6(d)) away from the tip of the probe. It is observed from Figure 7-5 that the acoustic beam can be cone shaped meaning that the width of distribution of cavitation bubbles increases by increasing the distance from the probe. The width of the intensity dips in the line

plots across the image in Figure 7-6 confirms the rise in width of cavitation bubbles' distribution in the sample with distance from the probe.

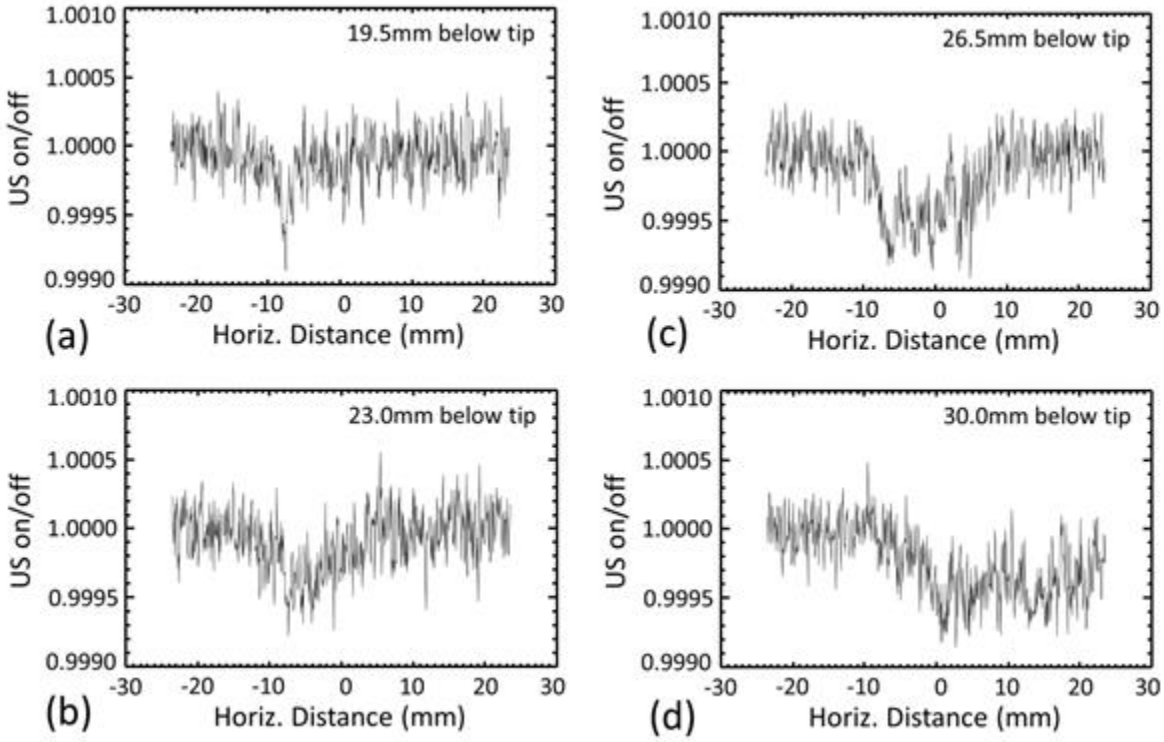

Figure 7-6 The intensity profile of images taken of the cavitation bubbles at different distances from the tip of the probe; 19.5 mm(a), 23 mm(b), 26.5 mm(c), 30 mm(d).

7.5 Conclusion

The pattern of cavitation bubbles in water driven by a 0.8835 MHz therapeutic ultrasound system at 14 watt output power was detected by synchrotron X-ray ABI. Since the flux of X-ray at 40 keV on the BMIT beamline is quite low, the imaging time was long. Although the acquisition time was somewhat long, the pattern of induced cavitation bubbles was revealed. The cavitation bubbles' pattern was observed in repetitive lines. The calculated distance between intervals revealed that the distance of frequent cavitation lines (intervals) is one-half of the acoustic wave length consistent with standing waves. The presence of bubbles was observed as a time-averaged

bubble region. The density and location of bubbles were inferred indirectly by measuring the ultra-small angle X-ray scattering distribution in the region of images where bubbles (cavitation) were formed. This set of experiments demonstrates the utility of synchrotron ABI for visualizing cavitation bubbles formed in water by a **clinical** ultrasound system working at high frequency and output power as low as a therapeutic system. This can be the first step toward more detailed characterization of cavitation bubbles formation in other clinical acoustic systems such as HIFU and lithotripsy.

7.6 References

1. Chemat S, Lagha A, AitAmar H, Bartels PV, Chemat F: **Comparison of conventional and ultrasound-assisted extraction of carvone and limonene from caraway seeds.** *Flavour and Fragrance Journal* 2004, **19:**188-195.
2. Ikeda T, Yoshizawa S, Tosaki M, Allen JS, Takagi S, Ohta N, Kitamura T, Matsumoto Y: **Cloud cavitation control for lithotripsy using high intensity focused ultrasound.** *Ultrasound in medicine & biology* 2006, **32:**1383-1397.
3. Delius M, Mueller W, Goetz A, Liebich H, Brendel W: **Biological effects of shock waves: kidney hemorrhage in dogs at a fast shock wave administration rate of fifteen Hertz.** *J Lithotripsy Stone Dis* 1990, **2:**103-110.
4. Evan AP, Willis LR, McAteer JA, Bailey MR, Connors BA, Shao Y, Lingeman JE, Williams JC, Fineberg NS, Crum LA: **Kidney damage and renal functional changes are minimized by waveform control that suppresses cavitation in shock wave lithotripsy.** *The Journal of urology* 2002, **168:**1556-1562.
5. Zhu S, Dreyer T, Liebler M, Riedlinger R, Preminger GM, Zhong P: **Reduction of tissue injury in shock-wave lithotripsy by using an acoustic diode.** *Ultrasound in medicine & biology* 2004, **30:**675-682.
6. Zhou Y-F: **High intensity focused ultrasound in clinical tumor ablation.** *World journal of clinical oncology* 2011, **2:**8.
7. Suslick K: **The yearbook of science and the future.** *Encyclopedia Britannica, Chicago* 1994, **138**.
8. Daniels S, Kodama T, Price D: **Damage to red blood cells induced by acoustic cavitation.** *Ultrasound in medicine & biology* 1995, **21:**105-111.
9. Child SZ, Hartman CL, Schery LA, Carstensen EL: **Lung damage from exposure to pulsed ultrasound.** *Ultrasound Med Biol* 1990, **16:**817-825.
10. Holland CK, Deng CX, Apfel RE, Alderman JL, Fernandez LA, Taylor KJ: **Direct evidence of cavitation in vivo from diagnostic ultrasound.** *Ultrasound in medicine & biology* 1996, **22:**917-925.
11. O'Brien WD, Zachary JF: **Comparison of mouse and rabbit lung damage exposure to 30 kHz ultrasound.** *Ultrasound in medicine & biology* 1994, **20:**299-307.
12. O'Brien WD, Zachary JF: **Rabbit and pig lung damage comparison from exposure to continuous wave 30-kHz ultrasound.** *Ultrasound in medicine & biology* 1996, **22:**345-353.
13. O'Brien WD, Zachary JF: **Lung damage assessment from exposure to pulsed-wave ultrasound in the rabbit, mouse, and pig.** *Ultrasonics, Ferroelectrics, and Frequency Control, IEEE Transactions on* 1997, **44:**473-485.
14. O'Brien WD, Jr., Simpson DG, Frizzell LA, Zachary JF: **Superthreshold behavior and threshold estimates of ultrasound-induced lung hemorrhage in adult rats: role of beamwidth.** *IEEE Trans Ultrason Ferroelectr Freq Control* 2001, **48:**1695-1705.
15. O'Brien Jr WD, Kramer JM, Waldrop TG, Frizzell LA, Miller RJ, Blue JP, Zachary JF: **Ultrasound-induced lung hemorrhage: Role of acoustic boundary conditions at the pleural surface.** *The Journal of the Acoustical Society of America* 2002, **111:**1102-1109.
16. O'Brien Jr WD, Simpson DG, Ho M-H, Miller RJ, Frizzell L, Zachary JF: **Superthreshold behavior and threshold estimation of ultrasound-induced lung**

hemorrhage in pigs: role of age dependency. *Ultrasonics, Ferroelectrics, and Frequency Control, IEEE Transactions on* 2003, **50:**153-169.
17. Tarantal AF, Canfield DR: **Ultrasound-induced lung hemorrhage in the monkey.** *Ultrasound in medicine & biology* 1994, **20:**65-72.
18. ter Haar G: **Therapeutic applications of ultrasound.** *Progress in biophysics and molecular biology* 2007, **93:**111-129.
19. Sokka S, King R, Hynynen K: **MRI-guided gas bubble enhanced ultrasound heating in in vivo rabbit thigh.** *Physics in medicine and biology* 2003, **48:**223.
20. Vykhodtseva N, Hynynen K, Damianou C: **Histologic effects of high intensity pulsed ultrasound exposure with subharmonic emission in rabbit brain in vivo.** *Ultrasound in medicine & biology* 1995, **21:**969-979.
21. Husseini GA, de la Rosa MAD, Richardson ES, Christensen DA, Pitt WG: **The role of cavitation in acoustically activated drug delivery.** *Journal of Controlled Release* 2005, **107:**253-261.
22. Coussios C, Farny C, Ter Haar G, Roy R: **Role of acoustic cavitation in the delivery and monitoring of cancer treatment by high-intensity focused ultrasound (HIFU).** *International Journal of Hyperthermia* 2007, **23:**105-120.
23. Lizzi F, Coleman D, Driller J, Silverman R, Lucas B, Rosado A: **A therapeutic ultrasound system incorporating real-time ultrasonic scanning.** In *IEEE 1986 Ultrasonics Symposium*. IEEE; 1986: 981-984.
24. Frohly J, Labouret S, Bruneel C, Looten-Baquet I, Torguet R: **Ultrasonic cavitation monitoring by acoustic noise power measurement.** *The Journal of the Acoustical Society of America* 2000, **108:**2012-2020.
25. Philipp A, Delius M, Scheffczyk C, Vogel A, Lauterborn W: **Interaction of lithotripter-generated shock waves with air bubbles.** *The Journal of the Acoustical Society of America* 1993, **93:**2496-2509.
26. Sass W, Matura E, Dreyer H, Folberth W, Seifert J: **Lithotripsy-mechanisms of the fragmentation process with focussed shock waves.** *Electromedica* 1993, **61:**2-12.
27. Zhong P, Cioanta I, Cocks FH, Preminger GM: **Inertial cavitation and associated acoustic emission produced during electrohydraulic shock wave lithotripsy.** *The Journal of the Acoustical Society of America* 1997, **101:**2940-2950.
28. Pishchalnikov YA, Sapozhnikov OA, Bailey MR, Williams Jr JC, Cleveland RO, Colonius T, Crum LA, Evan AP, McAteer JA: **Cavitation bubble cluster activity in the breakage of kidney stones by lithotripter shockwaves.** *Journal of Endourology* 2003, **17:**435-446.
29. Yoshizawa S, Yasuda J, Umemura S: **High-speed observation of bubble cloud generation near a rigid wall by second-harmonic superimposed ultrasound.** *J Acoust Soc Am* 2013, **134:**1515-1520.
30. Cleveland RO, McAteer JA: **The physics of shock wave lithotripsy.** *Smith's Textbook on Endourology* 2007, **1:**529-558.
31. Chapman D, Thomlinson W, Johnston R, Washburn D, Pisano E, Gmür N, Zhong Z, Menk R, Arfelli F, Sayers D: **Diffraction enhanced X-ray imaging.** *Physics in medicine and biology* 1997, **42:**2015.
32. Izadifar Z, Belev G, Izadifar M, Izadifar Z, Chapman D: **Visualization of ultrasound induced cavitation bubbles using the synchrotron X-ray Analyzer Based Imaging technique.** *Physics in medicine and biology* 2014, **59:**7541.

33. Kelly ME, Beavis RC, Fourney DR, Schültke E: **Diffraction-enhanced imaging of the rat spine.** *Canadian Association of Radiologists Journal* 2006, **57:**204.
34. Zhong Z, Thomlinson W, Chapman D, Sayers D: **Implementation of diffraction-enhanced imaging experiments: at the NSLS and APS.** *Nuclear Instruments and Methods in Physics Research Section A: Accelerators, Spectrometers, Detectors and Associated Equipment* 2000, **450:**556-567.
35. **Safety Action Notice SAN (SC) 06/44.** In *Physiotherapy ultrasound machines:calibration of acoustic power/intensity*. Edinburgh: Scottish Healthcare Supplies 2006.
36. Duck FA, Baker AC, Starritt HC: *Ultrasound in medicine.* CRC Press; 1998.
37. Kinsler LE, Frey AR, Coppens AB, Sanders JV: **Fundamentals of acoustics.** *Fundamentals of Acoustics, 4th Edition, by Lawrence E Kinsler, Austin R Frey, Alan B Coppens, James V Sanders, pp 560 ISBN 0-471-84789-5 Wiley-VCH, December 1999* 1999, **1**.
38. Scherf WW: **Amplitude Modulation of a Stationary Acoustic Field by Cavitation Bubbles.** DTIC Document; 1971.

Chapter 8 Conclusion and future research

8.1 Conclusion

The interaction between ultrasound and tissue can potentially affect cells due to ultrasound-induced thermal and mechanical bioeffects that occurs in the beam pathway. These bioeffects should be prevented or minimized during ultrasound diagnosis but can be effectively used for therapeutic purposes (e.g. focused ultrasound lithotripsy), if precisely controlled. The ultrasound-induced thermal and mechanical effects take place simultaneously as a result of ultrasound energy deposition in the tissue; as such, it would be very difficult to differentiate between these effects. Cavitation is a process which is recognized as a major cause of ultrasound-induced mechanical and thermal effects, and can be accentuated by the presence of ultrasound contrast agents in the tissue. It is clear from the evidence reviewed in chapter 2.3 of this thesis that cavitation can have hazardous bioeffects on the tissue under ultrasound therapy or imaging if not controlled.

One step toward improving the outcomes and safety of ultrasound diagnostic and therapeutic applications is to have a better understanding of cavitation bubble formation during the imaging or therapeutic procedures. A better insight into the ultrasound-induced cavitation process will eventually help with the determination of safe levels of acoustic intensity and frequency, duration of ultrasound exposure, and frequency of ultrasound session. One challenge is to visualize the cavitation bubbles in physiologically relevant media for mapping the cavitation bubble formation patterns under diagnosis or therapeutic ultrasound conditions without contrast agents. This study was a step forward to use synchrotron X-ray for visualization of cavitation bubble formation patterns in a physiologically relevant medium (e.g. water, saline) without contrast agent under clinical diagnostic/therapeutic ultrasound conditions.

First, this study aimed to exploit the interaction between a cavitation bubble and synchrotron-based X-ray to examine the suitability of synchrotron X-ray for visualizing ultrasound-induced cavitation bubbles. In the second part of this study, we examined phase-sensitive imaging modalities, DEI, ABI and PCI, for mapping the ultrasound-induced cavitation bubble formation patterns in water. A comparison between the aforementioned imaging methods led us to identify the most suitable synchrotron imaging technique as a protocol for investigating cavitation bubble formation for the rest of our study. Although studies have shown that PCI can be an effective imaging method for visualization of soft tissues, PCI was unable to visualize the ultrasound-induced cavitation bubble formation patterns as implemented in BMIT beamline in our study. In contrast, the ABI showed promises for visualization of cavitation bubbles as well as their formation patterns in water. Water was used as a representative for very soft tissues such as embryo and its surrounding fluid. Using the ABI approach, the density and location of bubbles were inferred indirectly by measuring the ultra-small angle X-ray scattering distribution in the region of images where cavitation bubbles were formed. Therefore, utilization of the synchrotron X-ray ABI in BMIT at CLS for visualizing ultrasound-induced cavitation bubble formation in water provided a foundation for further studies to characterize cavitation bubble formation patterns.

As inspired, we applied the developed ABI to map the ultrasound cavitation bubble formation patterns induced by different ultrasound devices with emphasis on clinical ultrasound devices operating at various ultrasound frequencies and amplitudes. Also, ABI was used to identify the cavitation threshold associated with the ultrasound beam propagation in water. Cavitation bubble formation patterns were successfully mapped using ABI at X-ray energy of 40 keV for two different ultrasound devices including a clinical ultrasound system. The low X-ray photon flux

corresponding to X-ray energy of 40 keV required a longer acquisition time for a higher signal to noise ratio, leading to success in mapping the cavitation bubble formation patterns at therapeutic output powers. One limitation of this study was the low X-ray photon flux corresponding to X-ray energy of 40 keV at the BMIT bending magnet beamline. Considering that the ultrasound-induced cavitation bubbles are very small and their life time is very short, the detection of an individual cavitation bubble essentially requires a high X-ray photon flux and very high speed X-ray camera. To overcome these limitations in our study, we used a local time-averaging approach based on which the probability of local cavitation bubble formation within a fixed window corresponding to the ultrasound beam propagation in the sample was determined from multiple X-ray images as described in chapters 6 and 7. This approach shows promises for detecting cavitation bubble formation patterns in water. Besides, the exposure time can be effectively lowered if the photon flux can be improved by using wiggler rather than bending magnet or a higher storage ring energy synchrotron. If the flux was much higher the imaging time could be shortened and bubbles probably would be detected at lower acoustic powers than what was measured in this study. As the higher ultrasound frequency and lower ultrasound output power were applied, the required imaging acquisition time dramatically increased. As demonstrated in chapters 6 and 7 the initial hypothesis of the thesis regarding the capability of synchrotron based phase based X-ray imaging techniques for visualization of ultrasound induced cavitation bubbles was confirmed correct with ABI but not with PCI. ABI could successfully visualize ultrasound induced cavitation bubbles and provide an overall distribution pattern and location of cavitation bubbles in water sample.

8.2 Recommendation for future work

Results from this study indicate that ABI shows promise for visualization and detection of ultrasound-induced cavitation bubble formation patterns in water. Before ABI technique can be applied to biological tissue and animal/human for cavitation bubble formation mapping, further studies are needed *in vivo*. In our studies, water was used as a physiologically relevant medium to assess the ability of ABI for mapping cavitation bubble formation patterns, but we do not exactly know how these results may relate to cavitation bubble occurrence in biological tissue, animal/human. Thus, animal studies will be required to assess the capability of ABI towards possible applications in human studies.

Cavitation thresholds and related safety considerations are usually determined experimentally through different detection techniques in water. Although water can be a good representative for human soft tissues, it may not reflect the real characteristics of human body. For example, X-ray attenuation and refractive index of water may not exactly represent those of most tissues in the body. Furthermore, the reflection of ultrasound waves corresponding to interfacial microstructural features of soft tissues, which possess different acoustic properties, can generate standing waves leading to more likelihood of cavitation bubble formation. The absence of organelles and their related interfacial features in water limits our ability to acquire the corresponding information attributed to ultrasound cavitation bubble formation. On the other hand, animal studies bring the concern that lies with scaling. Animal testing in small animals such as mice or rabbit can involve whole body exposure, whereas in the human only a small proportion of the total volume is exposed. The absence of human studies leaves us to pose the concern of potential bioeffects from ultrasound.

The acquisition time was somewhat long in our experiments that make it challenging for future tissue and animal studies. Acquisition time may be improved by optimizing the imaging method. The imaging method given in this study needs to be modified to achieve similar results with less acquisition time. From a diagnostic safety point of view, the lack of detectable contrast of cavitation bubbles in water at diagnostic ultrasound power and frequency may not rule out the cavitation bubble occurrence; however, it may only imply that the photon flux and the speed of the X-ray detector may have been insufficient to visualize the cavitation bubble formation. In terms of the safety level of ultrasound devices, one problem is how to rule out possible collateral effects which may have resulted from cavitation occurrence. A null finding doesn't necessarily mean that no effect exists because the null finding may be due to the insufficiently sensitive assay with respect to the detection of the cavitation bubbles. As such, further studies are recommended to refine the imaging parameters of the proposed imaging technique in this thesis for the detection of cavitation bubbles, if they exist, at corresponding low power and frequency diagnostic ultrasound exposure.

To lower the threshold of energy needed for visualization of cavitation bubbles, the accuracy of the threshold determination is critically dependent on the sensitivity of the detection system. Although ABI is a very sensitive method for the detection of bubbles, its performance relies on X-ray photon flux. The detection of small cavitation bubbles corresponding to low output powers and high frequency of diagnostic ultrasound requires higher X-ray flux. The benefits of diagnostic ultrasound currently outweigh the known risks. However, continued research is required to confirm or refute the potential risks of diagnostic ultrasonography. For future research, it is also recommended to perform the experiments in a higher storage ring energy synchrotron which can provide higher photon flux to enable us to eventually develop a protocol

for safety assessment of diagnostic ultrasound using ABI method. The refinement of the ABI technique should not be limited to diagnostic ultrasound but be implemented to assess and characterize cavitation bubble formation in other clinical acoustic systems such as HIFU and lithotripsy.